

**Scientific Cruise Report of the Kara-Sea  
Expedition 2001 of RV "Akademik Boris Petrov":  
The German-Russian Project on Siberian River  
Run-off (SIRRO) and the EU Project "ESTABLISH"**

---

**Edited by  
Ruediger Stein and Oleg Stepanets  
with contributions of the participants**

**Ber. Polarforsch. Meeresforsch. 419 (2002)  
ISSN 1618 - 3193**

**Scientific Cruise Report of the Kara Sea Expedition 2001 of  
RV "Akademik Boris Petrov": The German-Russian Project  
on Siberian River Run-off (SIRRO) and the EU-Project  
"ESTABLISH"**

**Wissenschaftlicher Fahrtbericht der Karasee-Expedition 2001  
mit FS "Akademik Boris Petrov": Das deutsch-russische  
Verbundprojekt "Siberian River Run-off (SIRRO)" und das  
EU-Projekt "ESTABLISH"**

---

Ruediger Stein  
Alfred Wegener Institute for Polar and Marine Research Columbusstrasse,  
Bremerhaven, Germany  
e-mail: rstein@awi-bremerhaven.de

Oleg Stepanets  
Vernadsky Institute of Geochemistry and Analytical Chemistry  
Kosygin Street, Moscow, Russia  
e-mail: stepanet@geokhi.ru

## Table of Content

<b>1. Introduction</b>	<b>1</b>
(O. Stepanets, R. Stein)	
<b>2. Itinerary</b>	<b>3</b>
(R. Stein, O. Stepanets)	
<b>3. Physical and Chemical Oceanography</b>	<b>6</b>
(V. Stanovoy, A. Latko, B. Shmelkov, J. Simstich)	
3.1. Hydrological conditions in the Kara Sea during summer cruise 2001.	6
(B. Shmelkov, A. Latko, V. Stanovoy)	
3.2. Short-periodic internal waves in the Kara Sea.	13
(V. Stanovoy, B. Shmelkov)	
3.3. Water temperature fluctuations in the marginal zones of the Svjataya Anna and Voronin Troughs.	22
(V. Stanovoy, B. Shmelkov)	
3.4. Temperature at the sediment surface - mini heat probe versus CTD	29
(J. Simstich, B. Shmelkov, V. Stanovoy)	
<b>4. Sediment trap investigations in the Kara Sea</b>	<b>33</b>
(C. Gebhardt, N. Lahajnar, B. Gaye-Haake, I. Fetzer, H. Deubel)	
<b>5. Marine Biology</b>	<b>41</b>
(H. Deubel, R. Beude, M. Engel, I. Fetzer, V.V. Larionov, E.-M. Noethig)	
5.1. Phytoplankton distribution in the Ob and Yenisei estuaries and adjacent Kara Sea	41
(V.V. Larionov)	
5.2. Phytoplankton biomass and production in the Ob and Yenisei estuaries and adjacent Kara Sea	45
(R. Beude, E.-M. Noethig)	
5.3. The pelagic larvae of macrofauna in the central Kara Sea	46
(I. Fetzer)	
5.4. Spatial distribution of zooplankton in the southern Kara Sea	50
(M. Engel)	
5.5. Are resting eggs an overwintering strategy of neritic calanoid copepods ?	52
(M. Engel)	
5.6. Benthic studies along a transect from the estuaries of Ob and Yenisei into the central Kara Sea	54
(H. Deubel)	

<b>6. Marine Geology</b>	<b>57</b>
(R. Stein, M.V. Bourtman, M. Chudetsky, H. Deubel, K. Dittmers, A. Eulenburg, G. Kolesov, M. Levitan, F. Schoster, J. Simstich, T. Steinke)	
6.1. Sediment sampling program	57
(F. Schoster, H. Deubel, K. Dittmers, A. Eulenburg, M. Levitan, F. Niessen, J. Simstich, R. Stein, T. Steinke)	
6.2. GeoChirp and ELAC sediment echograph profiling	64
(F. Niessen, K. Dittmers)	
6.3. Physical properties of the sediments	74
(K. Dittmers, F. Niessen)	
6.4. Composition of fraction >63 $\mu$ m of surface sediments from Ob, Taz, and Yenisei rivers and the southern Kara Sea	80
(M.A. Levitan)	
6.5. New data on heavy mineral distribution in southern Kara Sea surface sediments	87
(M.V. Bourtman, M.A. Levitan)	
6.6. Chemical characteristics of main lithofacies based on instrumental neutron-activation analysis data	101
(M.A. Levitan, G. Kolesov, M. Chudetsky)	
6.7. Lithostratigraphy of gravity cores ("Akademik Boris Petrov" Kara Sea Expedition SIRRO-2001)	112
(R. Stein)	
<b>7. Geochemistry</b>	<b>121</b>
(O. Stepanets, M.P. Bogacheva, A. Borisov, A.M. Bychkov, A. Eulenberg, B. Gaye-Haake, C. Gebhardt, B. Hollmann, L.A. Kodina, H. Koehler, V. Komarevsky, G.S. Korobeinik, N. Lahajnar, A. Ligaev, S.V. Ljutsarev, B. Meon, V.I. Peresytkin, F. Schoster, E. Sizov, G. Solovjeva, R. Stein, V.G. Tokarev, L.N. Vlasova, T.I. Waisman)	
7.1. Bacterial consumption and transformation of dissolved organic matter (DOM) in the rivers Ob and Yenisei and the adjacent Kara Sea	121
(B. Meon, H. Koehler)	
7.2. Geochemistry of carbon and silica: water column and sediment sampling. Material, methods and first results	127
(C. Gebhardt, N. Lahajnar, B. Gaye-Haake)	
7.3. Composition of particulate organic matter in the water column and sediments of the Yenisei River and inner Kara Sea	130
(R. Stein, B. Hollmann)	
7.4. Stable organic carbon isotope ratio, lignin and n-alkanes in the surface sediments of the inner Kara Sea.	134
(L.A. Kodina, V.I. Peresytkin)	

7.5.	Carbon isotope composition of phytoplankton biomass and calculation of the plankton material share in the Yenisei and Kara Sea POC load. (L.A. Kodina)	143
7.6	POC isotope composition in the Ob - River and Estuary as compared with the Yenisei system. (M.P. Bogacheva, S.V. Ljutsarev, L.A. Kodina)	151
7.7.	Geochemistry of hydrocarbon gases in the Kara Sea sediments. (G.S. Korobeinik, V.G. Tokarev, T.I. Waisman)	158
7.8.	New findings of ikaite in the Kara Sea sediments. (L.A. Kodina, V.G. Tokarev, L.N. Vlasova, A.M. Bychkov)	164
7.9.	Variability of element concentrations in suspended matter and sediments of the Kara Sea and the Yenisei and Ob rivers. (F. Schoster, A. Eulenberg, V. Rachold)	173
7.10.	Anthropogenic pollution of the Kara Sea and estuaries of the Yenisei and Ob rivers based on data of the 2000 and 2001 cruises. (O. Stepanets, A. Borisov, A.Ligaev, G. Solovjeva, E. Sizov, V. Komarevsky)	180
<b>8. Contributions of the "ESTABLISH" Project</b>		<b>191</b>
	(M.A.K. Sickel, J. Brown, S. Gerland, E.M. Korobova, O. Ch. Lind, V.G. Linnik, T. Panteleimonov, V.B. Pogrebov, V.V. Surkov, N.G. Ukraintseva)	
8.1.	Studies on plutonium speciation and radionuclide concentrations in the Ob and Yenisei estuaries and the Kara Sea under the EU project ESTABLISH (M.A.K. Sickel, O. Ch. Lind, J. Brown, S. Gerland)	191
8.2.	Benthic studies within the ESTABLISH Project (T. Panteleimonov, V.B. Pogrebov)	195
8.3.	Terrestrial investigations in the lower Yenisei during the 36 voyage of RV "Akademik Boris Petrov": Preliminary results. (E.M. Korobova, N.G. Ukraintseva, V.V. Surkov, V.G. Linnik)	197
<b>9. References</b>		<b>212</b>
<b>10. Annex</b>		<b>220</b>
10.1.	Station list	220
10.2.	Lithological core description	234
10.3.	Summary table of planned investigations by participating institutes	275
10.4.	List of participants	277



## 1 Introduction

*O.V. Stepanets<sup>1</sup> and R. Stein<sup>2</sup>*

<sup>1</sup>Vernadsky Institute of Geochemistry and Analytical Chemistry, RAS, Moscow

<sup>2</sup>Alfred Wegener Institute for Polar and Marine Research, Bremerhaven

Within the framework of the joint Russian - German project on “The Nature of Continental Run-Off from the Siberian Rivers and its Behavior in the Adjacent Arctic Basin (Siberian River Run-off - SIRRO)” and based on the results of the first three Kara Sea expeditions in 1997, 1999, and 2000 (Matthiessen and Stepanets, 1998; Stein and Stepanets, 2000, 2001), a fourth expedition with RV “Akademik Boris Petrov” was carried out in the Ob and Yenisei estuaries and adjacent inner Kara Sea in August-September 2001 (Fig. 1-1). The participating Russian and German scientists intended to study biological, geochemical and geological processes relevant for the understanding of the freshwater and sediment input by the Siberian rivers Ob and Yenisei and the impact on the environments of the inner Kara Sea.

In addition to SIRRO group, Russian and Norwegian scientists involved in the EU Copernicus project ESTABLISH (Estuarine Specific Transport and Biogeochemically Linked Interactions for Selected Heavy metals and radionuclides) participated in the 2001 expedition (see Chapter 8). The ESTABLISH project focuses on the marine-freshwater interface in the Yenisei Estuary in connection with modelling of the transport of contaminants (heavy metals and radionuclides) from inland to the open sea.

The scientific program of the expedition covered a wide range of objectives:

- (1) to characterize the supply of the rivers Ob and Yenisei with respect to their dissolved and suspension load, to identify processes modifying the river supply in the estuaries and the inner shelf sea, and finally to analyse the dispersal and deposition of the river supply in the Kara Sea;
- (2) to study the response of the planktic and benthic biota on variations in the river supply along the salinity gradient from the estuaries to the inner shelf;
- (3) to study the geochemistry of dissolved and particulate organic matter and hydrocarbon gases in the water column and the sediments;
- (4) to study the dispersal and distribution pattern of contaminants;
- (5) to study temporal and spatial changes in the late Quaternary paleoenvironment along transects from the estuaries of the rivers Ob and Yenisei towards the open Kara Sea; and
- (6) to study the extent and history of late Quaternary glaciations in the inner Kara Sea.

The research institutes involved in this expedition were from the Russian side the Vernadsky Institute of Geochemistry and Analytical Chemistry (GEOKHI) Moscow, the Arctic and Antarctic Research Institute (AARI) in St. Petersburg, the Shirshov Institute of Oceanology (IORAS) Moscow, the Institute of Geology of Ore Deposits, Petrography, Mineralogy and Geochemistry (IGEM) Moscow, the Murmansk Marine Biological Institute (MMBI), the Moscow State University, and SPA Typhoon, and

from the German side the Alfred Wegener Institute for Polar and Marine Research (AWI) Bremerhaven, the Research Center for Marine Geosciences (GEOMAR) Kiel, and the Institute for Biogeochemistry and Marine Chemistry (IFBM) Hamburg. From Norway, scientists from the Norwegian Radiation Protection Authority (NRPA) in Østerås and the Institute for Soil and Water Sciences, Agricultural University Norway (AUN) in Ås were on board "Akademik Boris Petrov".

This report presents the scientific program and initial results of the expedition and outlines future research to be performed on the material obtained during the expedition. In addition, some results from studies of the 1997, 1999, and 2000 material are also presented.

The success of our expedition is mainly based on the excellent cooperation between crew and scientists. We would like to thank captain Igor Vtorov and his crew for their untiring and able support during work onboard RV "Akademik Boris Petrov".

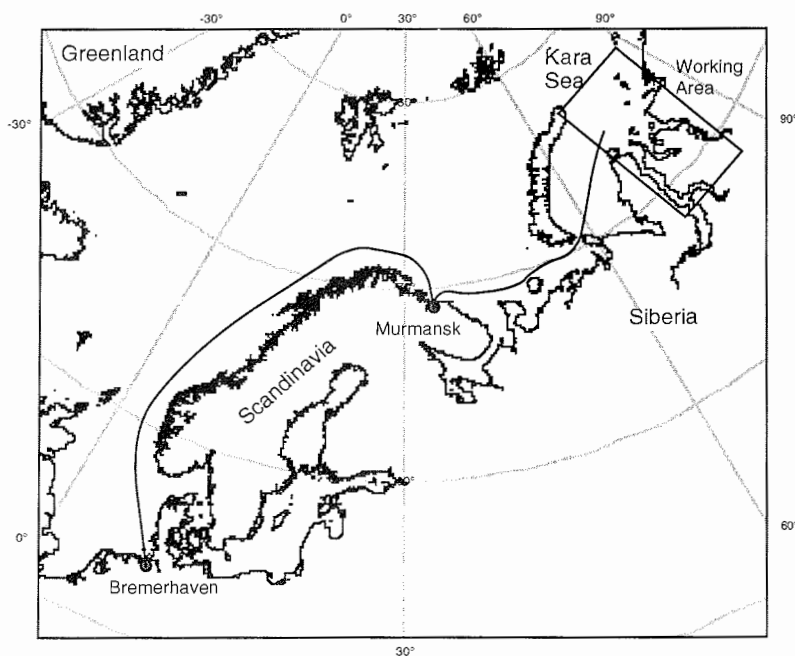


Fig. 1.1: Cruise track of the Kara Sea Expedition 2001 with RV "Akademik Boris Petrov" into the working area. More detailed information about the cruise track in the working area see Figure 6.4.



## 2 Itinerary

*R. Stein<sup>1</sup> and O.V. Stepanets<sup>2</sup>*

<sup>1</sup>Alfred Wegener Institute for Polar and Marine Research, Bremerhaven

<sup>2</sup>Vernadsky Institute of Geochemistry and Analytical Chemistry, RAS, Moscow

RV "Akademik Boris Petrov" left Murmansk early in the morning of August 11, 2001, onboard 35 crew members and 39 Russian, German and Norwegian scientists. On August 14, we reached our study area in the southern Kara Sea (Fig. 2-1).

During the expedition, an extensive sampling program was carried out on a total of 83 stations (Fig. 2-1). The stations for sediment sampling were carefully selected based on profiling results by means of a ELAC Sediment Profiler. Furthermore, the profiling results give detailed information about the seafloor topography and the thickness and structure of the youngest (Holocene?) sediment cover. The ELAC Sediment Profiler was continuously running during transit. In addition, two sediment traps were deployed north of the Ob and Yenisei Estuaries (Fig.2-1) to obtain data on the seasonal variation of particle flux during one year.

The following sampling equipment was used:

- 1) water column: CTD/Rosette, Large Volume Sampler "Batomat" (200l), Water Bucket, and Plankton Nets;
- 2) sediments and biota: Large Box Corer, Multicorer, Large Gravity Corer (with 3 m, 5 m, and 8 m core barrel), Benthos Dredge, and Epibenthos Sledge.

On August 14, we carried out a first station (BP01-01; 74° 59.1'N, 76° 23.4'E) where all sampling equipment was tested successfully. On August 15, we recovered the Yenisei sediment trap deployed in 2000 at 74° N, 80° E. The sediment trap worked perfectly over the last year, and all 24 sampling bottles were filled with suspended matter. In the afternoon of the same day, we reached the area directly east of the Island Sibiriakova (72°56'N) where a detailed Geochirp profiling survey was performed. Based on the profiling result, a geological sampling was selected and a gravity core of 6.5m length was recovered. During the next seven days a detailed water and surface-sediment sampling program was carried out in the Yenisei between 72°30'N and 70° N. At several stations, Yenisei freshwater endmember could be sampled successfully. On August 17, we reached our southernmost station BP01-08 (Fig. 2-1; 70° 04.1'N, 83° 03.9'E). Parallel to the marine work onboard "Akademik Boris Petrov", at several land stations soil and plant samples for studies of radionuclides were taken in the Yenisei coastal zone. Furthermore, surface-near sediment samples were recovered from very shallow water depths using a catamaran.

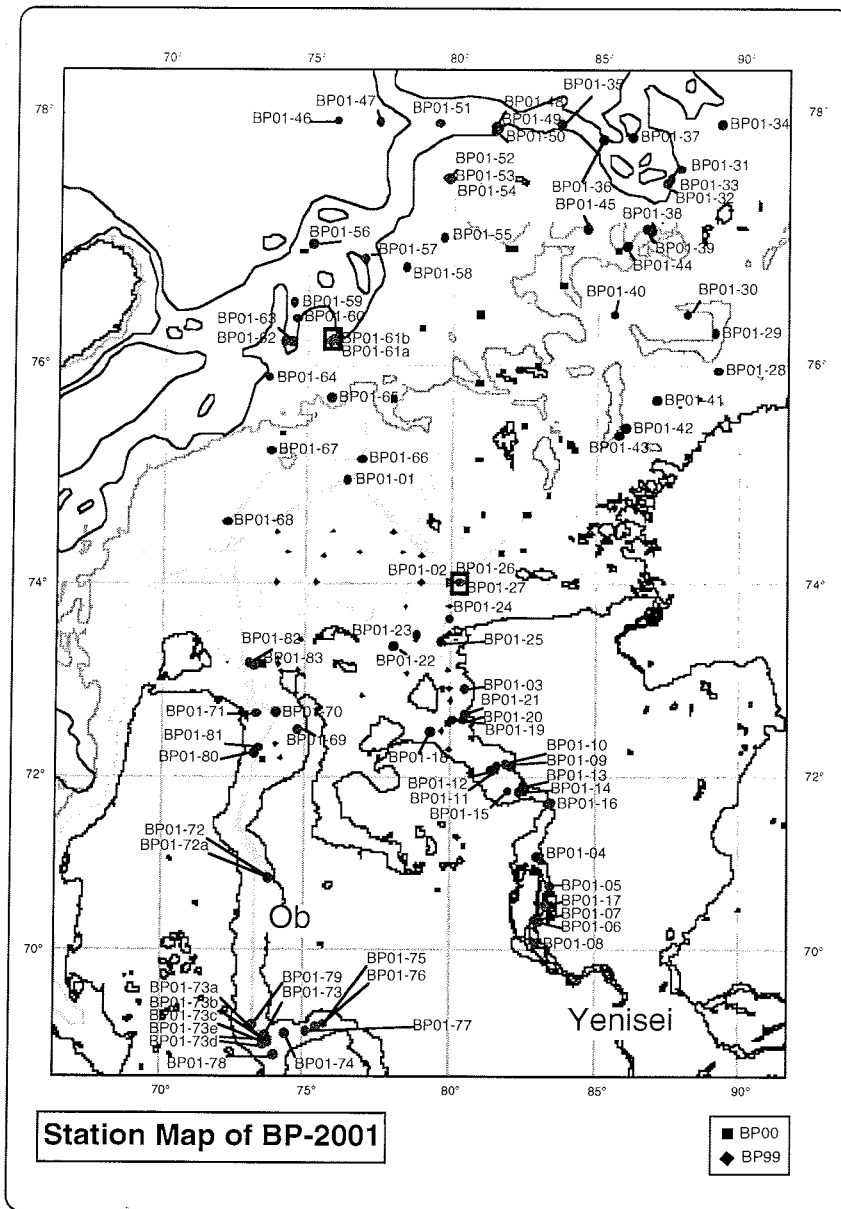


Fig. 2-1: Location of sampling stations and ELAC echosounding tracks of the “Akademik Boris Petrov” Expedition 2001. The large open squares mark the stations where the sediment traps were deployed. In addition, stations of the expeditions 1999 and 2000 are shown.

On August 22, we arrived at the northern Yenisei Estuary, where a long sediment core was obtained during the 1999 expedition (BP99-04). A Geochirp profiling survey was

carried out, and a second reference core (BP01-25/2) was taken at that position (73°24.9'N, 79° 40.6'E). In the early morning of August 23, we reached again the location, where we recovered the Yenisei sediment trap some days ago. After having finished a full water and sediment sampling program, we re-deployed the Yenisei mooring system (sediment trap plus current meter) a few nautical miles towards the east at 74° 00.07'N, 80° 19.87'E (Station BP01-27/1). At the same day, we left the Yenisei, heading towards the northeast. After a transit of 190 nm, a main station was carried out at 75°56.34'N, 89° 15.9'E (BP01-28) on August 24. During the next five days, we worked in the eastern part of our study area. We reached our northeasternmost location in the evening of August 25 (Fig. 2-1, BP01-34; 77°54.29'N, 89° 20.15'E).

Between August 30 and September 06, a detailed oceanographic, biological, geochemical, and geological measuring and sampling program of the water column as well as the sediments were carried out in the northern and northwestern part of our study area. In this area, an intensive ELAC echosounding survey was performed which allows a detailed mapping of the extent of the Last Glacial Maximum (LGM) Kara Sea ice sheet. The northwestern location (BP01-46; 77°55.43'N, 75° 57.35'E) was reached on August 30. On September 03, we deployed successfully our second mooring system (sediment trap plus current meter) at Station BP01-61a (76° 12.08'N, 75° 45.30'E). After having finished all work at Station BP01-68 (74° 35.05'N, 72° 14.97'E) we headed towards the south and reached the Ob Estuary in the morning of September 07.

During the following five days, we worked in the Ob and performed the full program of water and sediment sampling. On September 09, one main and several small stations were carried out in the mouth area of the River Taz (Fig. 2-1; Stations BP01-73 to BP01-79). On September 11, we had the last station at 73° 11.8'N, 73° 14.4'E (Station BP01-83). We finished our scientific work in our study area with a last Geochirp profile across Station BP01-83. In the evening of September 11, we started steaming towards the west. On September 15, we arrived at Murmansk.

### 3.1 Hydrological conditions in the Kara Sea during summer cruise 2001

*B. Shmelkov<sup>1</sup>, A. Latko<sup>1</sup> and V. Stanovoy<sup>2</sup>*

<sup>1</sup> Vernadsky Institute of Geochemistry and Analytical Chemistry, RAS, Moscow, Russia

<sup>2</sup> SSC RF Arctic and Antarctic Research Institute (AARI), St.Petersburg, Russia

#### Introduction

The hydrological survey was conducted during the period from 14 August till 11 September 2001 in the area between 78° and 68° 50' N and 72° and 90° E. For measurement of water salinity and temperature and for subsequent sampling of selected depth intervals a CTD-sonde of type "MARK - 3B" from "EG&G OCEAN PRODUCTS" connected to a rosette sampler (24 bottles, volume 1.7 L) was used. The sonde is suitable for measurements of electrical conductivity, temperature and pressure up to depths of 6000 m. The measurement precision for temperature in the range from -32°C up to +32°C is  $\pm 0.005^\circ\text{C}$ , for electrical conductivity in the range from 1 up to 65 mmho is  $\pm 0.005$  mmho, and for pressure in the range from 0 up to 320 db is  $\pm 0.1$  db. The instruments were calibrated in August 2000 by the company "GENERAL OCEANICS INC." MIAMI, USA. CTD measurements were conducted at 69 stations (Fig. 3.1). After profiling, the horizons for water sampling were selected based on the previous profile and absolute values of the water temperature and salinity.

#### Results and discussion

The ice conditions were quite easy in the summer 2001 (Fig. 3.2) and it was possible to carry out the survey up to 78° N. These easy ice conditions determine some features of the hydrological parameters distribution.

In August and beginning of September 2001 in the Kara Sea the water temperature in the upper layer was higher than the multiyear mean (Fig. 3.3). In the northern part of the investigation area this difference reached up to 2-4 °C. In the northeastern area the water salinity was higher than the multiyear mean (Fig. 3.3). In contrary to this the salinity values in the northern part of the investigation area were close to multiyear mean and in the northwestern part less than the multiyear mean.

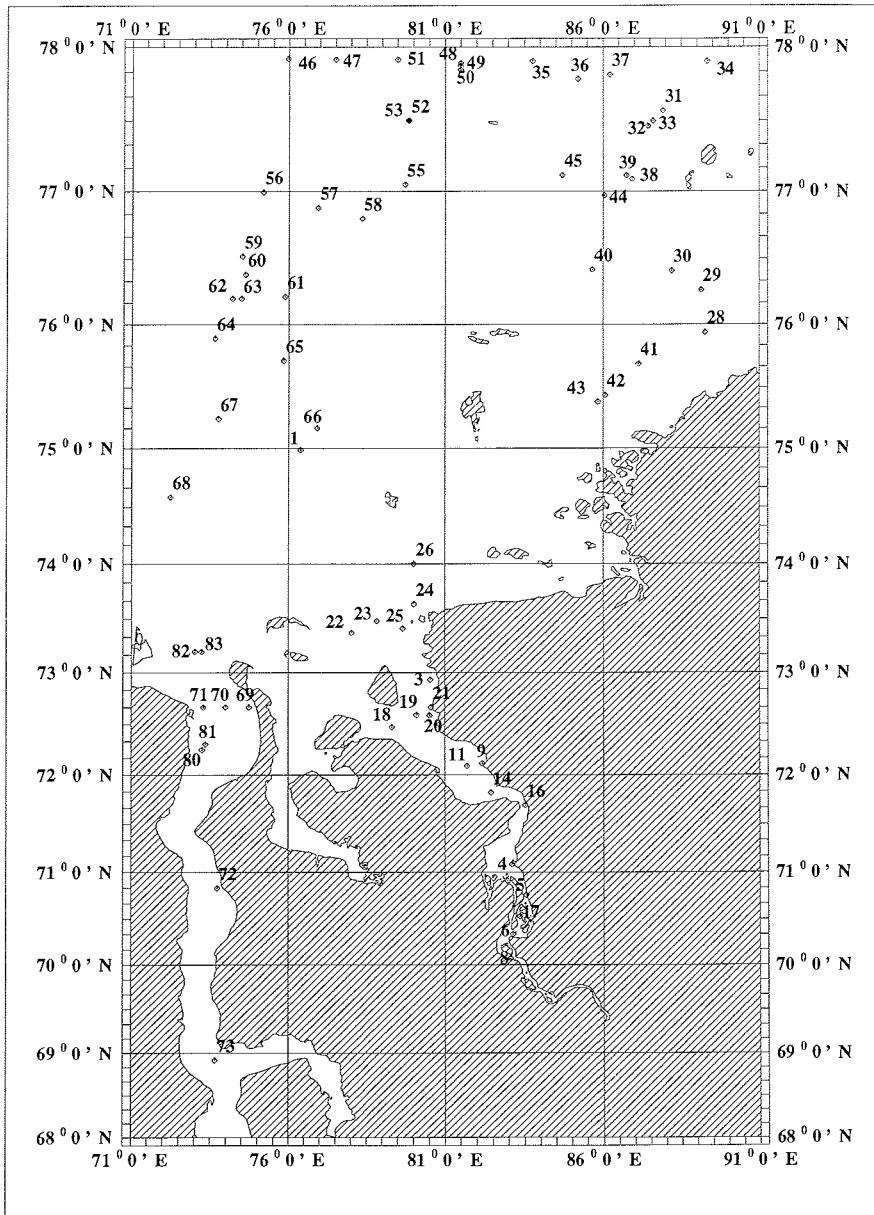


Fig.3.1 Hydrophysical stations on the 36<sup>th</sup> cruise of RV "Akademik Boris Petrov".

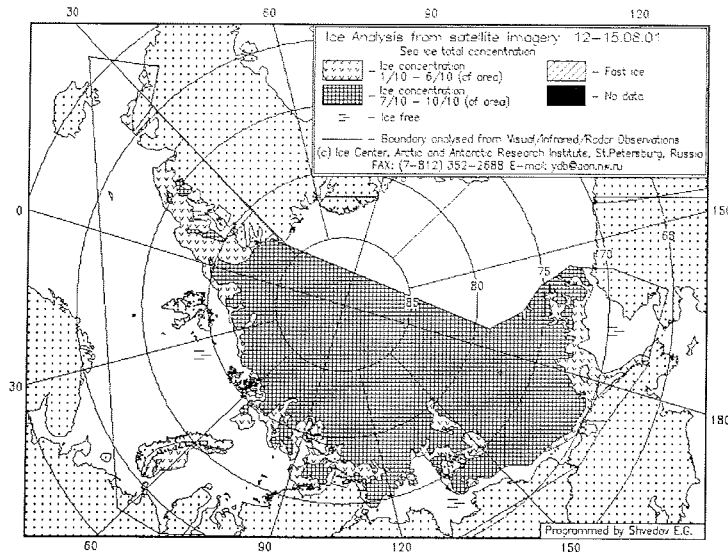


Fig. 3.2. Ice condition map

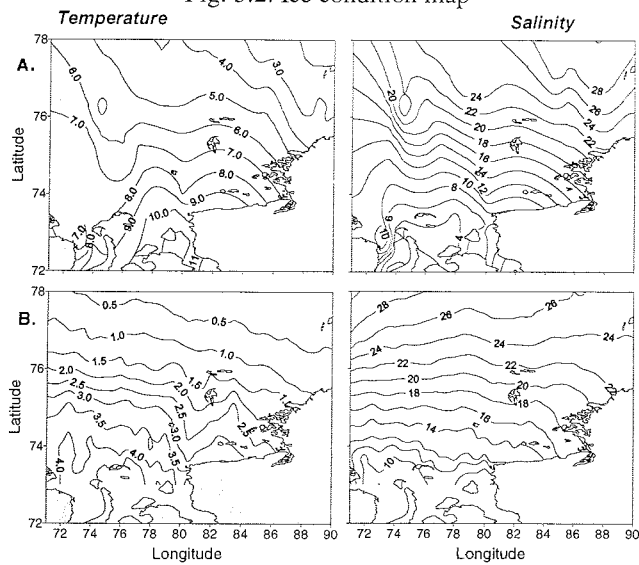


Fig. 3.3. Spatial distribution of the surface water temperature and salinity in summer 2001 (A) and mean multiyear for summertime (B).

In the northeastern part of the investigated area a vertical thermohaline structure with a well-pronounced upper mixed layer down to 10-15 m water depth and a seasonal pycnocline at the depths 15-25 m was observed (Fig. 3.4). In the pycnocline layer the vertical gradients of salinity and temperature reached up to 0.5 psu and 0.5 °C per 1 m, respectively. At the northern (northward from 77° N) stations in this area the layer of Arctic Basin Surface Water is observed below the pycnocline at 25-35 m water depth (Fig. 3.4). The temperature in this water is about 0.2-0.5 °C less than in the underlying

## Deep Kara Sea Water.

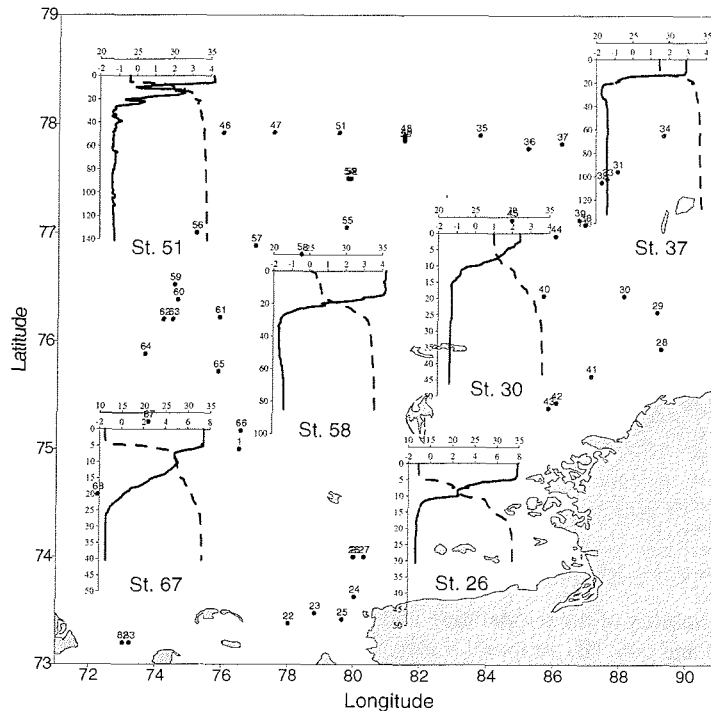


Fig. 3.4. Vertical distribution of the water temperature and salinity in summer 2001

In the northern and north-western deep regions of the investigated area at the marginal zones of the Svjataya Anna and Voronin Troughs significant vertical fluctuations of water temperature and thermic inversion layers at the depths 20-50 m caused by topography were observed. The values of vertical temperature fluctuations reached 2 - 3 °C per 10 m. More detailed description of this phenomenon is presented in the other paper of this volume (Chapter 3.2).

The one of the most important features of the hydrological regime of the central and southern parts of the Kara Sea is the significant temporal variability of the water temperature and salinity. In summertime the variability of intraseasonal (synoptic), tidal and less temporal scales is very strong in this region. The atmospheric processes, changing of the river run-off volume and dynamical forces cause this variability. For example we present the vertical distribution of the temperature and salinity at the station 1 (14 August) and station 66 (5 September) (Fig. 3.5a). The distance between these stations was not so much (see Fig. 3.1), but the vertical profiles are very different. Also in this figure (Fig. 3.5b) we present the variability of the less temporal scale. Usually at the CTD-stations there were a few casts for water sampling. The time difference between these casts was about 0.5 hours only, but during this time some changing of the salinity (density) distribution was observed.

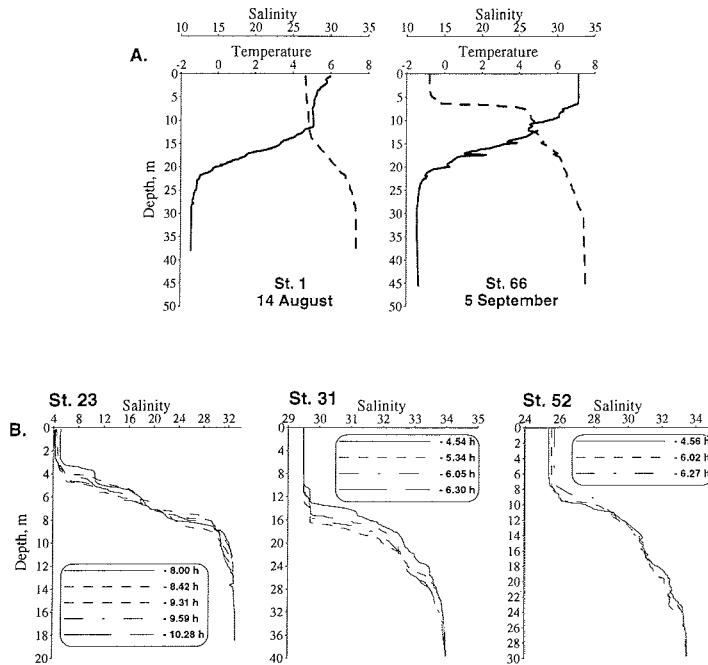


Fig. 3.5. Variability of the temperature and salinity vertical distribution of synoptic (A) and tidal (B) temporal scales.

Also the spatial variability of the pycnocline parameters was observed. In the Figure 3.6 the spatial distribution of the pycnocline depth is presented (Fig. 3.6a). This depth was determined as depth where Brunt-Vaisala frequency is maximal. In the same figure (Fig. 3.6b) we present the spatial distribution of the maximal values of the Brunt-Vaisala frequency.

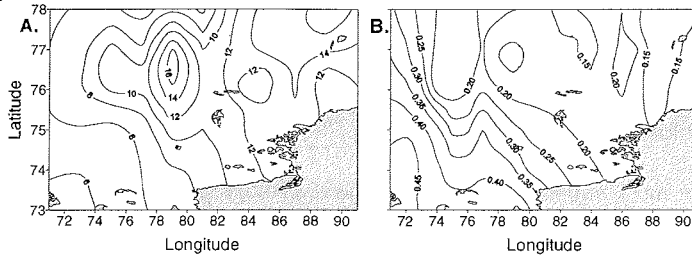


Fig. 3.6. The spatial distribution of the pycnocline depth (A) and maximal values of the Brunt-Vaisala frequency (B).

The vertical distribution of temperature and salinity in the Yenisei and Ob Gulfs in August and the beginning of September 2001 was typical for baroclinic estuaries (Fig. 3.7 – 3.9). The vertical gradients within the pycnocline layer reached up to 5-8 psu per 10 cm and up to 1.0 – 2.0 °C per 10 cm. The fine thermohaline structure is well pronounced.



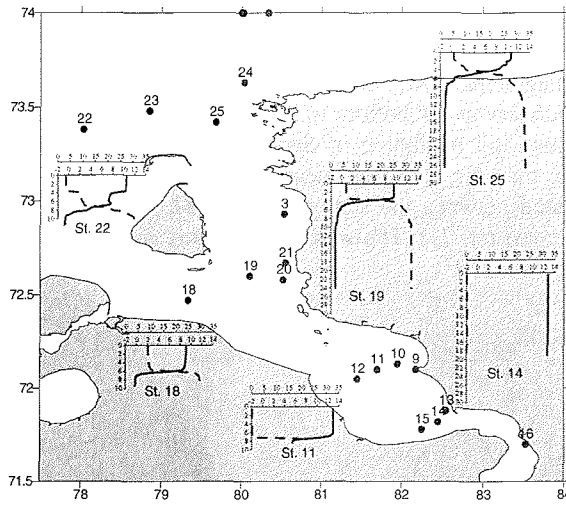


Fig. 3.7. Vertical distribution of the water temperature and salinity in summer 2001 in the Yenisei Gulf.

In the Yenisei estuary in August the boundary between fresh (1 psu) and saline water at the bottom was located in the region between the capes Shaitansky (st. 11) and Sopochnaya Karga (st. 14). Compared to the multiyear mean for August the boundary of fresh water at the bottom moved seaward in 2001, whereas the salinity values at the bottom were higher than the multiyear mean. In the surface layer the boundary between fresh and saline water was located between the stations 11 and 20, in the region of Krestovsky Island (Fig. 3.8), which is in good agreement with the mean multiyear values. The water temperature in the Yenisei Gulf was higher than the multiyear mean.

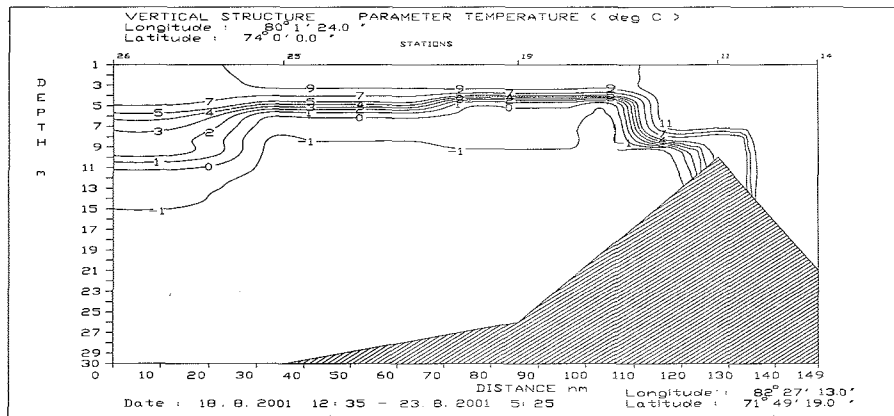


Fig. 3.8. Vertical distribution of the water temperature and salinity at the section along the Yenisei Gulf

In the Ob Gulf in the beginning of September the boundary between fresh and saline water at the bottom was located in the region between the stations 80 and 72 (Fig. 3.9). This is in the good agreement with the mean multiyear salinity distribution which shows the fresh water boundary at the bottom to be located between the latitudes  $71^{\circ} 30'$  and  $72^{\circ} 00'$  N in August and beginning of September. Also the values of salinity at the bottom were higher than the multiyear mean values. In the surface layer the fresh water boundary was located between the stations 70 and 82, with an inflow of saline water along the western coast (st. 71). The water temperature in the Ob Gulf was higher than the multiyear mean.

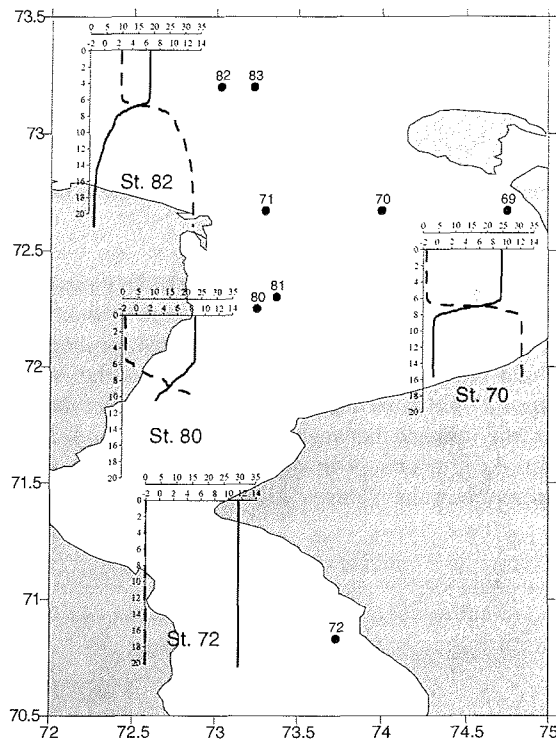


Fig. 3.9. Vertical distribution of the water temperature and salinity in summer 2001 in the Ob Gulf.

This paper contains only some preliminary results of the analysis of data obtained during the summer 2001 cruise of RV "Boris Petrov" in the Kara Sea.

### 3.2 Short-period internal waves in the Kara Sea

*V. Stanovoy<sup>1</sup> and B. Shmelkov<sup>2</sup>*

<sup>1</sup> SSC RF Arctic and Antarctic Research Institute (AARI), St.Petersburg, Russia

<sup>2</sup> Vernadsky Institute of Geochemistry and Analytical Chemistry, RAS, Moscow, Russia

#### Introduction

The internal waves are one of the main reasons of the processes of water entrainment and pycnocline erosion in the fresh waters spreading zone in the Kara Sea. Instability and destruction of the internal waves on the shelf and in the coastal zone results in more intensive mixing of water masses and amplification of the turbulent diffusion of the heat and salts. Until present time there are only a few measurements of the short-period waves in the Kara Sea. Within the framework of Russian-Swedish expedition "Tundra-94" in the southwest part of the Kara Sea the measurements of water temperature oscillations in the pycnocline during about 1 hour with the discretization 4 sec were executed. The analysis of these measurements has shown the presence of the internal waves with periods 10-12 and 2-3 minutes (Zakharchuk and Presnyakova 1997). Within the framework of the joint Russian-German expedition 1997 onboard of the RV "Academik Boris Petrov" the measurements of temporary variability of water temperature and salinity were executed from anchored vessel not far from the Dikson Island. The recording of hydrological parameters was carried out with the discretization 1 sec during almost 4 hours. The analysis of these measurements has shown internal waves with well-expressed periods 9.5, 5.3 and 2-3.5 minutes. It was noted the packet character of the short-period waves (Gribanov et al. 1999).

#### Data

Within the framework of the joint Russian-German expedition 2001 onboard of the RV "Academik Boris Petrov" the measurements of temporal variability of water temperature and salinity using CTD-sonde "Neil Brown-MKIII" were executed. After water sampling the additional profiling was carried out and the horizon for device deploying was selected. At 22 stations the CTD-sonde was deployed for long term measurements from the anchored vessel directly within the pycnocline layer or within the layer with some peculiarity of the vertical thermohaline structure. Also to exclude the influence of the vessel body the depth of observation was chosen more than 4.5 m.

The mean duration of these records is about 1 hour (Tab. 3.1). The numbers of CTD-stations in the table are from this expedition and their locations are presented in this volume (Fig. 3.10, Chapter 3.1). Unfortunately the simultaneous measurements of currents are absent.

Table 3.1. The long-term measurements of the water temperature and salinity

№ station	Horizon, m	Duration, min	Length of averaging row	Note
3	6.0	71	230	Pycnocline
11	7.5	65	391	Pycnocline
23	4.5	31	95	Pycnocline, long-periodic trend
26	7.8	78	156	Pycnocline, long-periodic trend
28	14.9	69	138	Peculiarity, long-periodic trend
31	15.1	60	121	Pycnocline
35	19.7	67	202	Peculiarity
38	14.5	81	243	Pycnocline, long-periodic trend
43	11.0	69	207	Peculiarity
45	18.0	59	178	Pycnocline, long-periodic trend
46	19.0	69	209	Pycnocline
48	22.7	72	217	Peculiarity
52	14.3	63	190	Peculiarity, long-periodic trend
56	19.0	35	107	Peculiarity, long-periodic trend
59	31.2	52	158	Peculiarity
62	23.7	81	243	Peculiarity, long-periodic trend
65	10.3	69	207	Peculiarity
67	14.6	63	189	Peculiarity
68	11.6	63	191	Peculiarity
70	8.5	128	768	Pycnocline, long-periodic trend
80	6.1	61	185	Pycnocline, long-periodic trend
82	8.0	60	181	Peculiarity

The depth of sensors varied because the sound was put down from the vessel board. We assumed that the oscillations of values of water temperature and salinity are a linear superposition of oscillations caused by vertical displacements of sensors and by internal waves. Using data of registration of the immersion depth of the sensors and data of sounding on CTD-station executed before record, the oscillations caused by vertical displacements of sensors were filtered. The minimum values of internal waves periods should be more than maximum value of the Brunt-Väisälä period therefore source rows were smoothed by the running averaging. All oscillations with period less than Brunt-Väisälä period are referred to turbulent pulsing.

### Results and discussion

The analysis of the long term records of water temperature and salinity have shown the existence of well pronounced short-period internal waves at the all CTD-stations. The salinity variations are about 0.3-0.5 psu per 10 min (in estuaries – up to 6-8 psu) and temperature variations reach values up to 0.5-1.0 °C per 10 min. The main periods of these waves are about 8-12, 5-6 and 2-3 minutes and amplitudes are from 0.5 to 3 m. In Table 3.2 the estimations of the wave amplitudes and main periods are presented. These values are presented for temperature and salinity separately. The spatial distributions of these parameters are presented on Figure 3.10.

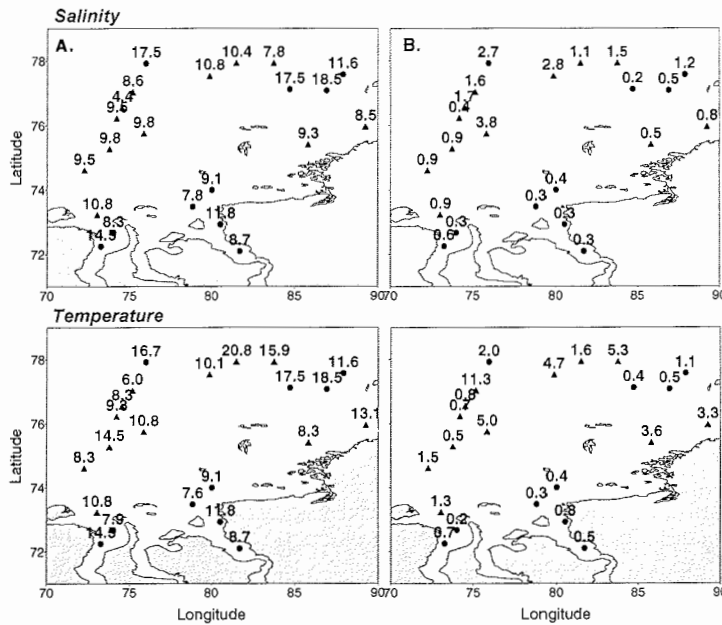


Fig. 3.10. The spatial distribution of the amplitudes (A) and periods (B) of internal waves for water temperature and salinity records.

- - measurements at the pycnocline layer;
- ▲ - measurements at the layer with some peculiarities.

It is necessary to note that the values of wave amplitudes and periods for temperature and salinity are the same (or closely) at the stations where measurements were executed at the pycnocline layer (Fig. 3.11). But these values are different at the stations where measurements were executed at the layer with some peculiarities (Fig. 3.12).

About the one half of the records has the well-expressed long-period trend (Tab. 3.1). The analysis of measurements on the daily and multidaily CTD-stations in the Kara Sea (the measurements were produced with a discretization 1 hour and more) has shown the presence of internal waves with tidal and subtidal (3-8 hours) periods (Gribanov et al. 1997; Pavlov et al. 1996). Thus the short-period waves exist on the background of the more long-period waves (Fig. 3.13).

Table 3.2: The estimations of the internal wave parameters.

№ station	Horizon, m	Salinity		Temperature	
		Wave amplitude	Wave period	Wave amplitude	Wave period
3	6	0.3	11.8; 5.1	0.8	11.8; 4.9
11	7.5	0.3	8.7; 5.0; 2.8	0.5	8.7; 2.4
23	4.5	0.3	7.8; 4.2; 2.0	0.3	7.6; 4.2; 2.0
26	7.8	0.4	11.9; 9.1; 5.5	0.4	11.9; 9.1; 5.5
28	14.9	0.8	13.1; 8.5; 5.2	3.3	13.1; 6.6; 3.8
31	15.1	1.2	11.6; 7.9; 6.0	1.1	11.6; 7.8; 6.0
35	19.7	1.5	18.5; 7.8; 3.9	5.3	15.9; 10.1; 7.4; 5.8; 4.3; 3.5
38	14.5	0.5	18.5; 6.9; 4.8	0.5	18.5; 6.9; 4.8
43	11	0.5	15.9; 9.3; 5.8; 3.7; 3.2	3.6	8.3; 5.7; 4.6; 3.2
45	18	0.2	17.5; 10.8; 4.9	0.4	17.5; 10.4; 4.9
46	19	2.7	17.5; 10.1; 5.0	2.0	16.7; 10.1; 5.0
48	22.7	1.1	10.4; 5.8; 3.4; 2.8	1.6	20.8; 10.1; 6.3; 4.2
52	14.3	2.8	10.8; 5.0; 2.9	4.7	10.1; 5.5; 3.9
56	19	1.6	8.6; 5.8; 2.3	11.3	7.8; 6.0; 3.5; 2.3
59	31.2	1.7	6.5; 5.4; 4.4; 2.1	0.8	8.3; 4.3; 3.3; 2.4
62	23.7	0.4	13.9; 9.5; 6.4; 5.2	0.7	9.3; 5.5; 4.3; 3.7
65	10.3	3.8	9.8; 7.1; 4.4; 3.7; 2.8	5	10.8; 6.9; 5.5; 3.4; 2.8; 2.4
67	14.6	0.9	9.8; 6.0; 3.6; 1.8	0.5	14.5; 6.9; 3.6; 1.8
68	11.6	0.9	9.5; 6.7; 3.5	1.5	8.3; 6.4; 3.5
70	8.5	0.3	13.9; 8.3; 4.5; 3.4	0.2	12.8; 7.9; 4.5; 3.4
80	6.1	0.6	14.5; 7.2; 4.2; 3.4	0.7	14.5; 7.1; 4.2; 3.4
82	8.0	0.9	10.8; 3.7; 2.8; 2.4; 2.0	1.3	10.8; 3.7; 2.8; 2.4; 2.0

At the some stations it was marked the nonlinearly temperature and salinity oscillations from the cnoidal waves caused by the bottom influence (Fig. 3.14) and up to soliton-like waves caused by the peculiarities of the vertical thermohaline structure (Fig. 3.15).

The strip-selected filtering has shown that the short-period oscillations of the water temperature and salinity with periods 2-5 minutes have the packet character and the periods of these packets are from 30 minutes up to 1 hour.

The analysis results give some possibility to conclude that in the Kara Sea the probability of the Kelvin – Helmholtz instability occurring is very high for internal waves with periods 2-5 minutes. The dynamic instability and destruction of short-period internal waves results in the turbulence and formation of the fine thermohaline structure.

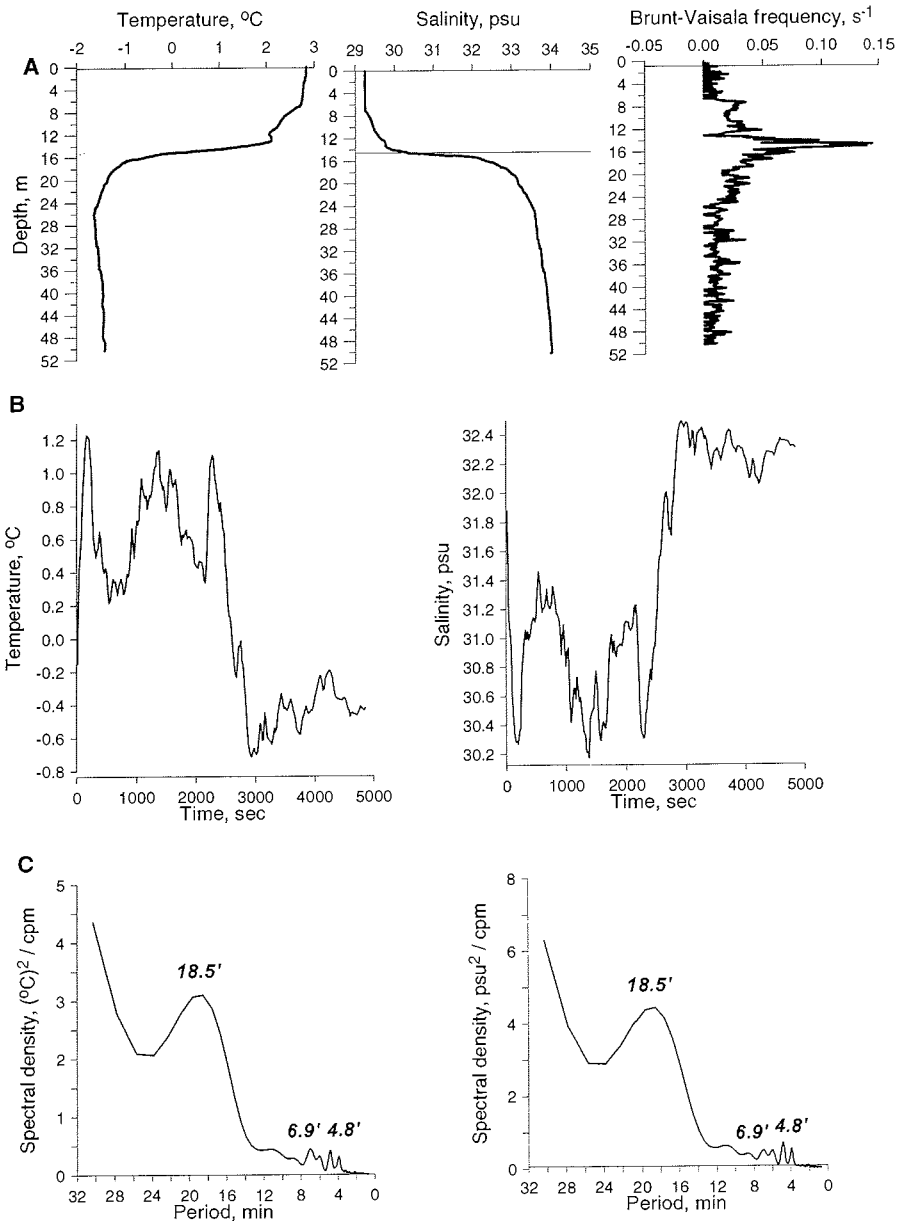


Fig. 3.11. Vertical distribution of the water temperature, salinity and Brunt-Vaisala frequency (A), oscillations of the temperature and salinity at the horizon 14.5 m (B) and spectra of these oscillations (C). Station No 38.

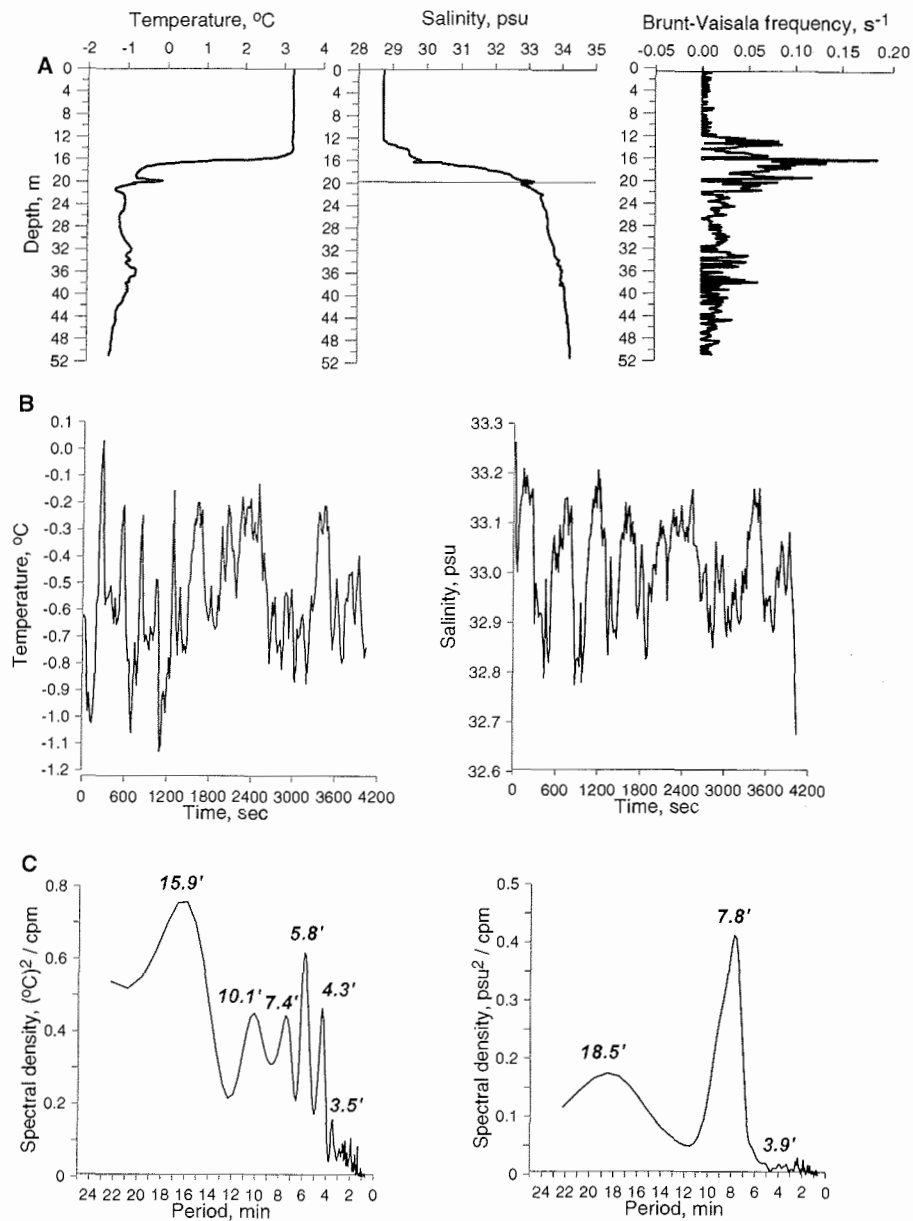


Fig. 3.12. Vertical distribution of the water temperature, salinity and Brunt-Vaisala frequency (A), oscillations of the temperature and salinity at the horizon 19.7 m (B) and spectra of these oscillations (C). Station No 35.



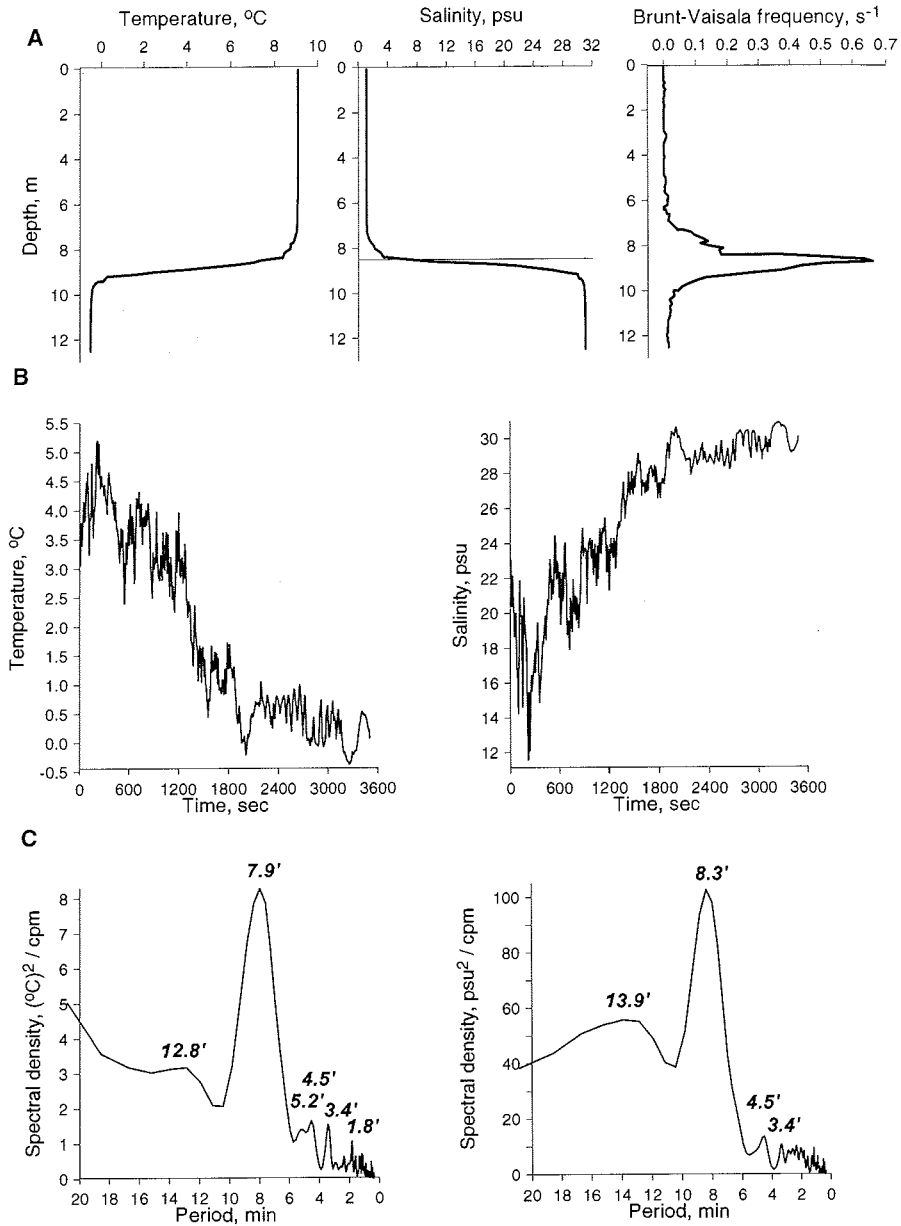


Fig. 3.13. Vertical distribution of the water temperature, salinity and Brunt-Vaisala frequency (A), oscillations of the temperature and salinity at the horizon 8.5 m (B) and spectra of these oscillations (C). Station No 70.

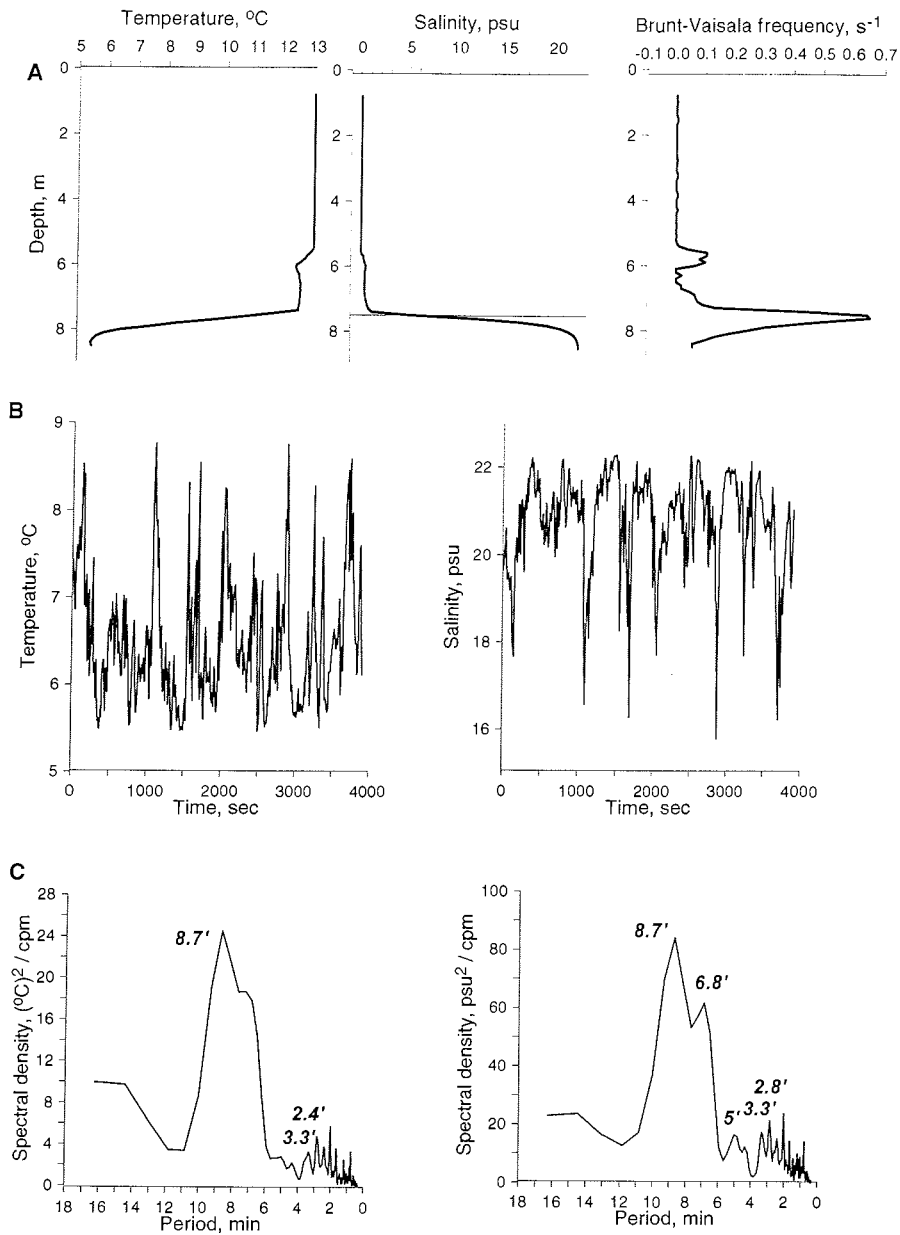


Fig. 3.14. Vertical distribution of the water temperature, salinity and Brunt-Vaisala frequency (A), oscillations of the temperature and salinity at the horizon 7.5 m (B) and spectra of these oscillations (C). Station No 11.

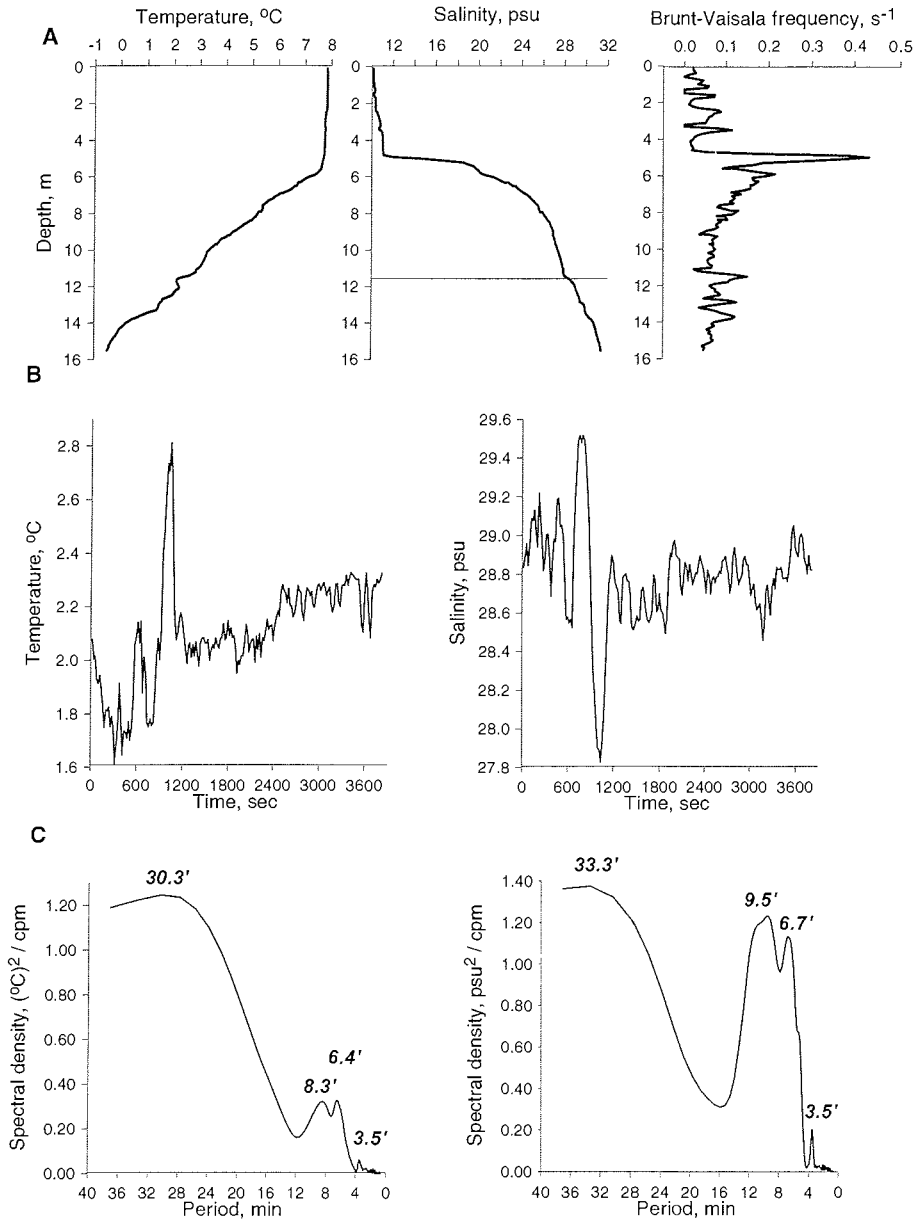


Fig. 3.15. Vertical distribution of the water temperature, salinity and Brunt-Vaisala frequency (A), oscillations of the temperature and salinity at the horizon 11.6 m (B) and spectra of these oscillations (C). Station No 68.

### 3.3 Water temperature fluctuations in the marginal zones of the Svjataya Anna and Voronin Troughs.

*V. Stanovoy<sup>1</sup> and B. Shmelkov<sup>2</sup>*

<sup>1</sup> SSC RF Arctic and Antarctic Research Institute (AARI), St.Petersburg, Russia

<sup>2</sup> Vernadsky Institute of Geochemistry and Analytical Chemistry, RAS, Moscow, Russia

#### Introduction

Within the framework of the joint Russian-German expedition 2001 onboard of the RV “Academik Boris Petrov” the measurements of water temperature and salinity using CTD-sonde “Neil Brown-MKIII” were executed. In the northern and northwestern parts of the investigated area of the Kara Sea the significant water temperature fluctuations and inversion layers within the upper layer were observed (Fig. 3.16).

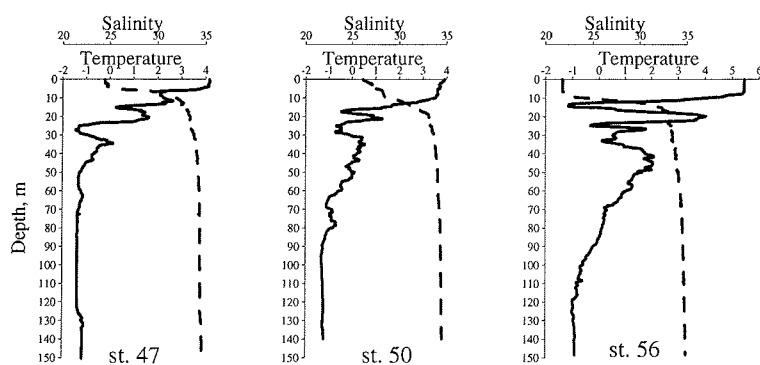


Fig. 3.16. Vertical distribution of the water temperature and salinity

Review of the historical data has shown that the similar thermohaline structure (more or less strong) was observed in this region in previous years. Thus the such phenomenon is not the feature of the summer 2001 but it is a feature of the investigated area represented the marginal zones (peripheries) of the Svjataya Anna and Voronin Troughs with depths about 100-150 m. In the present paper we will try to give some explanation of this phenomenon based on the observations of the cruise in summer 2001.

#### Discussion

The first possible reason of this phenomenon (and the easiest to explanation) is the spreading of some water masses into the Kara Sea from the Arctic Basin through the Svjataya Anna and Voronin Troughs or through the strait between the Novaya Zemlya and Franz-Iosif Land. Yes, indeed, we observed the layer of Arctic Basin Surface Water at the northern and northeastern CTD-stations below the pycnocline at 25-35 m water depth. The temperature of this water is about 0.2-0.5 °C less than temperature of the underlying Deep Kara Sea Water. And usually, it is marked the influence of the warm Atlantic Water and Barents Sea Water in this region (but not in the upper water layer). Anyway, this influence must be more or less permanent in the time and space.

During the water sampling at the stations several casts were executed usually. The time intervals between the casts were about 1-2 hours. In Figure 3.17 the temperature vertical distributions at the CTD-stations are presented. It is easy to see the strong temporal variability of the temperature.

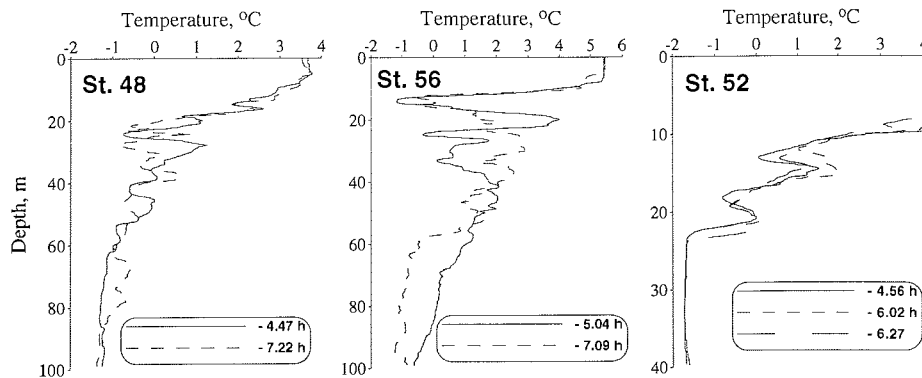


Fig. 3.17. Temporal variability of the temperature vertical distribution.

In Figure 3.18 the vertical distribution of the temperature in the upper water layer at the short section (stations 48, 49, 50) is presented. The spatial intervals between these stations are 1-2 navy miles. Also it is easy to see the strong spatial variability of the water temperature. Thus the temperature fluctuations not caused by the influence of some water masses but only by the influence of some dynamic processes.

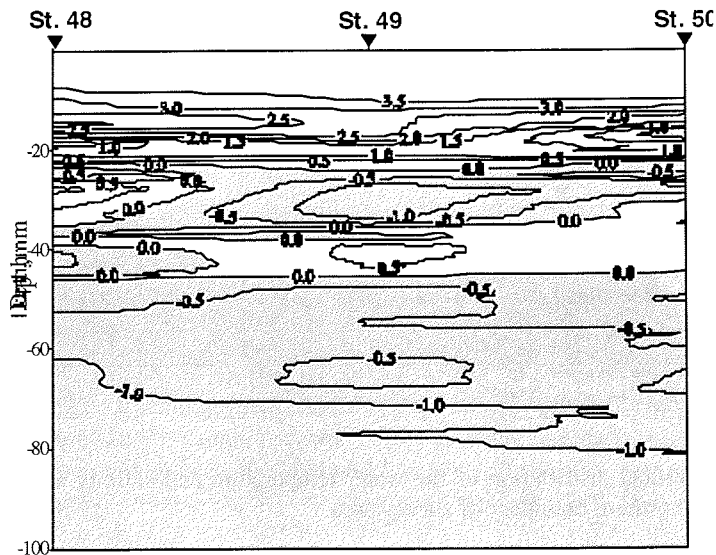


Fig. 3.18. Vertical distribution of the water temperature at the section.

For consideration we have following positions: 1). The temperature fluctuations take place in the zone of bottom rising (at the depths 100-150 m). At the deepest stations of survey area (st. 46 and 34) some temperature fluctuations are absent. 2). During the

summer cruise 2001 the section along the northern boundary of the investigated area was executed (Fig. 3.19). In contrary to the salinity the temperature distribution is quite strange. There are alternating cores of the more cold and more warm water. At the all sections in the investigated area there is similar picture (for example, Fig. 3.18). 3). The layer of cold Arctic Basin Water is an initial reason of temperature uniform structure. 4). At the all stations with temperature fluctuations we have the strong seasonal pycnocline and all fluctuations take place under it or/and in the lower part of pycnocline at the depths 10-60 m.

So we propose the following explanation of the observed phenomenon. The specific topography in the marginal zones of the troughs promotes the strong amplification of the internal waves. The strong pycnocline limits the growth of the wave amplitude and contributes to wave breaking. The existence of unstable layers (Fig. 3.20) confirms it.

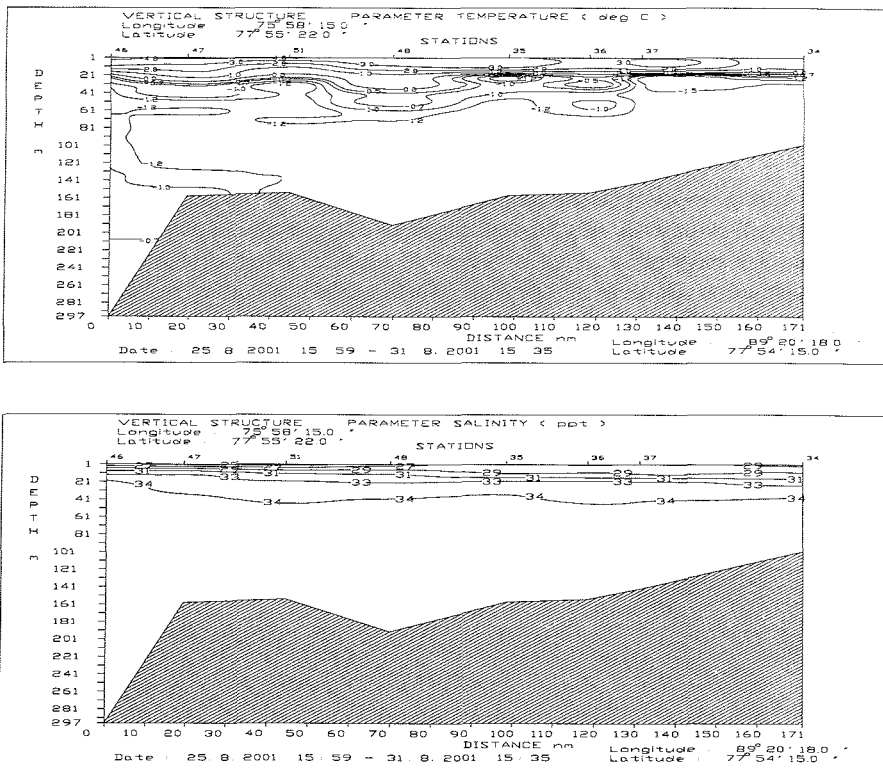


Fig. 3.19. The vertical distribution of the water temperature and salinity at the section along the northern boundary of survey area.

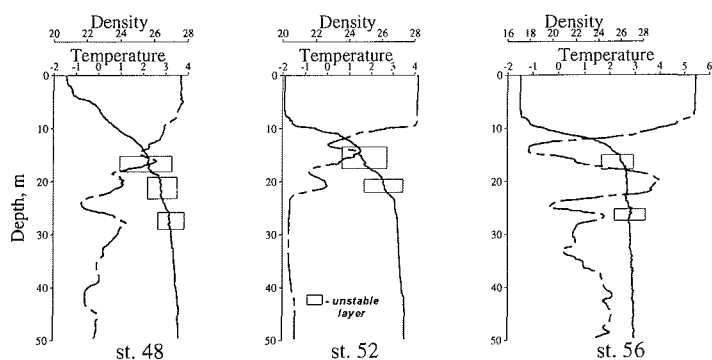


Fig. 3.20. The vertical distribution of the temperature and density

At the several stations with the investigated phenomenon the CTD-sonde was deployed within the layers with the temperature peculiarities during of about 1 hour. Unfortunately, the measurements were executed only at the one horizon. The analysis of these measurements has shown the very significant temperature oscillations and the difference between the main periods of the temperature and salinity oscillations (Fig. 3.21-3.23). It is necessary to mark that short-period waves are observed on the background of the more long-period (0.5-1 hour) waves. Also it is very possible that at the station 56 (Fig. 3.21) we observed the breaking of the internal waves at the measurement horizon.

### Conclusion

The topographic amplification of the internal waves is a main reason of the significant water temperature fluctuations and inversion layers within the upper layer in the marginal zones (peripheries) of the Svjataya Anna and Voronin Troughs.

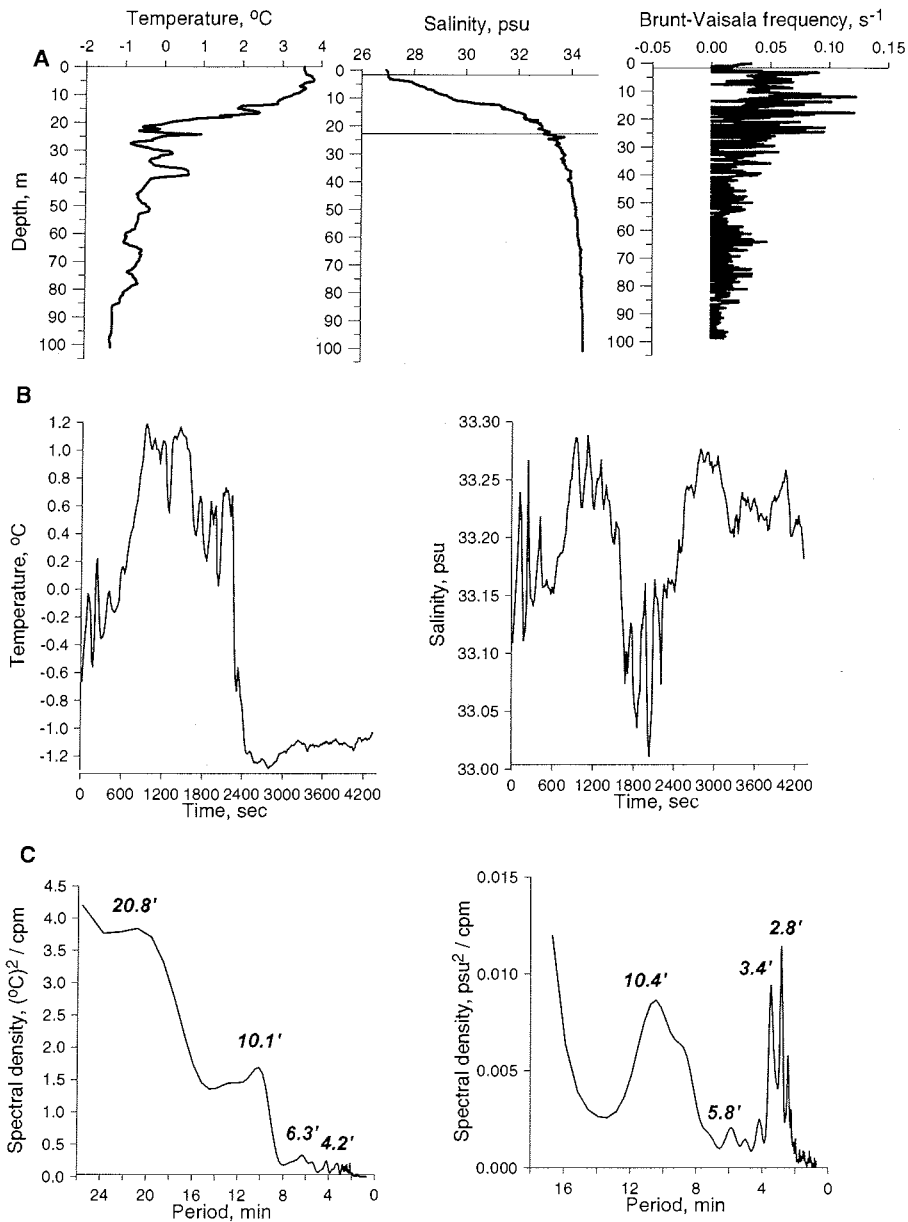


Fig. 3.21. Vertical distribution of the water temperature, salinity and Brunt-Vaisala frequency (A), oscillations of the temperature and salinity at the horizon 22.7 m (B) and spectra of these oscillations (C). Station No 48



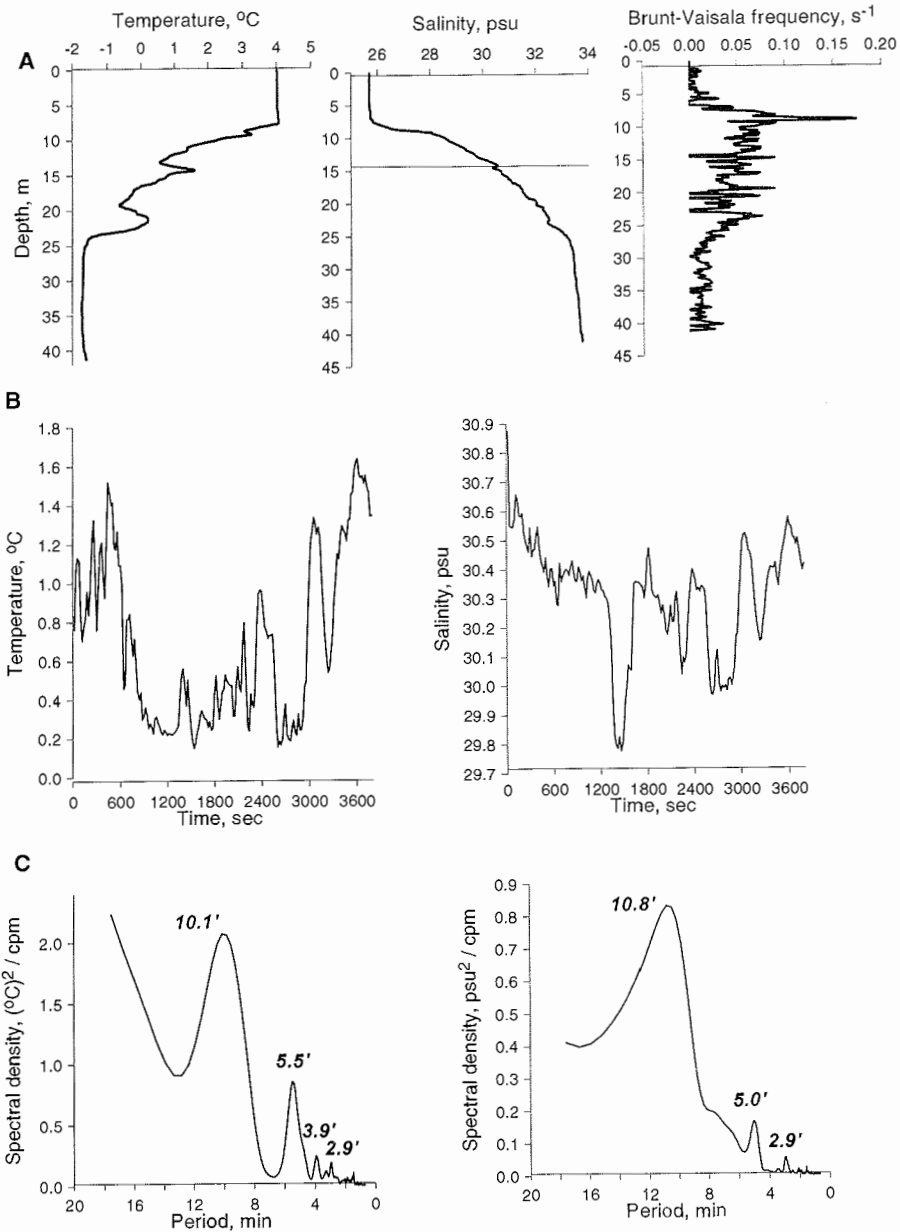


Fig. 3.22. Vertical distribution of the water temperature, salinity and Brunt-Vaisala frequency (A), oscillations of the temperature and salinity at the horizon 14.3 m (B) and spectra of these oscillations (C). Station No 52.

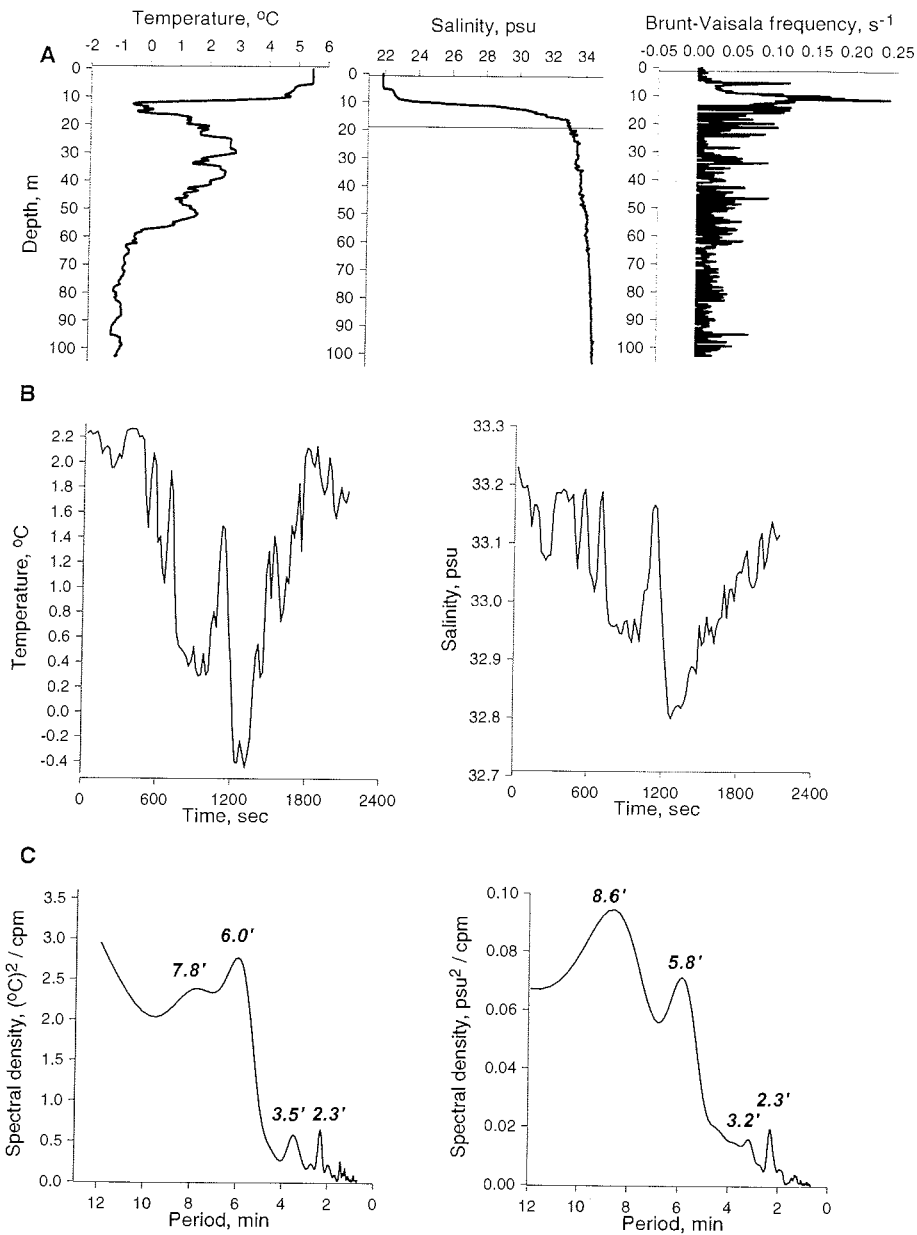


Fig. 3.23. Vertical distribution of the water temperature, salinity and Brunt-Vaisala frequency (A), oscillations of the temperature and salinity at the horizon 19 m (B) and spectra of these oscillations (C). Station No 56.

### 3.4 Temperature at the sediment surface – mini heat probe versus CTD

J. Simstich, B. Shmelkov, V. Stanovoy

#### Abstract

The water temperature directly at the sediment surface was measured with a mini heat probe. The obtained data were compared to the water temperature in the deepest depth levels, reached by CTD measurements, which usually is some meters above ground. The data show that the temperature between the two investigated depth levels differs no more than 0.01 K, which is negligible for geological questions like the oxygen isotope ratios in calcareous shells of benthic living organisms. However, in very shallow water (<20 m), where the pycnocline is close to the bottom, the measured temperatures may differ considerably.

#### Purpose

A well-established tool for the reconstruction of past marine environments is the ratio between the oxygen isotopes  $^{18}\text{O}$  and  $^{16}\text{O}$  ( $\delta^{18}\text{O}$ ) in calcareous shells of benthic living animals like foraminifera, ostracods, or mussels (Emiliani 1955). One factor determining this ratio is the water temperature during the precipitation of the carbonate shells, because the calcifying organisms fractionate with a temperature-dependent factor (Urey et al. 1951). Therefore the actual bottom water temperature directly on the sediment surface, which is the habitat for most of the animals, is of special interest. Before the expedition no information was available on the actual bottom water temperature in the Kara Sea, because for safety reasons the CTD (conductivity-temperature-depth) measuring devices normally stop some meters above the sea floor. In this work we present results of measurements of the bottom water temperature and compare them with the water temperature in the deepest reached CTD level.

#### The mini heat probe

To measure the temperature at the sediment surface we used a mini heat probe, which originally was constructed for in-sediment temperature measurements by Norbert Kaul and Bernd Heesemann of the Department for Earth Sciences, University of Bremen. The mini heat probe delivers one value every 2 seconds via 7 channels. These channels are connected to 7 temperature sensors, which are fixed equally spaced within a 50 cm long, sediment penetrating steel spine, thus enabling to measure the temperature in 7 different sediment depths (Fig. 3.24). A metal plate prohibits the complete penetration of the probe and keeps the uppermost sensor (channel 7) out of the mud and approx. 0.5 to 1 centimeter above the sea floor (Fig. 3.24). An additional sensor, connected to channel 8, measures the angle of the probe all the time during the measuring and shows, whether the probe is staying upright or has fallen down. The data can be achieved “real time” via a data cable from water depths of max. 50 m. In deeper water an offline operation mode with data storage in an internal memory is possible. The construction allows the deployment by hand, even from ice flows.

The water depth at most stations of the expedition “Kara Sea 2001” on board of RV “AKADEMIK BORIS PETROV” required the deployment of the mini heat probe in the offline mode over a winch. This was done several times, until, after a small accident, the plugs on top of the heat probe were damaged and caused failures of the internal data storage due to short interruptions of the power supply.

For the initial calibration of the sensors the mini heat probe and the ship’s CTD device were deployed for 15 minutes in the same water depth, simultaneously. The obtained values were compared (Fig. 3.25), and correction factors were calculated as differences between the temperature data from the mini heat probe and the CTD device for each channel separately. These calculated correction factors were applied to the regular measurements. During the actual measuring the heat sensors had approx. 5 min for adaption after penetration into the sediment. The values of the following 2-6 min. were averaged and are given in table 1 as the bottom water temperature.

Table 3.3: Results of the temperature measurements at the bottom ( $T_{\text{bot}}$ ) and the deepest CTD level ( $T_{\text{CTD}}$ ).

Station	Water depth (m)	Depth of $T_{\text{CTD}}$ (m)	$T_{\text{bot}}$ (°C)	$T_{\text{CTD}}$ (°C)	$T_{\text{CTD-bot}}$ (K)
BP01-26	33	30.6	-1.28	-1.28	0.00
BP01-28	51	50.6	-1.12	-1.12	0.00
BP01-30	47	No vertical penetration			
BP01-34	92	90.7	-1.41	-1.41	-0.01
BP01-35	160	150.1	-1.38	-1.39	-0.01
BP01-40	46	43.6	-1.35	-1.34	0.01
BP01-41	38	35.0	-1.14	-1.14	0.00
BP01-45	77	No vertical penetration			
BP01-46	295	No vertical penetration			

## Results and discussion

For unknown reasons the mini heat probe did not stay vertically during the measurements at three stations (Tab. 3.3). The values on channel 8, which measures the angle of the device, show that the probe was fallen down. Most probably the spine with the sensors did not penetrate vertically or even did not penetrate at all into the sediment. In these cases the temperature data in the internal memory were rejected, because it is not clear from which water depth above the sediment surface the measured temperature values actually are.

The results of the successful bottom temperature ( $T_{\text{bot}}$ ) measurements and the temperature in the deepest reached CTD levels ( $T_{\text{CTD}}$ ) can be seen in table 3.3. At all stations the difference between bottom and CTD temperature is very small and does not exceed 0.01 K (Tab. 3.3). The bottom temperature is a continuation of the vertical temperature trend in the water column. This means that the temperature at the bottom is colder/warmer than at the deepest CTD level, when the temperature in the deeper water column becomes likewise colder/warmer with depth.

The temperature difference between  $T_{\text{bot}}$  and  $T_{\text{CTD}}$  is too small to affect the oxygen isotopic composition ( $\delta^{18}\text{O}$ ) in calcitic shells of foraminifera by more than 0.003‰ (O’Neil et al. 1969; Shackleton 1974), or 0.002‰ in aragonitic shells of mussels

(Grossman and Ku 1986). These values are far below the measuring accuracy, which is 0.08‰  $\delta^{18}\text{O}$  (Erlenkeuser et al. 1999). As the main result we conclude that for studies of  $\delta^{18}\text{O}$  of benthic organisms in the Kara Sea the temperature at the sediment surface can be approximated by the temperature in the deepest reached CTD level, without making a significant error.

However, this approximation is not applicable in areas where a temperature gradient in the deep water causes a significant temperature difference between the deepest CTD level and the sea floor. Such situations probably exist in the shallow and estuarine areas of the Kara Sea where the pycnocline is situated close to the ground. For example, in areas where the water depth is below 20 m the salinity at the sediment surface deviates considerably from the salinity in the deepest CTD level (Simstich 2001). This might also be the case for temperature, because in the southern Kara Sea the depth of the thermocline is closely connected to the depth of the halocline, as can be seen in the CTD profiles (Shmelkov et al., this volume).

### **Conclusions**

From the comparison of the water temperature directly above the sediment surface with the temperature in the deepest reached CTD level we conclude that the temperature difference between these two depth levels is too small to significantly affect oxygen isotope ratios in calcareous shells of benthic organisms. Presumably, this does not apply to shallow areas where the pycnocline is situated close to the ground.

### **Acknowledgements**

We thank the crew of RV "AKADEMIK BORIS PETROV", especially Viktor Chorshev, Alexander Latko, and Vladimir Markovskiy for helping in many ways during the cruise. We are obliged to Norbert Kaul and Bernd Heesemann, University of Bremen, for carefully training the first author in the handling of the mini heat probe.

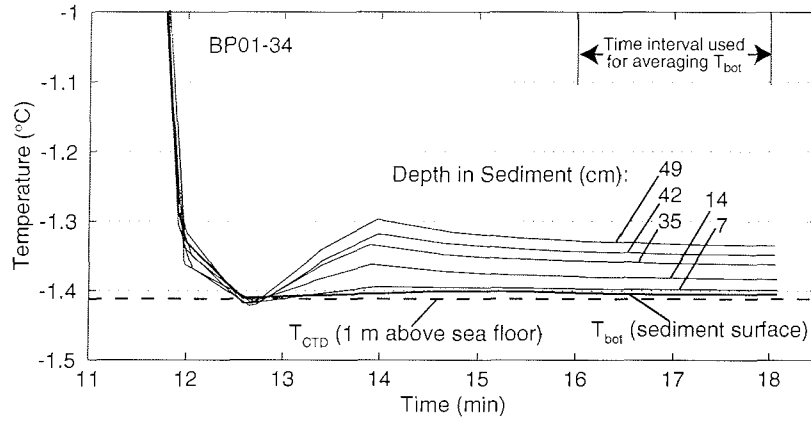


Fig. 3.24: Temperature in different depths at station BP01-34. The correction factors (see text and Fig. 3.25) are applied.

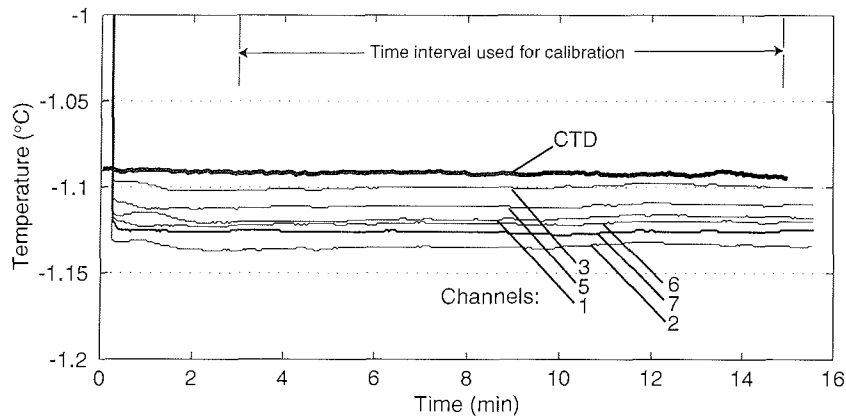


Fig. 3.25: Calibration data.

#### 4. Sediment Trap Investigations in the Kara Sea

A. C. Gebhardt<sup>1</sup>, N. Lahajnar<sup>1</sup>, B. Gaye-Haake<sup>1</sup>, I. Fetzner<sup>2</sup> & Hendrik Deubel<sup>2</sup>

<sup>1</sup>Institute for Biogeochemistry and Marine Chemistry, University of Hamburg

<sup>2</sup>Alfred Wegener Institut, Bremerhaven

##### Introduction

When studying the global biogeochemical cycle of elements such as carbon, silica, nitrogen and phosphorus, the transfer of particulate matter from the surface layer through the water column to the sediment-water interface as well as its incorporation into the sediment play a major role. Sediment traps provide a reliable means to sample sinking particulate matter and to calculate flux rates. Sediment trap investigations carried out in numerous regions of the world ocean have contributed to the better understanding of processes and factors controlling the formation, amount and composition of sinking particles (e.g. Honjo 1996; Ittekkot 1996). This information is essential for interpretation of the sedimentary record. Unfortunately, flux measurements from the high latitudes are scarce especially over longer periods because of logistical problems due to the ice coverage. The observed range of flux rates varies from only a few  $\text{mg m}^{-2} \text{d}^{-1}$  in permanently ice-covered regions (Hargrave et al. 1993) to values  $>300 \text{ mg m}^{-2} \text{d}^{-1}$  under the influence of ice-rafted material near the ice edge (Hebbeln and Wefer 1991).

The sediment trap recovered during the “Akademik Boris Petrov” is the first longtime sinking particle record from the Kara Sea and therefore provides essential information about the processes and fluxes in this area. Two new systems were deployed in order to prolong this record; one at the previous position near the Yenisey estuary and the other in the open Kara Sea (Fig. 4.1).

##### Methods

###### Recovery of Sediment Trap YEN02

During the “Akademik Boris Petrov” Cruise 2000 into the Kara Sea a cylindrical sediment trap mooring was deployed in the Yenisey river mouth (see Fig. 4.1) in order to record an annual cycle of the vertical particle flux and its seasonality. For sediment trap parameters refer to (Unger et al. 2001).

The sediment trap mooring was easily retrieved at the BP00-24a site. While all bottles could be recovered, the sediment trap itself was in a desolate status: the funnel was lost, probably during the recovery procedure. Nevertheless, the trap had turned to bottle 24 which was not closed as it was recovered during the last sampling interval. Data from the sediment trap timer board could be read after changing the batteries which were exhausted at time of recovery. Fortunately, the batteries had not been exhausted until the last turning process, meaning the system had turned correctly throughout the investigated time span (Tab. 4.1).

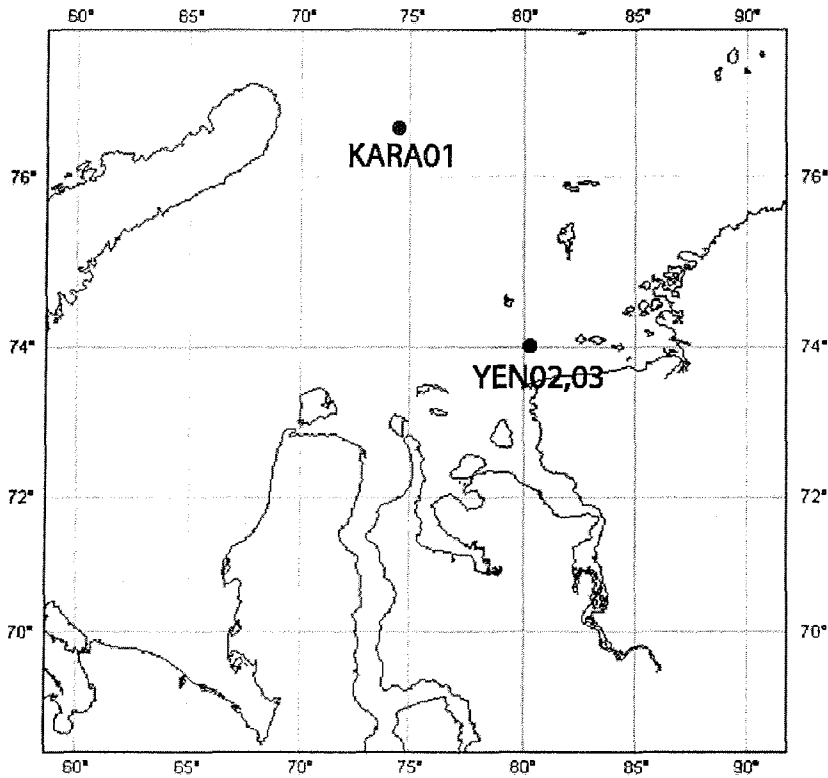


Fig. 4.1: Positions of sediment traps YEN02, YEN03 and KARA01

#### Deployment of Sediment Trap YEN03

In order to extend the particle flux measurements over a longer period and to get a better insight into the flux in the Yenisey river mouth, the sediment trap mooring was deployed for another year (YEN03). This time, the mooring was equipped with a current meter allowing to determine current direction and velocity as well as temperature of the water masses delivering the trap with particulate matter.

Sediment trap YEN02 which was recovered in desolate status was repaired onboard and equipped with a new funnel made primarily of a gravity core liner (diameter 120 mm) and a laboratory funnel. The new funnel system was covered by a mesh to avoid fish and other animals to swim actively into the funnel. Additionally, in order to stabilize the funnel, the trap was furnished with extra holding rods by the ship's mechanics.

To get a reasonable record resolution, the 24 sediment trap bottles were programmed to rotate weekly in arctic summer and river runoff maximum, respectively, whereas the sampling intervals were prolonged to 14 days in spring and autumn and to 28 days in



To get a reasonable record resolution, the 24 sediment trap bottles were programmed to rotate weekly in arctic summer and river runoff maximum, respectively, whereas the sampling intervals were prolonged to 14 days in spring and autumn and to 28 days in winter (Tab. 4.2). All bottles were filled with sea water (surface water from station BP01-01) poisoned with 3,3 g HgCl<sub>2</sub> and 35 g NaCl per liter to avoid bacterial activity.

The sediment trap mooring was deployed on August, 23, 10:06 UTC at station BP01-27 (74°00,07'N, 80°19,87'E), water depth 36 m. The trap was deployed on open hole; the first sampling interval was started on August, 24, 00:00 UTC in order to avoid sampling particles whirled up by the deployment procedure. The sediment trap itself was stationed 25 m below sea surface and 11 m above sea bottom, respectively. For detailed deployment information refer to Table 4.3.

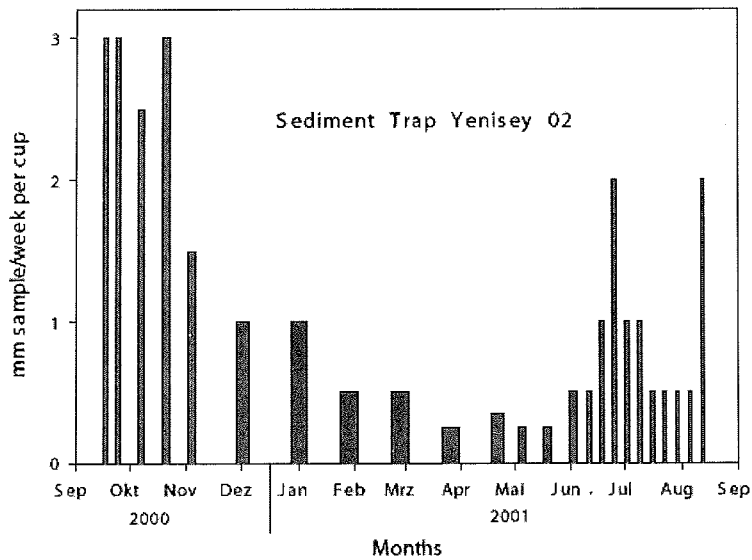


Fig. 4.2: Bulk collected material of YEN02 (in mm sample/week per bottle)

#### Deployment of Sediment Trap KARA01

During the "Akademik Boris Petrov" cruise in 2001 a second sediment trap mooring (KARA01) was deployed in the northwestern part of the investigated area (Fig. 4.1) in order to record the vertical particle flux in the distal part of the Ob and Yenisey estuaries as well as in the open Kara Sea. The position of the sediment trap was chosen primarily in order to get an open Kara Sea signal, i.e. at a site which is north enough not to be directly influenced by Ob and Yenisey. Nevertheless, the trap position could not be chosen farther north than 76°N because of often occurring pack and sea ice in that region.

be chosen farther north than 76°N because of often occurring pack and sea ice in that region.

Contrary to the YEN03 mooring, KARA01 consists of 12 bottles. The 12 bottle configuration was chosen as in this distal part a rather low vertical particle flux is expected. For better comparison the rotation scheme was synchronized to the YEN03 scheme by simply doubling the sampling intervals (Tab. 4.2). Likewise to YEN03, KARA01 was equipped with a current meter. This current meter not only records current direction, current velocity and temperature of the water masses delivering the trap with the particle flux in question, but also its turbidity. Likewise to YEN03, all bottles were filled with sea water (filtered surface water from station BP01-58) poisoned with 3,3 g HgCl<sub>2</sub> and 35 g NaCl per liter to avoid bacterial activity. The sediment trap mooring was deployed on September, 03, 12:53 UTC at station BP01-61a (76°31,16'N, 74°30,95'E), water depth 73 m. The trap was deployed on open hole; the first sampling interval was started at September, 04, 00:00 UTC in order to avoid sampling particles whirled up by the deployment procedure. The sediment trap itself was stationed 53 m below sea surface and 20 m above sea bottom, respectively. For detailed deployment information refer to Table 4.3.

Tab. 4.1: Rotation/recovery scheme for sediment trap YEN02

Bottle	Start of Interval	Moscow Time	Duration of Interval	Recovery Status
Bottle 1	09/16/2000	0:00	7 days	done
Bottle 2	09/23/2000	0:00	7 days	done
Bottle 3	09/30/2000	0:00	14 days	done
Bottle 4	10/14/2000	0:00	14 days	done
Bottle 5	10/28/2000	0:00	14 days	done
Bottle 6	11/11/2000	0:00	28 days	done
Bottle 7	12/09/2000	0:00	28 days	done
Bottle 8	01/06/2001	0:00	28 days	done
Bottle 9	02/03/2001	0:00	28 days	done
Bottle 10	03/03/2001	0:00	28 days	done
Bottle 11	03/31/2001	0:00	28 days	done
Bottle 12	04/28/2001	0:00	14 days	done
Bottle 13	05/12/2001	0:00	14 days	done
Bottle 14	05/26/2001	0:00	14 days	done
Bottle 15	06/09/2001	0:00	7 days	done
Bottle 16	06/16/2001	0:00	7 days	done
Bottle 17	06/23/2001	0:00	7 days	done
Bottle 18	06/30/2001	0:00	7 days	done
Bottle 19	07/07/2001	0:00	7 days	done
Bottle 20	07/14/2001	0:00	7 days	done
Bottle 21	07/21/2001	0:00	7 days	done
Bottle 22	07/28/2001	0:00	7 days	done
Bottle 23	08/04/2001	0:00	7 days	done
Bottle 24	08/11/2001	0:00	7 days	active

## First Results

The amount of sinking particles (in mm sample per cup and week, Fig. 4.2) shows two distinct peaks, one in June/July and one in September/October. The first peak most

likely reflects the maximum river discharge, whereas the second peak reflects the Arctic summer and therefore a period with enhanced primary productivity. Furthermore, during the Arctic winter months (December to Mai), almost no sample was collected. As the Ob and the Yenisey are thoroughly frozen during this time span and the Kara Sea is ice covered, this material most likely must be resuspended matter.

Tab. 4.2: Rotation scheme for sediment traps YEN03 and KARA01

Trap YEN03				Trap KARA01			
Bottle	Start of Interval	Moscow Time	Duration of Interval	Bottle	Start of Interval	Moscow Time	Duration of Interval
Bottle 1	08/24/2001	0:00	7 days				
Bottle 2	08/31/2001	0:00	7 days	Bottle 1	09/04/2001	0:00	17 days
Bottle 3	09/07/2001	0:00	14 days				
Bottle 4	09/21/2001	0:00	14 days	Bottle 2	09/21/2001	0:00	42 days
Bottle 5	10/05/2001	0:00	28 days				
Bottle 6	11/02/2001	0:00	28 days	Bottle 3	11/02/2001	0:00	56 days
Bottle 7	11/30/2001	0:00	28 days				
Bottle 8	12/28/2001	0:00	28 days	Bottle 4	12/28/2001	0:00	56 days
Bottle 9	01/25/2002	0:00	28 days				
Bottle 10	02/22/2002	0:00	28 days	Bottle 5	02/22/2002	0:00	56 days
Bottle 11	03/22/2002	0:00	28 days				
Bottle 12	04/19/2002	0:00	28 days	Bottle 6	04/19/2002	0:00	42 days
Bottle 13	05/17/2002	0:00	14 days				
Bottle 14	05/31/2002	0:00	7 days	Bottle 7	05/31/2002	0:00	14 days
Bottle 15	06/07/2002	0:00	7 days				
Bottle 16	06/14/2002	0:00	7 days	Bottle 8	06/14/2002	0:00	14 days
Bottle 17	06/21/2002	0:00	7 days				
Bottle 18	06/28/2002	0:00	14 days	Bottle 9	06/28/2002	0:00	28 days
Bottle 19	07/12/2002	0:00	14 days				
Bottle 20	07/26/2002	0:00	7 days	Bottle 10	07/26/2002	0:00	14 days
Bottle 21	08/02/2002	0:00	7 days				
Bottle 22	08/09/2002	0:00	7 days	Bottle 11	08/09/2002	0:00	14 days
Bottle 23	08/16/2002	0:00	7 days				
Bottle 24	08/23/2002	0:00	7 days	Bottle 12	08/23/2002	0:00	7 days

Most of the material in the bottles contained, besides detritus, many fecal pellets of animal origin (Tab. 4.4). There was a clear size grouping showing many small pellets probably from microplankton and small copepods (e.g. *Microcalanus* sp., *Drepanopus bungei*, *Pseudocalanus* spp.), medium sized pellets of bigger copepod species (*Calanus* spp.) and large ones mostly originating from Appendicularia (bottles 4-7, 13, 19-24). Many gelatinous housings of the Appendicularia *Larvacea* spp. (bottles 6, 7, 11, 19, 22, 23) and some comb jellies (*Ctenophoras* spp.) (bottles 6, 8, 12) were also transported into the cups. Active swimmers as copepods and pteropods *Limacina* spp. (bottle 14) were also trapped.

Several bottles contained quite large amounts of copepods. Single individuals of *Pareuchaeta glacialis* and *Calanus glacialis/hyperboreus* were caught. Interestingly some bottles contained many small copepods of the genus *Pseudocalanus* (bottles 1-5).

Probably the environmental conditions in this time of the year were such that they were transported to the vicinity of the trap in great numbers.

The presence of organic matter, copepods and fecal pellets correlates in time. During high occurrence of organic matter, which originates most likely from dying phytoplankton or riverine imported material, there is also a high concentration of copepods feeding on this material (bottles 24, 1-7). This may as well explain the abundant fecal pellets afterwards (bottles 4-7).

### **Ongoing work**

The sediment trap samples will be split and the aliquots will be analyzed for opal, organic carbon and nitrogen, carbon and nitrogen isotopes, amino acids, biomarkers and pigments; plankton counts will be done.

### **Acknowledgements**

We would like to express our thanks to the Captain and crew of R/V “Akademik Boris Petrov” for their excellent work during the recovery and deployment of the sediment traps. We would also like to thank all colleagues on board “Akademik Boris Petrov” for their assistance during the cruise.

	YEN03	KARA01
<b>Date of Deployment:</b>	08/23/2001	09/03/2001
<b>Time of Deployment:</b>	10:06 UTC	12:53 UTC
<b>Position of Anchor Drop:</b>	74°00,07'N, 80°19,87'E	76°31,16'N, 74°30,95'E
<b>Water Depth:</b>	36 m	73 m
<b>Trap:</b>	Hydro-Bios Multi Sediment Trap MST24 Funnel: Height 570mm, Diameter 120mm	Hydro-Bios Multi Sediment Trap MST12 Funnel: Height 760 mm, Diameter 138 mm
<b>Acoustic Release:</b>	Benthos Release Model 865-A Receive Frequency: 10 kHz Transmit Frequency: 12 kHz Enable Code: 1B Release Code: 1D	Benthos Release Model 865A Receive Frequency: 10 kHz Transmit Frequency: 12 kHz Enable Code: 1C Release Code: 1A
<b>Current Meter:</b>	<b>Aanderaa RCM9 Current Meter</b>	<b>Aanderaa RCM9 MkII Current Meter</b>
<b>Topfloat:</b>	none	Novatech (Canada) Frequency: 156,475 MHz or Channel 69 Transmission rate: continuous (ON/OFF pressure dependent) Transmission distance: approx. 5-10 nm
<b>Cup Water:</b>	Surface Water from Station BP01-01 Addition of env. 3.3g HgCl <sub>2</sub> /lt and 35g NaCl/lt	Filtrated surface water from Station BP01-58 Addition of env. 3.3g HgCl <sub>2</sub> /lt and 35g NaCl/lt

Tab. 4.3: Deployment Protocol for YEN03/KARA01

Bottle	Interval	OM	CP	AM	FP	PC	AP	CT	MY	ME	CH	CU	PT	IA
1	09/06/2000-09/23/2000	xx	xx											
2	09/23/2000-09/30/2000	xx	xx											
3	09/30/2000-10/14/2000	xx	xx											
4	10/14/2000-10/28/2000	xx	xx	x	x									
5	10/28/2000-11/11/2000	x	xx	x	x									
6	11/11/2000-12/09/2000	x	x		xxx	x	x	x						
7	12/09/2000-01/06/2001	x		x	xxx		x		x					
8	01/06/2001-02/03/2001	x	x	xx				x		x	x	x		
9	02/03/2001-03/03/2001	x												x
10	03/03/2001-03/31/2001	x												x
11	03/31/2001-04/28/2001	x	x				x							
12	04/28/2001-05/12/2001		x					x						
13	05/12/2001-05/26/2001		xx	x	x				x		x			
14	05/26/2001-06/09/2001		x	x							xx		x	
15	06/09/2001-06/16/2001		xx								x			
16	06/16/2001-06/23/2001	x	xx											
17	06/23/2001-06/30/2001	x												
18	06/30/2001-07/07/2001		x											
19	07/07/2001-07/14/2001	x			x		x				x			
20	07/14/2001-07/21/2001		x		x									
21	07/21/2001-07/28/2001	x			x									
22	07/28/2001-08/04/2001		x		x		x							
23	07/04/2001-08/11/2001		x		x		x							
24	08/11/2001-08/23/2001	x			x									

Tab. 4.4: Sample composition for recovered sediment trap YEN02 (macrofauna). OM: organic matter; CP: copepods; AM: amphipods; FP: fecal pellets; PC: polychaets; AP: apendiculariens; CT: ctenophores; MY: mysidaceens; ME: medusae; CH: chaetognaths; CU: cumaceens; PT: pteropods; IA: ice algae; x: sparse; xx: abundant; xxx: very abundant.

## 5.1 Phytoplankton distribution in the Ob and Yenisei estuaries and adjacent Kara Sea

V.V. Larionov, MBI Murmansk, Russia

### Materials and methods

Water samples for species composition studies and phytoplankton abundance and biomass estimation were collected on the majority of the «main» stations over the whole area of investigation. Sampling was carried out on standard depths from the surface layers (with the metallic zinc coating bucket), from the density change layer and from the near bottom layer (with the sampler of the «Rosette» system; parallel with the hydrological probing). Concrete stations and sampling depths are presented in Table. 88 samples on 31 stations were collected. Besides, on the majority of «short» stations located in the most variable areas from the point of view of hydrodynamics phytoplankton samples were collected (more than 20) from the surface layer for obtaining a more detailed picture of microalgal communities development in these areas.

Primary processing and preservation of samples were carried out according to accepted hydrobiological methods. Water samples collected (usually of 1 liter volume) were subjected then to concentrating by a standard inverse-flow method and fixed with 40% buffered formalin (final concentration is 1-2 %) for the microscopy to receive exact data on the taxonomic composition of the communities and biomass and abundance of each species of microalgae. This is in its turn will allow to estimate reliably the directions and rate of development of pelagic phytocenoses in different parts of the investigation area, to give description of the interrelation processes of phytoplankton of different origin (fresh water or sea water) species complexes and to give conclusions on lesser or greater significance of the of the biological chain in biogeochemical cycles upon the whole in this area.

Phytoplankton samples for the isotope analysis were collected from either the surface layer by the way of filtration of large volumes of water (in the range 100-1000 liters) through the plankton net with the mesh of 10 mcm diameter or in the fresh water areas, where phytoplankton was in the state of vigorous blossom was represented mainly by long filamentous forms -with the zooplankton net with mesh diameter 200 mkm. Then the samples obtained were fixed with the mercuric chloride solution and were subjected to standard preparation for the subsequent analysis. 21 samples were collected all in all (concrete stations are presented in Table).

### Preliminary results

Preliminary investigation of samples collected from the surface water layer on separate stations allows in this very moment to give a short qualitative estimation of the phytoplankton communities state in different parts of the investigated area.

In the southern parts of the estuary zones in the coastal area the micro- algae species complex is represented exclusively by the forms of fresh water and estuary origin which occurred traditionally there during several years of investigation. Diatom algae *Melosira granulata* and *M. varians* prevail. The minor part is composed of green algae, distinguishing by significant species diversity (filamentous forms of genera *Rhizoclonium* and *Ulothrix*, unicellular ones of genera *Pediastrum*, *Scenedesmus* etc.), diatoms *Asterionella formosa* and *Fragilaria crotonensis* and blue-green algae. The latter group is diverse as in respect of its representatives and includes greater in comparison to previous years number of filamentous forms (at the dominance of the genus *Oscillatoria*), which is more typical of the most mouth parts of the estuaries, especially for the Enisei bay. Upon the whole significant differences between the estuarine zones of the Ob and Enisei in respect of phytoplankton in species composition are not observed.

This uniform complex is distributed in the near Enisei part of the shallow water area. (Stations 8, 4, 11 and 19) up to 73° latitude, where already as singular amounts marine species occur – diatoms of genus *Chaetoceros* (Station 19). To the north the part of fresh water and estuary forms falls sharply: on station 23 they constitute not more than 70 % as for biomass and on Station 26 (74° latitude) – not more than 10 %. This per cent falls more in the north-east direction. (Stations 43 and 28) though at the significant decrease of species diversity. Though already in the more northern part of the area (Stations 45 and 31) their single representatives (mainly *Melosira granulata*) occur.

Sea water complex of microalgae in this eastern part of the investigation area is typical for the summer stage of the Arctic phytoplankton communities development. It includes diatoms of genera *Chaetoceros* and *Thalassiosira* and numerous representatives of the Phylum *Dinophyta*. The latter prevail insignificantly in the more southern (and more coastal at that!) part (Stations 23, 26, 43 and 28). For the northern (off-sea) area some dominance of diatoms is typical (mainly *C. diadema* and *T. nordenskiöldii*), which might be considered as the earlier stage of development (either early summer or late spring), which in the coastal zone began earlier, and during the moment of investigation a typically summer complex was observed there with prevalence of dinoflagellates. It is interesting to note Station 48, where one species of diatoms, *C. diadema*, dominated absolutely, – the phenomenon is absolutely untypical for the plankton phytocenoses of the Nordic seas.

On the Ob bay area the marine species occur more to the south in comparison with the near Enisei part of the shallow water area. – already on Station 70 dinoflagellates are distinguished by species diversity, though observed in the insignificant amounts. As for the off- sea part of the near Ob area to the north of 74° latitude (Stations 67 and 68) – quite a unique community which has never been described yet was found: the main part of the biomass in it (on station 67 is up to 95 %!) consists of the diatom *Nitzschia delicatissima*. This species (at the moment specialists consider is «composed», i.e. a group of close species) is typical for the Barents Sea coastal zone and even there it does not reach that part by biomass, and in the Kara Sea it is not typical at all. It might be



supposed that we are confronted with the anomaly during development of the community which is not a rare phenomenon.

In the north-western part of the investigation area a summer sea phytoplankton complex differing to some extent from those in the eastern part is observed. On Stations 56 and 46, located more to the north up to 80 % of biomass is constituted of dinoflagellates, the rest are mainly diatoms *Thalassionema nitzschioides* and species of genus *Chaetoceros*: *C. borealis* and *C. convolutus*. These microalgae occurred and in the eastern part of the area but in the lesser concentrations. The representatives of genus *Chaetoceros* mentioned are the oceanic species and are typical for the summer phytoplankton community in the off-sea area. It is interesting to note that on Station 61, located farther to the south, their part in biomass is about 30 %, species *Chaetoceros diadema*, constitutes more than half of biomass, and per cent of dinoflagellates is quite insignificant. This community is more similar to that found on Station 48, that with phytocenoses in the nearest parts of the area.

As seen from the description the spatial structure of phytoplankton communities in the western part of the investigation area is rather complicated, differs significantly from observed earlier in the neighboring areas situations and at the moment is rather difficult for the unequivocal explanation. Phytocenoses with dominance of one microalgae species cause special interest. All these phenomena might be caused by the impact of different (probably several) natural factors: changes in the ice situation, manifestation of the Ob river run-off effect, other climatic and hydrodynamic processes. Real reasons might be revealed only after the detailed analysis of the whole material obtained during the expedition.

Table 5.1: The phytoplankton investigations during the "Boris Petrov" cruise on the Ob-Yenisei shallow-water region at August-September 2001.

Station No.	Depths of phytoplankton sampling	Sampling for isotope analysis
1	0; 18; 35	
4	0; 19	+
8	0; 27	+
11	0; 7; 8.3	+
14	0; 18,4	
16	0; 27,3	
19	0; 4,5; 23	+
23	0; 4; 8; 18	+
26	0; 5,5; 30	+
28	0; 17	+
30	0; 12; 46	
34	0; 19; 90	+ (on the nearest Station No.31)
35	0; 17; 150	
40	0; 9; 43	
43	0; 10; 40	+
45	0; 18; 80	+
46	0; 20; 50; 300	+
48	0; 15; 188	+
51	0; 10; 138	
55	0; 15,5; 70	
56	0; 16; 170	+
61	0; 20; 100	+
64	0; 10; 95	
66	0; 10; 45	
67	0; 6; 40	+
68	0; 6; 20	+
70	0; 7,5; 15	+
72	0; 20	+
73	0; 9	+ (on the nearest Station No.79)
80	0; 7; 10	+
82	0; 7; 20	+

## 5.2 Phytoplankton biomass and production in the Ob and Yenisei estuaries and adjacent Kara Sea

R.Beude, E.- M. Nöthig

Alfred Wegener Institute for Polar and Marine Research, Bremerhaven

Arctic rivers representing very dynamic environments characterized by strong seasonal changes. The variable light conditions, seasonal ice cover, and the pulse of fluvial matter affect biological processes and transformation rates of organic matter at large geographical scales. The aim of this study was like in the years before (1997, 1999, 2000) to investigate the horizontal and vertical distribution of phytoplankton biomass with regard to the different physical and chemical conditions in order to estimate the significance of biological processes for the transformation of matter in arctic estuaries. Furthermore, together with the results from investigations of the other groups, a more complete picture of the pathway of primary produced carbon could be established in the future. During the expedition to the Kara Sea with 'Akademik Boris Petrov' in 2001 phytoplankton biomass (expressed as chlorophyll *a*) as well as primary production (oxygen method) were measured.

### Material and Methods

Water samples to estimate phytoplankton biomass and oxygen production rates were collected with a Niskin Rosette sampling system. On 46 stations subsamples were taken from 1 to 6 different water depths according to different water masses determined by the CTD profiles. In most cases, samples were taken at the surface, just above and below the pycnocline and close to the bottom. For the chlorophyll *a* determination 500 - 1000 ml of water were filtered through Whatman GF/F glasfibre filter and stored at -18° C and analyzed at AWI. The filters were extracted in 90 % acetone and analyzed with a Turner-Design fluorometer according to the methods described in Evans and O'Reily (1987). In addition, light measurements were carried out at 10 stations with a 4π LICOR probe, and oxygen production rates were measured at 12 stations with surface phytoplankton populations.

### First Results

Chlorophyll *a* concentrations ranged from 0.01 to 7.27 µg/L with maximum values in the surface layers in most cases. The lowest values were found at the most northern stations in the eastern part of the investigation area; highest phytoplankton biomass was found in both rivers at the southernmost stations decreasing continuously towards the estuary. Between 73°S and 75° chlorophyll *a* concentrations around 1 µg/L prevailed decreasing to values ranging from 0.13 µg/L to about 1µg/L north of 76 °N.

The light measurements showed light was available for phytoplankton in the rivers only in the upper 3-5 m, whereas in the estuary and the northern part of the investigation area light penetrated down to about 20 m. Analyses of the production measurements will give more information on the productivity of the phytoplankton populations in the investigation area. First results showed somewhat higher oxygen production in the rivers and fairly low production in the northern region.

### 5.3 The pelagic larvae of macrofauna in the central Kara Sea

I. Fetzner

Alfred Wegener Institut for Polar and Marine Research, Bremerhaven

#### Introduction

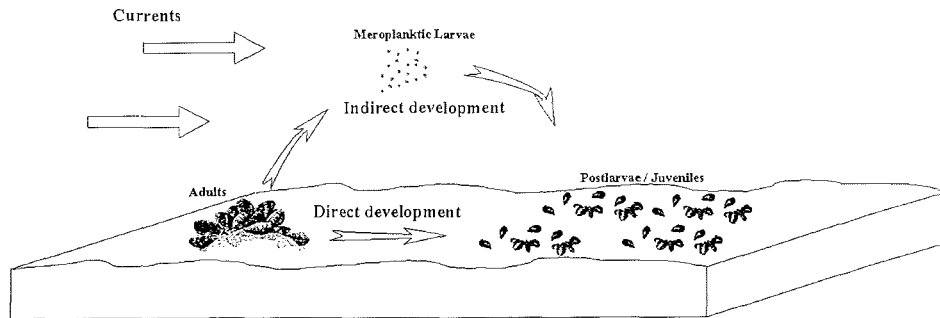
Formation, development and stability of benthic communities mainly depend on recruitment of larvae and juveniles from within or outside the community (Butman 1987). Only the permanent replacement of old individuals by young ones ensures the survival of species within a group (Burkovsky et al 1997). If and how new communities are formed depends very much on the reproduction modes of the species.

The bulk of benthic invertebrates in the boreo-atlantic region reproduces via pelagic larvae (Fig. 5.1), since this ensures a wide distribution of the species and a good ability for fast exploitation of new territories (Thorson 1950). Moreover the planktic stages are able to enter the euphotic zone and there instantaneously utilise the primary production in the upper water layers. But the pelagic stages very much depend on environmental factors and settlement success. Prevailing currents often carry them away to unfavourable sites resulting in high mortality.

The alternative strategy is direct development, which is lacking a pelagic phase (Fig. 5.1). This ensures that the juveniles settle in the vicinity of the adults and stay on the approved sites where already the adults survived. It guarantees a sufficient recruitment of the community. Most species with direct development also show brood protection, which reduces the mortality of the juveniles to a minimum. But since this method is very energy consuming those species can afford only very few offspring whereas specimens with planktic stages usually produce huge amounts of small larvae.

To what degree environmental factors influence the distribution and the mortality of the pelagic stages, and how far settlement success is important for the structure of benthic communities is so far unknown. But today it is commonly accepted that understanding benthos ecology without the knowledge of larval and juvenile recruitment is hardly impossible (Scheltema 1986). The absence of larvae in polar waters led Thorson (1936) to the hypothesis that many polar species reproduce directly without a pelagic stage, which he explained by the shortening of time for development and food accessibility in higher latitudes. Recent discoveries of an increasing quantity of pelagic larvae in Arctic and Antarctic waters created problems with this rule and shows how little is known on the ecology of meroplankton in the Arctic.

The aim of this study is to investigate the reproduction modes of benthic invertebrates in the Kara Sea and the spatial distribution of their larvae and juveniles to explain the invertebrate community structure with emphasis on environmental factors such as river runoff and its accompanying effects.



**Fig. 5.1:** Reproduction modes of benthic invertebrates

### Material and Methods

Larval plankton was collected with a Nansen Closing Net (NCN) with 55 $\mu$ m mesh size at a hauling speed of 0.5 m/sec at 31 Stations (Tab. 5.2, Fig. 5.2). To gather information about the spatial occurrence of the larvae in the water layers at each station three vertical net hauls was taken: under (haul 1), through (haul 2) and above (haul 3) the halocline. Close to the sea floor the larvae were fished by an Epi-Benthic sledge, mounted with an 80 $\mu$ m Supranet. The sledge was dredged at about 1-2 knots and between 3-6min according to plankton concentration. Samples for the distribution of postlarvae and juvenile stages were taken by a Multicorer (MUC; 28cm<sup>2</sup> surface). At each station 3-4 tubes were taken. After careful removal of the supernatant water, the upper 3-5cm of the sediment was preserved. All samples were stored, until further treatment in the laboratory, in 4% borax buffered formaline. BP00 stays as abbreviation for the expedition carried out in 2000.

**Table 5.2:** Overview of meroplankton sampling stations, date, station depth, haul range, number and duration of devices used (NCN=Nansen Closing Net, MUC=Multicorer, EBS= Epi-Benthic Sledge)

Station	Date	Lat. ° N	Lon ° E	Depth [m]	Haul [range]	1 Haul [range]	2 Haul [range]	3 NCN [N]	MUC [N]	EBS [min]
BP01- 1	14.08.01	74°59.12	76°23.41	38	35-23 m	23-0 m	12-0 m	3	4	4
BP01- 19	21.08.01	72°35.7	80°06.4	28	24-6m	6-0m	3-0m	3	3	
BP01- 23	22.08.01	73°29.0	78°50.9	22	20-9m	9-0m	3-0m	3		
BP01- 26	23.08.01	74°00.0	80°01.4	33	32-18m	18-0m	4-0m	3	3	4
BP01- 28	24.08.01	75°56.34	89°15.9	51	50-20m	20-0m	3-0m	3	4	
BP01- 30	24.08.01	76°24.75	88°10.76	47	48-27m	27-0m	5-0m	3	3	
BP01- 31	25.08.01	77°34.2	87°54.5	88	90-17m	17-0m	12-0m	3	3	
BP01- 34	25.08.01	77°54.29	89°20.15	91	90-30m	30-0m	18-0m	3	4	
BP01- 35	26.08.01	77°54.31	83°45.94	160	155-40m	40-0m	10-0m	3	4	
BP01- 37	26.08.01	77°48.9	86°11.9	144	130-23m	23-0m	13-0 m	3	4	
BP01- 38	27.08.01	77°5.29	86°55.48	110	100-20m	20-0m	10-0m	3	4	
BP01- 40	27.08.01	76°25.2	85°39.9	52	45-20m	20-0m	4-0m	3	4	
BP01- 41	28.08.01	75°41.4	87°07.8	42	34-23m	23-0m	6-0m	3	4	
BP01- 43	28.08.01	75°22.99	85°49.90	48	40-27m	27-0m	6-0m	3	4	3
BP01- 45	29.08.01	77°6.83	84°44.0	87	80-23m	23-0m	17-0m	3	4	5
BP01- 46	30.08.01	77°55.43	75°57.35	323	300-30m	30-0m	10-0m	3	4	
BP01- 48	31.08.01	77°53.49	81°29.94	202	180-30m	30-0m	5-0m	3	4	
BP01- 51	31.08.01	77°54.68	79°29.48	158	140-25m	25-0m	5-0m	3	4	
BP01- 52	01.09.01	77°29.94	79°52.0	75	58-25m	25-0m	8-0m	3	4	
BP01- 55	01.09.01	77°2.97	79°43.99	83	70-30m	30-0m	5-0m	3	4	6
BP01- 56	02.09.01	76°59.58	75°11.48	176	170-38m	38-0m	8-0m	3	4	
BP01- 58	02.09.01	76°48.12	78°21.24	94	75-35m	35-0m	15-0m	3	4	
BP01- 59	03.09.01	76°31.16	74°30.95	176	155-35m	35-0m	5-0m	3	3	
BP01- 61b	03.09.01	76°12.9	75°53.15	111	95-38m	38-0m	3-0m	3	4	5
BP01- 62	04.09.01	76°12.05	74°12.15	135	100-30m	30-0m	3-0m	3	3	
BP01- 65	05.09.01	75°42.98	75°50.79	63	48-30m	30-0m	3-0m	3	4	
BP01- 66	05.09.01	75°10.04	76°55.13	55	45-32m	32-0m	4-0m	3	4	
BP01- 67	06.09.01	75°14.65	73°45.78	49	38-25m	25-0m	4-0m	3	4	
BP01- 68	06.09.01	74°35.05	72°14.97	31	25-17m	17-0m	5-0m	3	4	5
BP01- 70	07.09.01	72°40.16	74°0.22	22	16-9m	9-0m	6-0m	3	4	
BP01- 82	11.09.01	73°11.83	73°01.65	29	22-9m	9-0m	6-0m	3	4	5
Σ=31				Min=22 Max=323				Σ=93	Σ=114	Σ=8

## Results and Discussion

During the expedition on 31 stations meroplankton (=93 samples) and juvenile benthos (=114 surfaces) samples were taken (Fig. 5.2). Additional close-bottom plankton samples with the EBS were obtained on 8 stations (Tab. 5.2).

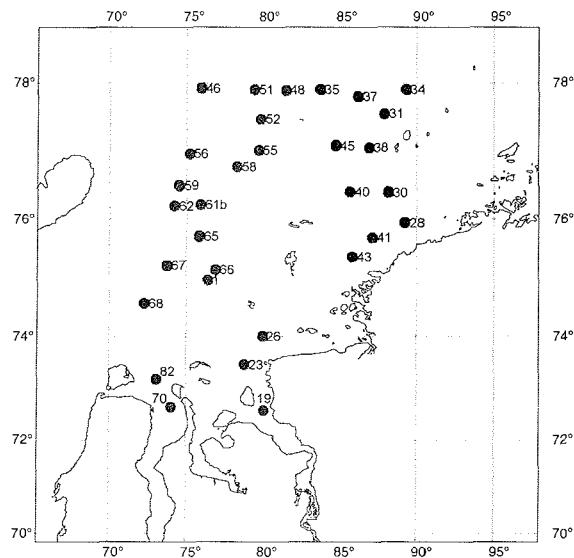
In general the meroplanktic inventory is comparable to that in BP00 (Fetzer 2001). Again pluteus larvae of brittle stars dominated the meroplankton at all stations. Here mainly larvae of *Ophiocten sericeum* were found. Formin (1989) reported that ophiurid larvae are typical representatives for the Kara Sea meroplankton and are present throughout the year. Generally the ophiuoplutei were present at all stations, although their main distribution area was the northern and middle part of the investigation area. Only within the estuaries no larvae were present. The reason for their distribution is the

freshwater inflow by the rivers, which restricts the stenohaline (=tolerant to narrow salinity range) adults, where the larvae finally descend from, to the northern parts. In their horizontal distribution the highest concentrations were usually present in the upper water layers (haul 2+3), above the pycnocline (Tab. 5.2). Here they usually outnumber the abundance of the larvae from below the pycnocline by 5-10fold. As observed earlier, the ophiurid larvae seem to be more tolerant to osmotic stress than their adults (Halsband and Hirche 1999, Fetzner 2001). In the upper water layers they may be able to utilise the phytoplankton and the river imported organic material as food source. Interestingly hardly any larvae were found in net samples of the deeper layers (>100m haul depth) in the northwest part of the investigation area (e.g. sts. 34, 35, 46, 48, 56, 59, 62). These stations lay at the shallow northern and western rim of the Kara Sea Shelf. Although ophiurids are the dominant taxon in high latitudes from the shallow waters down to the deep sea (Piepenburg and von Juterzenka 1994), it seems that only shallow living species, as e.g. *Ophiocten sericeum*, produced offspring at this time of the year, which may explain why larvae were found only at the shallow shelf area. *Asterias* sp. larvae were also quite common in the samples but not as abundant as in BP00. They mainly occurred in the deeper parts below the pycnocline.

In the middle and southern region high amount of polychete larvae were present in the samples. Besides spionid larvae (*Prionospio* sp.), larvae of *Phyllodoce groenlandicum*, *Pholoe minuta*, *Glycera capitata* and some species of the genus *Terebellida* were found. Although the spectrum of polychete species was not as wide as one year ago but the species present showed much higher abundances. Remarkable was that most of the polychete trochophora were much further developed and bigger as those present in the samples of BP00. Almost all of them were caught below the pycnocline close to the bottom. Most of them were about to metamorphose soon and obviously prepare to settle. This might be explained by the fact that the expedition was carried out about three weeks later than BP00. Obviously the polychete meroplankton was already in a later successional stage than the ones caught during BP00. Also here no planktic stages of polychetes were caught in the northern deeper waters. This lack as well is explained by the absence of the adults in these areas.

One big difference was the frequent occurrence of bivalve veligers in the plankton samples compared to BP00 (Fetzner 2001). The observed specimens were rather big and exclusively found in the lower net samples, so it seems that these animals were about to settle soon. In opposition to BP00 there were no mollusc larvae present. Either their larvae appear later in the year or had already settled. Since the specimen of BP00 were quite far developed the latter seems more likely.

The above-mentioned results still need to be evaluated by careful examination of the taken samples in the laboratory. After the identification of the juveniles and larvae in the home laboratory the data need to be compared to the adult fauna to get a better understanding of the complexity of the larvae-juvenile-adult interaction. To explain their distribution the found data need to be statistically correlated to biotic (e.g. abundance and distribution of the adult fauna) and abiotic (e.g. current regimes, salinity distribution, food availability) factors to help to understand their importance on the structure of the adult fauna and their role within the Kara Sea ecosystem.



**Fig. 5.2:** Map of meroplanktic sampling stations

#### 5.4 Spatial distribution of zooplankton in the southern Kara Sea

M. Engel

Alfred Wegener Institute for Polar and Marine Research, Bremerhaven

##### Introduction

The previous scientific cruises within the SIRRO project (BP-97, BP-99 and BP-00) covered in particular the Ob and Yenisei Rivers estuaries and the southern Kara Sea (Halsband and Hirche 1999, Fetzer and Arndt 1999, Suck 2001). Analysis of the plankton samples collected during these three expeditions produced detailed information on the spatial distribution and abundance of zooplankton species in the above regions (Fetzer and Hirche 2002). Nevertheless, the picture remained incomplete because little was known about other important parts of the Kara Sea, i.e. the areas north of 77°N and east of 85°E. To close this gap this year's cruise focused on these two regions.

##### Sampling of Mesozooplankton

Zooplankton samples were obtained at 39 stations (Tab. 5.3) using a Nansen-Closing-Net (NCN) with a mouth diameter of 0.75 m and a mesh size of 150  $\mu\text{m}$ . The net was hauled vertically with approximately 0.5  $\text{ms}^{-1}$ . At each station a near-bottom to surface haul was taken. When the previously made CTD cast gave evidence of the presence of a pycnocline an extra two hauls were usually made (one from near-bottom to below-pycnocline and a second from above-pycnocline to surface). Subsequently, samples were transferred to 250 ml Kautex bottles and preserved in 4% borax buffered formalin for later identification and counting.



Table 5.3: Zooplankton sampling stations

Station	Date	Time (GMT)	Latitude ° N	Longitude ° E	Depth (m)	Haul 1 Depth range	Haul 2 Depth range	Haul 3 Depth range
BP01-01	14.08.01	12:00	74°59.12	76°23.41	38	35-0 m	35-23 m	12-0 m
BP01-04	16.08.01	8:54	71°05.5	83°06.2	22	16-0 m	16-0 m	-
BP01-05	16.08.01	14:00	70°45.5	83°33.1	13	11-0 m	-	-
BP01-06	17.08.01	4:30	70°20.2	83°8.2	17	14-0 m	-	-
BP01-08	17.08.01	11:00	70°04.1	83°3.9	28	28-0 m	-	-
BP01-09	18.08.01	6:00	72°06.9	82°10.7	11	8-0 m	-	-
BP01-11	18.08.01	12:00	72°05.6	81°41.8	12	8-0 m	5-0 m	-
BP01-14	19.08.01	7:20	71°49.3	82°27.2	21	19-0 m	-	-
BP01-16	19.08.01	14:30	71°41.7	83°31.2	28	27-0 m	27-0m	-
BP01-19	21.08.01	11:00	72°35.7	80°06.4	28	24-0 m	24-8 m	3-0 m
BP01-23	22.08.01	7:00	73°29.0	78°50.9	22	20-0 m	20-9 m	3-0 m
BP01-26	23.08.01	4:30	74°00.0	80°01.4	33	32-0 m	32-18 m	4-0 m
BP01-28	24.08.01	4:15	75°56.34	89°15.9	51	50-0 m	18-0 m	-
BP01-30	24.08.01	13:30	76°24.75	88°10.76	47	47-0 m	47-27 m	5-0 m
BP01-31	25.08.01	4:30	77°34.2	87°54.5	88	88-0 m	88-17 m	12-0 m
BP01-34	25.08.01	15:20	77°54.29	89°20.15	91	90-0 m	90-30 m	18-0 m
BP01-35	26.08.01	4:30	77°54.31	83°45.94	160	155-0 m	155-40 m	12-0 m
BP01-37	26.08.01	13:52	77°48.9	86°11.9	144	130-0 m	130-23 m	13-0 m
BP01-38	27.08.01	4:30	77°5.29	86°55.48	110	100-0 m	100-20 m	10-0 m
BP01-40	27.08.01	16:30	76°25.2	85°39.9	52	45-0 m	45-20 m	4-0 m
BP01-41	28.08.01	4:00	75°41.4	87°07.8	42	35-0 m	35-23 m	6-0 m
BP01-43	28.08.01	11:30	75°22.99	85°49.90	48	40-0 m	40-27 m	7-0 m
BP01-45	29.08.01	8:00	77°6.83	84°44.0	87	80-0 m	80-33 m	17-0 m
BP01-46	30.08.01	4:53	77°55.43	75°57.35	323	300-0 m	30-0 m	10-0 m
BP01-48	31.08.01	4:30	77°53.49	81°29.94	202	180-0 m	30-0 m	-
BP01-51	31.08.01	14:30	77°54.68	79°29.48	158	140-0 m	140-25 m	5-0 m
BP01-52	01.09.01	4:19	77°29.94	79°52.0	75	58-0 m	58-25 m	8-0 m
BP01-55	01.09.01	11:48	77°2.97	79°43.99	83	60-0 m	60-30 m	15-0 m
BP01-58	02.09.01	12:20	76°48.12	78°21.24	94	75-0 m	75-35 m	15-0 m
BP01-59	03.09.01	4:30	76°31.16	74°30.95	176	155-0 m	155-35 m	5-0 m
BP01-61b	03.09.01	13:15	76°12.9	75°53.15	111	95-0 m	95-38 m	3-0 m
BP01-62	04.09.01	4:30	76°12.05	74°12.15	135	100-0 m	100-30 m	3-0 m
BP01-65	05.09.01	4:18	75°42.98	75°50.79	63	48-0 m	48-30 m	3-0 m
BP01-66	05.09.01	11:28	75°10.04	76°55.13	55	45-0 m	45-32 m	4-0 m
BP01-67	06.09.01	4:30	75°14.65	73°45.78	49	38-0 m	38-25 m	4-0 m
BP01-68	06.09.01	12:25	74°35.05	72°14.97	31	25-0 m	25-17 m	5-0 m
BP01-70	07.09.01	7:15	72°40.16	74°0.22	22	25-0 m !!	15-0 m !!	10-0 m !!
BP01-72	08.09.01	4:20	70°49.88	73°44.34	26	20-0 m	-	-
BP01-82	11.09.01	4:17	73°11.83	73°01.65	29	22-0 m	22-9 m	5-0 m

### **5.5 Are resting eggs an overwintering strategy of neritic calanoid copepods in the Kara Sea?**

M. Engel

Alfred Wegener Institute for Polar and Marine Research, Bremerhaven

A number of physical and hydrographical parameters in the Kara Sea display a high seasonal variability. Salinity, for example, cycles strongly, particularly in surface waters, due to dramatic changes in fresh water discharge from Ob and Yenisei Rivers (Pavlov and Pfirman 1995). In late summer, after discharge levels reached their maximum, the river plume can easily be detected even at 78°N. In winter and early spring, on the other hand, surface salinity increases significantly in the Kara Sea. Light intensity also varies on a seasonal basis. During the arctic winter values are small, as the sun stays below the horizon. As a result, photoautotrophic primary production is very low or ceases altogether. Additionally, sea ice, which covers the Kara Sea from approx. November to June (Gloersen et al. 1992), further reduces light penetration into the water. Consequently, herbivorous and brackish water organisms will experience a period of low food availability and inadequate salinity during that time of year.

Calanoid copepods dominate the Kara Sea zooplankton in terms of abundance (Fetzer and Hirche 2002) and biomass (Vinogradov et al. 1995) and therefore play an important role in the ecosystem. Some species are herbivores and many can be found living in intermediate salinities. In the temperate zone a number of neritic calanoids were found to produce resting eggs (Marcus 1996), to overcome adverse conditions. The eggs sink to the sea floor and, in the case of dormant eggs, will only hatch after conditions have improved and are favourable for development. True diapause eggs require a genetically fixed period of time to pass before hatching can occur. Whether species from the Kara Sea also use these strategies to secure population survival is unknown at present.

To answer this question

- unpreserved sediments will be incubated and the overlying water regularly screened for copepod nauplii. Thereby one will get an idea as to whether there are any copepod resting stages in the sediments or not.
- the organic compound will be separated from the sediment of a second set of unpreserved samples. Morphologically similar resting stages will be grouped and incubated. It is intended to raise any hatching nauplii to an identifiable stage. This should enable us to identify resting eggs in preserved samples down to species level.
- a preserved set of samples will be used to get information on the spatial distribution and abundance of resting eggs of neritic calanoid copepods in Kara Sea sediments.

Sediment samples were obtained at 32 stations (Tab. 5.4) using a Multicorer (MUC) equipped with transparent Plexiglas tubes (length 65 cm, inner diameter 6 cm) and capable of collecting up to 12 cores simultaneously. Usually three cores were taken per station. On two occasions samples had to be taken from a large box corer using MUC

Plexiglas tubes. The soft top layer (3-7 cm thick) of each core was spooned into a 500 ml Kautex bottle. Subsequently, the three samples were treated as follows:

#### Incubation of sediments

The bottle was topped up with 0.2 µm filtered seawater (approx. 34‰, 0°C) and placed in an incubator at 0°C and LD 20:4. The supernatant was decanted every 3-7 days by pouring it through a 55 µm sieve. The bottle was then refilled again with 0.2 µm filtered seawater (approx. 34‰, 0°C) and returned to the incubator. The material retained by the sieve was washed back into a plastic Petri dish and a few drops of Bengal rose solution was added. On the following day the Petri dish was screened for copepod nauplii. If present, they were transferred into a 0.5 ml Eppendorf cap and preserved in 4% borax buffered formalin for later identification and counting.

#### Incubation of similar morphotypes

The bottle was topped up with 0.2 µm filtered seawater (approx. 34‰, 0°C) and stored in an incubator at 0°C and DD until the return to Bremerhaven.

#### Distribution and abundance

For later identification and counting of copepod eggs the sample was preserved in 4% borax buffered formalin.

Table 5.4: Sediment sampling stations

Station	Date	Time (GMT)	Latitude ° N	Longitude ° E	Depth (m)	Number of tubes taken	Device used
BP01-01	14.08.01	12:00	74°59.12	76°23.41	38	4	MUC
BP01-11	18.08.01	12:00	72°05.6	81°41.8	12	3	MUC
BP01-14	19.08.01	7:20	71°49.3	82°27.2	21	3	GKG
BP01-19	21.08.01	11:00	72°35.7	80°06.4	28	3	GKG
BP01-26	23.08.01	4:30	74°00.0	80°01.4	33	3	MUC
BP01-28	24.08.01	4:15	75°56.34	89°15.9	51	4	MUC
BP01-30	24.08.01	13:30	76°24.75	88°10.76	47	3	MUC
BP01-31	25.08.01	4:30	77°34.2	87°54.5	88	3	MUC
BP01-34	25.08.01	15:20	77°54.29	89°20.15	91	3	MUC
BP01-35	26.08.01	4:30	77°54.31	83°45.94	160	3	MUC
BP01-37	26.08.01	13:52	77°48.9	86°11.9	144	3	MUC
BP01-38	27.08.01	4:30	77°5.29	86°55.48	110	3	MUC
BP01-40	27.08.01	16:30	76°25.2	85°39.9	52	3	MUC
BP01-41	28.08.01	4:00	75°41.4	87°07.8	42	3	MUC
BP01-43	28.08.01	11:30	75°22.99	85°49.90	48	3	MUC
BP01-45	29.08.01	8:00	77°6.83	84°44.0	87	3	MUC
BP01-46	30.08.01	4:53	77°55.43	75°57.35	323	3	MUC
BP01-48	31.08.01	4:30	77°53.49	81°29.94	202	3	MUC
BP01-51	31.08.01	14:30	77°54.68	79°29.48	158	3	MUC
BP01-52	01.09.01	4:19	77°29.94	79°52.0	75	3	MUC
BP01-55	01.09.01	11:48	77°2.97	79°43.99	83	3	MUC
BP01-56	02.09.01	4:30	76°59.58	75°11.48	176	3	MUC
BP01-58	02.09.01	12:20	76°48.12	78°21.24	94	3	MUC
BP01-59	03.09.01	4:30	76°31.16	74°30.95	176	3	MUC
BP01-61b	03.09.01	13:15	76°12.9	75°53.15	111	3	MUC
BP01-62	04.09.01	4:30	76°12.05	74°12.15	135	2	MUC
BP01-65	05.09.01	4:18	75°42.98	75°50.79	63	3	MUC
BP01-66	05.09.01	11:28	75°10.04	76°55.13	55	3	MUC
BP01-67	06.09.01	4:30	75°14.65	73°45.78	49	3	MUC
BP01-68	06.09.01	12:25	74°35.05	72°14.97	31	3	MUC
BP01-70	07.09.01	7:15	72°40.16	74°0.22	22	3	MUC
BP01-82	11.09.01	4:17	73°11.83	73°01.65	29	3	MUC

## 5.6 Macrobenthic studies along a transect from the estuaries of Ob and Yenisei into the central Kara Sea

H. Deubel

Alfred Wegener Institute for Polar and Marine Research, Bremerhaven

### Introduction

Biological studies of SIRRO 2001 are an important component to understand the full dimension of the cycle of organic matter in the open Kara Sea. The enormous fresh water inflow from the siberian rivers Ob and Yenisei is important for the distribution of macrobenthic organisms and hence determinant for the entire Kara Sea ecosystem. In this respect, sea floor living organisms are an important link between the water column and the sea bottom. Studies on the long-lived macrofauna are necessary to understand energy turnover and benthic-pelagic coupling in the area of the Kara Sea and the adjacent Arctic Ocean.

Within the scope of the Russian-German project SIRRO, the macrofauna of the estuarine areas of Ob and Yenisei as well as the adjacent southern Kara Sea has been studied extensively. However, for logistic reasons offshore parts of the Kara Sea, which are more difficult to reach, have been investigated insufficiently. In comparison with previous expeditions substantial changes of macrobenthic species composition with increasing latitude are indicated. During this expedition evenly distributed samples for incubation experiments were also collected in the Kara Sea (Tab. 5.5, see chapter 8.2).

### Sampling

The large-scale distribution of the Kara Sea macrobenthic organisms was studied handling two approaches. First, the benthic fauna was collected using a Large Box Corer (0.25m<sup>2</sup>). The macrofauna from 60 LBC were separated from the sediment by sieving on 500µm-screens and preserved by 7% with Natriumtetraborat buffered formaldehyde. In combination with the LBC samples and to capture larger quantities of macrobenthic animals a dredge with a frame size of 150 x 50cm was used. Subsamples of the dredge material were pre-sorted and deep-frozen (-80°C) for biochemical investigations. The retained dredge sample was also formalin fixated for subsequent examination.

For benthic respiration studies, the sampling program includes evenly distributed multi-corer samples, four replications on each station. The incubated sediment cores were closed with lids, kept in the dark and cooled in a water basin for 24h. In addition, water from the similar multi-corer was bottled (four replications á 100ml) and kept dark and cooled together with the sediment cores. Aboard oxygen was determined using standard methods (Winkler titration). Respiration rates were calculated from the differences in oxygen concentration between the incubated sediment cores and the bottled seawater.

### Preliminary results

Only preliminary results are available since most of the material will be sorted at the Alfred Wegener Institute in Bremerhaven. Molluscs, especially bivalvia, represented the most important macrobenthic group, followed by polychaeta, crustacea and echinodermata. *Portlandia* (cf.) *arctica* and *Tridonta borealis* dominated the bivalvia fauna. Gastropoda were very rare in the samples. Amphipods and isopods were the most abundant crustacea. Of some importance were the amphipoda *Pontoporeia affinis* and different species of the isopode *Saduria*. However, larger specimens of *Saduria entomon*, which had been abundant in previous expeditions, were found this year only sporadic. Comparable with other arctic shelf areas, echinodermata are an important macrobenthic element of the central Kara Sea. Very remarkable are *Ophiocten sericeum* and *Ophiopleura borealis*. These arctic species occurred only in the northern part of the investigation area, where the Kara Sea is more influenced by Atlantic waters. The sea star *Ctenodiscus crispatus* appeared in the dredge samples in relatively large numbers. In the northwestern Kara Sea the suspension feeding *Heliometra glacialis* and *Gorgonocephalus arcticus* inhabited the high arctic deeper areas.

At 8 evenly distributed stations a total of 32 respiration measurements were conducted. As expected, absolute oxygen consumption decreased within 24h. Sediment cores, which contained larger macrobenthic animals, had considerably higher oxygen demands compared to incubated cores without visible organisms.

Table 5.5: List of total benthological activities during the Kara Sea expedition SIRRO 2001

LBC = Large Box Corer; MUC = Multicorer; EBS = Epibenthos sledge

Station	Date	Depth (m)	SIRRO 2001				ESTABLISH	
			LBC	Dredge	MUC	EBS	Okean - Grab	Meiofauna sample
BP-01-01	14.08.2001	39	2	0	0	1	2	1
BP-01-03	15.08.2001	15	0	0	0	0	2	1
BP-01-04	16.08.2001	21	0	0	0	0	2	1
BP-01-05	16.08.2001	13	0	0	0	0	2	1
BP-01-06	17.08.2001	16	0	0	0	0	2	1
BP-01-08	17.08.2001	29	0	0	0	0	2	1
BP-01-09	18.08.2001	9	0	0	0	0	2	1
BP-01-11	18.08.2001	10	0	0	0	0	3	1
BP-01-14	19.08.2001	21	0	0	0	0	2	1
BP-01-16	19.08.2001	27	0	0	0	0	2	0
BP-01-17	20.08.2001	17	0	0	0	0	2	0
BP-01-18	21.08.2001	11	0	0	0	0	2	0
BP-01-19	21.08.2001	26	0	0	0	0	2	1
BP-01-20	21.08.2001	14	0	0	0	0	2	0
BP-01-22	22.08.2001	14	0	0	0	0	3	0
BP-01-23	22.08.2001	21	0	0	0	0	2	1
BP-01-24	22.08.2001	41	0	0	0	0	2	0
BP-01-26	23.08.2001	33	0	0	0	1	0	0
BP-01-28	24.08.2001	51	2	1	0	0	2	0
BP-01-30	24.08.2001	47	2	0	0	0	0	0
BP-01-31	25.08.2001	88	2	0	0	0	2	0
BP-01-34	25.08.2001	92	2	1	0	0	0	0
BP-01-35	26.08.2001	142	2	0	0	0	1	0
BP-01-37	26.08.2001	144	2	0	0	0	0	0
BP-01-38	27.08.2001	111	2	1	X	0	0	0
BP-01-39	27.08.2001	102	0	0	0	0	2	0
BP-01-40	27.08.2001	53	2	0	0	0	0	0
BP-01-41	28.08.2001	42	2	1	X	0	0	0
BP-01-42	28.08.2001	45	0	0	0	0	2	0
BP-01-43	28.08.2001	43	2	0	0	0	0	0
BP-01-45	29.08.2001	87	2	1	X	1	0	0
BP-01-46	30.08.2001	295	2	1	X	0	2	0
BP-01-48	31.08.2001	202	2	1	X	0	0	0
BP-01-49	31.08.2001	198	0	0	0	0	2	0
BP-01-51	31.08.2001	158	2	0	0	0	0	0
BP-01-52	01.09.2001	75	2	0	0	0	0	0
BP-01-55	01.09.2001	76	2	0	0	1	2	0
BP-01-56	02.09.2001	176	2	1	0	0	0	0
BP-01-58	02.09.2001	79	2	0	0	0	1	0
BP-01-59	03.09.2001	160	2	0	0	0	0	0
BP-01-60	03.09.2001	80	0	0	0	0	2	0
BP-01-61	03.09.2001	112	2	0	X	1	0	0
BP-01-62	04.09.2001	135	2	1	0	0	0	0
BP-01-63	04.09.2001	88	0	0	0	0	2	0
BP-01-64	04.09.2001	99	2	0	0	0	0	0
BP-01-65	05.09.2001	58	2	1	X	0	0	0
BP-01-66	05.09.2001	49	2	1	0	1	0	0
BP-01-67	06.09.2001	49	2	1	0	0	2	0
BP-01-68	06.09.2001	31	2	0	0	1	0	0
BP-01-70	07.09.2001	22	2	1	X	0	2	0
BP-01-72	08.09.2001	24	0	0	0	0	2	0
BP-01-73	09.09.2001	13	0	0	0	0	2	0
BP-01-77	09.09.2001	13	0	0	0	0	2	0
BP-01-80	10.09.2001	15	2	0	0	0	3	1
BP-01-82	11.09.2001	29	2	1	0	0	1	1
<b>total</b>			<b>60</b>	<b>14</b>	<b>8</b>	<b>7</b>	<b>70</b>	<b>13</b>

## 6.1 Sediment sampling program

*F. Schoster<sup>1</sup>, H. Deubel<sup>1</sup>, K. Dittmers<sup>1</sup>, A. Eulenburg<sup>1</sup>, M. Levitan<sup>3</sup>, F. Niessen<sup>1</sup>, J. Simstich<sup>2</sup>, R. Stein<sup>1</sup>, and T. Steinke<sup>1</sup>*

<sup>1</sup> Alfred Wegener Institute for Polar and Marine Research, Bremerhaven and Potsdam, Germany

<sup>2</sup> GEOMAR Research Center for Marine Geosciences, Kiel, Germany

<sup>3</sup> Vernadsky Institute of Geochemistry and Analytical Chemistry RAS, Moscow

In this expedition of “Akademik Boris Petrov 2001” main objectives were studying and sampling the northern part of the Kara Sea and the Ob Estuary and Ob River in the south (Fig. 6.1). Compared to the former expeditions of the “Akademik Boris Petrov” in the years 1999 and 2000 the working area and the working time were larger (Stein and Stepanets 2000, Stein and Stepanets 2001). The working area reached ca. from 72° E until 90°E and from 78°N down to 68°N. The working time was 29 days in the working area. Due to participating of members of a Russian/Norwegian-Project it was possible to get water and sediment samples also in the Yenisei River. In the southern region of the working area the samples were taken along the salinity gradient from the outer estuaries of Ob and Yenisei down to the fresh water endmember. The water column and the sediments were generally sampled at the same stations in order to study the relationship between modern processes in the surface waters and their reflection in the surface sediments.

Based on the sediment echograph profiling the geological stations were selected. After arriving and anchoring at the station in the shallower water (water depth <70 m) the water sampling started. When this was finished the geological sampling started usually with the Okean Grab, the Giant Box Corer and the Multicorer in order to take samples from the surface and near-surface sediments. For long sediment cores the Gravity Corer was used in lengths of 3, 5 and 8 m. At the stations with deeper water depths (water depths >70 m) anchoring was not possible. Changes in the position due to drifting were documented in the stationlist.

### Okean Grab

The Okean Grab is of light weight, and therefore, needs less time to get a small amount of surface sediment.

### Giant Box Corer

The Giant Box Corer (weight of ca. 500 kg; volume of sample 50\*50\*60 cm; manufactured by Fa. Wuttke, Henstedt-Ulzburg, Germany) was successfully used 96 times on 49 stations. Three times the box was destroyed due to hard sediment surface, only two box corers were disturbed, and four box corer were overfilled due to overpenetration. The recovery generally varied between 20 and 68 cm. The box cores were sampled for the following investigations:

- surface sediments
- stable isotope analysis of benthic calcareous organisms (Geomar)

- 10\*10 from the upper 1 cm (100 cm<sup>3</sup>) fixed with bengal-rose-methanol-solution
- 10\*10 from the upper 5 mm (50 cm<sup>3</sup>)
- benthic foraminifera and stable isotopes (Shirshov-Institute)
  - 1-3 times 10\*10 from the upper 1 cm (100 cm<sup>3</sup>) fixed with bengal-rose-methanol-solution
- studies on benthic macrofauna (AWI-Biology)
- organic geochemistry (Vernadsky-Institute)
- radionuclides analysis (Norway)
- radionuclides analysis (Taifun, Moscow)
  
- profiles (tubes 120 mm in diameter)
  
- sedimentology, grain-size and clay mineralogy (AWI-Geology)
- organic geochemical bulk parameters (TOC, CaCO<sub>3</sub>, C/N-ratio, Rock Eval pyrolysis) and biomarkers as well as  $\delta^{13}\text{C}$  of specific biomarkers (AWI-Geology)
- organic geochemistry, radio-nuclides (Vernadsky-Institute)
- benthic foraminifera (Shirshov-Institute)
- radionuclides analysis (Norway)
- radionuclides analysis (Taifun, Moscow)

### Multicorer

The standard 12-tubes-version multicorer (weight of 495 kg; manufactured by Fa. Wutke, Henstedt-Ulzburg, Germany) with an inner tube diameter of 6 cm was used. The penetration weight was always 250 kg. The multicorer was successfully used 49 times on 32 stations, and usually recovered undisturbed surface sediments and overlying bottom water. Three multicorer were empty due to technical problems.

surface sediments

- Benthic oxygen consumption measurements (AWI Biology)
  - 3-4 tubes
  - Copepodes (Juveniles) (AWI-Biology)
  - 3-4 tubes, 30 – 80 cm<sup>3</sup>
  - Phyto-zoo-plankton (AWI-Biology)
  - 2-3 tubes, 20 – 60 cm<sup>3</sup>
  - stable isotope analysis of benthic calcareous organisms (Geomar)
  - 1-3 tubes, 10 – 60 cm<sup>3</sup>, from the upper 1 cm fixed with bengal-rose-methanol-solution to stain living organisms
  - inorganic geochemistry (AWI-Geology)
  - 2 tubes, ca. 20 cm<sup>3</sup>
  - clay minerals (AWI-Geology)
  - 1 tube, 10 – 20 cm<sup>3</sup>
  - palynology (AWI-Geology)
  - 1 tube, 10 – 20 cm<sup>3</sup>
  - biomarkers and  $\delta^{13}\text{C}$  of specific biomarkers (AWI-Geology)
  - 1 tube, 10 – 20 cm<sup>3</sup>, stayed frozen at -20°C
  - organic geochemical bulk parameter (TOC, C/N, Rock Eval pyrolysis, CaCO<sub>3</sub>) (AWI-Geology); 1 tube, 10 – 20 cm<sup>3</sup>
- profiles



- organic geochemical analysis ( $C_{org}/N$ , carbonate, biogenic silica (Opal), carbohydrates, amino acids) (IfBM)

1 tube, samples ( $20\text{ cm}^3$ ) from the upper 3 cm, stored frozen at  $-20^\circ\text{C}$ , tube sampled at 5 cm intervals and additionally at lithological changes, stored at  $-20^\circ\text{C}$

- organic geochemistry (Vernadsky-Institute)

In addition, bottom water (100 ml), was sampled from the multicorer tubes for stable isotope measurements (Geomar).

#### Gravity Corer

The Gravity Corer has a penetration weight of 1.5 t and is used in 3, 5 and 8 m long core barrels. The diameter is 12 cm. The gravity corer was used on 55 stations for 62 times. Only two cores were empty due to stiff or hard sediment layers near to the surface. The other cores vary in the recovery of sediments from 0.10 up to 7.43 m (Fig. 6.2, Tab. 6.1). Most of the cores showed a brownish colored sediment at the top indicating that the near-surface sediments have been recovered. After recovery the cores were cut in segments of 100 cm length and stored in the cold. Double cores were taken at 9 stations (Tab. 6.1), 10 cores were opened, described and sampled for methane/pore water/heavy mineral investigations (Tab. 6.1). Core descriptions are presented in the annex.

Table 6.1: Penetration and recovery of gravity corer. (SL-3 (5 or 8): 3 (5 or 8) m core barrel (methane: methane and pore water sampling, CC: core catcher).

Core	Recovery	Penetration	Gear	Kodina-Core	Remarks
BP01-01/9	24	50	SL-5		
BP01-03/3	689	800	SL-8		
BP01-03/4	647	800	SL-8	x	
BP01-25/2	705	830	SL-8		Position BP99-04/7
BP01-26/3	526	650	SL-8	x	Position BP99-03/7; ikaite
BP01-28/7	488	600	SL-8		
BP01-29/2	174	300	SL-5		
BP01-30/6	0	30	SL-8		Basement ("Anstehendes")?
BP01-31/6	657	800	SL-8		
BP01-32/2	638	800	SL-8		
BP01-32/3	627	800	SL-8		
BP01-33/2	743	760	SL-8		
BP01-34/7	488	530	SL-5	x	Nannos, forams in ss
BP01-34/8	433	500	SL-8		
BP01-35/6	536	650	SL-8		
BP01-36/2	616	750	SL-8		
BP01-37/6	619	800	SL-8		
BP01-38/7	624	800	SL-8		
BP01-38/8	633	800	SL-8	x	
BP01-39/2	538	750	SL-8		
BP01-40/6	193	200	SL-8		stiff clay
BP01-41-7	457	500	SL-5		
BP01-42/2	572	800	SL-8		
BP01-43/7	344	400	SL-5		
BP01-43/8	329	400	SL-5	x	
BP01-44/2	309	350	SL-8		sandy?
BP01-45/6	490	750	SL-8		
BP01-46/2	234	250	SL-5		stiff clay (overconsolidated?)
BP01-47/3	259	350	SL-5	x	stiff clay (overconsolidated?)
BP01-47/4	405	500	SL-5		stiff clay (overconsolidated?)
BP01-48/7	469	700	SL-8		
BP01-49/2	384	450	SL-5		stiff clay (overconsolidated?)
BP01-50/2	211	250	SL-5		stiff clay (overconsolidated?); Stein (3cm) außen an CC
BP01-51/5	392	600	SL-8		
BP01-52/5	369	600	SL-8		
BP01-53/2	0	0	SL-5		end morain?
BP01-54/2	10	10	SL-5		extremely stiff clay
BP01-55/5	317	350	SL-5	x	H2S: ikaite
BP01-55/6	424	500	SL-5		no H2S!
BP01-56/5	245	400	SL-5		
BP01-57/2	274	300	SL-5		
BP01-58/5	589	800	SL-8		H2S
BP01-59/5	606	800	SL-8		
BP01-60/2	29	30	SL-5		end morain?
BP01-61/7	566	800	SL-8		
BP01-62/5	580	800	SL-8		
BP01-62/6	582	820	SL-8		
BP01-63/2	14	30	SL-3		end morain?
BP01-64/6	492	600	SL-5	x	surface missing
BP01-64/7	536	800	SL-8		
BP01-65/6	56	70	SL-5		
BP01-67/7	71	100	SL-5	x	

Core	Recovery	Penetration	Gear	Kodina-Core	Remarks
BP01-68/6	11	40	SL-5		
BP01-70/7	639	820	SL-8		
BP01-71/3	234	250	SL-5		
BP01-71/4	232	250	SL-5	x	
BP01-72a/2	467	510	SL-5		
BP01-73/5	222	250	SL-5		
BP01-80/6	150	200	SL-5		
BP01-82/7	229	300	SL-5		
BP01-82/8	213	300	SL-5	x	
BP01-83/2	730	780	SL-5		Position BP00-38/2
	24340				

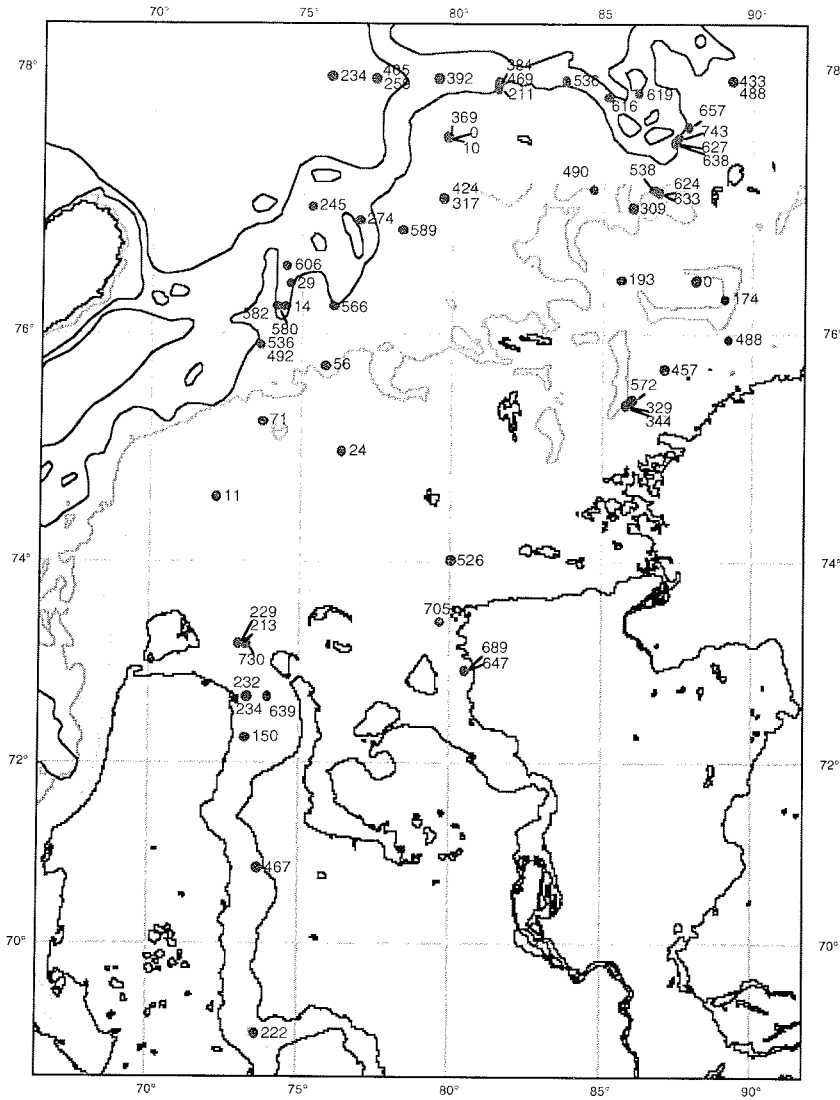


Fig. 6.1: Gravity Corer stations (SL) and recovery during „Akademik Boris Petrov“ Expedition 2001

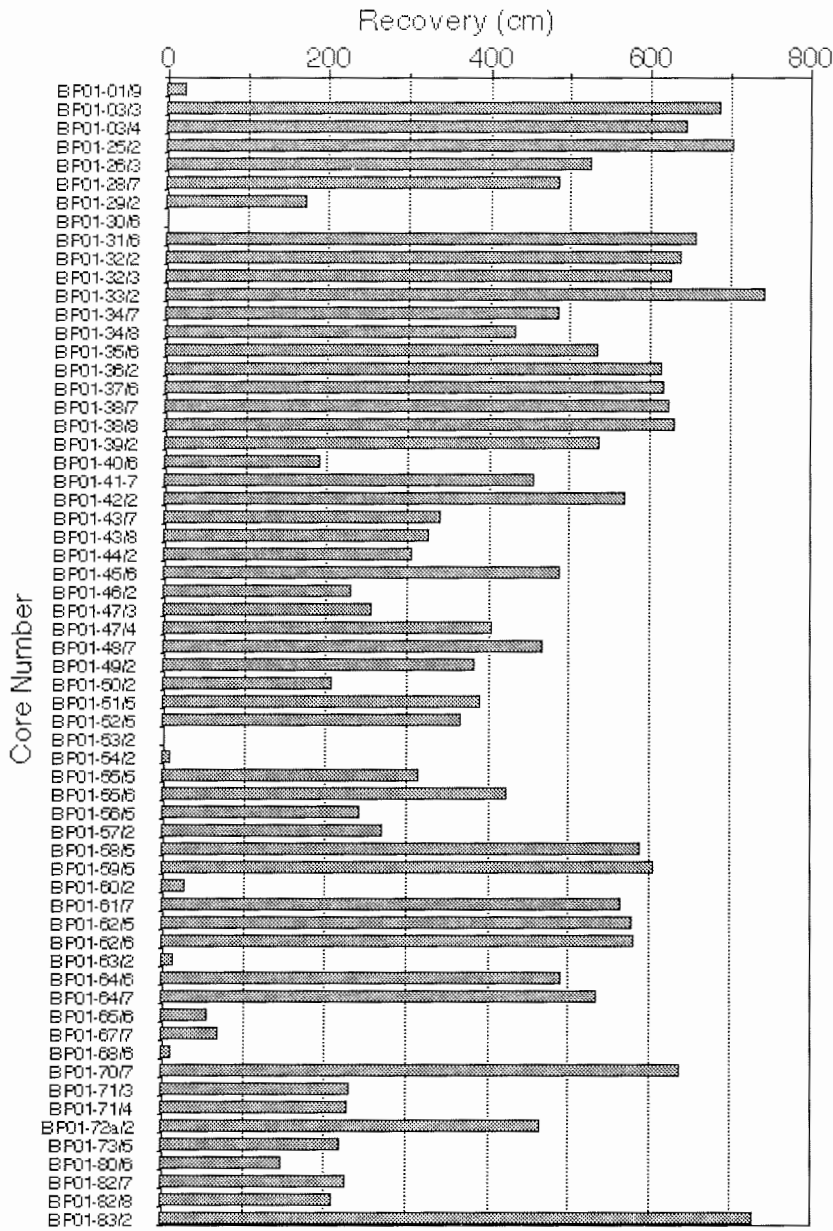


Fig. 6.2: Recovery of gravity cores during “Akademik Boris Petrov” Expedition 2001.

## 6.2. Chirp and ELAC sediment echograph profiling

(F. Niessen, K. Dittmers)

During cruise BP01 sediment echosounding was carried out using two different systems (Tab. 6.2):

1. The hull-mount echograph ELAC was set to an operating frequency of 12 kHz and was in operation during 24 h per day along all cruise lines in the area of investigation.
2. In addition to the ELAC a portable chirp system was used along selected lines. Transducers and underwater electronics are mounted in a catamaran towed by the vessel and are connected via deck cable to the control unit in the rear laboratory. The chirp frequency range was set to 2-8 kHz.

For both ELAC and GeoChirp signal output was improved by set of mobile system components which were hooked up in the rear laboratory of the vessel. These components are parts of the mobile sediment echosounding system of AWI. Previous results from the AWI Chirp system were described from arctic lakes (Hubberten et al. 1995, Niessen et al. 1999).

On RV Boris Petrov the system was connected as illustrated in Figure 6.3 and listed in Table 6.2. Amplification, filtering, data storage (analog), digitising including import of navigation data, processing and high quality on-line plus replay printing was carried out. The system has its own GPS antenna (during BP01 placed on a container on the helicopter deck of RV Boris Petrov), amplifier and receiver. Along cruise lines, where only the ELAC system was in operation, system trigger and signal output ports (pre-amplified by the hull-mount ELAC unit in the control room behind the bridge according to Table 6.2) were connected via the ship-wiring-system into the portable AWI-system in the rear laboratory (Fig. 6.3). In comparison to the use of the ELAC system on previous cruises of RV Boris Petrov (Stein & Stepanets 2000, 2001) this new configuration had the following advantages:

1. fast availability of sediment-echosounding information in the main working laboratory
2. screen-display of both GPS positions and ELAC subbottom information on-line without time lag
3. printing GPS positions and time on subbottom analog profiles in one-minute intervals for improving station selection
4. enhancement of geological information in acoustic subbottom images by selective signal amplification, filtering and processing (stack)
5. flexible (scale, contrast) high-quality printing of subbottom profiles on two line-scan recorders
6. simultaneous noise-less analog tape storage (DAT) of trigger, signal and GPS data
7. full data replay on demand

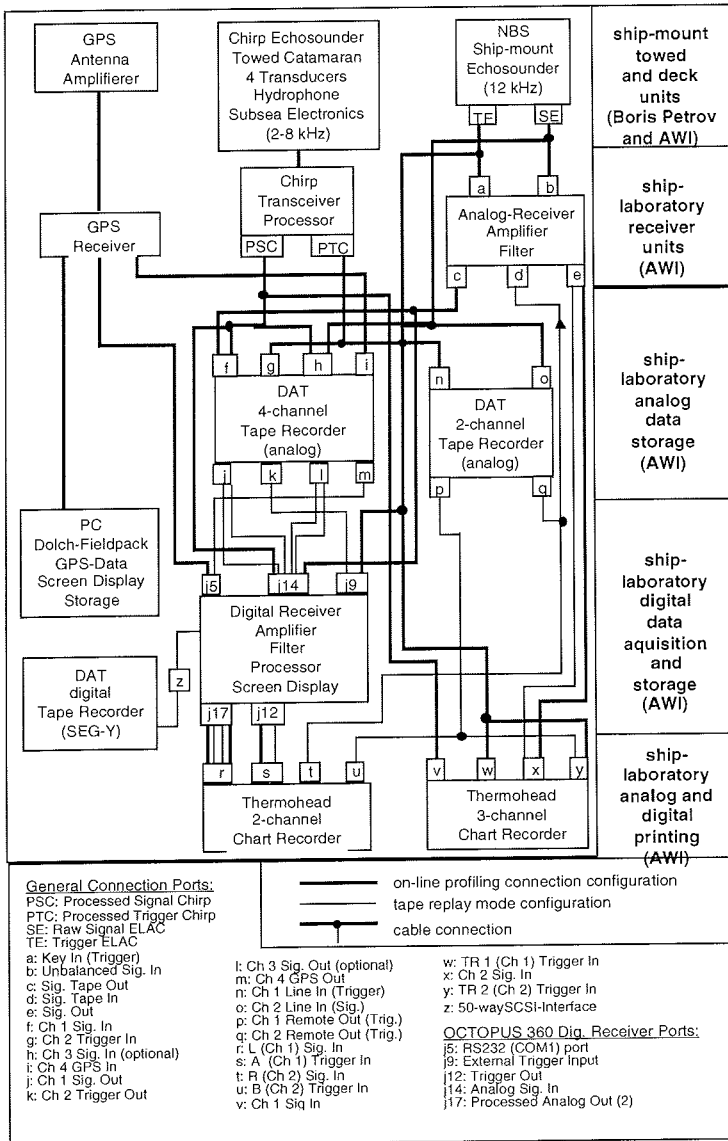


Figure 6.3: Connection diagram of different system components of the high-resolution sediment echosound systems used during BP01. For technical details of the individual components see Tab. 6.3.

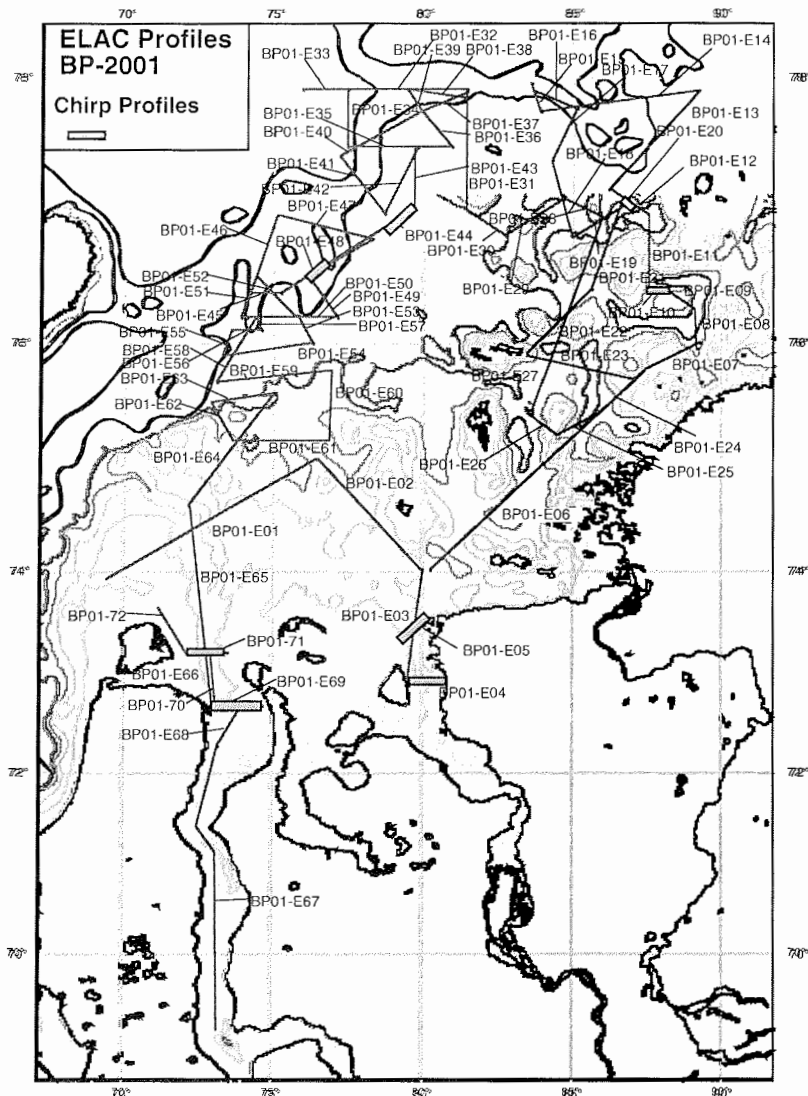


Figure 6.4: Map of ELAC and Chirp profiles recorded during BP01.

Unfortunately the DAT digital tape recorder for storing individual seismic traces in SEG-Y format (Fig. 6.3) failed shortly after the beginning of the data acquisition and could not be repaired on board. Along those lines, where the GeoChirp system was used in addition to the ELAC system, chirp trigger and signal were given a higher priority and connected with the GPS, 4-channel DAT recorder and digital receiver. In this mode, ELAC signal and trigger were stored on a 2-channel DAT-recorder simultaneously with the 4-channel data storage of the chirp (Fig. 6.3). As a result of the stable good weather



and calm sea during almost the entire cruise we did not apply heave filtering to the data. Two-way travel times in seismic images are converted to meter using a sound velocity of 1500 m/s.

Tab. 6.2: Technical specifications of sediment echosound system components used during BP01.

Component (Fig.1)	Model	Manufacturer	Settings
		Country	
NBS-Echosounder	ELAC-LAZ 72	Honeywell-Nautic Germany	Pulse: 12 kHz, level 3 Amplification: 11 (max) Range: 1 (0-200) 100x1
Chirp-Echosounder	GeoChirp	GeoAcoustics UK	Mode: High Penetration Trigger: 4:1 (<100m) Trigger: 2:1 (>100m)
Analog Receiver	5210	GeoAcoustics UK	Filter: 3-15 kHz Gain: 20 + 24 dB, 0 dB input Tape Output: filtered
DAT Recorder 4-Channel	PC204Ax	Sony Japan	Amplification: CH1-4: 0.5-5-5-5 Speed: normal
DAT Recorder 2-Channel	Walkman	Aiwa Japan	Speed: normal
Digital Receiver	360	Octopus UK	Sample Rate: 24 kHz Initial Gain: x10 Filter: 3.5-9.98 kHz
Chart Recorder 2-Channel	Waverly 3710	Dowty UK	Sweep: 150 or 300 ms Grid-Line-Spacing: 15 ms (10 m)
Chart Recorder 3-Channel	120-138	Ultra UK	Sweep: 150 or 300 ms Grid-Line-Spacing: 15 ms (10 m)

In total of 5200 km of ELAC profiles were recorded along 72 lines (Fig. 6.4, Tab. 6.3). In addition 8 chirp profiles with a total length of about 144 km were recorded for more detailed analysis of different acoustic facies and stratigraphy within the area of investigation (Fig. 6.4, Tab.6.3). The objectives are two-fold: (i) to search for evidence of glaciation in the Kara Sea during the last glacial maximum (LGM, marine isotope stage 2), and, (ii) to trace paleoriver channels on the open Kara shelf and to study the glacial and post glacial depositional history with respect to Siberian river runoff. These studies will be part of PhD thesis (K. Dittmers) currently carried out at AWI.

The different acoustic character of the chirp and ELAC systems are compared along a W-E line across the outer part of the Yenesei Estuary (Fig. 6.5, see also Stein & Stepanets 2000). Along this profile the total sound penetrations of both systems are almost similar and limited by a strong basal reflector located at about 16 m subbottom in the centre of the acoustic images (Fig. 6.5). Above the basal reflector, the Chirp profile is differentiated by numerous distinct reflectors whereas the ELAC image appears more diffuse. Some stratification is defined by different ELAC acoustic

backscatter of the upper and lower half of the sediments overlying the base reflector, respectively. The acoustic facies of relatively thick muds associated with channel-overbank morphologies (Fig. 6.5) is typical for the outer areas of the Ob and Yenesei estuaries.

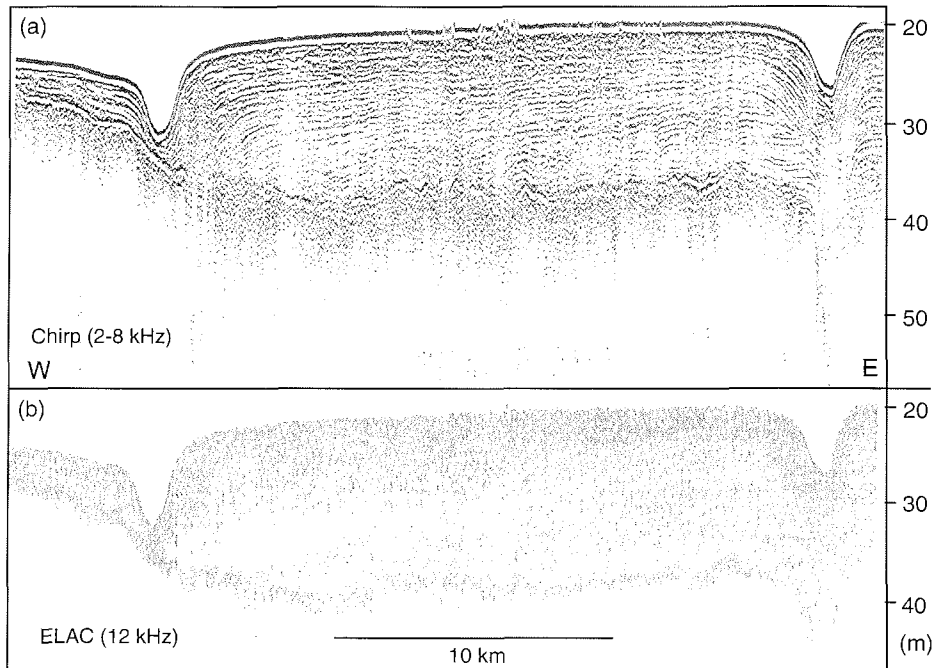


Figure 6.5: Comparison of Chirp (a) and ELAC (b) sediment echosound profiles from the Yenisei estuary. Note that both profiles were recorded simultaneously. Profile no. BP-C01 (a) and BP-E04 (b), start and end positions in Tab.6.3.

Based on both relief and acoustic penetration/resolution different types of acoustic facies are identified in the inner and middle shelf areas under investigation. In ELAC images the north-west area is characterised by hummocky morphologies superimposed on several major subbottom ridges and furrows (Fig. 6.6). Sea floor backscatter is high and undifferentiated sediment penetration restricted to a few meters in general. A preliminary ship-board interpretation suggests that the relief has been formed by advances and retreats of a LGM Barents-Kara Sea ice sheet. The eastern boundary of this north-western facies forms a relatively sharp line which can be mapped (Stein et al. submitted). Furthermore, in places of this north-western acoustic facies, sediment penetration can increase up to 20 m above the strong reflector observed in this area (Fig. 6.7). These sediment complexes appear well stratified, are of limited width (on the order of 5 km) and associated with channel-overbank morphologies somehow similar to sediments found in the outer Ob and Yenesei estuaries (Fig. 6.5). The fact that these sediment complexes overly formerly glaciated terrain implies deposition after deglaciation. A possible association of these sediment complexes with early Holocene Siberian river runoff will be investigated by AWI in more detail.

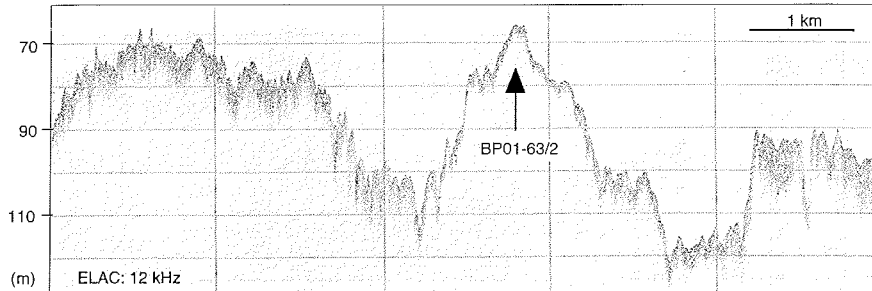


Figure 6.6: Section of ELAC profile BP-E50 between  $76^{\circ}12'N$ ,  $74^{\circ}39.8'E$  (left: 03.09.01, 01:15UTC) and  $76^{\circ}12'N$ ,  $74^{\circ}21.2'E$  (right: 03.09.01, 01:40UTC) as typical example of the north-western facies. Arrow marks location of core BP01-63/2.

In contrast to the north-western facies, the central and south-eastern acoustic facies is characterised by smooth relief. The relatively flat sea floor is cut by several wide channels or paleovalleys (Fig. 6.8). Acoustic penetration is usually minor associated with strong backscatter and lack of stratification. Within the channels or valleys the penetrated sediment cover is on the order of 10 m exhibiting several weak reflectors (Fig. 6.8).

In the north-eastern area of investigation the sea floor bathymetry is more variable showing deeper water associated with wider depressions separated by ridges. In depressions an additional acoustic facies is observed which is characterised by deep sound penetration and well stratified records comprising numerous distinct reflectors. In ELAC acoustic images penetration can be more than 25 m. Often the top 5 m of the sequences show higher backscatter whereas the lower part of the sequence is more transparent intercalated with thin but distinct sub-parallel reflectors (Fig. 6.9). In greater sediment depth reflections become very weak and no typical basal reflector is visible in this facies. In a chirp profile from this area (Fig. 6.10) reflectors can be observed to a sediment depth of approximately 60 m. Below this depth backscatter becomes too weak to interpret the record. Also, no distinct basal reflector is notable in chirp images in the deepest areas of these depressions. In contrast to the distinct sub-parallel reflectors in the lower sequence, the top layer is acoustically transparent and more variable in thickness from about 8 m to only a few cm in places (Fig. 6.10).

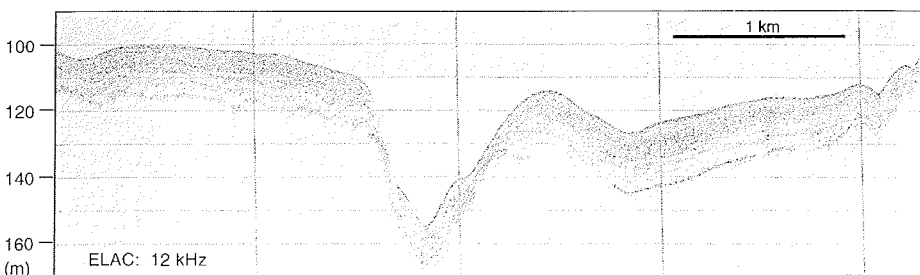


Figure 6.7: Section of ELAC profile BP01-E58-E59 between  $75^{\circ}42.7'N$ ,  $73^{\circ}18.37'E$  (left: 04.09.01, 16:50UTC) and  $75^{\circ}40.08'N$ ,  $73^{\circ}15.2'E$  (right: 04.09.01, 17:10UTC) as typical example of channel-overbank complexes overlying north-western facies.

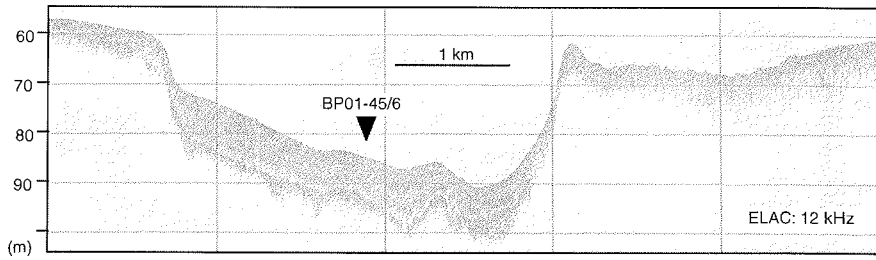


Figure 6.8: Section of ELAC profile BP01-E17 between 77°09N, 84°41.4E (left: 26.08.01, 22:48UTC) and 77°04.4N, 84°45E (right: 27.08.01, 23:12UTC) as typical example of the south-eastern facies.

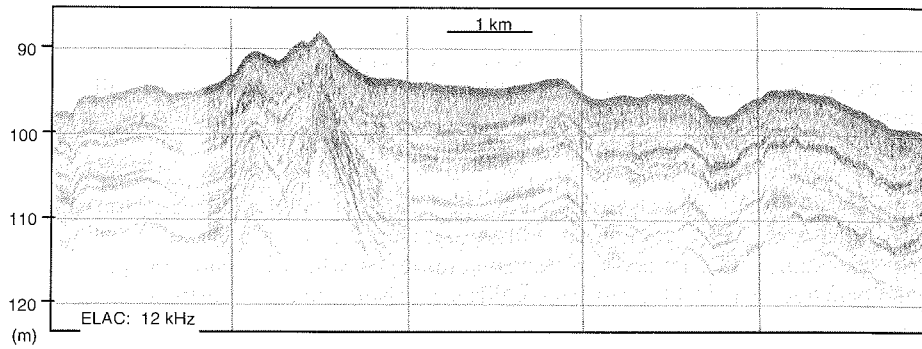


Fig. 6.9: Section of ELAC profile BP01-E11 between 77°21N, 86°57E (left: 25.08.01, 01:40UTC) and 77°24.8N, 87°14.1E (right: 25.08.01, 02:05UTC) as typical example of the north-eastern facies.

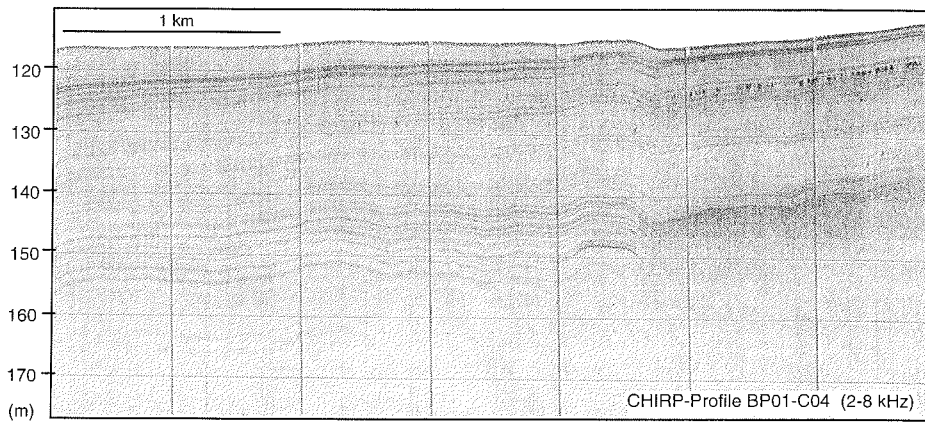


Figure 6.10: Section of Chirp profile BP01-C04 between 77°05.2N, 86°55.8E (left: 27.08.01, 23:45UTC) and 77°06.4N, 86°47.5E (right: 27.08.01, 23:58UTC) as typical example of the north-western facies.

Tab. 6.3: List of ELAC and Chirp profiles recorded during BP01

Date	Number	Beginning Latitude (N)	Longitude (E)	End Latitude (N)	Longitude (E)	Direction	Remarks
14.08.	BP01-E01	73°55'	69°30'	75°	76°30'	SW-NE	BP01-01
14./15.08.	BP01-E02	75°	76°30'	74° 0.3'	80°0.45'	NW-SE	BP01-01, -02
15.08.	BP01-E03	74° 0.3'	80°0.45'	72°56'	79°35'	NNE-SSW	
15.08.	BP01-E04	72°56'	79°35'	72°56'	80°45.2'	W-E	
22.08.	BP01-E05	73°20'	79°23'	73°32.6'	80°08'	SW-NE	BP01-03, BP99-08, BP99-09; Chirp Profile BP01-C01
23./24.08.	BP01-E06	74°0.07'	80°19.87'	73°46'	87°28'	SW-NE	BP01-25/BP99-04, BP99-05, BP00-23; Chirp Profile BP01-C02
24.08.	BP01-E07	75°46'	87°28'	75°59'	89°23'	mix	BP01-41, -42, -43
24.08.	BP01-E08	75°56.4'	89°15.9'	76° 16.03'	89°07.69'	SSE-NNW	BP01-28
24.08.	BP01-E09	76° 16.03'	89°07.69'	76°24.75'	88°10.76'	SE-NW	BP01-28, -29
24.08.	BP01-E10	76°24.7'	88°14.8'	76°24.7'	87°33'	E-W	BP01-29, -30
24./25.08.	BP01-E11	76°24.7'	87°33'	77°	87°33'	S-N	BP01-30; Chirp Profile BP01-C03
25.08.	BP01-E12	77°	87°33'	77°11'	86°15'	SE-NW	BP01-38, -39
25.08.	BP01-E13	77°11'	86°15'	77°54.29'	89°20.15'	SW-NE	BP01-31, -32, -33, -34
25.08.	BP01-E14	77°54.29'	89°20.15'	77°45'	84°	ENE-WSW	BP01-36, -37
26.08.	BP01-E15	77°45'	84°	77°57'	83°40'	SSE-NNW	BP01-35
26.08.	BP01-E16	77°54.3'	83°45.94'	77°47.1'	85°12.6'	NW-SE	BP01-35, -36
26./27.08.	BP01-E17	77°48.9'	86°12.7'	77°24.5'	84°24'	NE-SW	BP01-37
27.08.	BP01-E18	77°24.5'	84°24'	76°50'	85°	NNW-SSE	BP01-45
27.08.	BP01-E19	76°50'	85°	77°05.2'	86°55.8'	SW-NE	BP01-38, -44
27.08.	BP01-E20	77°05.2'	86°55.8'	77°06.79'	86°44.87'	SE-NW	BP01-38, -39; Chirp Profile BP01-C04
27.08.	BP01-E21	77°06.79'	86°44.87'	76°25.2'	85°39.9'	NNE-SSW	BP01-39, -40
28.08.	BP01-E22	76°25.2'	85°39.9'	75°54'	83°35'	NE-SW	BP01-40
28.08.	BP01-E23	75°54'	83°35'	75°41.35'	87°08.1'	ENE-WSW	BP01-41
28.08.	BP01-E24	75°41.35'	87°08.1'	75°23'	85°49.9'	NE-SW	BP01-41, -42, -43, part of BP01-E06

Date	Number	Beginning Latitude (N)	Longitude (E)	End Latitude (N)	Longitude (E)	Direction	Remarks
28.08.	BP01-E25	75°23'	85°49.9'	75°13'	84°33'	NE-SW	
28.08.	BP01-E26	75°13'	84°33'	75°23'	83°41'	SE-NW	BP00-32, -33, -34, -35
29.08.	BP01-E27	75°23'	83°41'	76°58.25'	86°02.2'	SSW-NNE	BP01-40, -44
29.08.	BP01-E28	76°58.23'	86°01.9'	77°06.8'	84°44'	SE-NW	BP01-44, -45
29.08.	BP01-E29	77°06.8'	84°44'	76°50'	82°50'	NE-SW	BP01-45
29.08.	BP01-E30	76°50'	82°50'	77°02'	81°30'	SE-NW	BP00-36
29.08.	BP01-E31	77°02'	81°30'	77°55'	81°30'	S-N	BP01-48, -49, -50
30.08.	BP01-E32	77°55'	81°30'	77°55'	76°	E-W	BP01-46, -47, -51
30.08.	BP01-E33	77°55'	76°	77°55'	77°30'	W-E	BP01-46, -47
30.08.	BP01-E34	77°55'	77°30'	77°30'	77°30'	N-S	BP01-47
30.08.	BP01-E35	77°30'	77°30'	77°30'	81°	W-E	BP01-52, -53, -54
31.08.	BP01-E36	77°30'	81°	77°45'	80°	SE-NW	
31.08.	BP01-E37	77°45'	80°	77°53.5'	81°30'	SW-NE	BP01-48
31.08.	BP01-E38	77°50.9'	81°30'	77°54.7'	79°29.5'	ESE-WNW	BP01-50, -51
31.08.	BP01-E39	77°54.7'	79°29.5'	77°45'	80°	NW-SE	BP01-51
31.08.	BP01-E40	77°45'	80°	77°26'	77°15'	NE-SW	
01.09.	BP01-E41	77°26'	77°15'	77°	78°47'	NW-SE	
01.09.	BP01-E42	77°	78°47'	77°30'	79°52'	SW-NE	BP01-52
01.09.	BP01-E43	77°30'	79°46.2'	77°03'	79°44'	N-S	BP01-54, -55
01.09.	BP01-E44	77°03'	79°44'	76°23'	75°20'	NE-SW	BP01-55; Chirp Profile BP01-C05
02.09.	BP01-E45	76°23'	75°20'	76°23'	74°20'	E-W	BP01-60
02.09.	BP01-E46	76°23'	74°20'	76°59.6'	75°10.3'	SW-NE	BP01-56, -59
02.09.	BP01-E47	76°59.6'	75°10.3'	76°48.1'	78°21.2'	WNW-ESE	BP01-56, -57, -58
02.09.	BP01-E48	76°48.1'	78°21.2'	76°31.7'	76°16.4'	NE-SW	BP01-58; Chirp Profile BP01-C05
02.09.	BP01-E49	76°31.7'	76°16.4'	76°12'	77°12'	NW-SE	

73

Date	Number	Beginning		End		Direction	Remarks
		Latitude (N)	Longitude (E)	Latitude (N)	Longitude (E)		
03.09.	BP01-E50	76°12'	77°12'	76°12'	74°	E-W	BP01-61, -62, -63
03.09.	BP01-E51	76°12'	74°	76°31.2'	74°31'	SW-NE	BP01-59
03.09.	BP01-E52	76°31.2'	74°31'	76°12.1'	75°45.3'	NW-SE	BP01-59, -60, -61
03.09.	BP01-E53	76°12.9'	75°53.1'	75°59'	76°22'	NW-SE	BP01-61
04.09.	BP01-E54	75°59'	76°22'	75°53'	73°28'	ENE-WSW	BP01-64
04.09.	BP01-E55	75°53'	73°28'	76°05'	73°42'	SSW-NNE	
04.09.	BP01-E56	76°05'	73°42'	76°05'	74°42'	W-E	
04.09.	BP01-E57	76°05'	74°42'	76°12'	74°12'	SE-NW	BP01-62
04.09.	BP01-E58	76°12'	74°29.3'	75°40'	73°12'	NE-SW	BP01-63, -64
05.09.	BP01-E59	75°40'	73°12'	75°45'	77°	WSW-ENE	BP01-65
05.09.	BP01-E60	75°43'	75°50.8'	75°10'	76°55.1'	NW-SE	BP01-65, -66
05.09.	BP01-E61	75°10'	76°55.1'	75°10'	73°46'	E-W	BP01-66
06.09.	BP01-E62	75°10'	73°46'	75°30'	73°02'	SE-NW	
06.09.	BP01-E63	75°30'	73°02'	75°34'	75°10'	WSW-ENE	
06.09.	BP01-E64	75°34'	75°10'	74°35'	72°15'	NE-SW	BP01-67, -68
06.09.	BP01-E65	74°35'	72°15'	72°40'	73°05'	NNW-SSE	BP01-68
07.09.	BP01-E66	72°40'	73°05'	72°40'	74°45'	W-E	BP01-69, -70, -71
09./10.09.	BP01-E67	69°03.3'	73°13.7'	72°15'	73°15'	general S-N	BP01-79, -80
	BP01-E68	72°15'	73°15.2'	72°40'	74°05'	SW-NE	BP01-80, -81
	BP01-E69	72°40'	74°05'	72°40'	73°10'	E-W	BP-01-70, -71; Chirp BP01-C07
	BP01-70	72°40'	73°10'	73°11.8'	73°01.7'	S-N	BP01-82
	BP01-71	73°12'	73°33'	73°12'	72°10'	E-W	BP01-82, -83; Chirp BP01-C08
	BP01-72	73°12'	72°10'	73°35^	72°	SSE-NNW	

Marine Geology

### 6.3. Physical Properties of the Sediments

K. Dittmers and F. Niessen

Alfred Wegener Institute for Polar and Marine Research, Bremerhaven and Potsdam, Germany

#### Introduction

During the cruise of Boris Petrov 2001 the physical properties of 82 sediment cores with a total length of 240 m were logged with a MultiSensorCoreLogger. Density, p-wave velocity and magnetic susceptibility of the cores were measured.

Logging of these properties allows a first interpretation of sediment properties of unopened cores. Variation in the parameters reflect changes in sediment composition and porosity, so an indication for the lithology of the cores can be given (Thomson and Oldfield 1986, Weber et al. 1997). For example, a diamicton layer will show higher density, lower p-wave amplitude, higher p-wave velocity and - depending from the magnetisation of the accumulated grains- higher or lower magnetic susceptibility than the surrounding pelitic sediment.

Magnetic susceptibility is defined as the dimensionless proportional factor of an applied magnetic field in relation to the magnetization in the sample (expressed in SI units). Variations in magnetic susceptibility in sediments of the Eurasian part of the Arctic Ocean correlate with the content of ferrimagnetic grains (magnetite, titanomagnetite or maghemite; Thompson and Oldfield 1986). These minerals are more abundant in volcanic and metamorphic rocks (e.g. Putoran Plateau Basalts). Thus susceptibility acts as a good indicator for terrestrial derived material. Furthermore the Ob and Yenisei river signals can be differentiated, because of their very different geologies of the catchment areas. The Ob drains great parts of the West Siberian lowlands consisting of sedimentary rocks with low values in magnetic susceptibility. In contrast the Yenisei has a hinterland geology with source rocks of higher magnetic susceptibility, such as the volcanites of the Putoran Plateau.

#### Method

The Geotek MultiSensorCoreLogger (MSCL14) allows the logging of core thickness, p-wave travel time, attenuated gamma counts, magnetic susceptibility and temperature. For determining densities, gamma rays of a  $^{137}\text{Cs}$ -source are used. Magnetic susceptibility is measured with a BARTINGTON MS2C coil sensor the volume susceptibility (dimensionless, all values presented here are in  $10^{-5}$  in the SI-System). Dense material absorbs more gamma-radiation than light material, so this inverse relation can be used to correlate gamma—ray-absorption with density. Magnetic susceptibility is commonly used as an indicator for the mineralogical composition of the sediments and for lateral core correlation (e.g., Kleiber and Niessen 2000). It is defined as the dimensionless proportional factor of an applied magnetic field in relation to the magnetisation in the sample.

Technical details of the Multi Sensor Core Logger and the set up are given in Tab. 6.4. The logger was calibrated according to the method of Best et al. (1999).



After data processing, p-wave amplitude, p-wave velocity (normalized for 20°C), gamma density, magnetic susceptibility, acoustic impedance and fractional porosity can be computed.

In addition to normal p-wave measurements transmission seismograms were recorded (Breitzke et al. 1996, Breitzke 2000) which reveal grain size information.

Prior to logging the cores were stored in the laboratory for at least 24 hours to equilibrate with room temperature (mean temperature: 20°C). All cores were logged in 1 cm intervals. High-resolution logging was performed for Holocene key cores in increments of 0.5 cm. After each gravity core, a calibration liner filled with water and a stepped aluminium insert was logged (Best et al. 1999). This method serves to simulate different porosities and logging environments because aluminium as the solid component has a density and gamma-ray absorption coefficient close to natural dry grain density (2,7 g/cm<sup>3</sup>) (see Weber et al. 1997).

### Settings

Sensor offsets from the reference point:

γ-sensor	22 cm
p-wave-sensor	36 cm
susceptibility loop:	80 cm

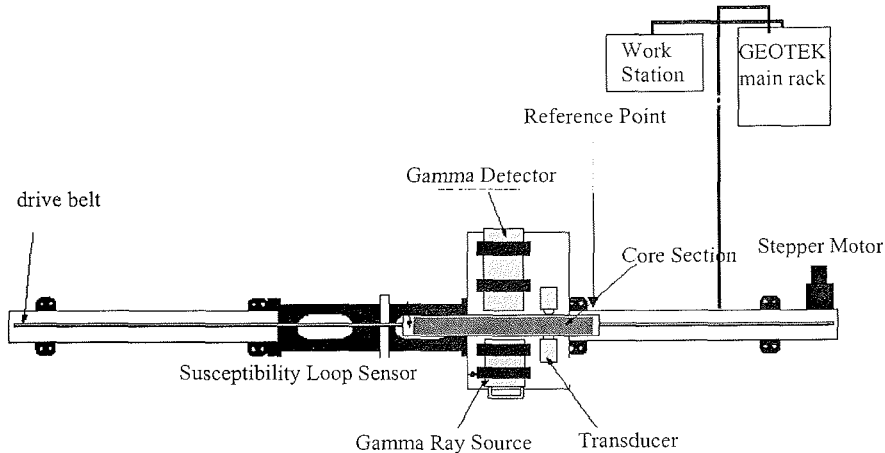


Fig. 6.11: Top view of set up of the MultiSensorCoreLogger

Sensors:

- a) Ultrasonic Transducers to measure the travel time of compressional p-waves through the core. 250 kHz piezo-electric ceramic transducers, spring-loaded against the sample. Accurate to about 0.2%, depending on core condition.
- b) A gamma ray source and detector for measuring the attenuation of gamma rays through the core. 137-Cs gamma source in a lead shield with 5 mm collimator. Density resolution of better than 1% depending upon count time.
- c) A magnetic susceptibility sensor to determine the amount of magnetically susceptible material present in the sediments. Bartington loop sensor with 140 mm coil diameter.
- d) Core diameter: The diameter of the core, including the liner, is measured using a pair of displacement transducers connected to the spring loaded compressional wave transducers. This enables the compressional wave velocity and density (from the gamma ray attenuation measurements) to be corrected for changes in core diameter.
- e) Temperature: An IR thermal sensor is employed 10 cm above the core. Surface core temperatures are logged and can be used to correct p-wave velocities for temperature changes that may occur during the logging process.

Table 6.4.: Sensor specifications

<p><b>P-wave Velocity and Core diameter</b></p> <p>Plate Transducer diameter: 5 cm          Transmitter pulse frequency: 250 kHz          Transmitted pulse repetition rate: 1 kHz          Received pulse resolution: 50 ns</p>
<p><b>Density</b></p> <p>Gamma ray source: Cs-137          Source activity: 356 MBq          Source energy: 0.662 MeV          Collimator diameter: 5.0 mm (SL), 2.5 mm (KAL)          Gamma detector: Gammasearch2, model SD302D, ser. no. 3019 , John Caunt Scientific Ltd., 15 sec counting time; 1 sec for quickies</p>
<p><b>Magnetic Susceptibility</b></p> <p>Loop sensor type: BARTINGTON MS-2C, ser. no. 130          Loop sensor diameter: 14 cm          Alternating field frequency: 565 Hz, counting time 10 s, precision <math>0.1 \times 10^{-5}</math> SI          Magnetic field intensity: about 80 A/m RMS</p>

The following figure (Fig. 6.12) shows an example of typical onboard measurements. In this case two parallel cores of one station were logged before one of the cores was opened on board. We used a special setup, which allowed logging of the cores very quickly (about 5 minutes per core meter, quicky -mode).

The physical properties are a useful tool for core correlation as well as sediment sampling of the opened cores. In combination with sediment echosounding (Niessen and Dittmers this volume) they are a useful tool for acoustic stratigraphy. Magnetic susceptibility proved to be an excellent tool for core correlation. In Fig. 6.13 the physical properties of all opened cores are listed. You find this data set on the Pangaea web site: [www.pangaea.de](http://www.pangaea.de).

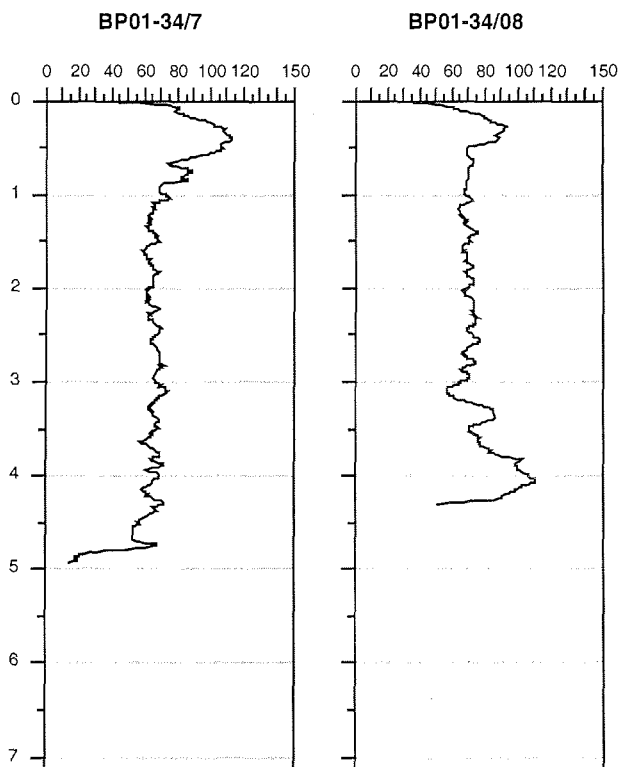
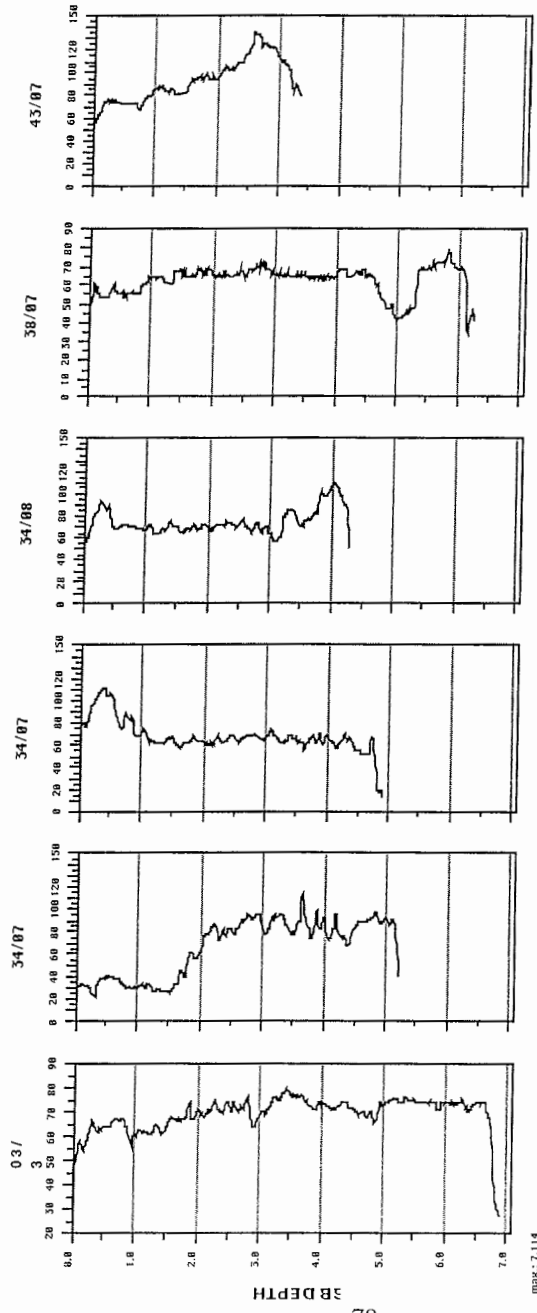
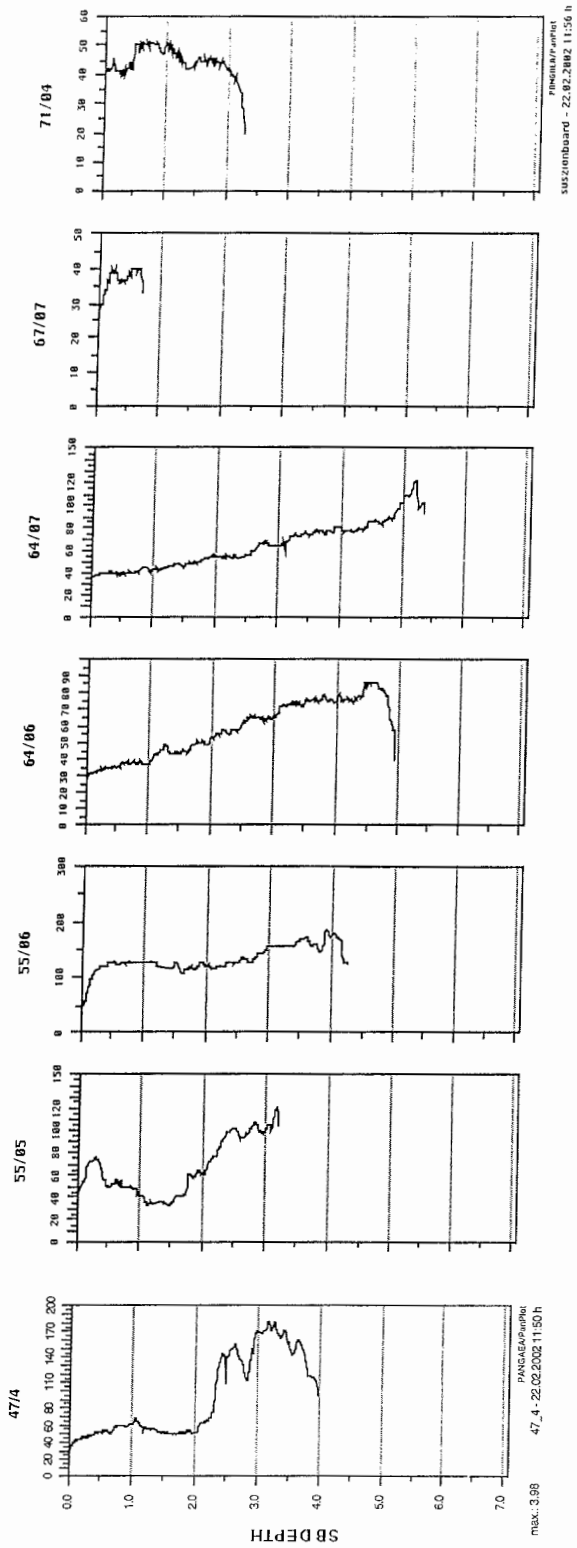


Fig. 6.12: Magnetic susceptibility of cores BP01-34/07 and BP01-34/08 which are situated in the north eastern corner of the working area. Although the cores have different lengths they include the same time interval. According to the curve the shorter core BP01-34/8 seems to penetrate older sediments than BP01-34/07.

Fig. 6.13: Magnetic susceptibility of cores all measured cores from the 2001 years expeditions.



Continued with Fig. 6.13:



#### 6.4 Composition of fraction $>63 \mu\text{m}$ of surface sediments from Ob, Taz, and Yenisei rivers and the southern Kara Sea

M.A.Levitan<sup>1,2</sup>

1 – Vernadsky Institute of Geochemistry and Analytical Chemistry RAS, Moscow, Russia;

2 – Shirshov Institute of Oceanology RAS, Moscow, Russia

##### Introduction

Facies pattern of recent sedimentation traditionally includes the results of joint study of environments and environments' reflection in lithology (grain-size, mineralogy, geochemistry, sedimentation rates, etc.) and taphocoenoses of recent sediments. In this relation a lot of information can be obtained by means of study the composition of sand (and gravel) fractions.

##### Facts and methods

During the SIRRO R/V "Akademik Boris Petrov" (2001) cruise we have sampled the surface-layer (0-1 cm) sediments of 41 stations (from 39 box-corers and 2 grab-samplers). The volume of individual sample was  $50 \text{ cm}^3$ . The samples have been undergone to wet sieving through sieves 63 and  $125 \mu\text{m}$ . Then two grain-size fractions ( $63\text{-}125$  and  $>125 \mu\text{m}$ ) have been dried at  $105^\circ\text{C}$  and examined separately under the binocular microscope. A counting has been done in semi-quantitative manner.

Table 6.6: Composition of fr.  $>125 \text{ mkm}$  (%). Surface layer (0-1 cm). Cruise BP-01.

Station	1	2	3	4	5	6	7
17	1	2	10	20	20	35	7
16	1	5	10	7	20	45	7
14	5	20	10	15	20	25	2
12	1	1	2	1	2	3	90
3	0	0	4	5	15	35	40
24	2	2	4	8	31	50	2
26	1	2	2	5	37	48	0

##### Preliminary results

Our results are represented in Tables 6.5 and 6.6. In both fractions the main components are biogenic remains, rock fragments and mineral grains. The comparison revealed a strong difference between two studied fractions (Fig. 6.14): in general the fraction  $>125 \mu\text{m}$  has a much higher amount of biogenic remains and rock fragments than the fraction  $63\text{-}125 \mu\text{m}$ . Only several samples of fraction  $63\text{-}125 \mu\text{m}$  were enriched in biogenic remains, and in all cases they have been represented by plant remains. All these samples have been obtained from river sediments or from sediments of the marginal filter. In the mineral part of this fraction quartz and feldspars dominate; the amount of mica, black ore (opaque) minerals and coloured transparent minerals – as a rule – has a subordinate significance (Table 6.6). As the fraction  $>125 \mu\text{m}$  has a

much more diverse composition, we will concentrate our efforts on results of just this fraction.

Table 6.7: Composition of fr. >125 mkm (%). Surface layer (0-1 cm). Cruise BP-01.

Station	6	4	3	2	Black ore	1	5	C.m.+ M	Color min.	Mica
75	42	22	20	10	0	3	0	3	2	1
73	30	20	14	30	0	4	0	4	2	2
72	15	50	23	8	0	4	0	4	3	1
80	8	26	10	15	1	5	35	5	5	0
70	0	7	7	5	0	0	80	0	0	0
82	2	40	30	20	0	4	3	4	3	1
68	0	50	37	3	1	6	2	6	4	2

It should be mentioned that during SIRRO BP01 we managed to reach a more northern latitude (Fig. 6.15) than during 49-th cruise of R/V "Dmitry Mendeleev" (1993) and SIRRO BP00. That is why we got samples from facies zone IID (Levitan et al. 1996) and can divide this zone on two subzones (IID/1 and IID/2). IID/1 sediments cover the northern and north-western slope and rise of the Ob-Yenisei shoal. They are represented by a rather thick (several meters of Holocene) sequence, and characterize the regime of accumulation. IID/2 sediments form a thin veneer (up to first dozen centimeters) drapping a typical glacial topography of the St. Anna Trough bottom northward from IID/1 area. These sediments characterize the regime of transition or very low sedimentation rates.

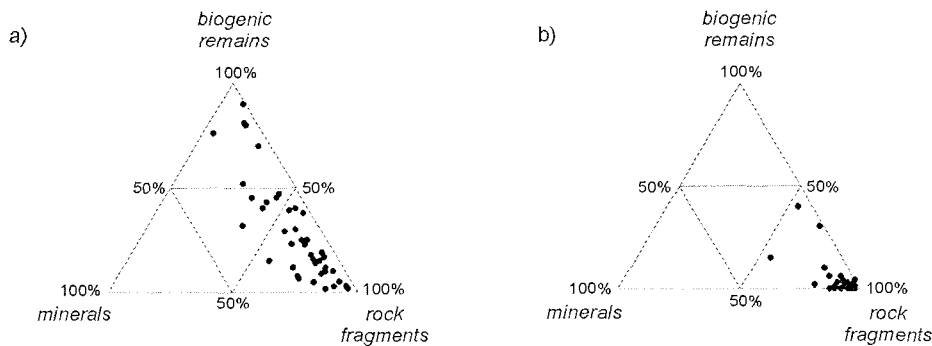


Figure 6.14. Composition of fraction >125  $\mu\text{m}$  (a) and fraction 63-125  $\mu\text{m}$  (b)

The mineral part of the fraction >125  $\mu\text{m}$  consists of the same minerals as were listed above for the fraction 63-125  $\mu\text{m}$  (Table 6.5). The rock fragments mainly include sedimentary and metasedimentary rocks (sandstones, siltstones, shales, schists, ferruginous crusts, etc.) of sandy size. Rather often these fragments are hematite-stained. Biogenic remains include remains of macrozoobenthos, meiobenthos (polychaets, bivalves, calcareous and agglutinated benthic foraminifers, sponge spicules, ostracods, mollusk (bivalve) clutches (Table 6.5), and terrestrial macroflora (plant remains, spores and pollen). The plant remains dominate among terrestrial macroflora absolutely. It is quite obvious that a comparison of our data of biogenic remains distribution with literature data on taphocoenoses distribution in trawls or box-corers (grab-samplers) has no sense because of methodical differences.

A composition of the fraction  $>125 \mu\text{m}$  is shown on Figure 6.15. An amount of biogenic remains *per se* (or biogenic remains/siliciclastics ratio) cannot be considered in the Kara Sea as the very important facies indicator because of too different nature of these remains (autochthonous for macro- and meiobenthos, and allochthonous for plant remains). The role of this indicator increases within of individual taphocoenosis areas which are shown on Figure 6.15. These areas are distinguished by the dominance of any group of biogenic remains. There are 7 large and 2 small taphocoenosis areas. The north-western area is characterized by the dominance of agglutinated benthic foraminifers (in IID/2 sediments – large (up to 2 mm) ball-like forms) which are accompanied by bivalves and ostracods mainly. For the north-eastern area the dominance of polychaets is typical (sometimes together with bivalves). The central (largest) area is distinguished by bivalves abundance. Bivalves here are accompanied by benthic foraminifers, ostracods, polychaets. The eastern area is characterized by calcareous benthic foraminifers with ostracods. In the western area polychaets are most typical. The northern part of Ob estuary is occupied by polychaets and plant remains. The surface sediments of southern Ob estuary and Taz river are characterized by plant remains (sometimes with ostracods and mollusk clutches). Plant remains are also most typical for sediments of Yenisei river and Yenisei Gulf. In the sediments of St. BP01-56 polychaets form the dominate group, and St. BP01-66 sediments are characterized by dominance of mollusk clutch.

Such way, we would like to underline the importance of plant remains as facies indicator of sediments which are accumulated in rivers and mixing zones of fresh and sea water (Fig. 6.16) – facies IIa and IIB (Levitan et al. 1996). As we mentioned above, the same is also true for the fraction  $63\text{-}125 \mu\text{m}$ . It is clear that this event is related to the land proximity and specific hydrodynamic regime. Other taphocoenoses are due to the peculiarities of food (it's quality and quantity) and feeding mode, sediment's character, hydrodynamics of bottom water, etc. An amount of biogenic remains is also influenced by the siliciclastics' dilution.

A concentration of rock fragments in the fraction  $>125 \mu\text{m}$  (Fig. 6.15) can be explained by different mechanisms: riverine supply, coastal abrasion, bottom erosion, sea ice and iceberg melting, dilution by biogenic remains and minerals. For example, amount of rock fragments ca. 20% and higher (Table 6.5; Fig. 6.15, 6.16) in Ob estuary and Yenisei river is due to riverine supply and bottom erosion; in the northernmost part of Ob estuary – to coastal abrasion (?); in St. BP01-28 sediments – to coastal abrasion and first ice melting; in St. BP01-67 sediments – to bottom erosion; in the sediments of north-western and northern slope of Ob-Yenisei shoal (St. BP01-56, 35, 38) – to bottom erosion and high hydrodynamic activity of bottom water. A dilution by biogenic remains can be avoided by recalculation on biogenic-free matter. The results of this operation showed that biogenic dilution was a factor of secondary importance – all listed above areas of enhanced rock fragment abundance remained their locality. Only in the northern part of Ob estuary the area with more than 20% of rock fragments became much larger and occupied this region entirely. We cannot describe the provenance of studied area based on petrography of rock fragments: in most cases these particles are too small for correct determination of the rock type.



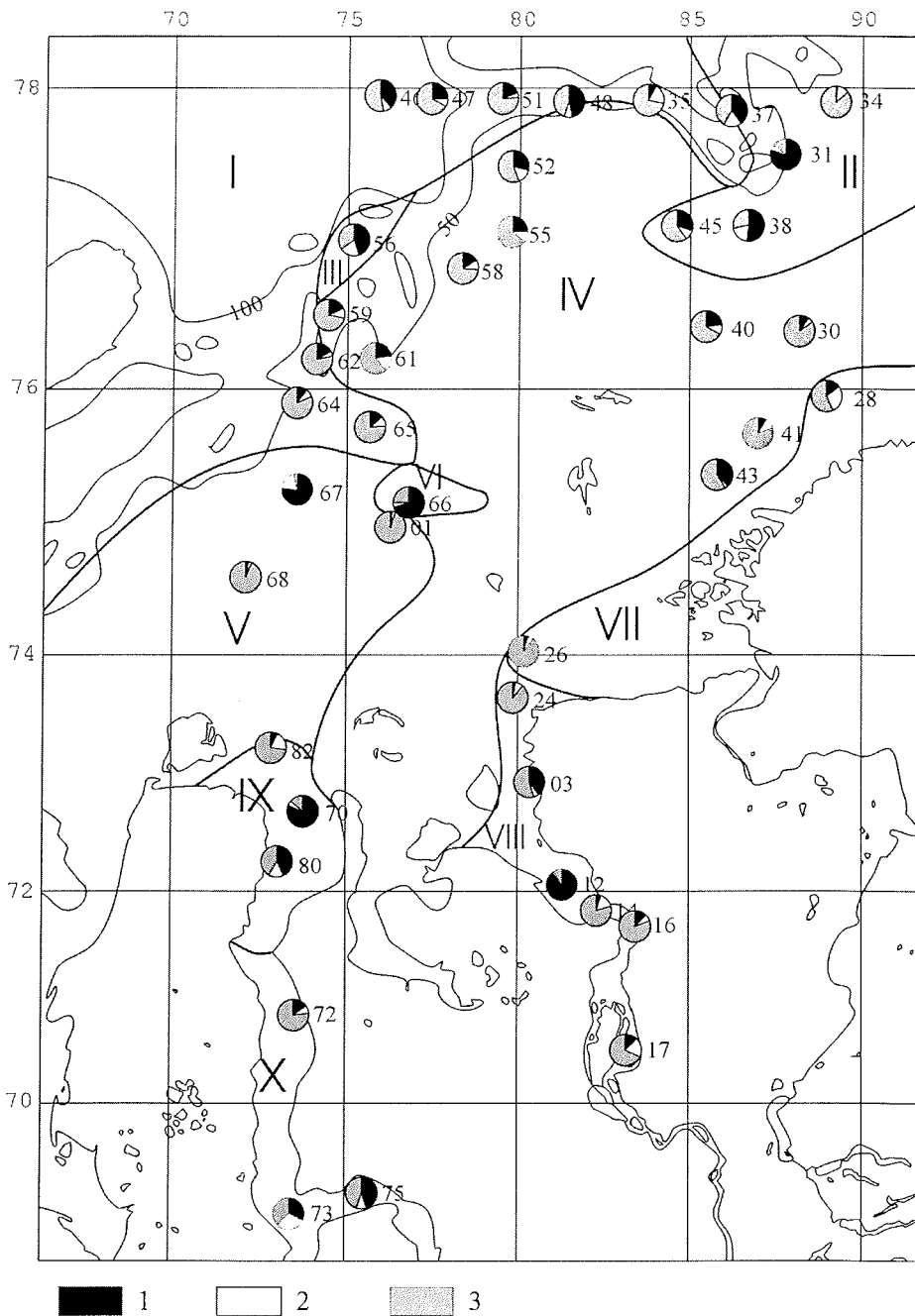


Fig. 6.15. Taphocoenoses and composition of fr. >125 μm. 1 – biogenic remains; 2 – rock fragments; 3 – minerals. Taphocoenoses with dominance of: I – agglutinated benthic foraminifers; II – polychaets; III – polychaets and agglutinated benthic foraminifers; IV – bivalves; V – polychaets; VI – mollusk clutches; VII – agglutinated benthic foraminifers; VIII – plant remains; IX – polychaets and plant remains; X – plant remains

As a rule, quartz and feldspars dominate among mineral grains in the fraction  $>125 \mu\text{m}$  (Table 6.5). We should mention that transparent colourless grains of quartz are the most numerous ones among the quartz grains. This observation is in accordance with the conclusion of Levitan et al. (1998). Mica group is represented by muscovite, biotite and – very rare – by plates of green mica. Usually their abundance doesn't exceed several percent but sometimes (especially, in the fraction 63-125  $\mu\text{m}$  – St. BP01-12) it reaches 15%. The reasons of such event are still unknown.

An important problem is connected with black ore minerals (Table 6.14; Fig. 6.16). They are absent in both sand fractions of Taz, Ob rivers, and Ob estuary sediments. In general there is a positive correlation between amount of opaque minerals in both fractions. We can pay attention to two main areas of black ore minerals concentration in fraction  $>125 \mu\text{m}$ . The first area is located in Yenisei river sediments (St. BP01-17) and related to direct supply of these minerals from Putoran basalts. The second area occupies a vast region near Ob-Yenisei shoal break and slope, and probably is related to processes of active reworking of bottom sediments in high energetic environment due to enhanced hydrodynamic activity of bottom water. Recalculation of black ore minerals on biogenic-free matter confirmed this idea.

It is well known that coloured transparent minerals form more rich assemblage in the fraction 63-125  $\mu\text{m}$  than in the fraction  $>125 \mu\text{m}$ . The study of heavy minerals in the fraction 63-125  $\mu\text{m}$  now is in progress. The results will be presented later.

### **Conclusions**

Such way, the study of fractions 63-125 and  $>125 \mu\text{m}$  brought a lot of information in the understanding of facies pattern in the eastern Kara Sea. Here we would like to underline the role of plant remains as a facies indicator of Taz, Ob and Yenisei fresh waters, and the lack of black ore minerals in Taz and Ob sediments in contrast to Yenisei sediments.

### **Acknowledgements**

The assistance of J.Simstich in sampling is greatly appreciated. This is grant RFBR # 02-05-64017.

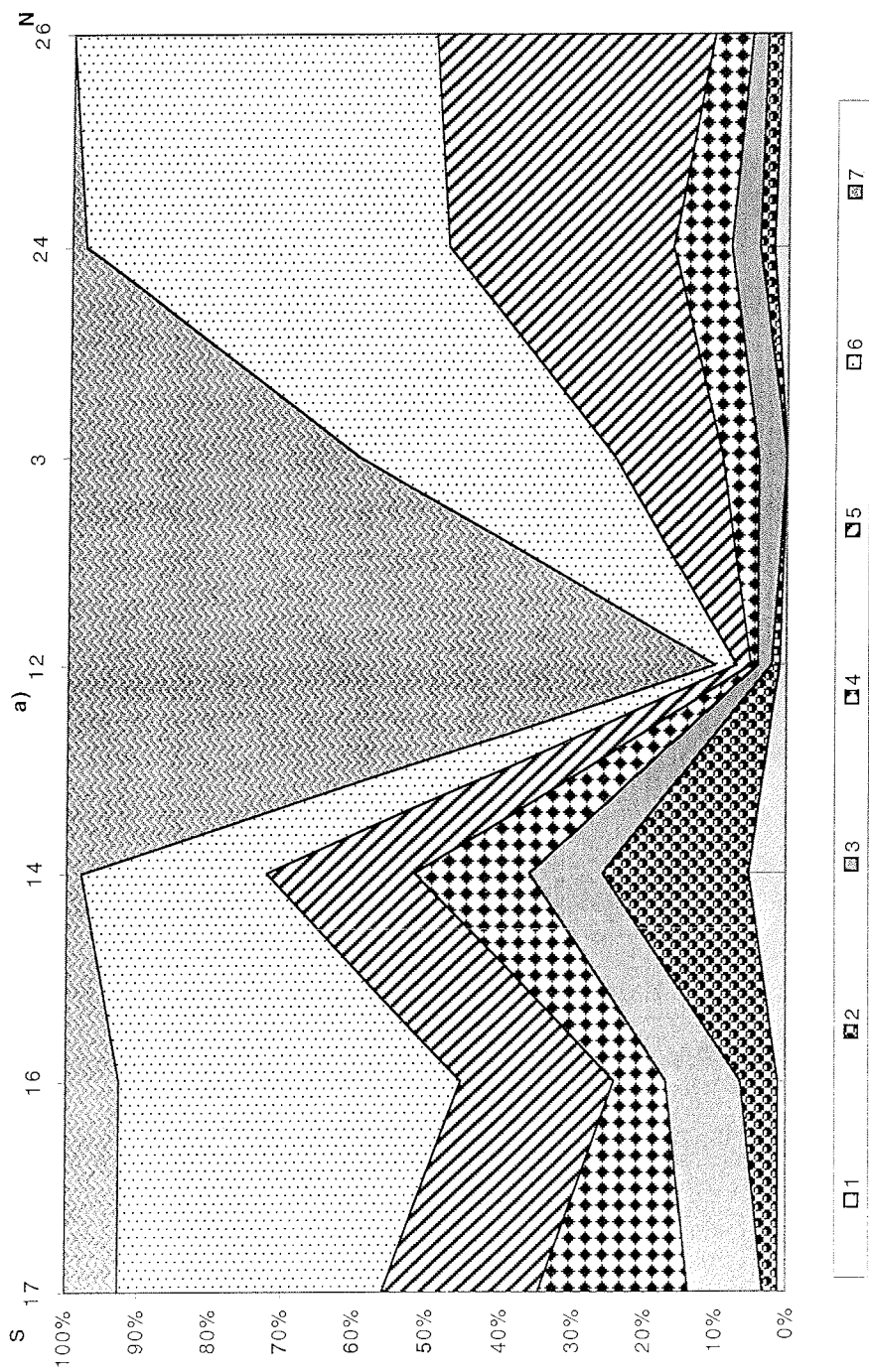


Fig. 6.16. Composition of fr. >125 μm along Yenisei (a) and Ob (b) transects. Fig. 6.16a: 1 – mica; 2 – coloured minerals; 3 – black ore minerals; 4 – rock fragments; 5 – feldspars; 6 – quartz; 7 – plant remains.

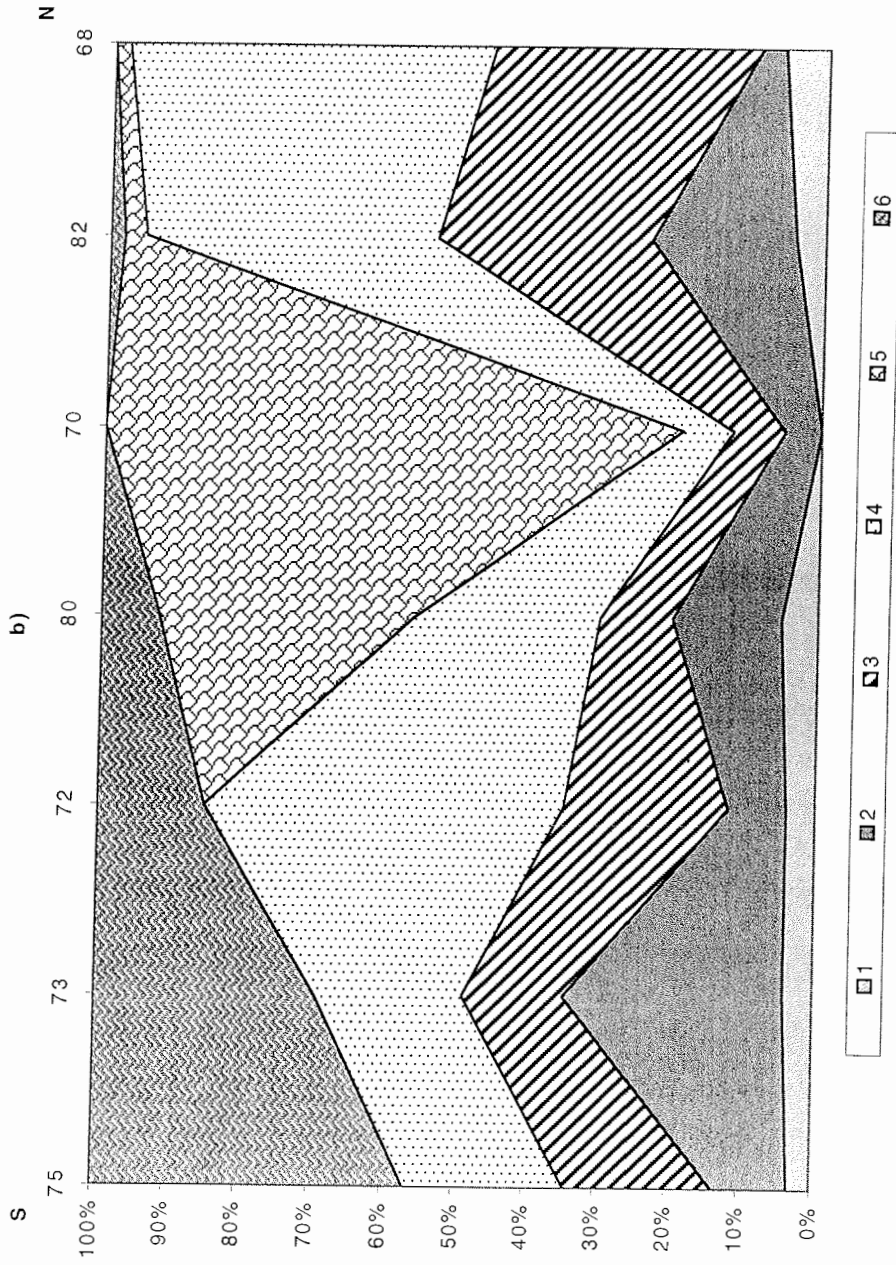


Fig. 6.16b: 1 – sum of mica, coloured and black ore minerals; 2 – rock fragments; 3 – feldspars; 4 – quartz; 5 – polychaets; 6 – plant remains

## 6.5 New data on heavy mineral distribution in the Southern Kara Sea surface sediments

M.V. Bourtman<sup>1,2</sup>, M.A. Levitan<sup>1,2</sup>

1 – Shirshov Institute of Oceanology RAS, Moscow, Russia;

2 – Vernadsky Institute of Geochemistry and Analytical Chemistry RAS, Moscow, Russia

### Introduction

Among the traditional methods of marine geological investigations the study of heavy minerals is one of the main procedures helpful for the identification of source areas and transport pathways of terrigenous matter. The last 10 years of investigations of the Kara Sea modern sedimentation system led to the development of a detailed scheme of facies zonality for the Late Holocene sediments in this region (Levitan et al. 1996; Levitan 2001, 2002). According to this concept, there are four main facies subzones (FIIA – FIID) in the Ob-Yenisei (FII) zone, which are also divided into local parts. In particular, the zone of river sediments FIIA consists of the area of bottom erosion FIIA/1 and subzone FIIA/2 of winnowing of fine- and concentrating of coarse-size fractions due to strong currents. Zone of fresh and sea water mixing FIIB contains two subunits: FIIB/1, the area of hydrodynamic barrier with domination of coarse fractions, and FIIB/2, where fine material prevails. The transit zone FIIC is divided into five parts: FIIC/1 - area of bedrock outcrops, FIIC/2 - subzone of Quaternary relict sediments, FIIC/3 - area of recent sandy reworked sediments, and two units in paleoriver valleys (channels): FIIC/4, filled by sediments and FIIC/5 - empty valleys with bedrock outcrops due to strong currents. FIID, the facies zone of accumulation in the northern troughs, consists of FIID/1 - the area of northern and north-western Ob-Yenisei shoal slope characterized by high sedimentation rate, and FIID/2 - the subzone of low sedimentation rate.

### Facts and Methods

Surface (0-1 cm) sediments from 41 geological stations (Fig. 6.17) sampled by means of box corer during the SIRRO R/V "Akademik Boris Petrov" (2001) cruise were investigated in fraction 63-125  $\mu\text{m}$ . The samples were separated by bromoform (density 2.87  $\text{g/cm}^3$ ) for heavy and light subfractions. Heavy grains were mounted to permanent slides with meltmount ( $n=1,68$ ), identified and counted using a polarisation microscope. Unfortunately, 15 examined samples contain just a few heavy grains; these results can only be useful for mapping and conclusions as supplementary information. It is necessary to note that we used only data with 200 and more grains in each sample and mineral groups (clinopyroxenes with aegirine-augite, amphiboles, etc.) for mapping and description.

## Results

The results of mineralogical analyses are shown in Table 6.7. Among the heavy minerals in most of studied samples clinopyroxenes, epidote group and “black ore” minerals dominate (almost everywhere more than 15 %). The garnet and amphiboles content also exceeds 10 % in some of the investigated samples. The concentration of other minerals and mineral groups does not reach 10 %.

*Clinopyroxenes.* The maximum amount of clinopyroxenes (Fig. 6.17) was found in the sediments of river valleys, in the eastern and northwestern parts of the investigated area. In the south of the region the content of these grains increases northward from the FIIA/1 (16.2 %) to FIIC/3 (39.6 %) subzone along the Yenisei transect. Very high amount of clinopyroxenes (31.7 %) was also discovered in the sediments of station BP01-72 in the Ob estuary. The surface sediments of FIID/1 and FIID/2 facies subzones are also characterized by high and medium amount of clinopyroxenes (19,4 – 28.6 %). Distribution of grains of this group in the sediments of FIIC/3 and FIIC/4 areas varies and, probably, rather depends on the general region peculiarities (geological structure) than reflects any local facies regularities. In particular, one of the largest content of clinopyroxenes (35,3 %) in sediments from the FIIC/4 zone (station BP01-28) is formed by well-rounded semi-transparent “old” grains never met in other studied samples here. The local decrease of these minerals is found in the central and midwestern parts of the study area (also subzones FIIC/3 and FIIC/4).

*Epidote group minerals.* The amount of epidote group minerals varies from 12,3 % in the Yenisei sediments to 37,0 % in the mid-east of the study area. Minimum values of epidote content were described in the sediments of the Yenisei transect, eastern part of FIIC/4 subzone and at the north-eastern area. Generally, the sediments of the Ob estuary as well as those from FIIC and FIID facies zones, are enriched by epidote (Fig. 6.18).

*Black ore minerals.* Black ore minerals definitely dominate in the south-east of the area (Fig. 6.19). These minerals prevail in the bottom sediments along the Yenisei transect and even exceed 50 % in the sample from station BP01-17. However, the sediments taken at station BP01-24 (at the northern end of this transect) contain very low quantity of black ore minerals – 6.9 %. This can be explained by the intensive accumulation of sand-size grains earlier, along the hydrodynamical barrier zone FIIB/1 located southward of this station. The Ob sediments have a low amount of this group minerals (maximum 13,3 %). Two other maxima of black ores are found in samples from stations BP01-68 (FIIC/3) and BP01-45 (FIIC/4). Here grains were redeposited from the Mesozoic rocks. Black ores content in the sediments of the northern part of the investigated region (FIIC and FIID zones) increases northward varying from 10 to almost 29 %. There is one exception with very low amount of these grains in the reworked and redeposited sediments of station BP01-55 (FIIC/3 subzone), also explained by the composition of underlying rocks.

*Amphibole minerals.* Relative content of amphiboles varies from 1,4 to 14,4 % (Fig. 6.20). Hornblende strongly dominates over the other amphibole minerals and composes 89 – 100 % of amphiboles. The amount of amphiboles is decreasing northward and exceeds 10 % at the northwest of subzone FIID/2. The maximum content of these grains (12.4 %) was found in surface sediments from station BP01-24 (described earlier)

located just near the coastal source. The Ob sediments are also enriched by amphiboles supplied by the river from the West Siberian Plain.

*Garnet.* The amount of garnet in bottom sediments does not reach 15 %. There are no strong variations of its distribution. In general, minimum values of garnet content are located in the northwest of the shoal slope (zone FIID) and at the end of the Yenisei transect (zone FIIB) to the north of the hydrodynamic barrier area. The enrichment of sediments by garnet grains is increasing northward. On the whole, the garnet distribution depends on the influence of local sources, sediments composed by redeposited terrigenous grains containing higher amount of these minerals.

*Titanous minerals.* The minerals of this group are represented by sphene and rutile grains. The amount of Ti minerals varies from 1,1 to 8,7 %. The areas of sediments enriched by sphene and rutile are just close to their local sources: Yamal Peninsula, Taimyr coastal zone and at the north of the region with Mesozoic terrigenous underlying rocks.

*Fe oxides and rock fragments.* The amount of Fe oxides is about 3 % in average with the maximum value in the Yenisei estuary bottom sediments (6,7 %). The rock fragments content does not exceed 2 % in general, although there are some local anomalies with high amount of these grains in samples from paleo-valleys of FIIC/4 subzone and at the southwest of the shoal slope (FIID/1). It is necessary to note that the samples from the stations that we used just as the supplementary information (with insufficient heavy subfraction amount) are strongly enriched by rock fragments and Fe oxides at the Ob transect, both Ob and Yenisei barrier zones (FIIB/1), the areas of dominant redeposition (FIIC/3) and in the upper shoal slope (FIID/1).

*Clinopyroxene/epidote ratio.* Clinopyroxene/epidote ratio is an important indicator of the riverine terrigenous matter in the sediments of the Ob-Yenisei facies zone (Levitan et al. 1996). In accordance with the geological difference of the source provinces drained by both large rivers, the Yenisei bottom sediments have a higher value of this parameter than the Ob samples (Table 6.8). In general, this ratio is decreasing northward from the estuaries to the facies subzones IIC and IID (Fig. 6.21).

## Discussion and conclusions

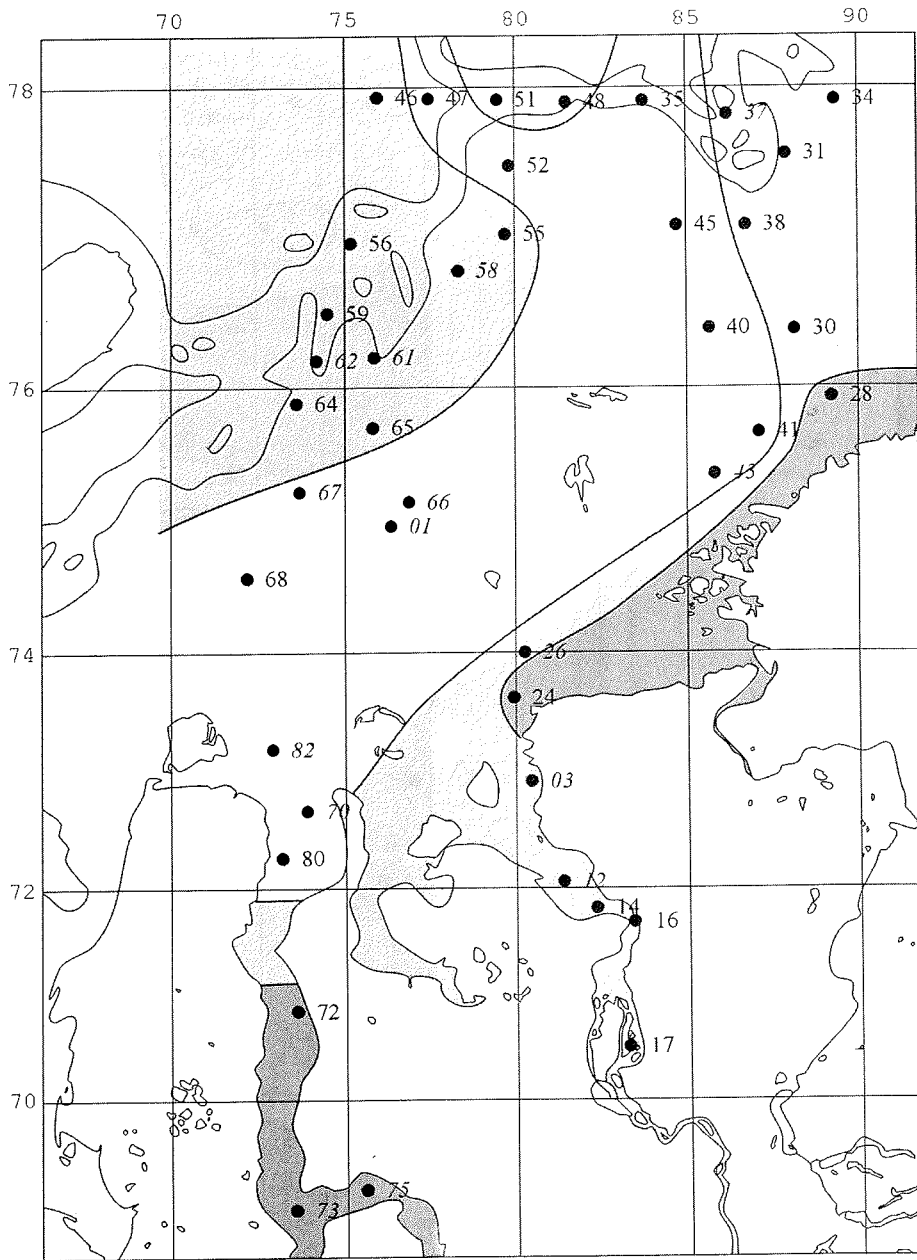
The distribution of heavy minerals in surface sediments have been studied according to the facies zonality of the eastern Kara Sea. Generally, a few main groups of heavy minerals dominate in the fine sand fraction of sediments: clinopyroxenes, black ores, epidotes, garnet, titanous minerals, Fe oxides and rock fragments. The distribution of black ores and the last four listed grain groups shows that they are located very close to the sources. The increasing of their amount (especially, Fe oxides and rock fragments) may be used as an indicator of local genesis of studied terrigenous grains. The variations of epidote content in sediments mostly depends on the presence of other mineral groups even along the Ob transect. The sources of clinopyroxenes are the Yenisei river and Taimyr Peninsula. The clinopyroxenes/epidote ratio distribution using as the indicator of Yenisei supply in the sediments exhibits a sublatitude zonality well coincided with the main facies units.

The mineral composition of FIIA/2 subzone samples (Table 6.8) in the south of estuaries demonstrates the dominance of local sources (the river coasts are located just close to studied sediments) for the formation of modern deposits. The hydrodynamic barrier zone FIIB/1 is characterized by strong accumulation of main mineral groups as from far continental sources (clinopyroxenes and epidote) so from the local ones (black ores, Fe hydroxides and rock fragments). But the distribution of amphiboles demonstrate that these minerals probably can overcome the barrier due to their high buoyancy comparably with other heavy grains. The samples from the FIIB/2 unit contain just a few heavy grains represented mostly by rock fragments. The composition of FIIC/3 unit sediments demonstrates the strong influence of local sources: underlying bedrocks and old Quaternary terrigenous sediments formed by riverine matter. A definite role in this relation can play also the supply of sediment matter from numerous small islands in the zone. In turn, FIIC/3 sediments are partly eroded and transported to the FIIC/4 and FIID subzones. The sediments of the paleo-valleys (FIIC/4) and shoal slope (FIID/1) contain material both from far sources (especially, Yenisei run-off, and probably redeposited from the FIIC/3 subzone area) and local sources. Increasing of clinopyroxenes, Fe hydroxides, rock fragments and CIPx/Ep ratio in FIIC/4 sediments in comparison with FIIC/3 sediments (Table 6.8) proves that channels are the pathways of riverine sediments northward the mixing zone. The role of local sources increasing for the FIID/2 area sediments – it follows from the high amount of garnet in the east and amphiboles in the west of this subzone.

#### **Acknowledgment**

We would like to express our gratitude to the analysts V.P. Kazakova and A.N. Rudakova for performing the separation of sand fraction.  
This is grant RFBR # 02-05-64017.





< 20%    
  20-30%    
  > 30%

Figure 6.17. Distribution of Clinopyroxenes in surface sediments of the Eastern Kara Sea (rel. %). Samples from the stations with numbers in italic contained less than 100 grains

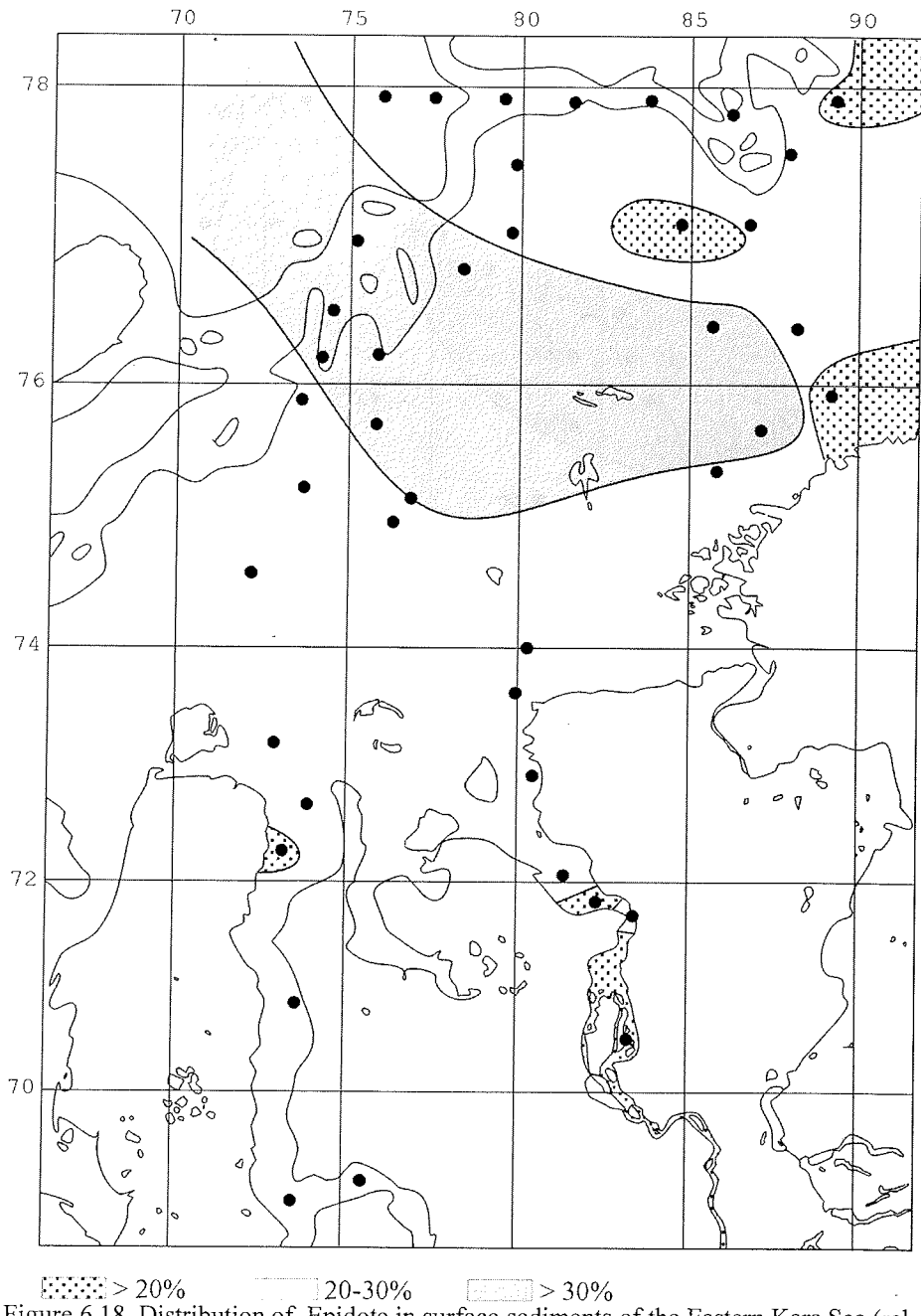


Figure 6.18. Distribution of Epidote in surface sediments of the Eastern Kara Sea (rel. %)

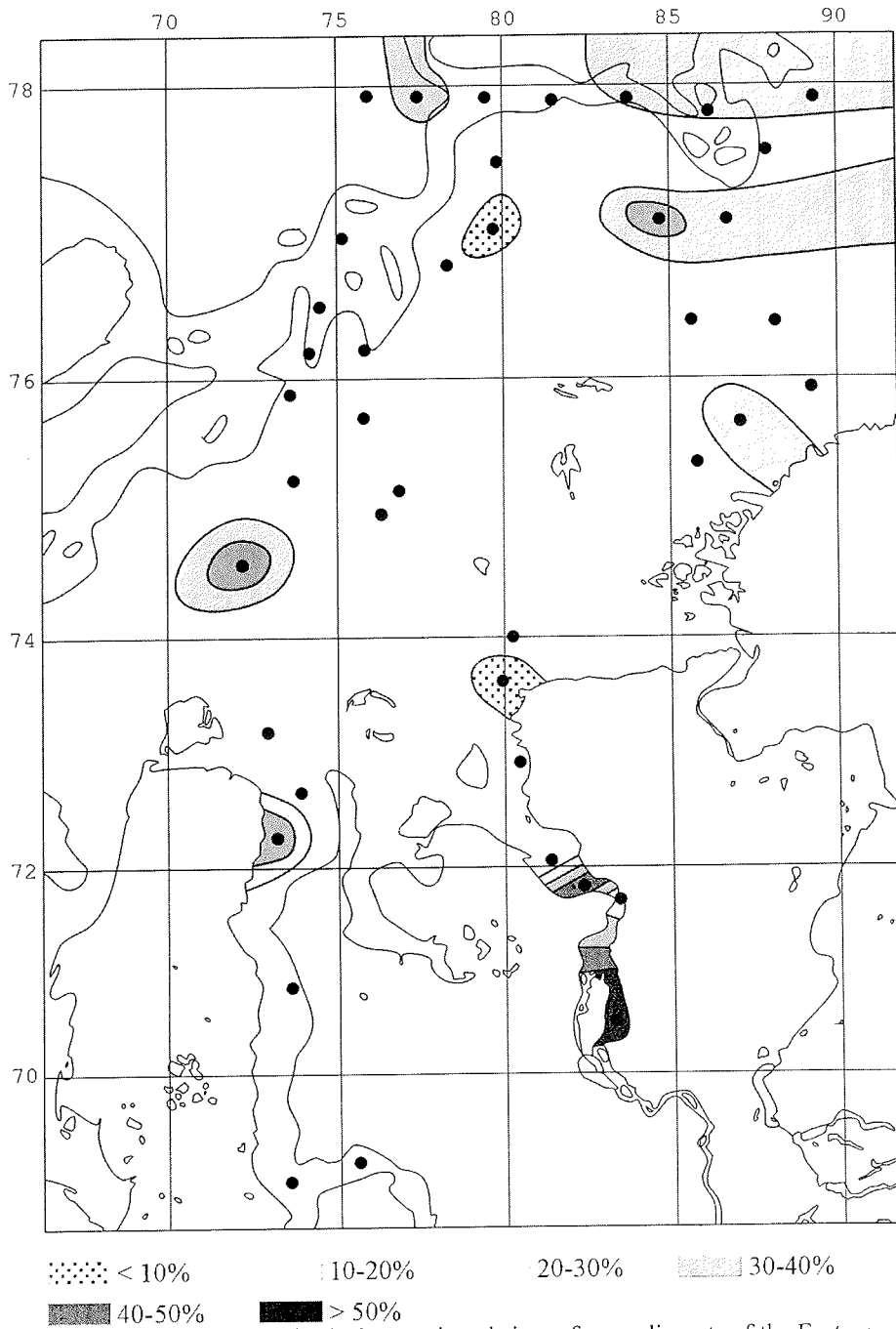


Figure 6.19. Distribution of Black ore minerals in surface sediments of the Eastern Kara Sea (rel. %)

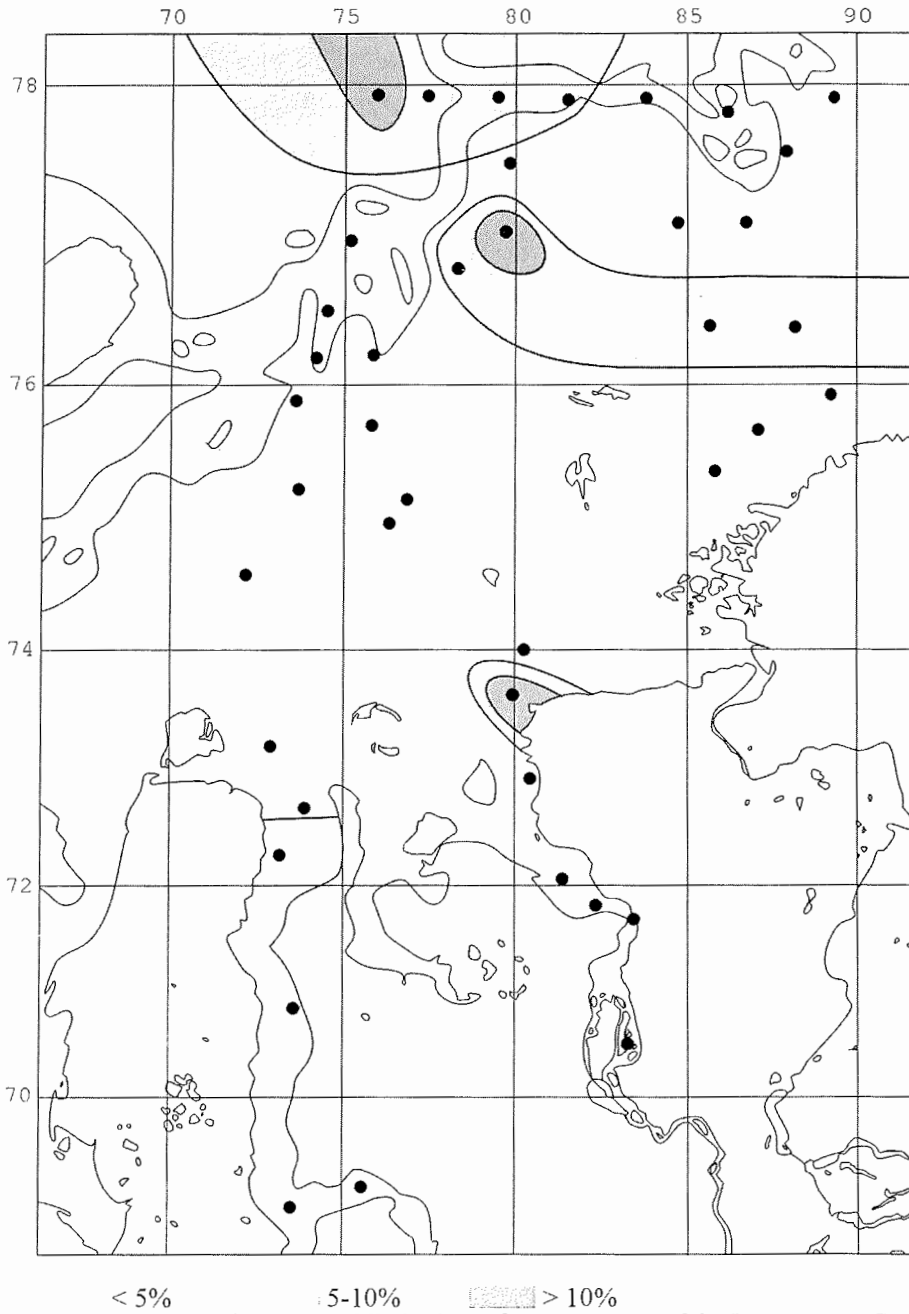


Figure 6.20. Distribution of Amphiboles in surface sediments of the Eastern Kara Sea (rel. %)

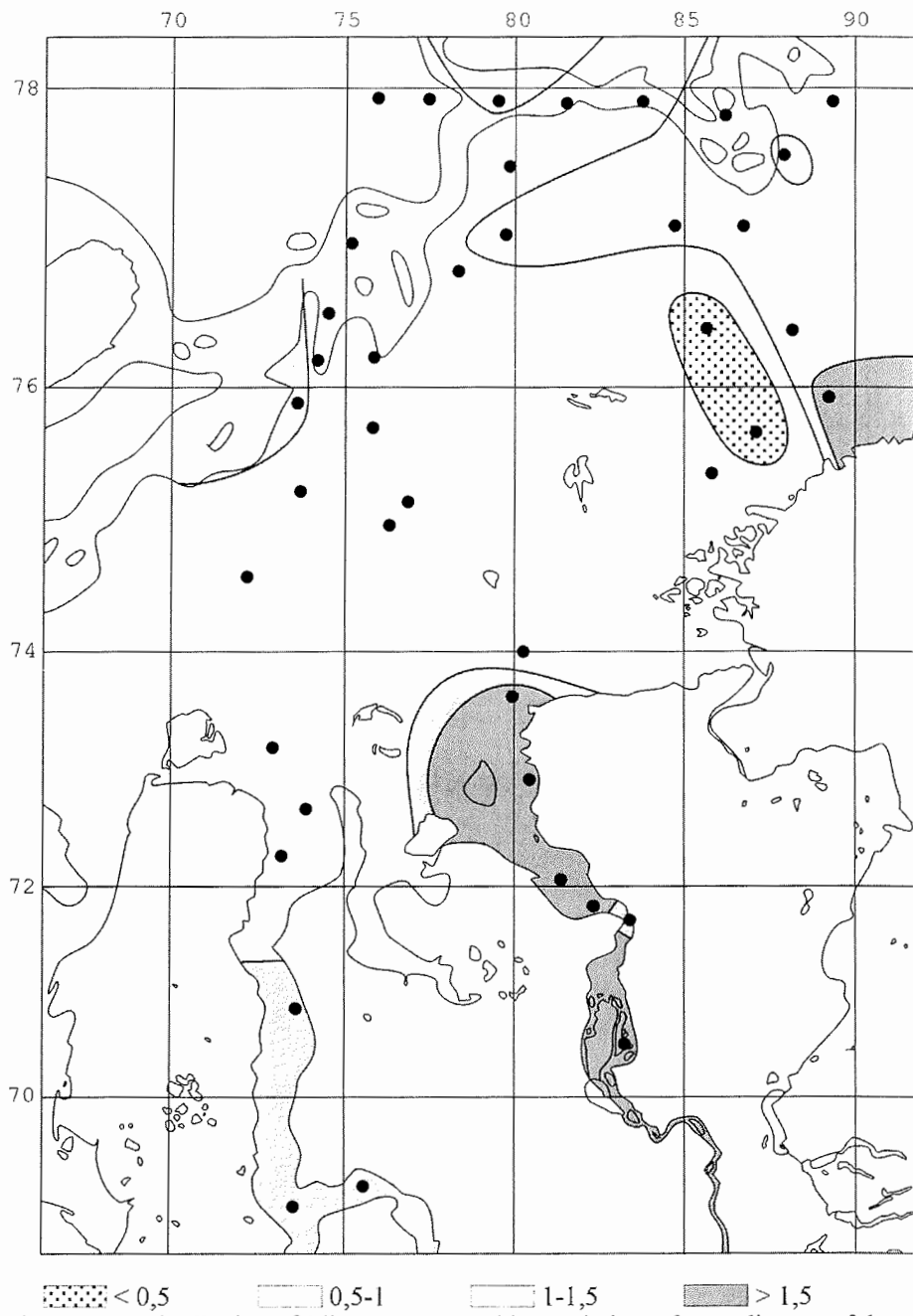


Figure 6.21. Distribution of Clinopyroxene/Epidote ratio in surface sediments of the Eastern Kara Sea

Table 6.7: Heavy minerals in the Eastern Kara Sea surface sediments (rel.%)

Station BP01	CIPx	Ep	BI ore	Garn	HBI	Brown HBI	Fe hydr	Act- Trem	Staur	Ca- grain	Tourm	Spinel	Apatite	Sphene	Fluor	Ru	Chlortd
14	21,0	12,3	45,6	3,2	2,4	0,8	6,7	0,0	0,0	0,4	0,4	0,4	0,0	0,0	0,0	2,4	0,0
16	27,7	24,1	23,7	5,9	2,4	0,0	6,7	0,0	0,0	0,4	0,0	1,2	0,4	0,0	0,0	3,2	0,0
17	22,5	12,5	50,6	1,5	0,7	0,7	3,0	0,0	0,7	0,0	0,4	0,7	0,7	0,7	0,0	0,4	0,4
24	37,3	22,6	6,9	3,2	11,1	1,4	3,2	0,0	0,0	0,5	0,9	0,0	0,5	1,4	0,0	2,8	0,0
28	33,8	18,7	11,9	4,7	2,5	0,7	4,0	0,0	0,4	0,4	0,0	0,4	1,8	2,2	0,0	3,2	0,4
30	24,2	24,2	17,7	8,1	4,0	1,2	6,0	0,4	0,4	0,0	0,0	0,0	0,0	1,6	0,0	1,2	0,0
31	20,2	26,4	19,4	7,4	3,7	0,8	3,7	0,0	0,0	0,0	0,4	0,4	0,4	1,2	0,0	5,0	0,0
34	21,8	16,2	28,8	14,0	1,7	0,9	4,4	0,0	0,0	0,0	0,0	0,0	1,3	0,4	0,0	3,5	0,0
35	17,4	26,9	20,2	13,0	3,2	0,8	4,3	0,0	0,0	0,0	0,4	0,0	0,8	0,8	0,0	5,5	0,0
38	19,7	20,5	21,6	11,6	3,1	0,4	2,3	0,0	0,0	0,4	0,8	0,4	1,5	1,9	0,0	4,2	0,0
40	14,8	37,0	13,9	9,3	3,7	0,9	5,1	0,0	0,0	0,0	0,0	1,4	0,0	2,8	0,0	5,6	0,0
41	11,5	30,9	21,2	11,9	2,6	1,1	3,7	0,0	0,0	1,1	0,0	0,0	1,5	2,2	0,0	3,0	0,0
45	12,3	13,1	33,3	13,7	0,8	0,5	3,0	0,0	1,1	0,8	0,0	0,8	1,9	1,4	0,0	4,1	0,3
46	21,6	26,4	13,9	3,5	10,0	0,0	4,8	0,0	0,0	0,0	0,9	0,0	1,7	0,4	0,0	4,3	0,4
47	19,2	26,8	21,1	6,8	4,9	0,4	3,4	0,4	0,8	0,0	0,4	0,0	1,5	0,4	0,4	2,6	0,0
48	21,1	27,4	19,7	10,8	5,8	1,3	3,1	0,0	0,4	0,0	0,0	0,4	0,9	0,4	0,0	4,0	0,0
51	25,0	26,7	16,4	9,5	7,3	0,0	4,3	0,0	0,0	0,0	0,4	0,4	0,4	0,4	0,0	2,6	0,4
52	14,8	25,7	15,7	13,5	2,6	0,9	8,3	0,4	0,4	0,4	0,4	0,4	2,2	0,9	0,0	7,8	0,0
55	22,0	23,1	6,8	6,1	10,2	3,0	6,1	0,8	0,0	0,4	1,5	1,1	0,8	2,3	0,0	2,3	0,4
56	23,2	33,6	15,1	3,9	3,5	0,0	2,3	0,0	0,0	0,0	0,4	0,4	1,2	1,5	0,0	2,3	0,8
59	22,6	30,4	17,8	7,0	4,8	0,0	2,2	0,0	0,0	0,4	0,4	0,0	0,4	0,9	0,0	4,8	0,4
64	27,5	21,8	10,7	7,5	5,7	0,0	4,6	0,0	1,1	0,0	0,7	0,0	0,7	2,1	0,4	3,6	0,4
65	21,5	32,4	17,0	8,5	2,8	0,0	2,8	0,0	0,0	0,0	0,0	0,0	0,8	0,8	0,0	5,3	0,0
68	13,4	20,1	31,2	9,7	3,7	0,7	3,7	0,0	0,0	0,0	0,0	0,0	0,3	0,3	0,0	4,4	0,7
72	29,3	25,7	13,3	4,0	5,6	0,0	2,0	0,0	0,0	0,0	0,4	0,8	0,4	0,8	0,4	2,0	0,4
80	15,8	19,8	30,4	6,7	4,3	0,8	2,0	0,0	0,4	0,0	0,0	0,4	2,0	2,0	0,0	5,5	0,0

Table 1: cont.

Station BP01	Enst- Hyp	O1	Sill	Bi	Chlorite	Andal.	Aug- Aug	Artveds > 200 grains counted	Zr	Chrom Spinel	Rock fragm.	Voulk. glass	Musc	Cass	Brook.	Monaz	Pyrite
14	0,8	0,0	0,0	0,0	0,4	0,0	0,4	0,0	0,8	0,0	1,2	0,0	0,4	0,0	0,0	0,4	0,0
16	0,0	0,0	0,0	0,4	1,2	0,0	0,0	0,0	0,0	0,0	1,2	0,0	0,0	0,0	0,0	1,6	0,0
17	2,6	0,4	0,4	0,0	0,0	0,0	0,4	0,0	0,0	0,0	0,0	0,4	0,4	0,0	0,0	0,0	0,0
24	1,4	0,5	0,0	0,0	2,3	0,0	2,3	0,0	0,5	0,0	1,4	0,0	0,0	0,0	0,0	0,0	0,0
28	0,0	1,1	1,1	0,0	2,5	0,0	1,4	0,0	0,7	0,0	6,1	1,4	0,0	0,0	0,4	0,4	0,0
30	1,2	2,0	0,0	0,0	0,8	0,4	0,8	0,0	1,2	0,8	2,0	0,4	0,0	0,0	0,0	0,8	0,4
31	1,7	0,8	0,0	0,4	1,2	0,0	0,8	0,4	1,7	0,0	2,1	0,0	0,0	1,2	0,0	0,4	0,0
34	0,4	0,4	0,4	0,0	0,0	1,3	0,0	0,4	1,7	0,4	0,9	0,0	0,0	0,4	0,0	0,4	0,0
35	0,4	0,4	0,4	0,4	0,8	0,4	2,0	0,0	0,4	0,0	1,2	0,0	0,0	0,4	0,0	0,0	0,0
38	2,3	2,3	0,0	0,0	1,5	0,0	0,8	0,0	1,2	0,0	0,8	0,8	0,4	0,8	0,0	0,8	0,0
40	0,9	0,9	0,0	0,0	1,4	0,0	0,5	0,5	0,0	0,5	0,0	0,0	0,5	0,0	0,0	0,5	0,0
41	1,9	0,0	0,0	0,0	1,9	0,0	0,7	0,0	1,9	0,0	0,4	0,4	1,1	0,7	0,0	0,4	0,0
45	0,5	1,4	0,3	0,0	0,0	0,0	0,8	0,0	2,7	0,3	6,0	0,3	0,0	0,5	0,0	0,0	0,0
46	3,9	0,9	0,0	0,4	0,9	0,0	1,7	0,4	0,4	0,0	1,7	0,0	1,3	0,0	0,0	0,4	0,0
47	0,0	0,8	0,4	0,0	1,9	0,4	0,4	0,8	3,4	0,0	1,9	0,0	0,0	0,8	0,0	0,4	0,0
48	0,4	0,4	0,0	0,0	0,4	0,0	0,4	0,0	0,9	0,0	0,4	0,4	0,4	0,4	0,0	0,0	0,0
51	0,9	0,4	0,4	0,4	0,4	0,4	0,9	0,0	0,9	0,0	0,9	0,4	0,0	0,0	0,0	0,0	0,0
52	0,9	0,4	0,0	0,9	0,4	0,0	0,0	0,0	0,0	0,0	1,7	0,4	0,4	0,0	0,0	0,0	0,0
55	2,7	1,1	0,4	0,0	1,1	0,4	2,7	0,4	0,0	0,4	3,8	0,0	0,0	0,4	0,0	0,0	0,0
56	2,7	0,8	0,4	0,0	3,9	0,4	1,2	0,8	0,0	0,0	1,2	0,0	0,8	0,0	0,0	0,0	0,0
59	2,2	0,4	0,0	0,0	1,3	0,0	0,9	0,0	0,9	0,4	1,3	0,0	0,0	0,0	0,0	0,4	0,0
64	0,7	0,4	0,4	0,7	0,7	0,0	1,1	0,0	1,1	0,4	7,1	0,4	0,0	0,0	0,0	0,4	0,0
65	2,0	0,4	0,0	0,0	0,4	0,0	2,0	0,4	1,6	0,0	0,0	0,0	0,4	0,4	0,0	0,4	0,0
68	0,7	0,0	0,0	0,7	0,0	0,0	0,3	0,0	6,7	0,0	1,7	0,0	0,0	1,0	0,0	0,7	0,0
72	1,2	0,0	0,4	0,0	4,4	0,0	2,4	0,0	0,4	0,0	3,6	0,4	1,6	0,4	0,0	0,0	0,0
80	0,8	0,0	0,0	0,0	1,2	0,0	0,4	0,0	4,7	0,0	0,4	0,0	0,0	1,2	0,0	1,2	0,0

Table 1: cont.

Station BP01	ClPx	Ep	Bl ore	Garn	HBl	Brown HBl	Fe hydr	Act- Trem	Staur	Ca- grain < 100 grains counted	Tourm	Spinel	Apatite	Sphene	Fluor	Ru	Chlorid
1	18,5	12,3	6,2	6,2	4,9	2,5	9,9	0,0	0,0	0,0	1,2	0,0	2,5	1,2	0,0	1,2	0,0
3	30,4	21,7	0,0	8,7	0,0	0,0	13,0	0,0	0,0	0,0	0,0	0,0	0,0	0,0	0,0	0,0	0,0
12	20,0	20,0	0,0	6,7	13,3	0,0	6,7	0,0	0,0	0,0	0,0	0,0	0,0	0,0	0,0	0,0	0,0
26	21,6	9,8	4,9	2,0	3,9	0,0	22,5	0,0	0,0	1,0	1,0	1,0	0,0	0,0	0,0	0,0	0,0
37	41,7	37,5	0,0	2,1	2,1	0,0	0,0	0,0	0,0	0,0	2,1	0,0	0,0	0,0	0,0	0,0	0,0
43	36,8	2,6	0,0	0,0	7,9	13,2	10,5	0,0	0,0	0,0	7,9	0,0	0,0	0,0	0,0	0,0	0,0
58	16,0	6,4	1,1	1,1	7,4	2,1	36,2	0,0	0,0	1,1	0,0	1,1	0,0	0,0	0,0	0,0	0,0
61	12,9	9,7	0,0	5,4	8,6	1,1	34,4	0,0	0,0	0,0	1,1	2,2	0,0	1,1	0,0	0,0	0,0
62	13,5	5,8	0,0	1,9	1,9	0,0	55,8	0,0	0,0	0,0	0,0	0,0	0,0	0,0	0,0	1,9	0,0
66	26,2	35,4	1,5	0,0	4,6	0,0	10,8	0,0	0,0	0,0	1,5	4,6	1,5	0,0	0,0	1,5	0,0
67	11,1	30,6	0,0	5,6	2,8	0,0	13,9	0,0	0,0	0,0	0,0	0,0	0,0	2,8	0,0	0,0	0,0
70	15,6	18,0	0,8	7,0	5,5	0,0	27,3	0,0	0,0	0,0	0,8	0,0	0,0	0,8	0,8	0,8	0,0
73	17,1	4,3	1,4	2,9	5,7	0,0	15,7	0,0	0,0	0,0	1,4	0,0	0,0	0,0	0,0	0,0	0,0
75	10,4	8,3	0,0	5,2	6,3	1,0	37,5	0,0	1,0	0,0	2,1	1,0	0,0	2,1	1,0	2,1	0,0
82	37,7	18,0	0,0	0,0	8,2	0,0	4,9	0,0	0,0	0,0	3,3	0,0	0,0	0,0	0,0	0,0	0,0



Table 1: cont.

Station BP01	Enst- Hyp	Oi	Sill	Bi	Chlorite	Andal.	Aeg- Aug	Arfveds < 100 grains counted	Zr	Chrom Spinel	Rock fragm.	Voulk. glass	Musc	Cass	Brook.	Monaz	Pyrite
3	8,7	0,0	0,0	0,0	8,7	0,0	8,7	0,0	0,0	0,0	0,0	0,0	0,0	0,0	0,0	0,0	0,0
12	0,0	0,0	0,0	13,3	6,7	0,0	6,7	0,0	0,0	0,0	0,0	0,0	0,0	6,7	0,0	0,0	0,0
26	2,9	0,0	0,0	1,0	0,0	0,0	1,0	0,0	0,0	0,0	27,5	0,0	0,0	0,0	0,0	0,0	0,0
37	6,3	0,0	0,0	0,0	4,2	0,0	4,2	0,0	0,0	0,0	0,0	0,0	0,0	0,0	0,0	0,0	0,0
43	10,5	0,0	0,0	0,0	7,9	0,0	2,6	0,0	0,0	0,0	0,0	0,0	0,0	0,0	0,0	0,0	0,0
58	4,3	1,1	0,0	1,1	2,1	0,0	4,3	0,0	0,0	0,0	14,9	0,0	0,0	0,0	0,0	0,0	0,0
61	2,2	1,1	0,0	1,1	8,6	0,0	5,4	0,0	1,1	0,0	3,2	0,0	0,0	1,1	0,0	0,0	0,0
62	0,0	0,0	0,0	0,0	0,0	0,0	3,8	0,0	0,0	0,0	15,4	0,0	0,0	0,0	0,0	0,0	0,0
66	9,2	0,0	0,0	0,0	1,5	0,0	1,5	0,0	0,0	0,0	0,0	0,0	0,0	0,0	0,0	0,0	0,0
67	8,3	0,0	0,0	0,0	8,3	0,0	0,0	0,0	0,0	0,0	16,7	0,0	0,0	0,0	0,0	0,0	0,0
70	2,3	0,0	0,0	0,0	1,6	0,0	0,0	0,0	0,0	0,0	17,2	0,0	0,0	0,0	0,0	0,0	0,0
73	2,9	2,9	0,0	0,0	7,1	0,0	1,4	0,0	0,0	0,0	37,1	0,0	0,0	0,0	0,0	0,0	0,0
75	3,1	1,0	0,0	1,0	4,2	0,0	2,1	1,0	2,1	0,0	6,3	1,0	0,0	0,0	0,0	0,0	0,0
82	6,6	0,0	0,0	1,6	6,6	0,0	3,3	0,0	0,0	0,0	9,8	0,0	0,0	0,0	0,0	0,0	0,0

Table 6.8:

Heavy mineral content in different lithofacies (rel.%)

Lithofacies	CIPx	Ep	Garnet	Black ores	Amphib.	Ti min.	Fe hydrox.	Rock frag.	CIPx/Ep
A2 (Yen.)									
n=1	22,9	12,5	1,5	50,6	1,5	1,1	3	0	1,8
B1 (Yen.)									
n=2									
min	21,4	12,3	3,2	23,7	2,4	2,4	6,7	1,2	1,1
max	27,7	24,4	5,9	45,6	3,2	3,2	6,7	1,2	1,7
mean	24,6	18,2	4,6	34,6	2,8	2,8	6,7	1,2	1,4
B1 (Ob)									
n=2									
min	16,2	19,8	4	13,3	5,1	2,8	2	0,4	0,8
max	31,7	25,7	6,7	30,4	5,6	7,5	2	3,6	1,2
mean	24	22,8	5,4	21,8	5,4	5,2	2	2	1
C3									
n=4									
min	12,3	20,1	6,1	6,8	3,7	4,7	2,8	0	0,4
max	24,6	32,4	11,9	31,2	14,4	6,2	6,1	3,8	1,1
mean	18,6	26,6	9	19	6,4	5,1	4,1	1,5	0,7
C4									
n=6									
min	13,1	13,1	3,2	6,9	1,4	2,8	3	0	0,4
max	39,6	37	13,7	33,3	12,4	8,7	8,3	6,1	1,9
mean	23,8	23,6	8,8	16,6	5,8	5,8	4,9	2,9	1,1
D1									
n=8									
min	19,4	16,2	3,9	10,7	3,1	3	2,3	0,4	0,7
max	28,6	33,6	14	28,8	7,3	6,3	4,6	7,1	1,4
mean	23,3	26,2	9,1	18,5	5,2	4,9	3,6	1,9	0,9
D2									
n=2									
min	19,6	26,4	3,5	13,9	6,4	3	3,4	1,7	0,7
max	23,4	26,8	6,8	21,1	10,4	4,8	4,8	1,9	0,8
mean	21,5	26,6	5,2	17,5	8,4	3,9	4,1	1,8	0,8

## 6.6 Chemical characteristics of main lithofacies based on instrumental neutron-activation analysis data

M.Levitan<sup>1,2</sup>, G.Kolesov<sup>1</sup>, M.Chudetsky<sup>1,3</sup>

1 – Vernadsky Institute of Geochemistry and Analytical Chemistry RAS, Moscow, Russia

2 – Shirshov Institute of Oceanology RAS, Moscow, Russia

3 – Institute of Oil and Gas Problem RAS, Moscow, Russia

### Introduction

Chemical analysis is of great importance for understanding of sedimentological and geochemical processes in different environments. It allows to reveal source provinces, main transport pathways, grain-size and mineralogical regularities, role of different sorption agents, etc. Earlier we pointed that chemical composition is the one of the best facies indicators for the Kara Sea surface sediments (Levitan et al. 1996).

In the field of inorganic geochemistry of the Kara Sea bottom sediments first results have been obtained by means of “wet chemistry” and semi-quantitative methods of spectral analysis (Kulikov 1961; Gurevich 1995). Then different modifications of XRF method – on-board variant (Gurvich et al. 1994; Krasnyuk and Vanshtein 1999; Sizov et al. 2001) and coast laboratory variant (Schoster and Stein 1999) – have been used. In our short report we present first results of instrumental neutron-activation analysis (INAA) of bottom sediments.

### Facts and methods

During the cruises of RV “Akademik Boris Petrov” (2000, 2001) we took surface sediment samples at 54 stations by means of box-corer. The location of stations is shown in (Stein and Stepanets 2001; 2002 – this volume). The first centimeter of the core top was collected. In coast laboratory the samples were dried and ground. A determination of major, minor and trace elements have been performed by instrumental neutron-activation analysis. Its main parameters look as follows (Kolesov 1994): neutron flux  $1.2 \times 10^{13}$  neutron/cm<sup>2</sup> x s, irradiation time 20 h, sample weight 20-50 mg. The activity determination was performed using 4096-channel pulse height analyser with the high-purity Ge semi-conductor detector having the high resolution.

International reference standards (KH-1, JDO-1, So-1, JSD-1, JLK-1, BM, SDO-2) have been used to check the analyses. The accuracy of determination for different elements is as follows: La, Sm, Na, Se, Co – 3-5 rel. %; Eu, Yb, Lu, Cs, Cr, Fe, As, Th, U – 5-10 rel. %; Ce, Tb, K, Rb, Ca, Ba, Zn, Sb – 10-15 rel. %; Nd, Sn, Hf, Ta, Zr – 15-20 rel. %; other elements – more than 20 rel. %.

### Preliminary results

Our raw data are represented in Table 6.9. It is important to underline that amount of elements with asterisk is calculated but not determined directly. Note that several

element concentrations are expressed in weight % (Na, K, Ca, Fe), and other elements – in ppm.

Denotes of lithofacies are given according to (Levitan 2001; 2002 – this issue). It's useful to remind that FIIA/2 (briefly, A2) means river alluvium, FIIB/1 (B1) – proximal alluvial-marine sediments from the mixing zone of fresh and sea water, FIIB/2 (B2) – distal alluvial-marine sediments from the same zone, FIIC/3 (C3) – residual marine silts and sands from transitional zone accumulated with low sedimentation rate, FIIC/4 (C4) – marine muds from paleoriver channels located in the same zone and accumulated with high sedimentation rate, FIID/1 (D1) – marine sediments from the area of Ob-Yenisei Shoal break and slope accumulated with high sedimentation rate, FIID/2 (D2) – marine sediments from the area of marginal troughs bottom accumulated with low sedimentation rate.

Our results for abovelisted lithofacies are presented in Table 6.10 as lowest, highest and mean concentrations. We should notice that number of samples from lithofacies A2 (n=3), B1 (n=1) and D2 (n=3), of course, is not enough for statistics. Nevertheless, we have obtained quite definite trends. A2 sediments are characterized by highest mean amount of such elements as Zn, Th, U, Zr, light REE, and Ba. It is due to very coarse grain-size composition and almost full lack of clay fraction (Levitan 2001). It's well known, for example, that during weathering light REE enrich the detrital components, and heavy REE are mainly concentrated in solutions (Balashov 1976). Such way, most part of abovelisted elements is concentrated in lattices of detrital minerals and in the rock fragments.

B1 sediments are strongly enriched in Hf and, very probably, Zr. This event is mainly related to relatively high coarse/fine grain-size fractions ratio (Levitan, 2001). Nevertheless, higher amount of clay and the participance of marine sediment matter cause the difference of chemical composition from A2 sediments (Table 6.10).

Geochemistry of B2 sediments is of great importance. Dominant part of mixing zone sediments is represented just by B2 lithofacies. In this environment one can observe giant mass accumulation of clay minerals, transformation of dissolved organic matter and Fe in particulate forms and their accumulation, enhanced primary production (Lisitzin 1994). As result, B2 sediments are very fine clayey muds with the high content of Fe oxides and hydroxides, and relatively high TOC amount (Romankevich and Vetrov 2001). That's why they have quite definite geochemical specifics, and enrichment by such elements as Fe, To, Eu, Tb, Dy, Ho, Er, Tm, Yb, Cs, Ca, Sc, Cr. Probably, most part of these elements is accumulated in B2 sediments by sorption processes from the water column and organic complexes on clay minerals – especially on smectite (Geodekyan et al. 1997), on Fe hydroxides, on particulate organic matter. May be, a less significant role can be played by biotransportation. Small fraction of typical B2 elements can be contained in the lattices of clay minerals.

Comparison of Ob and Yenisei estuarine B2 sediments (Table 6.11) revealed that Ob sediments are enriched in the most studied elements: La, Ce, Pr, Nd, Sm, Eu, Gd, Tb, Dy, Ho, Er, Na, Rb, Cs, Sr, Ba, Fe, Ni, Se, As, Sb, Th, Br, Ag. The highest enrichment is recorded for La, Ce, Na, Rb, Sr, As, Sb, Br, Ag. Other elements have very close concentrations in Ob and Yenisei B2 sediments. This difference is caused by: 1) different geological composition of watershed territory; 2) slightly higher detrital/clay

mineral ratio in Ob sediments and 3) higher amount of Fe hydroxides in Ob B2 lithofacies. In general, this problem needs further investigation.

It is very important to point out the extremely significant role of the northern limit of B2 subzone as a facies and geochemical barrier. No less than 90% of riverine discharge is accumulated southward this boundary (Lisitzin 1994). What proportion of different elements supplied by rivers is accumulated here, has still to be clarified. In principle it's clear that elements in soluble form and connected with clay fraction have more chance to cross the boundary than "detrital" elements.

A thin veneer of C3 relatively coarse sediments covers ca. 70% of FIIC subzone. Here, the main process of sediment matter supply is the bottom erosion of Quaternary and Cretaceous sediments which underly C3 sediments. Less important sources are riverine discharge, sea ice sediments, aerosoles, and local supply from small islands (Izvestiya Tzik and others). Strong bottom currents produce resuspension, winnowing and bottom erosion. As result, fine (clay) fractions are winnowed and accumulated as C4 sediments in the local channels and other depressions. C3 sediments consist mainly of feldspar-quartz clastics, sometimes with significant role of accessories (Levitan et al. 1996, 1998). Amount of quartz determines the chemical composition (Gurvich et al. 1994) because it dilutes the majority of elements for exception of Si. Thus, C3 sediments are enriched in Ag, W, Mo related to feldspars and accessories, and depleted in almost all other studied elements (Table 6.10).

C4 sediments are rather close to B2 sediments based on chemical composition (Table 6.10) because of their almost same grain-size (Levitan 2001) and mineralogical (Levitan et al. 1996) composition. But different sources of sediment matter and their different relative proportion are expressed in enrichment of C4 sediments by Au, Gd and Sr. Also they have a higher amount of such elements as Ba, W, Br, U, Sb, As, Se, Ni and Co than B2 sediments.

FIID facies zone (Levitan et al. 1996) is studied not enough yet. D1 sediments mainly have more or less coarse composition with rather high amount of black ore minerals and rock fragments (Levitan 2002, this volume). They are accumulating with relatively high sedimentation rate in environment with active hydrodynamics and sharp bottom topography gradient. As result, D1 sediments are characterized by association of A2 elements (Table 6.10) and elements which are mainly transported in soluble forms (Na, Rb, Se, Sb, Br, Au). Also amount of several elements (Ni, Co) can be related to early diagenetic processes which are more strongly developed in this zone. Interestingly, no one studied element forms a highest concentration in D1 sediments. Such way, we propose that local reworking of old river sediments serve as an important source of matter for D1 lithofacies. This conclusion concides with our data on sand fraction composition (Levitan 2002, this volume).

D2 sediments form a very thin veneer of relatively fine sediments on the old glacial bottom; topography northward D1 subzone. Typically they are accumulating with very low sedimentation rate. It seems that supply of sediment matter from D1 subzone, the longest exposition of water/sediment surface, rather strong diagenesis (deep position of brown/green boundary), active bottom currents are the main reasons of formation of characteristic element association: Co, Ni, Se, As, Sb, Br, Na, K, Rb. Light REE also are relatively abundant in D2 sediments (Table 6.10).

If we join all analyses for samples of FIIC and FIID subzones (Table 6.12) we receive a mean composition of pure marine shelf sediments of the Kara Sea. Comparison of these data with average composition of terrigenous sediments near north-western Africa (Dubinin and Rozanov 2001) and pericontinental terrigenous sediments (Gurvich et al. 1980) revealed that the Kara Sea sediments belong to the typical hemipelagic siliciclastic deposits.

### **Conclusions**

Different source provinces and mechanical differentiation play the most important role in the formation of lithofacies geochemical structure. It seems that geochemical differentiation and diagenetic processes have a really subordinate significance in this relation. We can conclude that individual facies zones and subzones in the Kara Sea do have relatively independent sedimentological and geochemical peculiarities.

### **Acknowledgements**

We are grateful to V.N.Zaikin and L.A.Zadorina for technical assistance for preparation of samples for chemical analysis.  
This is grant RFBR # 02-05-64017.

Table 6.9: Chemical composition (INAA) of surface sediments from BP00 and BP01 cruises

	N	Cruise	Station	La ppm	Ce ppm	Pr* ppm	Nd ppm	Sm ppm	Eu ppm	Gd* ppm	Tb ppm	Dy* ppm	Ho* ppm	Er* ppm
1	1	BP01	01	3,42	7,52	0,94	4,02	1,14	0,16	1,74	0,29	1,9	0,46	1,41
2	2	BP01	26	29,2	54,2	5,9	22,2	5,22	1,66	9,08	1,13	7,0	1,61	4,58
3	3	BP01	28	26,8	48,0	5,2	19,7	4,65	1,07	6,21	0,99	6,0	1,39	4,06
4	4	BP01	30	30,1	59,3	6,65	25,0	6,35	1,29	7,4	1,09	6,03	1,29	3,43
5	5	BP01	31	27,3	49,9	5,47	20,3	4,97	1,09	6,5	1,03	6,22	1,42	4,19
6	6	BP01	34	18,7	34,5	3,6	13,5	3,29	0,82	4,42	0,67	4,19	0,93	2,67
7	7	BP01	35	52,5	95,3	9,5	34,2	7,9	1,44	8,6	1,23	6,98	1,41	3,73
8	8	BP01	37	27,9	51,0	5,66	21,2	5,04	1,15	6,0	0,89	5,03	1,12	2,99
9	9	BP01	38	35,0	62,6	6,47	22,4	5,04	1,5	6,03	0,92	5,12	1,13	3,0
10	10	BP01	40	28,5	53,0	5,85	22,2	5,41	1,12	6,22	0,93	5,32	1,17	3,11
11	11	BP01	41	20,1	37,8	4,11	15,0	3,82	1,18	4,9	0,76	4,52	1,04	2,86
12	12	BP01	43	30,1	57,8	6,27	23,0	5,78	1,33	6,52	0,97	5,38	1,17	3,05
13	13	BP01	45	26,8	49,0	5,31	20,0	4,96	1,13	5,75	0,85	4,79	1,06	2,75
14	14	BP01	46	27,2	47,1	5,02	18,6	4,33	0,91	5,18	0,8	4,71	1,09	2,98
15	15	BP01	48	24,6	43,0	4,6	17,1	4,02	0,96	5,41	0,83	4,95	1,14	3,17
16	16	BP01	51	28,9	52,0	5,49	20,1	4,68	1,07	4,88	0,66	3,58	0,7	1,78
17	17	BP01	52	29,7	57,6	6,51	25,0	6,5	1,45	7,51	1,09	6,13	1,3	3,48
18	18	BP01	55	22,8	42,3	4,76	17,3	4,36	0,82	5,32	0,8	4,6	1,03	2,75
19	19	BP01	56	23,5	42,3	4,68	17,9	4,19	1,42	5,32	0,81	4,7	1,06	2,81
20	20	BP01	59	31,4	57,8	6,07	22,3	5,31	1,33	6,01	0,9	5,2	1,14	3,08
21	21	BP01	61	29,2	53,2	5,87	22,1	5,15	1,11	6,47	0,98	5,7	1,27	3,5
22	22	BP01	62	27,2	49,9	5,53	21,7	5,23	1,36	6,35	0,95	5,35	1,18	3,15
23	23	BP01	64	32,7	60,2	6,5	23,8	5,78	1,53	6,41	0,97	5,5	1,22	3,32
24	24	BP01	65	24,6	43,2	4,7	16,8	4,18	1,39	5,3	0,8	4,58	1,01	2,73
25	25	BP01	66	29,5	54,8	5,99	22,4	5,43	1,64	6,52	0,97	5,45	1,19	3,2
26	26	BP01	67	30,4	56,8	6,02	22,5	5,43	1,1	6,7	1,01	5,99	1,31	3,7
27	27	BP01	68	27,2	48,9	5,25	19,9	4,57	1,04	5,72	0,93	5,78	1,35	4,02
28	28	BP01	70	33,9	60,8	6,48	23,1	5,68	1,58	6,39	0,95	5,4	1,18	3,14
29	29	BP01	73	36,2	65,5	7,1	25,8	6,3	1,08	6,8	0,98	5,4	1,15	2,97
30	30	BP01	75	41,6	71,7	7,33	25,0	5,8	1,25	7,35	1,14	6,95	1,53	4,37
31	31	BP01	80	21,5	39,0	4,04	14,7	3,57	0,91	4,48	0,67	4,21	0,93	2,69
32	32	BP01	82	29,6	55,0	6,02	22,7	5,74	1,51	6,98	1,06	6,1	1,35	3,75
33	2	BP00	3	30,2	54,8	5,8	21,0	4,89	0,6	6,47	1,01	6,03	1,38	3,99
34	14	BP00	4	21,1	37,7	4,01	14,7	3,56	1,05	4,5	0,67	4,11	0,88	2,48
35	13	BP00	5	20,6	37,0	3,92	14,3	3,44	2,52	4,48	0,67	4,19	0,93	2,69
36	15	BP00	7	28,7	54,6	6,0	22,6	5,66	1,34	6,61	1,0	5,78	1,25	3,42
37	12	BP00	8	25,7	47,0	5,19	19,6	4,63	1,29	5,98	0,92	5,47	1,23	3,48
38	5	BP00	9	19,6	36,2	4,08	15,3	3,96	1,11	5,02	0,78	4,51	1,03	2,76
39	20	BP00	13	24,7	44,9	5,0	19,1	4,7	1,59	5,78	0,89	5,23	1,19	3,32
40	19	BP00	28	28,6	49,9	5,1	18,2	4,01	1,14	5,0	0,75	4,47	0,97	2,63
41	7	BP00	16	27,1	49,1	5,33	20,1	4,86	1,14	6,07	0,96	5,81	1,32	3,83
42	10	BP00	15	22,0	41,0	4,72	18,7	4,65	2,02	6,3	0,99	5,98	1,34	3,8
43	3	BP00	19	21,8	38,2	4,04	14,7	3,57	1,0	4,79	0,73	4,49	1,03	2,78
44	1	BP00	22	22,5	42,0	4,82	19,1	4,59	0,78	6,0	0,91	5,32	1,19	3,28
45	17	BP00	22	25,2	46,0	5,03	19,1	4,53	1,62	5,9	0,94	5,66	1,31	3,8
46	21	BP00	23	23,6	43,1	4,7	17,9	4,14	1,43	5,28	0,81	4,68	1,07	2,89
47	8	BP00	24	26,5	46,8	5,03	19,0	4,41	1,13	5,49	0,84	4,93	1,12	3,09
48	18	BP00	29	28,3	49,9	5,12	18,6	4,16	1,05	5,1	0,76	4,48	0,98	2,67
49	11	BP00	26	27,0	49,0	5,45	20,3	4,98	1,61	6,43	0,99	5,97	1,32	3,72
50	9	BP00	30	26,1	47,8	5,14	19,7	4,71	1,29	6,2	0,99	5,99	1,35	3,97
51	4	BP00	31	29,5	53,0	5,71	21,7	5,03	1,56	6,28	0,99	5,97	1,32	3,83
52	16	BP00	35	26,5	48,3	5,4	20,3	4,99	1,59	6,42	1,0	5,99	1,34	3,83
53	22	BP00	36	29,6	52,8	5,6	20,4	4,76	1,38	5,83	0,88	5,11	1,15	3,12
54	6	BP00	38	33,9	63,5	7,08	27,0	6,74	1,93	8,02	1,2	7,0	1,49	4,1

	Tm*	Yb	Lu	Rb	Cs	Ca	Sr	Ba	Sc	Cr	Fe	Co	Ni	Zn
	ppm	ppm	ppm	ppm	ppm	%	ppm	ppm	ppm	ppm	%	ppm	ppm	ppm
1	0,23	1,41	0,26	6,77	1,07		125	250	4,18	8,36	1,31	4,68	30	
2	0,68	4,02	0,65	61,6	4,5	1,42	350	530	18,0	91,0	6,33	22,5	130	60
3	0,6	3,49	0,57	87,2	4,71	1,83	575	280	16,0	82,8	5,28	21,5	20	30
4	0,48	2,53	0,4	49,3	2,86	1,26	650	335	13,1	83,8	4,48	21,7	70	50
5	0,61	3,5	0,57	76,2	4,27	1,54	200	570	13,4	69,3	4,64	17,2		170
6	0,41	2,12	0,38	76,1	1,63	1,44	225	555	7,76	42,6	2,54	11,6	20	30
7	0,51	2,64	0,41	88,5	4,72	1,26	310	455	14,0	74,2	5,08	29,6		70
8	0,44	2,22	0,36	99,2	4,18	0,35	515	345	15,1	77,2	5,94	36,6	170	80
9	0,44	2,22	0,36	92,8	3,82	1,55	94	330	15,6	85,9	5,75	23,2		50
10	0,45	2,27	0,38	78,6	3,64	1,76	195	770	13,8	71,9	4,75	19,6	150	90
11	0,44	2,38	0,4	89,1	2,8	1,21	105	685	11,0	67,4	3,22	13,0		30
12	0,44	2,12	0,35	118,3	4,8	2,2	430	810	19,2	84,1	6,3	25,9		50
13	0,4	1,92	0,33	86,2	4,85	1,66	435	350	13,5	66,1	4,82	17,4		60
14	0,45	2,48	0,41	109,8	4,55	1,33	195	760	15,0	81,1	5,04	18,4	120	80
15	0,47	2,62	0,43	82,5	3,66	1,08	205	420	12,1	84,0	3,96	21,3	10	70
16	0,23	1,13	0,17	65,6	3,61	1,83	170	450	13,2	79,7	4,39	24,2	180	50
17	0,48	2,55	0,4	101,1	3,94	1,5	480	485	14,5	83,3	4,61	24,6	90	40
18	0,41	1,96	0,35	66,4	3,47	1,6	110	130	10,9	54,5	3,48	17,4		60
19	0,43	2,2	0,37	76,4	3,37	1,02	40	615	12,4	73,3	4,17	21,0	330	60
20	0,44	2,77	0,38	147,8	4,46	1,54	300	675	15,0	82,4	5,49	31,8	180	80
21	0,51	2,75	0,45	84,5	4,42	3,37	495	435	14,3	80,5	5,17	28,2		80
22	0,45	2,29	0,38	97,9	4,3	1,41	275	440	16,0	87,4	5,6	27,3		70
23	0,47	2,59	0,42	105,0	5,97	0,76	145	785	17,4	89,9	6,31	32,0		70
24	0,4	1,92	0,34	87,4	3,14	1,43	160	390	12,7	82,6	4,2	20,8		60
25	0,46	2,27	0,37	70,3	5,33	1,73	430	465	17,4	83,4	5,94	22,9	60	20
26	0,53	2,9	0,47	109,8	2,91	1,65	355	280	16,2	88,1	5,6	24,4		80
27	0,61	3,58	0,6	65,3	2,02	1,48	240	620	9,4	71,0	2,79	11,0	90	40
28	0,45	2,26	0,37	90,2	5,42	1,35	470	420	16,5	87,3	6,98	23,3	60	60
29	0,42	1,93	0,33	80,1	3,41	0,84	215	475	14,5	83,4	4,58	19,7		90
30	0,62	3,52	0,57	104,7	4,66	1,62	190	720	17,3	91,7	5,21	22,3		100
31	0,41	2,12	0,38	39,3	1,87	0,71	265	275	8,89	60,0	3,33	13,1	30	40
32	0,54	2,92	0,47	176,1	4,48	1,15	525	330	15,1	77,6	6,22	21,7		70
33	0,57	3,3	0,54	110,5	8,8	1,36	250	735	18,1	91,2	6,3	33,9	350	100
34	0,37	1,81	0,33	51,0	2,28	1,61	240	475	11,1	57,4	2,82	11,9		40
35	0,41	2,11	0,38	65,0	3,49	1,27	155	460	12,3	92,4	3,39	13,8	170	60
36	0,48	2,62	0,42	69,8	7,07	1,51	280	430	20,7	89,3	7,06	26,8	330	90
37	0,51	2,77	0,46	81,5	5,86	1,2	255	530	18,4	84,0	5,78	21,4	130	100
38	0,43	2,19	0,37	51,9	6,73	1,31	715	410	14,2	66,2	4,6	23,4	120	40
39	0,48	2,72	0,44	71,3	4,79	2,09	115	550	20,7	92,2	6,13	29,0	80	90
40	0,38	1,89	0,33	56,2	3,26	1,17	260	665	9,22	49,5	2,67	12,1		30
41	0,56	3,23	0,53	94,6	5,09	2,43	370	455	23,1	106,2	6,33	30,0		40
42	0,56	3,13	0,52	56,4	6,01	2,8	270	470	23,7	115,6	6,01	27,0		40
43	0,43	2,31	0,4	68,9	4,08	1,36	210	535	9,92	58,0	3,01	13,2		40
44	0,47	2,57	0,42	74,9	3,96	1,78	420	21	18,5	86,4	5,9	23,0	30	80
45	0,57	3,3	0,54	77,4	7,83	2,13	165	345	21,1	99,0	6,01	25,5	90	90
46	0,43	2,26	0,39	96,3	4,65	1,5	450	395	18,4	85,9	5,16	22,2		50
47	0,46	2,51	0,42	57,9	5,24	1,26	335	520	15,6	77,7	5,2	27,8	80	50
48	0,38	1,83	0,33	48,7	3,29	1,12	765	790	9,21	52,6	2,93	12,6	70	60
49	0,54	3,01	0,5	82,6	7,98	1,25	240	300	17,3	87,1	6,32	29,0	160	80
50	0,57	3,32	0,54	77,8	5,04	1,57	155	510	18,5	82,3	5,58	20,4	60	70
51	0,56	3,17	0,52	76,3	6,29	1,55	215	735	16,0	73,6	5,33	22,2	150	90
52	0,56	3,1	0,51	66,7	7,88	1,11	120	335	19,5	84,1	6,11	25,9	140	150
53	0,46	2,5	0,41	70,8	4,03	1,2	405	500	14,9	98,7	4,65	23,4	110	70
54	0,57	3,1	0,49	97,8	9,33	1,17	180	490	19,0	105,2	6,74	24,3	90	60



	Se	As	Sb	Th	U	Br	Hf	Ta	Zr	Au	Ag	W	Mo
	ppm	ppm	ppm	ppm	ppm	ppm	ppm	ppm	ppm	ppm	ppm	ppm	ppm
1	0.45	11.4	0.2	1.74	8.79	1.75	1.18	0.2	12			6.17	312.6
2	3.16	58.2	1.7	7.73	2.28	8.12	3.26	0.83	20	0.024			0.85
3	1.89	45.2	2.0	8.27	5.94	10.8	3.05	0.52	38	0.037			9.03
4	3.7	55.0	2.25	9.1	0.86	8.9	3.49	0.33	49			3.24	2.67
5	4.28	55.1	1.78	7.65	4.49	35.9	4.52	0.42	26			1.32	14.0
6	3.06	30.1	0.49	4.05	5.07	12.7	3.61	0.093	59				3.11
7	6.87	72.5	2.46	19.1	4.79	37.2	3.95	0.56	130				2.03
8	4.12	94.2	2.59	8.6	4.16	41.0	2.85	0.52	45	0.025		1.48	24.1
9	2.78	68.4	3.08	7.9	3.19	38.3	3.85	0.38	38			1.23	
10	3.21	46.7	3.4	7.61	8.23	42.5	2.96	0.56	82	0.019	3.54		20.2
11	2.78	20.4	1.52	5.83	1.76	21.4	4.55		105		3.84	3.42	
12	8.42	66.2	1.65	7.86	6.48	37.7	3.03	0.63	52			3.6	
13	2.68	54.4	2.16	7.93	4.54	40.0	8.15	0.62	130	0.01		7.63	
14	5.8	65.4	2.02	7.9	2.55	34.0	3.35	0.26	35			2.22	
15	1.25	47.3	1.63	6.79	4.96	32.6	2.65	0.17	21	0.009		2.24	9.73
16	3.43	58.1	2.55	7.53	1.03	34.1	3.41	0.25	99			2.36	4.42
17	3.33	52.5	3.73	7.99	1.17	36.2	4.63	0.62	64			1.58	17.0
18	2.8	44.9	1.38	5.72	3.43	18.4	5.88	0.67	170			7.8	9.29
19	4.75	50.9	1.31	6.27	3.59	12.3	5.08	0.15	88			7.81	
20	3.87	79.6	2.82	8.25	1.11	19.6	3.1	0.59	165			2.73	15.0
21	4.0	72.5	2.74	8.19	0.67	39.0	2.79	0.63	105	0.033		2.24	4.82
22	1.23	59.1	3.42	9.14	3.3	48.0	2.98	0.31	44	0.014	0.87	2.42	28.3
23	1.91	76.0	4.12	9.29	3.59	45.6	3.98	0.61				1.32	20.8
24	0.38	62.3	0.61	6.13	4.18	35.1	3.1	0.42	65			3.87	19.7
25	2.1	58.3	1.54	9.42	3.79	55.0	3.33	0.84	65			1.27	
26	3.21	81.5	2.98	8.88	1.66	47.6	3.93	0.88	110				
27	2.79	23.1	2.01	6.54	2.72	25.6	9.3	0.55	195			3.0	
28	0.9	54.2	1.05	9.46	2.64	44.1	3.87	0.87	110			1.22	
29	2.35	19.5	1.33	13.8	2.18	0.95	4.56	1.25	68			2.42	
30	2.47	9.1	1.13	8.82	6.68	1.26	3.32	0.74		0.006		2.37	2.87
31	4.19	19.9	0.69	4.92	1.16	2.47	10.4	0.49		0.019		4.37	
32	1.32	63.2	2.42	7.97	1.28	14.6	3.34	0.89	60		3.65	3.05	14.7
33	2.87	73.1	1.7	10.0	1.84	10.3	5.4		230	0.049			
34	0.11	18.1	0.92	5.41	1.85	3.6	7.33	0.96	145	0.008	0.059		
35	0.61	14.3	0.9	5.78	2.92	3.95	6.42	1.44	215				
36	0.3	62.7	1.57	9.31	2.05	11.4	4.09	1.36	80				
37	0.32	31.9	1.34	8.49	3.5	8.58	4.64	0.43	115	0.016	0.067		
38	0.64	42.1	1.38	7.13	2.57	6.38	3.02	2.46	130	0.004			
39	1.67	36.2	1.17	8.69	0.73	7.37	4.72	1.45	100				
40	0.72	24.4	0.86	7.08	1.97	3.96	8.72	0.39	95				
41	0.49	17.4	0.39	7.96	2.62	6.6	4.74	2.9	24	0.001			
42	1.27	12.7	0.099	7.12	3.38	3.42	5.27	0.19	125				
43	1.24	25.6	1.06	5.9	1.57	4.54	11.0	0.43	210				
44	0.64	39.4	0.93	6.41	1.8	4.51	3.29	1.05	60				
45	0.26	28.5	0.92	8.05	1.9	5.7	4.38	2.35	55				
46	0.36	33.4	0.42	7.56	1.62	7.25	4.3	2.23	115		0.24		
47	0.63	55.6	1.86	8.05	2.26	11.0	4.53	1.63	110				
48	0.13	25.1	0.45	6.36	0.34	5.15	16.1	1.01	330	0.005			
49	0.86	67.5	2.37	10.1	0.73	11.3	4.08	0.82	125		0.34		
50	0.1	47.7	1.13	8.14	1.82	8.98	5.26	1.47	95	0.003			
51	0.2	47.9	1.32	9.17	1.76	8.53	6.38	2.35	200				
52	0.6	44.0	1.51	8.69	1.82	9.5	3.83	1.61	55		0.28		
53	0.51	42.6	1.87	9.53	1.17	7.48	6.56	1.23	150				
54	0.27	28.4	1.34	11.5	2.34	7.75	5.42	1.66	55	0.016			

Table 6.10: Chemical characteristics of main lithofacies

lithofacies		La	Ce	Pr*	Nd	Sm	Eu	Gd*	Tb	Dy*	Ho*	Er*	Tm*	Yb	Lu	Rb	Cs	Ca	Sr
		ppm	ppm	ppm	ppm	ppm	ppm	ppm	ppm	ppm	ppm	ppm	ppm	ppm	ppm	ppm	ppm	%	ppm
A2	max	41,60	71,70	7,33	25,80	6,30	1,25	7,35	1,14	6,95	1,53	4,37	0,62	3,52	0,57	104,70	4,66	1,62	215,00
	min	21,80	38,20	4,04	14,70	3,57	1,00	4,79	0,73	4,49	1,03	2,78	0,42	1,93	0,33	68,90	3,41	0,84	190,00
	mean	33,20	58,47	6,16	21,83	5,22	1,11	6,31	0,95	5,61	1,24	3,37	0,49	2,59	0,43	84,57	4,05	1,27	205,00
	dispersion	104,76	317,66	3,37	38,32	2,11	0,02	1,82	0,04	1,55	0,07	0,75	0,01	0,69	0,02	335,37	0,39	0,16	175,00
	- n	8,36	14,55	1,50	5,05	1,19	0,10	1,10	0,17	1,02	0,21	0,71	0,09	0,68	0,10	14,95	0,51	0,32	10,80
B1-Ob	"mean"	21,50	39,00	4,04	14,70	3,57	0,91	4,48	0,67	4,21	0,93	2,69	0,41	2,12	0,38	39,30	1,87	0,71	265,00
	max	33,90	63,50	7,08	27,00	6,74	2,02	8,02	1,20	7,00	1,49	4,10	0,57	3,30	0,54	176,10	9,33	2,80	525,00
	min	22,00	41,00	4,70	17,90	4,14	0,78	5,28	0,81	4,68	1,07	2,89	0,43	2,26	0,37	56,40	3,96	1,15	115,00
	mean	26,94	49,49	5,46	20,76	5,07	1,51	6,30	0,97	5,69	1,27	3,55	0,51	2,83	0,46	92,78	5,73	1,82	329,44
	dispersion	20,91	69,62	0,74	8,66	0,67	0,14	0,63	0,01	0,43	0,02	0,16	0,00	0,16	0,00	1.166,36	3,09	0,34	22.659,03
B2	max	4,31	7,87	0,81	2,77	0,77	0,36	0,75	0,10	0,62	0,12	0,38	0,05	0,38	0,06	32,20	1,66	0,55	141,92
	min	2,51	5,68	0,66	2,55	0,73	0,41	0,99	0,11	0,66	0,15	0,50	0,07	0,56	0,09	20,08	1,77	0,29	146,94
	mean	27,84	51,56	5,63	21,10	5,14	1,37	6,48	0,96	5,64	1,25	3,48	0,50	2,72	0,45	81,77	5,12	1,50	350,33
	dispersion	6,74	34,62	0,46	6,96	0,57	0,18	1,04	0,01	0,46	0,03	0,27	0,01	0,34	0,01	432,14	3,35	0,09	23.133,81
	- n	2,51	5,68	0,66	2,55	0,73	0,41	0,99	0,11	0,66	0,15	0,50	0,07	0,56	0,09	20,08	1,77	0,29	146,94
C3	max	29,60	54,60	6,00	22,60	5,66	1,56	6,61	1,00	5,99	1,35	4,02	0,61	3,58	0,60	89,10	7,07	1,61	765,00
	min	3,42	7,52	0,94	4,02	1,14	0,16	1,74	0,29	1,90	0,46	1,41	0,23	1,41	0,26	6,77	1,07	1,12	105,00
	mean	23,82	43,20	4,66	17,25	4,15	1,12	5,19	0,80	4,75	1,06	2,97	0,44	2,35	0,40	62,88	3,88	1,40	290,38
	dispersion	50,49	153,66	1,64	22,06	1,13	0,12	1,46	0,03	1,18	0,06	0,51	0,01	0,44	0,01	456,33	3,50	0,03	46.672,76
	- n	6,83	11,91	1,23	4,51	1,02	0,33	1,16	0,18	1,04	0,23	0,69	0,10	0,64	0,09	20,52	1,80	0,18	207,56
C4	max	30,40	59,30	6,65	25,00	6,50	2,52	9,08	1,13	7,00	1,61	4,58	0,68	4,02	0,65	118,30	8,80	2,20	650,00
	min	20,60	37,00	3,92	14,30	3,44	0,60	4,48	0,67	4,19	0,93	2,69	0,40	1,92	0,33	49,30	2,86	1,11	120,00
	mean	27,84	51,56	5,63	21,10	5,14	1,37	6,48	0,96	5,64	1,25	3,48	0,50	2,72	0,45	81,77	5,12	1,50	350,33
	dispersion	6,74	34,62	0,46	6,96	0,57	0,18	1,04	0,01	0,46	0,03	0,27	0,01	0,34	0,01	432,14	3,35	0,09	23.133,81
	- n	2,51	5,68	0,66	2,55	0,73	0,41	0,99	0,11	0,66	0,15	0,50	0,07	0,56	0,09	20,08	1,77	0,29	146,94
D1	max	52,50	95,30	9,50	34,20	7,90	1,53	8,60	1,23	6,98	1,42	4,19	0,61	3,50	0,57	147,80	5,97	3,37	495,00
	min	18,70	34,50	3,60	13,50	3,29	0,82	4,42	0,66	3,58	0,70	1,78	0,23	1,13	0,17	65,60	1,63	0,76	40,00
	mean	29,60	53,81	5,73	21,30	5,05	1,21	6,04	0,90	5,24	1,15	3,14	0,45	2,46	0,40	90,05	4,04	1,53	236,50
	dispersion	81,11	270,51	2,45	29,66	1,53	0,05	1,34	0,03	0,95	0,05	0,42	0,01	0,37	0,01	542,33	1,25	0,51	14.622,50
	- n	8,54	15,60	1,48	5,17	1,18	0,22	1,10	0,16	0,92	0,20	0,62	0,09	0,58	0,09	22,09	1,06	0,68	114,72
D2	max	35,00	62,60	6,47	22,40	5,04	1,50	6,03	0,92	5,12	1,13	3,00	0,45	2,48	0,41	109,80	4,55	1,55	515,00
	min	27,20	47,10	5,02	18,60	4,33	0,91	5,18	0,80	4,71	1,09	2,98	0,44	2,22	0,36	92,80	3,82	0,35	94,00
	mean	30,03	53,57	5,72	20,73	4,80	1,19	5,74	0,87	4,95	1,11	2,99	0,44	2,31	0,38	100,60	4,18	1,08	268,00
	dispersion	18,62	65,00	0,53	3,77	0,17	0,09	0,23	0,00	0,05	0,00	0,00	0,00	0,00	0,00	73,72	0,13	0,41	48.307,00
	- n	3,52	6,58	0,59	1,59	0,33	0,24	0,39	0,05	0,18	0,02	0,01	0,00	0,12	0,02	7,01	0,30	0,52	179,46

108

lithofacies	Ba	Sc	Cr	Fe	Co	Ni	Zn	Se	As	Sb	Th	U	Hf	Ta	Au	Ag	W	Mo
	ppm	ppm	ppm	%	ppm	ppm	ppm	ppm	ppm	ppm	ppm	ppm	ppm	ppm	ppm	ppm	ppm	ppm
A2	720,00	17,30	91,70	5,21	22,30	-	100,00	2,47	25,60	1,33	13,80	6,68	11,00	1,25	0,01	-	2,42	2,87
	475,00	9,92	58,00	3,01	13,20	-	40,00	1,24	9,10	1,06	5,90	1,57	3,32	0,43	0,01	-	2,37	2,87
	576,67	13,91	77,70	4,27	18,40	-	76,67	2,02	18,07	1,17	9,51	3,48	6,29	0,81	0,01	-	2,40	2,87
	16.308,33	13,88	308,29	1,28	21,97	-	1.033,33	0,46	69,60	0,02	15,96	7,79	17,00	0,17	-	-	0,00	-
	104,27	3,04	14,34	0,93	3,83	-	26,25	0,55	6,81	0,11	3,26	2,28	3,37	0,34	-	-	0,03	-
B1-Ob	275,00	8,89	60,00	3,33	13,10	30,00	40,00	4,19	19,90	0,69	4,92	1,16	10,40	0,49	0,02	-	4,37	-
B2	550,00	23,70	115,60	6,98	30,00	90,00	90,00	1,67	63,20	2,42	11,50	3,38	5,42	2,90	0,02	3,65	3,05	14,70
	21,00	15,10	77,60	5,16	21,70	30,00	40,00	0,26	12,70	0,10	6,41	0,73	3,29	0,19	0,00	0,24	1,22	14,70
	386,22	19,57	95,04	6,16	25,11	70,00	64,44	0,80	34,82	0,97	8,30	2,03	4,37	1,51	0,01	1,95	2,14	14,70
	23.600,94	8,17	149,56	0,27	8,91	650,00	377,78	0,27	259,98	0,46	2,19	0,64	0,58	0,74	0,00	5,81	1,67	-
	144,84	2,70	11,53	0,49	2,81	22,80	18,32	0,49	15,20	0,64	1,40	0,75	0,72	0,81	0,01	1,71	0,92	-
C3	790,00	20,70	98,70	7,06	26,80	330,00	90,00	2,80	62,70	2,01	9,53	8,79	16,10	2,46	0,01	3,84	7,80	312,60
	130,00	4,18	8,36	1,31	4,68	30,00	30,00	0,10	11,40	0,20	1,74	0,34	1,18	0,20	0,00	0,06	3,00	9,29
	506,92	12,46	65,65	3,90	16,90	120,00	56,67	0,92	36,36	1,17	6,78	2,65	6,27	1,09	0,01	1,95	4,85	113,86
	36.648,08	19,28	518,08	2,35	42,02	8.600,00	442,42	1,18	285,84	0,29	4,31	4,33	14,04	0,54	0,00	7,15	4,22	29.649,29
	183,93	4,22	21,87	1,47	6,23	86,75	20,14	1,04	16,24	0,52	1,99	2,00	3,60	0,70	0,00	1,89	1,84	140,59
C4	810,00	19,50	92,40	6,33	33,90	350,00	150,00	8,42	81,50	3,73	10,10	8,23	8,15	1,63	0,05	3,54	9,03	20,20
	280,00	12,30	66,10	3,39	13,80	20,00	20,00	0,32	14,30	0,90	5,78	0,73	2,96	0,33	0,01	0,07	0,85	2,67
	479,00	16,19	83,40	5,41	23,49	129,17	68,00	2,51	53,63	2,07	8,39	3,20	4,32	0,84	0,03	1,06	3,89	13,29
	31.186,43	5,38	50,09	0,76	23,57	6.917,42	1.088,57	4,10	270,53	0,61	1,15	4,96	2,06	0,18	0,00	2,75	10,39	87,15
	170,61	2,24	6,84	0,84	4,69	79,63	31,87	1,96	15,89	0,75	1,03	2,15	1,39	0,41	0,01	1,44	2,98	7,62
D1	785,00	17,40	89,90	6,31	32,00	330,00	170,00	6,87	79,60	4,12	19,10	5,07	5,08	0,63	0,03	0,87	7,81	28,30
	420,00	7,76	42,60	2,54	11,60	10,00	30,00	1,23	30,10	0,49	4,05	0,67	2,65	0,09	0,01	0,87	1,32	4,42
	540,00	13,56	76,33	4,74	24,42	144,00	75,00	3,47	60,12	2,33	8,63	3,26	3,61	0,38	0,02	0,87	2,76	13,87
	15.083,33	6,75	181,33	1,11	44,37	17.630,00	1.338,89	2,98	235,45	1,12	15,86	2,95	0,61	0,04	0,00	-	3,46	74,31
	116,51	2,47	12,77	1,00	6,32	118,76	34,71	1,64	14,56	1,00	3,78	1,63	0,74	0,20	0,01	-	1,76	7,98
D2	760,00	15,60	85,90	5,94	36,60	170,00	80,00	5,80	94,20	3,08	8,60	4,16	3,85	0,52	0,03	-	2,22	24,10
	330,00	15,00	77,20	5,04	18,40	120,00	50,00	2,78	65,40	2,02	7,90	2,55	2,85	0,26	0,03	-	1,23	24,10
	478,33	15,23	81,40	5,58	26,07	145,00	70,00	4,23	76,00	2,56	8,13	3,30	3,35	0,39	0,03	-	1,64	24,10
	59.558,33	0,10	18,99	0,23	88,97	1.250,00	300,00	2,29	250,68	0,28	0,16	0,66	0,25	0,02	-	-	0,27	-
	199,26	0,26	3,56	0,39	7,70	25,00	14,14	1,24	12,93	0,43	0,33	0,66	0,41	0,11	-	-	0,42	-

109

Marine Geology

Table 6.11: Comparison of B2 chemical characteristics for Ob and Yenisei estuaries

Cruise	Station	lithofacies	La	Ce	Pr*	Nd	Sm	Eu	Gd*	Tb	Dy*	Ho*	Er*	Tm*	Yb	Lu	Rb	Cs	Ca	Sr	
			ppm	ppm	ppm	ppm	ppm	ppm	ppm	ppm	ppm	ppm	ppm	ppm	ppm	ppm	ppm	ppm	ppm	ppm	%
BP01	70	B2-Ob	33,9	60,8	6,48	23,1	5,68	1,58	6,39	0,95	5,4	1,18	3,14	0,45	2,26	0,37	90,2	5,42	1,35	470	
BP01	82	B2-Ob	29,6	55	6,02	22,7	5,74	1,51	6,98	1,06	6,1	1,35	3,75	0,54	2,92	0,47	176,1	4,48	1,15	525	
BP00	38	B2-Ob	33,9	63,5	7,08	27	6,74	1,93	8,02	1,2	7	1,49	4,1	0,57	3,1	0,49	97,8	9,33	1,17	180	
B2-Ob	max		33,9	63,5	7,08	27	6,74	1,93	8,02	1,2	7	1,49	4,1	0,57	3,1	0,49	176,1	9,33	1,35	525	
	min		29,6	55	6,02	22,7	5,68	1,51	6,39	0,95	5,4	1,18	3,14	0,45	2,26	0,37	90,2	4,48	1,15	180	
	mean		32,47	59,7667	6,5267	24,267	6,0533	1,6733	7,13	1,07	6,16667	1,34	3,6633	0,52	2,76	0,443	121,37	6,41	1,2233	391,7	
BP00	13	B2-Yen.	24,7	44,9	5	19,1	4,7	1,59	5,78	0,89	5,23	1,19	3,32	0,48	2,72	0,44	71,3	4,79	2,09	115	
BP00	16	B2-Yen.	27,1	49,1	5,33	20,1	4,86	1,14	6,07	0,96	5,81	1,32	3,83	0,56	3,23	0,53	94,6	5,09	2,43	370	
BP00	22	B2-Yen.	22,5	42	4,82	19,1	4,59	0,78	6	0,91	5,32	1,19	3,28	0,47	2,57	0,42	74,9	3,96	1,78	420	
BP00	22	B2-Yen.	25,2	46	5,03	19,1	4,53	1,62	5,9	0,94	5,66	1,31	3,8	0,57	3,3	0,54	77,4	7,83	2,13	165	
BP00	23	B2-Yen.	23,6	43,1	4,7	17,9	4,14	1,43	5,28	0,81	4,68	1,07	2,89	0,43	2,26	0,39	96,3	4,65	1,5	450	
BP00	15	B2-Yen.	22	41	4,72	18,7	4,65	2,02	6,3	0,99	5,98	1,34	3,8	0,56	3,13	0,52	56,4	6,01	2,8	270	
B2-Yen.	max		27,1	49,1	5,33	20,1	4,86	2,02	6,3	0,99	5,98	1,34	3,83	0,57	3,3	0,54	96,3	7,83	2,8	450	
	min		22	41	4,7	17,9	4,14	0,78	5,28	0,81	4,68	1,07	2,89	0,43	2,26	0,39	56,4	3,96	1,5	115	
	mean		24,18	44,35	4,9333	19	4,5783	1,43	5,88833	0,917	5,44667	1,23667	3,4867	0,51167	2,8683	0,473	78,483	5,3883	2,1217	298,3	
			Ba	Sc	Cr	Fe	Co	Ni	Zn	Se	As	Sb	Th	U	Hf	Ta	Au	Ag	W	Mo	
			ppm	ppm	ppm	%	ppm	ppm	ppm	ppm	ppm	ppm	ppm	ppm	ppm	ppm	ppm	ppm	ppm	ppm	
BP01	70	B2-Ob	420	16,5	87,3	6,98	23,3	60	60	0,9	54,2	1,05	9,46	2,64	3,87	0,87				1,22	
BP01	82	B2-Ob	330	15,1	77,6	6,22	21,7		70	1,32	63,2	2,42	7,97	1,28	3,34	0,89		3,65	3,05	14,7	
BP00	38	B2-Ob	490	19	105,2	6,74	24,3	90	60	0,27	28,4	1,34	11,5	2,34	5,42	1,66	0,016				
B2-Ob	max		490	19	105,2	6,98	24,3	90	70	1,32	63,2	2,42	11,5	2,64	5,42	1,66	0,016	3,65	3,05	14,7	
	min		330	15,1	77,6	6,22	21,7	60	60	0,27	28,4	1,05	7,97	1,28	3,34	0,87	0,016	3,65	1,22	14,7	
	mean		413,3	16,8667	90,033	6,6467	23,1	75	63,3333	0,83	48,6	1,60333	9,6433	2,08667	4,21	1,14	0,016	3,65	2,135	14,7	
BP00	13	B2-Yen.	550	20,7	92,2	6,13	29	80	90	1,67	36,2	1,17	8,69	0,73	4,72	1,45					
BP00	16	B2-Yen.	455	23,1	106,2	6,33	30		40	0,49	17,4	0,39	7,96	2,62	4,74	2,9	0,001				
BP00	22	B2-Yen.	21	18,5	86,4	5,9	23	30	80	0,64	39,4	0,93	6,41	1,8	3,29	1,05					
BP00	22	B2-Yen.	345	21,1	99	6,01	25,5	90	90	0,26	28,5	0,92	8,05	1,9	4,38	2,35					
BP00	23	B2-Yen.	395	18,4	85,9	5,16	22,2		50	0,36	33,4	0,42	7,56	1,62	4,3	2,23		0,24			
BP00	15	B2-Yen.	470	23,7	115,6	6,01	27		40	1,27	12,7	0,099	7,12	3,38	5,27	0,19					
B2-Yen.	max		550	23,7	115,6	6,33	30	90	90	1,67	39,4	1,17	8,69	3,38	5,27	2,9	0,001	0,24	0	0	
	min		21	18,4	85,9	5,16	22,2	30	40	0,26	12,7	0,099	6,41	0,73	3,29	0,19	0,001	0,24	0	0	
	mean		372,7	20,9167	97,55	5,9233	26,117	66,667	65	0,782	27,9333	0,65483	7,6317	2,00833	4,45	1,695	0,001	0,24			

Table 6.12: Chemical composition of the eastern Kara Sea surface sediments

	La	Ce	Pr*	Nd	Sm	Eu	Gd*	Tb	Dy*	Ho*	Er*	Tm*	Yb	Lu	Rb	Cs	Ca	Sr
	ppm	ppm	ppm	ppm	ppm	ppm	ppm	ppm	ppm	ppm	ppm	ppm	ppm	ppm	ppm	ppm	%	ppm
max	52,5	95,3	9,5	34,2	7,9	2,52	9,08	1,23	7,	1,61	4,58	0,68	4,02	0,65	147,8	8,8	3,37	765,
min	3,42	7,52	0,94	4,02	1,14	0,16	1,74	0,29	1,9	0,46	1,41	0,23	1,13	0,17	6,77	1,07	0,35	40,
mean	27,15	49,61	5,35	19,9	4,78	1,24	5,91	0,89	5,21	1,16	3,2	0,47	2,51	0,42	79,18	4,4	1,44	297,54
dispersion	42,6	142,69	1,46	19,28	1,09	0,13	1,41	0,03	0,87	0,04	0,39	0,01	0,36	0,01	566,65	2,83	0,2	29862,8
-	6,45	11,8	1,2	4,34	1,03	0,35	1,17	0,16	0,92	0,21	0,62	0,09	0,6	0,09	23,51	1,66	0,44	170,69
n	41	41	41	41	41	41	41	41	41	41	41	41	41	41	41	41	40	41

	Ba	Sc	Cr	Fe	Co	Ni	Zn	Se	As	Sb	Th	U	Hf	Ta	Au	Ag	W	Mo
	ppm	ppm	ppm	%	ppm	ppm	ppm	ppm	ppm	ppm	ppm	ppm	ppm	ppm	ppm	ppm	ppm	ppm
max	810,	20,7	98,7	7,06	36,6	350,	170,	8,42	94,2	4,12	19,1	8,79	16,1	2,46	0,05	3,84	9,03	312,6
min	130,	4,18	8,36	1,31	4,68	10,	20,	0,1	11,4	0,2	1,74	0,34	1,18	0,69	0,	0,06	0,85	2,67
mean	502,68	14,3	75,9	4,78	21,81	130,37	66,5	2,36	51,37	1,89	7,92	3,05	4,69	0,76	0,02	1,29	3,36	35,9
dispersion	28890,12	11,84	272,25	1,68	47,24	8088,32	890,	3,83	385,7	0,83	5,91	3,81	6,37	0,31	0,	2,78	5,68	6401,89
-	167,89	3,4	16,3	1,28	6,79	88,25	29,46	1,93	19,4	0,9	2,4	1,93	2,49	0,55	0,01	1,54	2,34	77,1
n	41	41	41	41	41	27	40	41	41	41	41	41	41	39	14	7	25	14

## 6.7 Lithostratigraphy of gravity cores ("Akademik Boris Petrov" Kara Sea Expedition SIRRO-2001)

*R. Stein*

Alfred Wegener Institute, Columbusstraße, Bremerhaven, Germany

### Introduction

During the "Akademik Boris Petrov" Kara Sea Expedition SIRRO-2001, a total of 61 gravity cores with lengths between 0.10 and 7.43 meters were obtained (Fig. 6.22; cf. Fig. 6.2). Onboard "Akademik Boris Petrov", a selected set of 10 sediment cores were already opened, described and sampled for smear-slide analyses (see Appendix 10.2). In addition, 18 cores were opened, photographed, and described at AWI. Color slides from the core sections are available at AWI (request to R. Stein, AWI) as well on <http://www.pangaea.de>. Furthermore, from all these cores sediment slabs were taken for X-Ray photographs. In several of the opened cores, abundant bivalves were found which were sampled for future AMS<sup>14</sup>C dating (Tab. 6.13). In almost all of the core tops, dark brown sediments were observed, indicating that the (near-) surface sediments were recovered in the cores.

The main purpose of this chapter is to summarize the major lithologies of the sedimentary sequences based on lithological core descriptions and to obtain a lithostratigraphic framework. These data should be the basis for future sampling and more detailed sedimentological, micropaleontological, and geochemical studies of the BP2001 sediment cores.

### Lithostratigraphy

For presentation and description of the major lithologies, 15 sediment cores have been selected and grouped into four groups: the Yenisei cores (Fig. 6.23), the Ob cores (Fig. 6.24), the cores from the northeastern part of the study area (Fig. 6.25), and the cores from the northwestern part of the study area (Fig. 6.26). The complete core descriptions of all cores and smear-slide data are presented in the Appendix 10.2.

Core BP01-03/4 taken from the central part of the Yenisei marginal filter, mainly consists of very dark gray and dark olive gray, bioturbated silty clay to clayey silt (Fig. 6.23). The lithology is very similar to that of Core BP99-04/7 from the northern part of the marginal filter, representing young Holocene sediments and reflecting the high-sedimentation-rate environment (Stein 2001). In Core BP01-26/3 obtained from the area north of the Yenisei (Fig. 6.22), the sediment composition is much more variable. Three lithological units can be distinguished (Fig. 6.23). Unit I is composed of dark olive, very dark gray, and black, bioturbated silty clay. At the base of the unit, a large ikaite crystal (about 5 cm in diameter) was found (cf. Chapter 7.9). The underlying Unit II is characterized by olive gray silty clay to clayey silt with intercalated sandy layers. Unit III consists of silty clay to clayey silt with minor amounts of sand. The unit is less bioturbated than Unit I, and distinct color variations between olive gray, dark olive gray, dark gray, very dark gray, and black with sharp

boundaries are obvious. Furthermore, significant amount of diatoms are present in this unit (see smear-slide data, Appendix 10.2). This variability in lithology probably reflects distinct changes in the depositional environment (e.g., changes in riverine sediment supply).

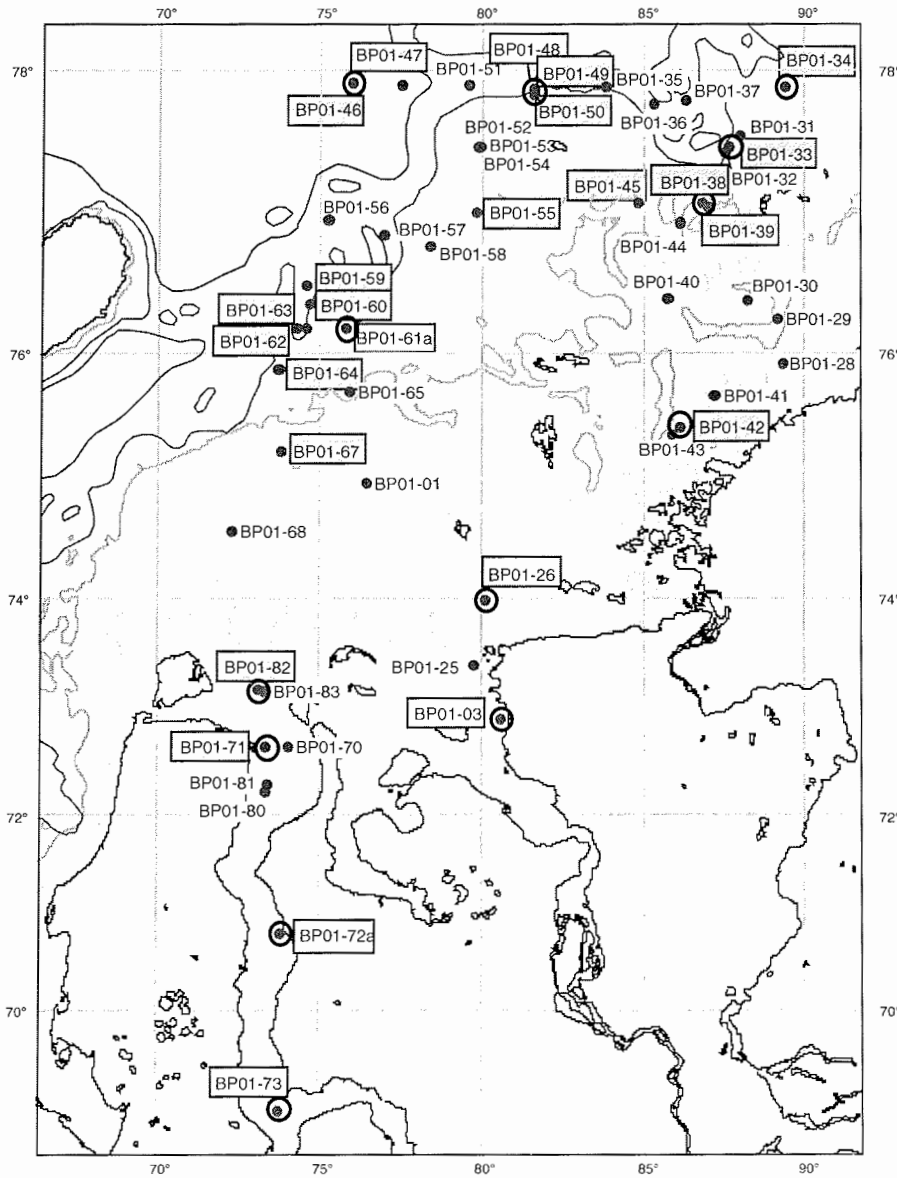


Fig. 6.22: Location of gravity cores obtained during "Akademik Boris Petrov" Expedition 2001. The cores marked by gray boxes were opened and described (see Appendix 10.2). For the circled cores, lithologies are presented in this chapter.

The sediment cores obtained from the Ob area are characterized by very different lithologies (Fig. 6.24). The two northern cores BP01-71/4 and BP01-82/8 are mainly composed of very dark gray and dark olive gray, bioturbated clays (Unit I). In Core BP01-71/4, more sandy layers are occasionally intercalated. The lowermost part of the core (200 - 232 cm) consists of dark olive gray sandy silty clay (Unit II). Core BP01-72a/2 was obtained from a narrow sediment-filled pocket/channel where the ELAC profiler showed a penetration of several meters below the seafloor. Two main lithological units can be distinguished. Below a more sandy, very dark gray and dark olive gray Unit I, most of the core is composed of laminated, dominantly black and very dark gray silty clay (Unit II). These laminated sediments may reflect a short-term variability in the depositional environment controlled by factors such as river supply, oxygenation, organic-carbon preservation, etc. The southernmost Core BP01-73/5 taken in front of the mouth of the River Taz, is mainly composed of alternation between 0.5-2 cm thick, clayey sand silt layers and 0.2-0.5 cm thick clayey silty sand layers. These variations may have been caused by (cyclic) variations in the hydraulic regime.

The northeasternmost Core BP01-34/7 mainly consists of dark gray, very dark gray, and dark olive gray silty clay units, intercalated with two units characterized by mud clasts (Fig. 6.25). Core BP01-33/2 can be divided into three lithological units (Fig. 6.25). Unit I is composed of dark olive gray and very dark gray, bioturbated silty clay. Between 450 and 690 cm core depth, (finely) laminated dark olive gray and very dark gray, relatively stiff silty clay to clayey silt is the typical lithology. The lowermost part of the core (Unit III) consists of dark olive gray and black clayey silty sand. Cores BP01-38/7 and BP42/2 only consists of one lithological unit characterized by dark olive gray, very dark gray, and black (Holocene) silty clay to clayey silt (Fig. 6.25). Further sedimentological studies are necessary to interpret the different lithologies of these cores in relationship to changes in the depositional environment.

The sedimentary sequence of northwesternmost Core BP01-46/7 can be divided into two lithological units (Fig. 6.26). Unit I is composed of dark olive gray, very dark gray, and black (Holocene), bioturbated silty clay to clayey silt. Unit II (211-234 cm core depth) consists of very dark gray to black, firm clayey sandy silt with several pebbles and stones (diamicton). Between both units, a thin horizon of laminated very dark gray silty clay was observed. Cores BP01-48/07, BP01-49/2, and BP01-50/2 taken very close to each other (cf., Fig. 6.22), can be correlated based on the upper three lithological units preserved in all three cores (Fig. 6.26). Below a very dark brown and dark grayish brown sandy silty clay unit (Unit I), very dark gray and dark olive gray, bioturbated silty clay to clayey silt (Unit II) was observed. The underlying Unit III is composed of very dark gray and dark olive gray silty clay with intercalated sandy layers. Unit IV, not present in Core BP01-48/7, is characterized by very stiff silty sandy clay (and one stone) in Core BP01-49/2 and by silty sandy clay with abundant stones/pebbles (diamicton) in Core BP01-50/2. In the latter core, the diamicton of Unit IV is underlain by four types of lithologies: dark olive gray sandy silty clay (Unit V), sandy silty clay with intercalated sandy laminae (Unit VI), dark olive gray clayey silty sand (Unit VII), and sandy silty clay with intercalated sandy laminae (Unit VIII).



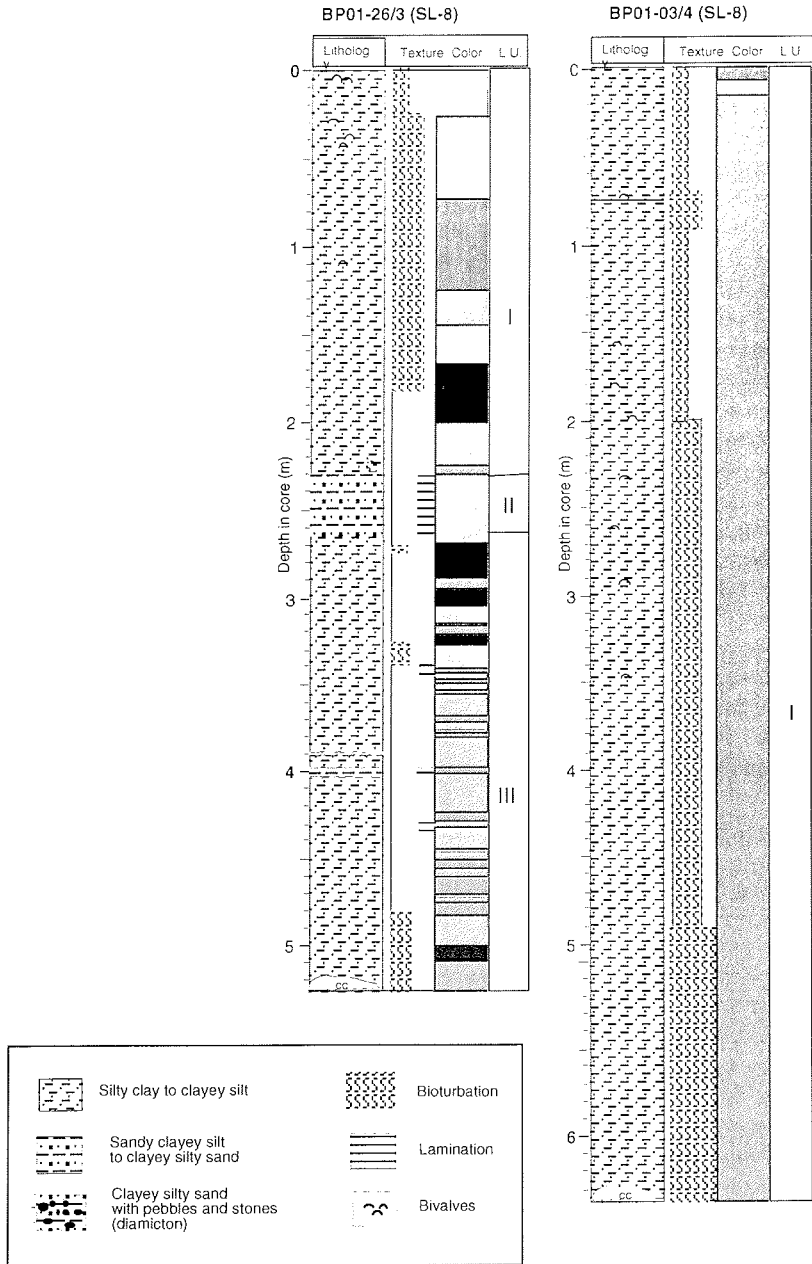


Fig. 6.23: Lithologies of Yenisei sediment cores. Distinct changes in sediment color between mainly gray and olive gray to black are marked by different gray scales (for detailed color codes see Appendix 10.2). For location of cores see Fig. 6.22.

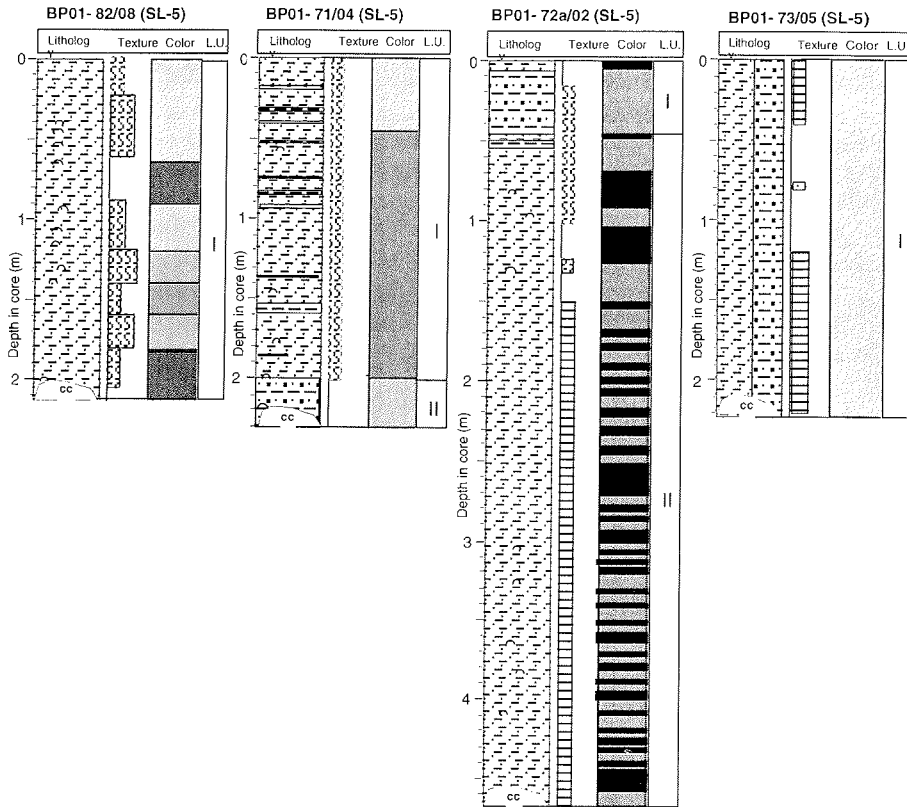


Fig. 6.24: Lithologies of Ob sediment cores. Distinct changes in sediment color between mainly gray and olive gray to black are marked by different gray scales (for detailed color codes see Appendix 10.2). For location of cores see Fig. 6.22, for legend see Fig. 6.23.

Cores BP01-46/7, BP01-48/7, BP01-49/2, and BP01-50/2 were obtained from an area close to the proposed margin of the Last Glacial Maximum (LGM) Kara Sea Ice Sheet (see Chapter 6.2). The different lithologies of these cores (laminated sediments, very stiff silty clayey sand, and diamicton) may be related to glacial processes. A detailed study of these cores as well as the other cores taken from this area (see Appendix 10.2) may give information about the extension and the history of LGM glaciation in this area.

Core BP01-61/07 (see Fig. 6.22 for location) is only composed of bioturbated silty clay to clayey silt (Unit I), probably representing young (Holocene) sediments and assuming high sedimentation rates. A study of these sediments will allow a high-resolution reconstruction of Holocene depositional environments.

## **Outlook**

Based on (a) the lithological core description, (b) future AMS<sup>14</sup>C dating of the sediment cores, (c) sedimentological, mineralogical, micropaleontological, and geochemical data sets, (d) detailed topographic maps, and (e) the evaluation of sediment echograph and Geochirp profiles, a detailed reconstruction of the paleoenvironment (e.g., changes in paleo-river discharge, history of late Quaternary glaciation, etc.) and a calculation of sedimentary and organic carbon budgets will be performed.

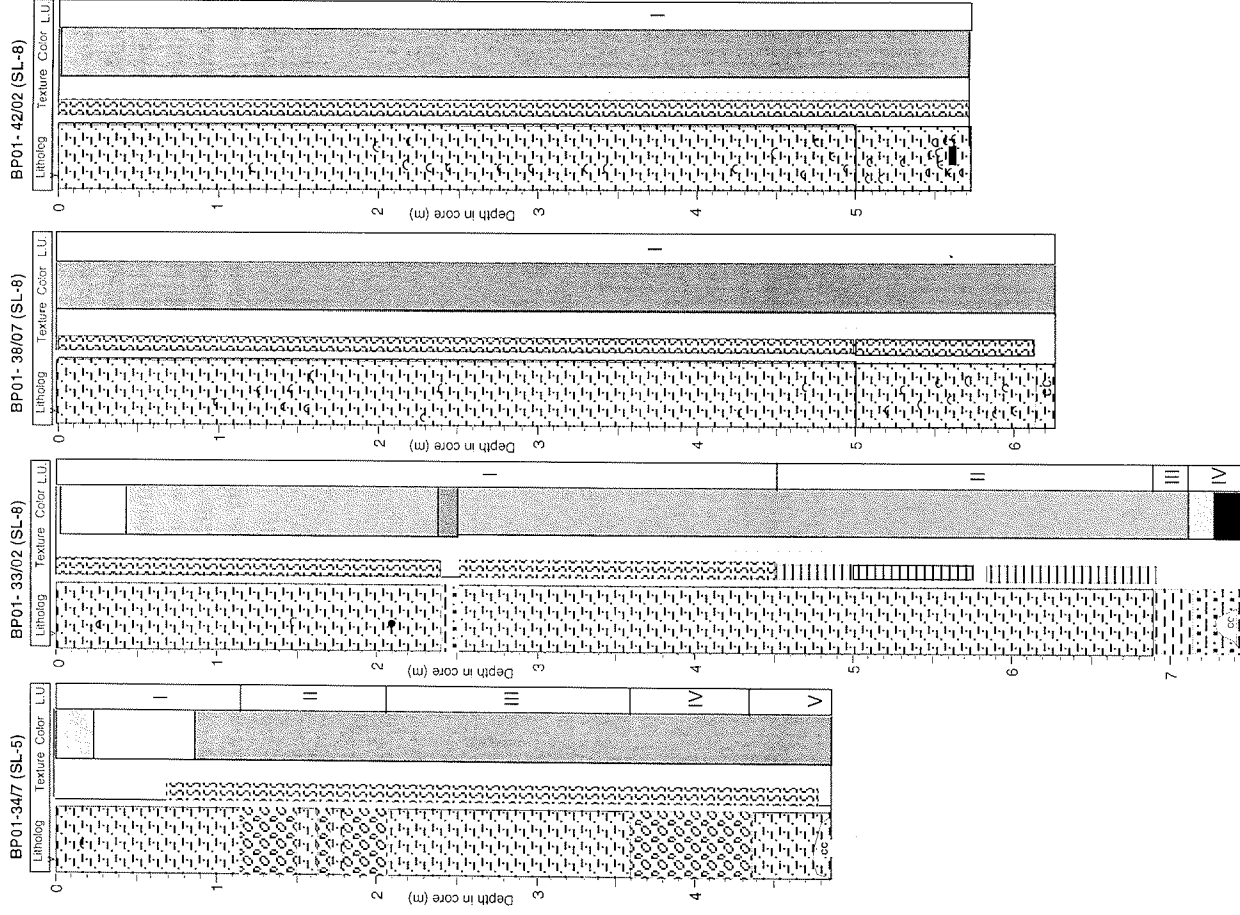


Fig. 6.25: Lithologies of sediment cores from the eastern and northeastern part of the study area. Distinct changes in sediment color between mainly gray and olive gray to black are marked by different gray scales (for detailed color codes see Appendix 10.2). For location of cores see Fig. 6.22, for legend see Fig. 6.23.

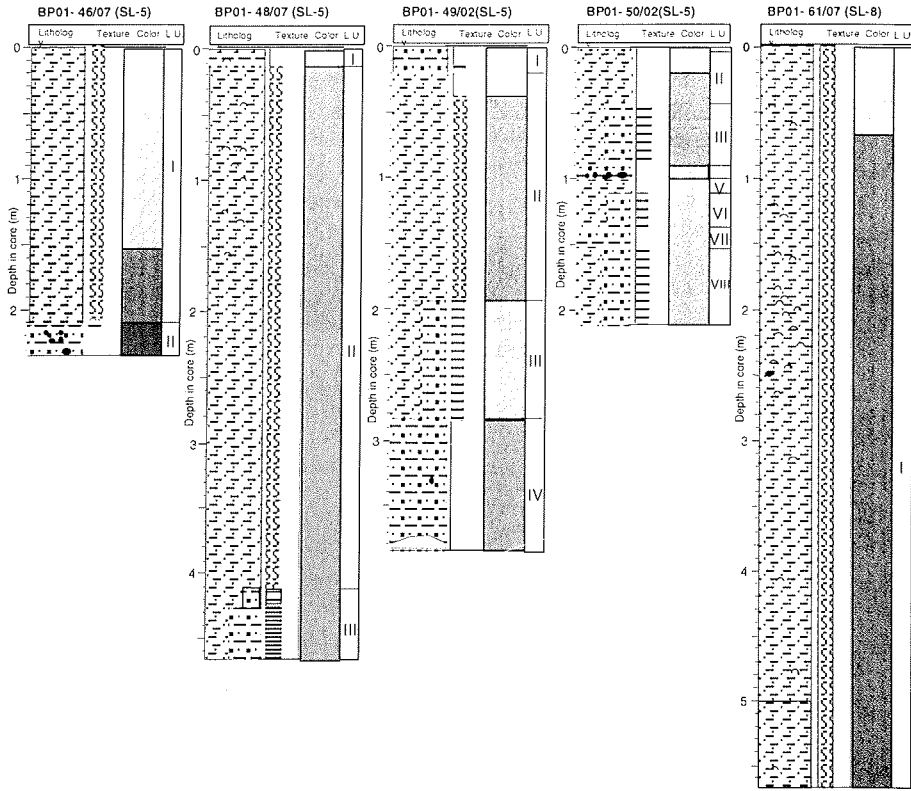


Fig. 6.26: Lithologies of sediment cores from the northwestern part of the study area. Distinct changes in sediment color between mainly gray and olive gray to black are marked by different gray scales (for detailed color codes see Appendix 10.2). For location of cores see Fig. 6.22, for legend see Fig. 6.23.

Table 6.13: Compilation of all bivalve samples taken from cores and available for AMS-14C dating

<b>BP01-33/02</b> Depth (cm)	<b>BP01-39/02</b> Depth (cm)	<b>BP01-42/02</b> Depth (cm)	<b>BP01-45/06</b> Depth (cm)	<b>BP01-46</b> Depth (cm)	<b>BP01-61/07</b> Depth (cm)
23-24	51	120	13	40	60
24	60	200	15		120
30	76	214	27		127
47	121	217,5	27,5	<b>BP01-48/07</b>	130
85	127	232	47	Depth (cm)	157
144	128	246,5	52		160
	152	275	63	10	183
	169	293,5	70	42	190
<b>BP01-37/06</b>	170	330	85	73	194
Depth (cm)	172	342	169	75	200
	179	427,5	170	87	203
128	187	450	171,5	101	215
160-161	195	468	210	125	225
174	200	477	267	131	239
195	245	487	277	158	242
219	256	494	285		265
240	262,5	504	302,5		313
245	280	508	304	<b>BP01-49/02</b>	407
245,5	287,5	516	308	Depth (cm)	478
260	296	530	326		552
284	349	545	350	20	
308	391	547,5	365	52	
	460	550	375		<b>BP01-62/05</b>
	470	553	380		Depth (cm)
<b>BP01-38/07</b>	480	554	460	<b>BP01-59/05</b>	
Depth (cm)	481	557	488	Depth (cm)	222
	500	560	491		280
5	509	562	499	179	330
99,5	511	567	567	386	346
124	525		599	465	355
140				468	360
144				479	440
156				480	477
160				502	
227					
238					<b>BP01-72a/02</b>
429					Depth (cm)
478					
520					80
529					95
540					129
552					304
560					364
561					379
571.5					408
588					
595					
600					

## 7.1 Bacterial consumption and transformation of dissolved organic matter (DOM) in the rivers Ob, Yenisei and the adjacent Kara-Sea.

B. Meon, H. Köhler

Institute of Biogeochemistry and Marine Chemistry, University of Hamburg, Germany

### Introduction

Heterotrophic bacteria are the most abundant organisms in the oceans ( $0.5 \times 10^6 - 10^7$  cells/ml) and constitute a key component in the oceanic organic carbon cycle (Azam et al. 1983; Williams 2000). Due to their almost unique ability to use dissolved organic matter (DOM) as carbon and energy source heterotrophic bacteria are the major sink of DOM thus shaping both the amount and composition of more than 95 % of the total organic carbon (TOC) in the oceans. While algal-derived organic carbon is predominantly labile and easily available to the bacterial community, riverine DOM is believed to be refractory due to the diagenetic processing the material has undergone on its way from the terrestrial source to the river mouth. Conservative mixing of riverine dissolved organic carbon (DOC) along the salt gradient from the freshwater to the marine endmembers supports the notion of a recalcitrant riverine DOC pool. However, the amount of terrestrially-derived carbon in the oceans and the influx of DOC through rivers are not balanced i.e. significantly less terrestrially-derived carbon than expected can be measured in the marine environment (Hedges et al. 1997). Apparently there exists a major sink for terrestrial DOM that so far escaped recognition.

The Kara-Sea receiving the huge freshwater discharge of two of the largest rivers in the Arctic, Ob and Yenisei, is an ideal testground to investigate physicochemical DOM transformation processes during estuarine mixing and bacterial utilization of riverine DOM. A comprehensive overview of the sampling stations covered by the BP 2001 cruise is given in various other contributions of this volume.

In addition to taking water samples for routine DOC, dissolved organic nitrogen (DON) and inorganic nutrient monitoring, we measured an array of bacterial parameters at selected main stations covering the rivers Ob, Yenisei and the adjacent Kara-Sea. Furthermore, we performed a number of mixing experiments to address the impact of riverine DOM on bacterial growth in medium and high salinity water of the Kara-Sea. Finally, we investigated the potential impact of photooxidation on riverine DOC concentration and transformation. Since information on the role of heterotrophic bacteria in the carbon cycle of the Arctic Ocean is still limited our study will be an important contribution to a better understanding of microbial processes and carbon fluxes in high latitude oceanic regimes.

### Material and Methods

#### Dissolved organic matter (DOM) and inorganic nutrients

Water samples for the determination of DOC, fluorescent properties, dissolved amino acids and dissolved carbohydrates were filtered through precombusted GF/F-filters and stored in combusted ampoules ( $-20^\circ\text{C}$ ). GF/F-filtered samples for dissolved organic

nitrogen (DON; fixed with mercury chloride) and inorganic nutrient measurements were stored in the cold (4°C) or frozen (-20°C).

#### Ultrafiltration of DOM

In order to isolate DOM from the salty water matrix, prefiltered (0.2µm) large volume samples (150-500 l) were ultrafiltered using a tangential flow disc tube system (Pall Rochem). Filters (Desal, Osmonics) with cut-off sizes of about 150, 450, 800 and 2000 Daltons were applied, thus achieving concentrated samples for up to 4 different size classes of the DOM. All samples were concentrated to about 1.5 l and stored frozen at -20°C for detailed analyses. Analyses will include the elemental and isotopic composition of all size-fractions, allowing more detailed conclusions about the origin and diagenetic state of DOM.

In close cooperation with the Vernadsky Institute in Moscow analyses of <sup>127</sup>Cs and <sup>90</sup>Sr will be carried out in both the concentrated and permeated sample water. These results will improve our understanding about the interactions between DOM and artificial radionuclides.

#### Humic matter

For the isolation of humic matter filtered (0.2 µm) water samples (90 l) were acidified (HCl, pH 2) and pumped through a column filled with XAD-8 resin (Thurman and Malcolm, 1981). Hydrophobic substances (humic and fulvic acids) which are adsorbed by the resin under acidic conditions were eluted with an alkaline solution (0.1 M NaOH). Analyses on the humic matter extracts will include NMR-spectroscopy as well as the elemental and isotopic composition of humic and fulvic acids.

#### Lignin phenols

The DOM of pycnocline water samples previously collected during the BP 2000 cruise revealed elevated C/N ratios compared with surface and deep water samples. In order to gain more information on the source of the dissolved material in the pycnocline we concentrated DOM on C18 columns. During the BP 2001 cruise water from CTD-casts from the surface and the pycnocline of 15 selected stations was filtered (0.2 µm) and acidified with HCl to reach a pH of 2. Using a peristaltic pump we extracted 1 – 6 l of acidified sample water on C 18 columns (Varian Inc.) that had been prerinsed with 50 ml of MeOH and 1 l of deionized water (pH 2) just before sample processing. A subsequent rinse with 1 l of deionized water was applied to flush inorganic salts from the resin. The columns were stored frozen (-20°C). The absorbed material will be analyzed for lignin-phenols that are indicative for plant-derived material of terrestrial origin.

#### Bacterial numbers

Surface water samples (20 ml) from the Ob, Yenisei and depth profiles in the estuaries and the Kara Sea were fixed with 1 ml 0.2 µm-filtered formaldehyde (37 %) and stored in the cold. After a maximum of 2 days the fluorescent dye DAPI (2 µg/ml sample) was added to 2 - 5 ml of the fixed samples to stain the bacteria. After 3 minutes the stained bacteria were gently filtered on black polycarbonate filters. The filters were placed on a drop of immersion oil on a microscope slide. Finally the filters were covered by a cover slip on which a drop of oil had been smeared and frozen (-20°C) until counting with a epifluorescence microscope.



### Bacterial production

Bacterial production measurements of water samples followed a modified procedure by Kirchman (1993). In short,  $^3\text{H}$ -labeled leucine (final concentration: 10 nM) was added to 10 ml of a water sample. The samples were incubated for 1 to 2 h in the dark, generally at the in situ surface temperature of the respective station. After incubation the samples were filtered on 0.22  $\mu\text{m}$  GSTF-filters (Millipore) using a Hofer box. Immediately after filtration 2 ml of ice-cold 5 % TCA was added to the filters. After 2 minutes the TCA supernatant was discarded using vacuum filtration followed by a rinse with 2 ml of filtered, ice-cold seawater (or river water, depending on the salinity of the water sample). The filters were air dried and stored in scintillation vials. A sample set consisted of 3 replicates and a TCA-killed control with samples taken from the surface, the pycnocline and close to the bottom. In order to calculate bacterial production from leucine uptake as accurate as possible we performed experiments to determine uptake/biomass conversion factors (Kirchman and Ducklow 1993) for the study area (Yenisei and Kara-Sea) rather than using non-site specific conversion factors from the literature. In total we performed about 770 individual assays during BP 2001 covering the depth profiles of 30 stations.

### Bacterial uptake of sugars and amino acids

To estimate the contribution of sugars and amino acids to bacterial production we measured bacterial uptake of  $^3\text{H}$ -glucose and a  $^3\text{H}$ -labeled amino acid mixture in the rivers Ob, Yenisei and depth profiles of the adjacent Kara-Sea. The labeled compounds (final concentration: 0.5 nM) were added to 10 ml of sample water. The incubations lasted between 4 and 12 hours and were performed in the dark at the in situ surface temperature of the respective station. After the incubation the samples were filtered on 0.22  $\mu\text{m}$  GSTF-filters (Millipore) followed by a rinse of the filters with 0.2  $\mu\text{m}$ -filtered water taken at the sampling site. A sample set consisted of 2-3 replicates and one TCA-killed control. The filters were air dried and stored in scintillation vials. We performed 360 individual assays covering 17 stations in the study area.

### Bacterial respiration

Bacterial respiration was measured in 0.8  $\mu\text{m}$ -filtered water samples using high precision automated potentiometric Winkler determination of dissolved oxygen. Filtered water samples were allowed to sit for at least 30 minutes in PP-bottles before they were siphoned into 120 ml BOD-bottles carefully avoiding bubble formation. At least two bottle volumes of sample water were used to flush the BOD-bottles before the stoppers were added. One set of replicates (usually 4) was immediately fixed with Winkler reagents followed by the determination of dissolved oxygen in the titrator using 0.0125 N thiosulfate as titrant solution for 50 ml of sample aliquots. A second set of replicates was incubated for 22 to 50 h in the dark at the in situ water temperature before fixation and analysis of dissolved oxygen was performed. Differences in dissolved oxygen concentration between the start and the end of the experiments allow an estimate on bacterial oxygen consumption. Routinely, TCA-killed water samples were incubated along with untreated samples to check for abiotic oxygen consumption. The time consuming experimental design of the method allowed only a limited number of measurements. We measured bacterial respiration in surface and/or pycnocline water samples at 8 stations during the BP2001 cruise.

#### Carbon limitation of bacterial growth

We experimentally investigated possible carbon limitation of bacterial growth at 5 stations located in the rivers Yenisei, Ob and the Kara-Sea. Unfiltered surface water samples were filled into 2-l polycarbonate bottles. One bottle served as control and one bottle was spiked with glucose (2  $\mu\text{M}$  final concentration) as carbon source. The bottles were incubated for about 72 hours in the dark at surface water temperature. In regular time intervals, subsamples were taken for bacterial production measurements using the method described above.

#### Impact of riverine water on bacterial growth in the Kara-Sea

In order to address the impact of riverine water on the growth of bacterial communities in the Kara Sea during estuarine mixing we performed 2 mixing experiments. We added 0.5 l of bacteria-free (0.2  $\mu\text{m}$ -filtered) water of the Yenisei-endmember to polycarbonate bottles containing 1.5 l of freshly sampled surface water from the stations BP01-35 and BP01-66, respectively. The respective control bottles contained 1.5 liter of freshly sampled surface water and 0.5 l bacteria-free water from the same sampling site. Each experiment consisted of 2 replicates and one control. The bottles were incubated for 3-4 days in the dark at the surface water temperature. In regular intervals subsamples for bacterial production measurements and the determination of bacterial numbers and DOC concentrations were taken following the procedures described above.

#### Degradation of riverine DOM by bacteria

Raw water of the Yenisei, Ob and the Taz was stored in 20-50 l PP-tanks in the dark at approximately 4°C to study the degradation of riverine DOM by the natural bacterial communities and evaluate the amount of labile, semi-labile and refractory DOM present in the riverine water. Subsamples for DOC determination were taken in regular intervals during the cruise and sampling proceeded after arrival of the tanks at the Alfred-Wegener Institute in Bremerhaven.

#### Photooxidation of riverine DOM

Photooxidation by UV radiation is an important removal and transformation factor of DOM (Mopper and Kieber, 2000). We performed three experiments to address the potential of photooxidation of riverine DOM in the Kara Sea. Filtered water (0.2  $\mu\text{m}$ ) of the Yenisei and Ob freshwater endmembers was exposed in quartz bottles to ambient sunlight on deck of the ship. The dissolved oxygen concentration in the sample water was determined at the beginning and at the end of the experiment using automated potentiometric Winkler determination (see above). In addition to oxygen measurements we took samples for DOC determinations in order to assess the formation of CO and CO<sub>2</sub> from dissolved organic carbon by photooxidation. The maximum exposure periods were 12 and 19 days, respectively, for water from the Yenisei and 2.5 days for Ob water.

#### Flocculation experiment

The abiotic conversion of DOM to particulate organic matter (POM) due to flocculation and sorption processes during estuarine mixing of riverine and marine water masses was investigated in a simple mixing experiment. Water from the Yenisei endmember and high salinity water from the Kara Sea were mixed in various proportions to give salinity values of 0, 2.5, 5.1, 6.8, 10.2 and 33.8 psu, respectively. We particularly focused on the salinity range between 0 and 10 psu because results from a previous experiment

indicated the predominance of flocculation processes in low-salinity mixtures. The mixed water samples were stored in 20 l plastic vessels in the dark at ambient temperature. After 2 days small volume subsamples were siphoned out of the vessels for DOC determination. The remaining water was filtered on precombusted GF/F filters for the determination of particulate organic carbon (POM). Samples for DOC and POM determinations of the endmembers were taken at the beginning of the experiment to calculate a theoretical mixing curve and assess deviations in the carbon partitioning caused by mixing.

### Preliminary Results and Discussion

Bacterial respiration rates from 8 stations in the Kara Sea and the rivers Ob and Yenisei, respectively, are presented in Table 7.1. The measured rates range from below the limit of resolution (i.e. the difference in oxygen concentration between start and end of the incubations did not differ significantly when applying the student t-Test) to  $2.2 \mu\text{M O}_2 \text{ d}^{-1}$ , with most of the values around or below  $1 \mu\text{M}$  and highest values encountered in the Ob bay (BP01-72) and north of the Ob bay (BP01-01). The few respiration data so far reported for the Arctic Ocean (Cota et al. 1996) give only numbers for community respiration on an area basis thus allowing no direct comparison to our study. A compilation of data on community respirations in various other oceanic regimes is presented by Williams (2000) with values generally ranging between  $0.9$  and  $4.1 \mu\text{M O}_2 \text{ d}^{-1}$ . Considering the fact that bacterial respiration generally represents only a fraction (about 40 %) of the community respiration our data from the Kara Sea agree well with other oceanic regimes indicating an active bacterial community in arctic shelf areas. Interestingly, bacterial respiration in the pycnocline was generally higher than in the respective surface water sample suggesting favorable conditions for bacterial growth in the pycnocline, maybe due to the accumulation of particulate organic material in the steep density gradient. Bacterial production measurements that are currently processed in our laboratory, together with primary production measurements (E. Noethig and co-workers) will complete the data set and allow a more detailed and substantiated interpretation of the bacterial carbon demand and utilization in the Kara Sea.

The photoreactivity of the riverine DOM pool of the Yenisei is illustrated in Figure 7.1. Under sunny weather conditions we measured a photochemical dissolved oxygen consumption of  $43 \mu\text{M O}_2$  ( $3.6 \mu\text{M O}_2 \text{ d}^{-1}$ ) for Yenisei water within 12 days. The subsequent onset of cloudy conditions slightly decreased the rate to  $2.9 \mu\text{M O}_2 \text{ d}^{-1}$  with a total of  $64 \mu\text{M O}_2$  being consumed after 19 days of exposure to natural sunlight. A second experiment during cloudy conditions resulted in a decrease of  $1.8 \mu\text{M O}_2 \text{ d}^{-1}$  (Fig. 7.1) which is similar to a decrease of  $1.5 \mu\text{M O}_2 \text{ d}^{-1}$  measured in water of the Ob (data not shown). These oxygen consumption rates are more than an order of magnitude lower than reported values for the Amazon river system ( $3.6 \mu\text{M O}_2 \text{ d}^{-1}$ ; Amon and Benner 1996), reflecting the smaller photon flux in high latitudes. The magnitude of photooxidation processes in the estuaries of Ob and Yenisei is certainly restricted to the uppermost layer of the water column due to the strong light attenuation by the riverine humic substances. However, upon mixing with water of the Kara-Sea, the penetration of light increases and light quanta will reach photoreactive substances in deeper water layers. Integrated over the polar summer photooxidation in arctic waters might be an important factor for DOM transformation processes and the formation of labile bioreactive substrates from soil derived, recalcitrant carbon (Obenosterer et. al. 1999).

DOC concentrations of samples taken at the beginning and at the end of the experiments will reveal the potential for the direct formation of CO and CO<sub>2</sub> from DOC by photooxidation.

Table 7.1: Bacterial respiration in the Ob, Yenisei and the adjacent Kara Sea.

Station	Latitude °N	Longitude °E	Depth layer	Bacterial respiration ( $\mu\text{M O}_2/\text{d}$ )
BP01-01	74°59.12	76°23.41	surface	n.s.
			pycnocline	2.19
BP01-04	71°05.5	83°06.2	surface	n.s.
			pycnocline	0.62
BP01-45	77°29.94	79°52.0	surface	0.41
			pycnocline	0.92
BP01-52	76°31.16	74°30.95	surface	n.s.
			pycnocline	0.34
BP01-59	75°42.98	75°50.79	surface	1.38
			pycnocline	0.77
BP01-65	74°35.05	72°14.97	surface	0.57
			pycnocline	1.01
BP01-68	70°49.88	73°44.34	surface	1.96
			pycnocline	

n.s. = no significant difference between start and end of incubation

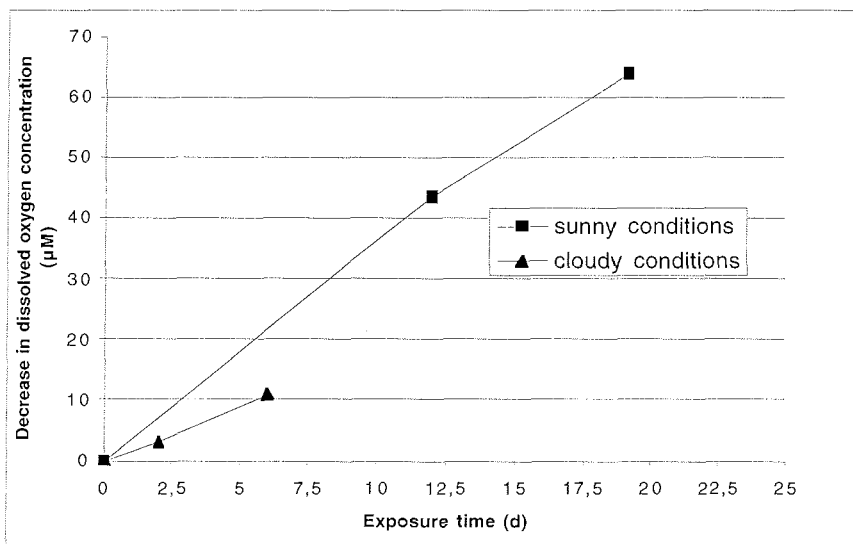


Figure.7.1: Photorespiration in 0.2  $\mu\text{m}$ -filtered water from the Yenisei. Incubations were conducted in quartz bottles on deck during the BP 2001 cruise in August 2001 under natural light conditions.

## 7.2 Geochemistry of carbon and silica: water column and sediment sampling. Material, methods and first results

A. C. Gebhardt, N. Lahajnar, B. Gaye-Haake  
Institute for Biogeochemistry and Marine Chemistry, University of Hamburg

### Introduction

The Arctic Ocean makes up only 1.5% of the global ocean, but receives about 10% of the global river discharge (Aargard 1994). More than one third of the total freshwater discharge to the Arctic Ocean occurs into the Kara Sea, mainly via Ob and Yenisey (Milliman et al. 2000) which are the second and, respectively, third largest Arctic rivers (Telang et al. 1991). During the "Akademik Boris Petrov" expedition 2001 sampling of sediments and suspended matter was carried out along the salinity gradient from the estuaries to the offshore area. The samples will be analyzed to determine sources, cycling processes and burial rates of organic matter in the Kara Sea. Organic composition and stable isotope analyses of suspended matter, sinking particles and recent sediments can be used to determine the degradational state and source of organic matter and its potential to be buried in the sediments.

### Shipboard sampling program and methods

During the "Akademik Boris Petrov 2001" expedition special emphasis was put on the northern and northeastern part of the Kara Sea and on the Ob river. At the southernmost sampling locations water masses of pure riverine nature ( $\approx 0\%$  salinity) were found in the Ob as well as in the Yenisey. Particulate matter from these stations are expected to represent the riverine material delivered by the Ob and Yenisey to the Kara Sea at the end of the high discharge period during summer. Transects from the Ob and Yenisey, respectively, to the Kara Sea will give an insight into processes taking place on particulate matter on its way from the rivers to the ocean, passing the marginal filter (Lisitsyn 1995). Sampling of particulate matter was carried out on 48 stations (Tab. 7.2). Sampling depths were chosen according to the CTD profiles. In most cases, a rather distinct thermohalocline separated an upper low saline from a deeper higher saline water mass. Therefore, one sample was taken from the surface, one from the deeper water mass and one from the thermohalocline. Surface samples were taken by means of a bucket, whereas the thermohalocline sample was taken with a 24-bottle Niskin rosette and the deep water sample with a large volume sampler (Bathomat, 200lt). One part of the samples was filtered through preweighted polycarbonate membrane filters (Whatman) with a pore size of 0.4  $\mu$ m for biogenic silica (opal) analysis. The remaining water was filtered through preweighted glass fiber filters (GF/F Whatman) for organic compound analysis and calculation of total suspended matter concentrations. The filters were dried onboard at 40° for 24 hours. In addition to the particulate matter samples, surface sediment were collected at 30 stations (Tab. 7.2) from a multiple corer. The samples were stored frozen and freeze-dried in the home laboratory for further analyses.

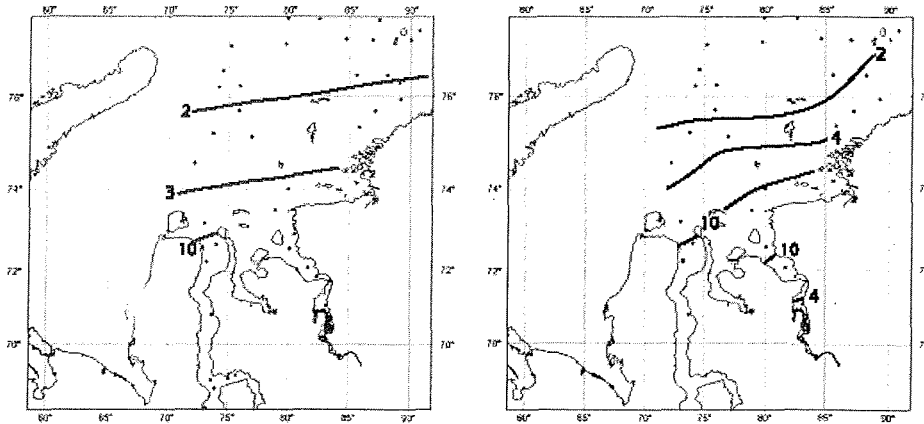


Figure 7.2: Total suspended matter (TSM) concentrations (in mg/l). Left panel: surface water; right panel: deep water.

### First results

As a first approach, the amount of total suspended matter (TSM) per filter was calculated. TSM of surface water shows a clear gradient from high values in the rivers to low values in the open Kara Sea (Fig. 7.2) with generally higher values in the Ob compared to the Yenisey. In the more southern part of the Ob Bay, where the Taz enters the Ob, very high TSM values are observed in the surface water corresponding to the very muddy waters observed in this region. TSM in the deep water also shows a gradient from high to low values along a river – open Kara Sea transect. Again, TSM is higher in the Ob, even though some values from the Yenisey Bay are higher due to resuspension processes.

### Ongoing analyses

The particulate material as well as the sediment samples will be analyzed for organic compound, biogenic silica (opal), amino acids, hexosamines and nitrogen isotopes. The particulate matter furthermore will be analyzed for carbon isotopes.

### Acknowledgements

We would like to express our thanks to the Captain and crew of R/V “Akademik Boris Petrov” for their excellent work. We would also like to thank all colleagues on board “Akademik I s Petrov” for their assistance during the cruise.

Table 7.2: Samples collected during “Akademik Boris Petrov” expedition 2001.

Station	Filter	Surface Sediment	Station	Filter	Surface Sediment	Station	Filter	Surface Sediment
BP01-01	x	x	BP01-32	x		BP01-59	x	x
BP01-03	x		BP01-34	x	x	BP01-61	x	x
BP01-04	x		BP01-35	x	x	BP01-62	x	x
BP01-05	x		BP01-37	x	x	BP01-65	x	x
BP01-06	x		BP01-38	x		BP01-66	x	x
BP01-07		x	BP01-40	x		BP01-67	x	x
BP01-08	x	x	BP01-41	x	x	BP01-68	x	x
BP01-11	x		BP01-43	x	x	BP01-70	x	x
BP01-14	x		BP01-45	x	x	BP01-72	x	
BP01-16	x	x	BP01-46	x	x	BP01-73	x	
BP01-19	x		BP01-48	x	x	BP01-75	x	x
BP01-23	x		BP01-49		x	BP01-77	x	
BP01-26	x	x	BP01-51	x	x	BP01-78	x	
BP01-28	x	x	BP01-52	x	x	BP01-79	x	
BP01-29	x		BP01-55	x	x	BP01-80	x	
BP01-30	x	x	BP01-56	x	x	BP01-82	x	
BP01-31	x	x	BP01-58	x	x			

### 7.3 Geochemistry of particulate organic matter in the water column and sediments of the Ob and Yenisei estuaries and the inner Kara Sea

*R. Stein, B. Hollmann*

Alfred Wegener Institute, Bremerhaven, Germany

#### Introduction

Major objectives are the characterization and quantification of particulate organic matter accumulated in the Ob and Yenisei estuaries and the adjacent Kara Sea. Information on the quantitative amounts of organic carbon derived from the respective sources (i.e. terrestrial/freshwater vs. marine) can be deduced from detailed organic-geochemical investigations of the suspended matter in the water column and the sedimentary organic carbon fraction. Both, bulk data (TOC, C/N-ratios, hydrogen index) as well as quantitative and qualitative biomarker distributions (*n*-alkanes, fatty acids, sterols, hopanoids, etc.) and  $\delta^{13}\text{C}$  of biomarkers will be used to characterise and identify the different sources of the particulate and sedimentary organic carbon pool. The studies of sediments will include surface sediments as well as samples from selected sediment cores.

#### Sampling of particulate organic matter and surface sediments

123 water samples 48 stations were obtained either by use of a Niskin rosette water sampler, large volume sampler (Bathomat, 200 L) or a water bucket. Sample locations were selected according to the salinity gradient recorded by the CTD-system. Water sampling stations, depth of the subsamples and the respective salinity are given in Table 7.3. In general, three water depths were sampled at each of the selected stations: surface water, the pycnoclyne (mixed-water) layer and near-bottom water. The water samples were filtered through precombusted glas-fiber filters (Whatman GF/F, 47mm diameter). The particulate organic matter collected on these filters was pre-extracted onboard with a mixture of 10ml Dichlormethane/Methanol (1:1) and stored under light-protection at -20°C. The quantitative and qualitative distribution of individual biomarkers (*n*-alkanes, fatty acids, sterols, hopanoids) will be used to investigate the biological sources (marine vs. terrestrial) and the conversion of the particulate organic matter prior to sedimentation.

In addition to the water samples, at GKG and MUC stations (see station list, Annex 10.1) surface samples were taken for future organic-geochemical investigations. The sediment samples were stored frozen (-20°C) and under light-protection in precleaned 100 ml glass-bottles.



Table 7.3: Stations used for sampling of particulate organic matter of the water column.

Station	sample-depth(m)	salinity	volume(l)	sampler
BP01-01	0	26.6	22.4	bucket
	18	29.7	21.25	CTD/RS
	35	33.4	20.0	BAT
BP01-03	0	4.4	18.0	bucket
BP01-04	0	0.0	15.0	bucket
	5	0.0	15.0	BAT
BP01-05	0	0.0	18.0	bucket
	11	0.0	18.0	BAT
BP01-06	0	0.0	18.0	bucket
BP01-08	0	0.0	18.0	bucket
	28	0.0	18.0	BAT
BP01-11	0	0.0	8.5	bucket
	3	0.0	8.5	BAT
	7	0.8	7.6	CTD/RS
	8	9.6	8.5	BAT
BP01-14	0	0.0	12.0	bucket
	15	0.0	12.0	BAT
BP01-16	0	0.0	18.0	bucket
	22	0.0	18.0	BAT
BP01-19	0	6.0	18.0	bucket
	10	31.3	12.0	BAT
	18	32.5	9.0	BAT
BP01-23	0	4.8	19.0	bucket
	7	17.7	19.5	CTD/RS
	15	33.0	19.0	BAT
BP01-26	0	12.3	19.5	bucket
	15	28.8	41.0	BAT
	28	33.5	18.0	BAT
BP01-28	0	22.7	22.3	bucket
	17		21.0	CTD/RS
	30	33.4	19.4	BAT
BP01-29	0	25.8	21.7	bucket
BP01-30	0	27.2	22.2	bucket
	12		21.6	CTD/RS
	30	33.9	20.7	BAT
BP01-31	0	28.9	22.5	bucket
	15		21.6	CTD/RS
	80	34.1	20.1	BAT
BP01-32	0	29.8	22.6	bucket

BP01-34	0	28,9	21,5	bucket
	19		18,0	CTD/RS
	60	34,3	20,8	BAT
BP01-35	0	28,8	21,6	Bucket
	17	32,4	21,7	CTD/RS
	100	34,5	20,6	BAT
BP01-37	0	28,3	21,7	bucket
	15	31,3	21,95	CTD/RS
	100	33,9	20,5	BAT
BP01-38	0	29,0	22,0	bucket
	14,5	30,6	25,6	CTD/RS
	60	34,1	20,7	BAT
BP01-40	0	23,3	22,1	bucket
	9	28,8	22,3	CTD/RS
	30	32,9	21,2	BAT
BP01-41	0	23,5	21,6	bucket
	10	26,6	21,8	CTD/RS
	28	32,9	20,9	BAT
BP01-43	0	20,6	21,0	bucket
	10	23,9	21,1	CTD/RS
	27	33,4	21,2	BAT
BP01-45	0	29,0	22,5	bucket
	18	31,4	21,0	CTD/RS
	50	33,9	19,6	BAT
BP01-46	0	25,0	21,2	bucket
	20	34,1	22,0	CTD/RS
	140	34,9	55,3	BAT
BP01-48	0	25,7	21,7	bucket
	15		22,0	CTD/RS
	100		40,1	BAT
BP01-51	0	23,5	21,9	bucket
	10	29,6	21,0	CTD/RS
	100	29,6	41,3	BAT
BP01-52	0	25,1	21,8	bucket
	12	29,4	22,8	CTD/RS
	40	33,6	41,1	BAT
BP01-55	0	25,9	22,0	bucket
	16	28,4	21,1	CTD/RS
	42	32,9	40,4	BAT
BP01-56	0	21,5	22,6	bucket
	16	31,9	22,4	CTD/RS
	100	34,4	40,8	BAT
BP01-58	0	24,1	21,0	bucket
	20	28,3	21,7	CTD/RS
	60	33,7	40,7	BAT

BP01-59	0	21,8	21,9	bucket
	16	29,9	22,4	CTD/RS
	120	34,3	36,0	BAT
BP01-61b	0	18,5	23,0	bucket
	20	29,2	21,9	CTD/RS
	80	34,1	41,7	BAT
BP01-62	0	23,0	22,9	bucket
	12	29,4	22,5	CTD/RS
	90	34,1	41,9	BAT
BP01-65	0	18,5	21,0	bucket
	8	26,9	21,8	CTD/RS
	42	32,8	41,0	BAT
BP01-66	0	12,9	20,9	bucket
	10	26,6	22,5	CTD/RS
	38	33,4	24,0	BAT
BP01-67	0	11,2	21,5	bucket
	6	23,8	22,5	CTD/RS
	27	32,1	27,0	BAT
BP01-68	0	9,8	18,0	bucket
	6	21,4	22,0	CTD/RS
	4		11,0	BAT
	15	30,2	31,0	BAT
BP01-70	0	0,7	9,0	bucket
	7	29,9	9,0	CTD/RS
	12	31,2	9,0	BAT
BP01-72	0	0,0	9,0	bucket
	12	0,0	7,5	BAT
BP01-73	0	0,0	7,0	bucket
BP01-75	0	0,0	6,0	bucket
BP01-77	0	0,0	6,0	bucket
BP01-78	0	0,0	6,0	bucket
BP01-79	0	0,0	6,0	bucket
BP01-80	0	0,7	10,5	bucket
	4		10,0	BAT
BP01-82	0	10,0	20,4	bucket
	7	23,6	21,0	CTD/RS
	4	10,3	21,0	BAT
	15	32,2	24,0	BAT

#### 7.4 Stable carbon isotope ( $\delta^{13}\text{C}_{\text{org}}$ ) ratio and lignin-derived phenol distribution in surface sediments of the inner Kara Sea

\*L.A. Kodina, \*\* V.I. Peresyphkin

\*V.I.Vernadsky Institute of Geochemistry and Analytical Chemistry RAS

\*\*P.P.Shirshov Institute of Oceanology RAS

##### Abstract

The sources of organic carbon were studied in the inner part of the Kara Sea by a combined isotopic ( $\delta^{13}\text{C}_{\text{org}}$ ) and molecular (n-alkanes, lignin) approach. A wide range of  $\delta^{13}\text{C}_{\text{org}}$ -values from  $-22,4\text{‰}$  to  $-27,6\text{‰}$  was determined over the study area. The organic carbon isotope composition allows to distinguish two groups of sediments: Station group I sediments are dominated by organic carbon of a planktonic origin enriched in  $^{13}\text{C}$  ( $\delta^{13}\text{C}_{\text{org}}$  :  $-22,4$  to  $-23,9\text{‰}$ ,  $\text{Ø}$   $-23,0\text{‰}$ ). Sediments of this type are clustered in the western part of the Kara Sea area, which is influenced by the Barents Sea water.

Station group II comprises sediments characterized by  $^{13}\text{C}$  depleted organic carbon (from  $-24,3\text{‰}$  to  $-27,6\text{‰}$ ,  $\text{Ø}$   $-26\text{‰}$ ). These sediments are located in the eastern part of the study area, including the Ob and Yenisei estuaries. Enhanced lignin-derived phenol concentrations are typical for these sediments. A special subgroup of station group II sediments was further distinguished in the area under indirect river influence, situated northwards of the estuaries. Isotopically depleted organic matter and the predominance of short chain n-alkanes in these sediments is typical for plankton-derived organic matter (OM). Rock-Eval pyrolysis data ( $\text{HI}>300\text{mgHC/gTOC}$ ) as well as the distribution pattern of lignin phenols further supports the planktonic origin of the OM in sediments of this group. Organic carbon isotope depletion results from the great Siberian rivers run-off, meaning that marine phytoplankton assimilates the isotopically depleted inorganic carbon driven with the river water. The subdivision of sediments with respect to the predominating organic matter source was further supported by the distribution pattern of n-alkanes and lignin-derived phenols.

##### Introduction

This paper reports on the sources and distribution pattern of sedimentary organic carbon in the inner part of the Kara Sea. The area of investigation extends from the archipelago Novaya Zemlya in the west to a longitude of  $80^{\circ}30'\text{E}$ . Surface sediment samples were collected during the 22 cruise R/V "Akademik Boris Petrov" in September-October 1995. The study area was covered by a set of about 80 sedimentary stations (Galimov et al. 1996). For this work, 18 stations were selected (Fig. 7.3) and the nature of sedimentary organic matter was investigated by its isotopic ( $\delta^{13}\text{C}_{\text{org}}$ ) and molecular (n-alkanes, lignin) composition.

Stable carbon isotope ratios of  $\text{C}_{\text{org}}$  are widely applied as indicator of the nature of sedimentary organic matter. This method is based upon the general observation that terrestrial OM is enriched in  $^{12}\text{C}$  compared to marine OM. The difference between

these two genetic types of organic matter averages about 5-7‰. In some cases, an excellent correlation between lignin-derived phenol concentrations and light  $\delta^{13}\text{C}_{\text{org}}$ -values was reported for recent marine sediments (Hedges & Mann 1979).

Lignin is a major biopolymer of higher plants, and lignin phenols are highly specific of vascular plant tissues (Manskaya & Kodina 1975). Aldehydes, acids and ketones of vanillyl (V) -, syringyl (S) - and p-hydroxybenzyl (P)- types are the major nitrobenzene oxidation products of lignin (Sarkanen & Ludwig 1971; Hedges & Mann 1979). In aquatic environments, lignin phenols are unique tracers for terrestrial organic matter (Opsahl et al. 1999; Huang et al. 1999).

n-Alkane concentrations and their carbon atom number distribution are considered to be a geochemical indicator to distinguish between autochthonous, aquatic bioproduction and terrigenous OM. The predominance of long chain ( $\text{C}_{25} - \text{C}_{33}$ ), odd-numbered n-alkanes and high CPI values are characteristic of aliphatic hydrocarbons derived from terrestrial plants, whereas short chain alkanes ( $\text{C}_{15} - \text{C}_{19}$ ) are indicative for enhanced bioproduktivty in the Arctic basin (Schubert & Stein 1997; Fahl & Stein 1999; Fernandes & Sicre 2000).

## Methods

The air-dried crushed sediment samples were oxidized with alkaline (8% NaOH) nitrobenzene at 175°C in small stainless steel autoclaves for 2.5 h, followed by centrifugation. Nitrobenzene reduction products were removed from the alkaline supernatant with dimethyl chloride. Lignin derivatives were extracted from the acidified solution with methylene chloride, silylated with trimethylsilyldiethylamine in pyridine (1:1v/v) at room temperature and analysed by high resolution gas chromatographic procedure (Peresykin 1990). Lignin-derived phenols are quantified on a Yanako G180-T.F.R. (Japan) instrument equipped with a FID and a silicone coated quartz capillar column (OVS-1, 30 m x 0,32 mm I.D.). Chromatographic conditions for the separation of phenols was as follows: 8 min at 80°C, heating rate 4°/min to 280°C, detector and injector temperature 300°C, He flow rate 1,5-2,0 ml/min. Data acquisition, peak detection and peak area processing was done by the integrator Chromatopak C-R3A (Shimadzu, Japan). Calibrated standard mixtures of phenols were used for lignin phenol quantification. The lowest detection limit for individual phenols is 0,01µg, the reproducibility is within 5%.

n-Alkanes were ultrasonically extracted from air-dried samples with methylene chloride and quantified with the GC-procedure described above, using squalane as an internal standard.  $\text{C}_{\text{org}}$  concentrations in sediments were determined by dry combustion of the samples in an oxygen flow, and coulombometric  $\text{CO}_2$  titration by the express device AN 7529 (Russia). Reproducibility of data for a  $\text{C}_{\text{org}}$  concentration range from 0,01 to 4% is within 0,005% C. Stable carbon isotope ratios were determined on a Varian Mat-230 instrument (Finnigan) relative to a working standard related with the International standard PDB. Sample preparation for isotope analysis consisted of sediment pretreatment with acid followed by combustion in the high-vacuum glas system in an oxygen flow. The resulting  $\text{CO}_2$  was cleaned and collected on a system of cold traps. The reproducibility for  $\delta^{13}\text{C}$ -values is within 0,2‰ vs. PDB.

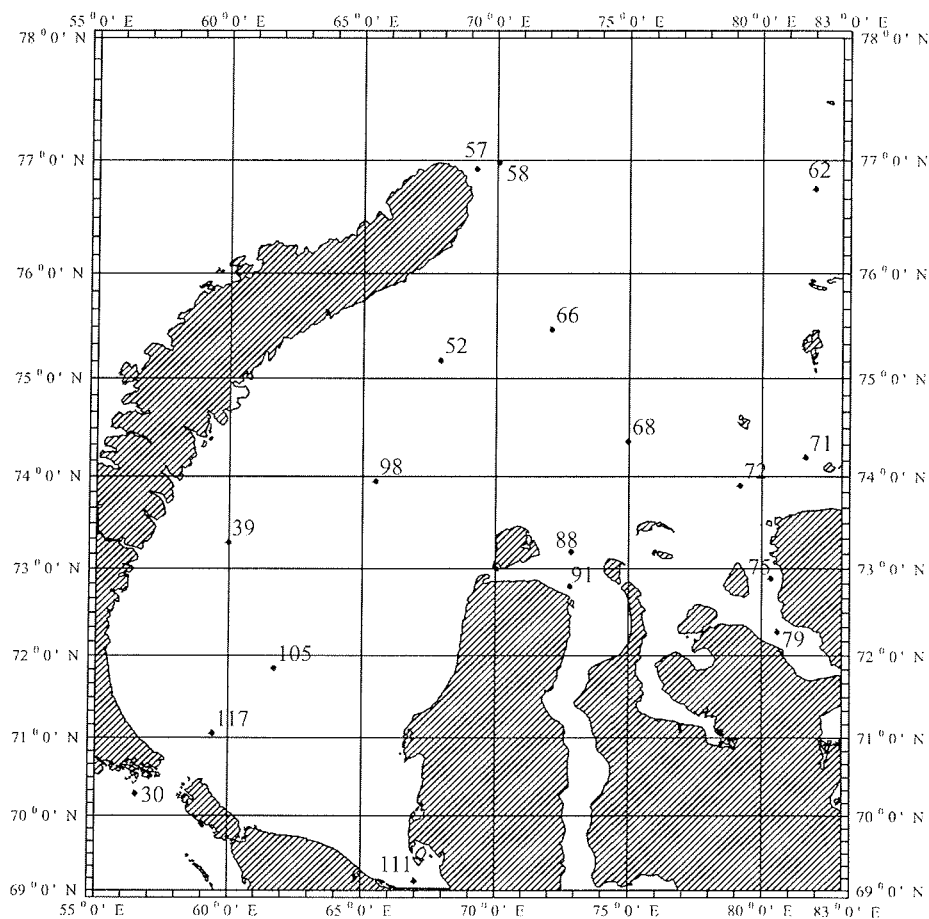


Fig.7.3.Sediment sampling stations in the Kara Sea "Akademik Boris Petrov" Cruise 1995.

### Results and discussion.

Stable carbon isotope ratio stands out of the other geochemical parameters as a solid indicator for bulk sedimentary organic matter. Organic carbon isotope composition forms the basis for the further classification of OM according to its genetic type. A wide range of the  $\delta^{13}\text{C}_{\text{org}}$ -values from  $-22,4\text{‰}$  to  $-27,6\text{‰}$  was determined for the sediments of the study area. The upper and lower  $\delta^{13}\text{C}_{\text{org}}$ -value can be considered two represent two distinct endmembers of OM:

$-22,4\text{‰}$  corresponds to autochthonous plankton-derived ("marine") OM, and  $-27,6\text{‰}$  represents terrigenous land-derived OM. According to the  $\delta^{13}\text{C}_{\text{org}}$ -values, the stations were subdivided into two groups.

Group I ("marine") includes stations mostly enriched in  $^{13}\text{C}$ , with the  $\delta^{13}\text{C}_{\text{org}}$ -values ranging from  $-22,4$  to  $-23,9\text{‰}$  and a mean of  $-23,0\text{‰}$ . The stations belonging to this group, and their corresponding  $\delta^{13}\text{C}_{\text{org}}$ -values are given below:

St.	39	62	52	98	105	30	58	57
$\delta^{13}\text{C}_{\text{org}}$ , ‰	-23,9	-23,9	-23,6	-23,5	-23,4	-22,9	-22,5	-22,4

As seen in Figure 7.3, plankton-derived organic matter is most commonly encountered in the western part of the area, including clayey sediments of the Novaya Zemlya Trough and adjacent area (St. 57, 58, 52, 30). This area is influenced by the nutrient-rich Barents Sea water and ice caps of the Novaya Zemlya archipelago. Ice-edge phytoplankton blooms are considered to be the major source for the supply of  $^{13}\text{C}$  enriched OM to the organic carbon pool in the Kara Sea.

The presence of autochthonous bioproduction over the inner Kara Sea water area (St.98, 105) may be related directly to the highly developed current system, including the circular current in the central part of the sea. In addition, the distribution pattern of sedimentary material in the Kara Sea is controlled by sea-ice transport (Kodina et al. 2000). This is in general agreement with the presence of not only isotopic but also molecular signals of algae in sediments all over the Kara Sea water area. However, from the averaged data given in Table 7.4 for n-alkane distribution clearly indicates an additional admixture of terrestrial material in sediments for some stations (e.g. St. 58, 62), where plankton-derived organic carbon dominates. Thus, some sediments of the group I, generally dominated by short chain n-alkanes, display a second maximum in the long chain n-alkane range.

Station group II is characterized by a  $^{13}\text{C}$  depleted organic carbon isotope composition, averaging -26‰ (range from -24,3‰ to -27,6‰). Stations of group II and their sedimentary organic carbon isotope composition are given below:

St.	117	111	66	68	72	71	79	75	88	91
$\delta^{13}\text{C}_{\text{org}}$ ‰	-24,3	-24,3	-24,7	-25,3	-25,4	-26,4	-26,6	-26,8	-27,6	-27,6

The presence of terrigenous organic carbon is most prominent in the riverine-influenced area of the Yenisei and Ob estuaries (St.75, 79, 71, 72, 88, 91). The bulk of the terrestrial material driven with river water is deposited in the “marginal filter” area (Stein 2001; Bogacheva et al. 2001). This is well reflected by the n-alkane distribution pattern in the sediments of the mixing zone and adjacent area, characterized by higher CPI values (2,25 against 1,57 for group I, Tab. 7.4) and lower levels of short chain n-alkanes. Absolute maxima of n-alkane concentrations are present in the long chain carbon atom number range (C25-C31), derived from waxes of higher landplants. Nonetheless, an additional input of organic carbon derived from aquatic primary producers is indicated by enhanced  $\text{C}_{17}$  and  $\text{C}_{19}$  concentrations for some stations (St. 66, 68, 72, 117). Peaks of  $\text{C}_{16}$  and  $\text{C}_{23}$  evidence OM reworking by bacteria.

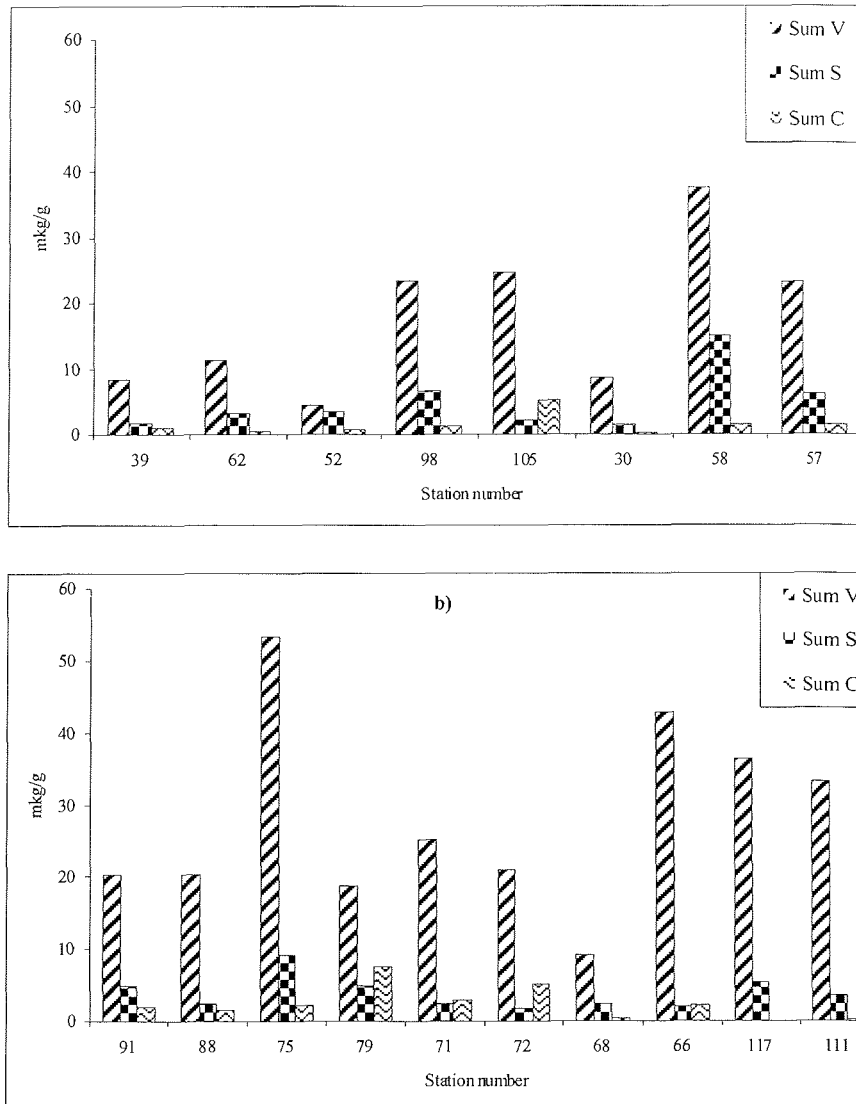


Fig. 7.4. Distribution pattern of lignin phenols in surface sediments of the groups I and II.

V- sum of vanillin, vanillic acid and acetovanillone;  
 S – sum of syringaldehyde, syringyl acid and acetosyringone;  
 C- sum of coumaric and ferulic acids.

A major part of the dissolved river discharge, namely nutrients and dissolved carbon (organic and inorganic, DOC/DIC), may pass through the marginal filter and propagate essentially northwards and northeastwards. Surface transported riverine water with dissolved compounds spreads northwards as far as 78°N. Dissolved nutrients support growth of phytoplankton and all further communities of the food



chain. DIC and DOC are included into Arctic food webs. Therefore, the terrestrial isotopic signal can travel through the marginal filter and can become incorporated into the new-formed autochthonous OM, resulting in a shift of marine  $\delta^{13}\text{C}_{\text{org}}$  towards more terrestrial values.

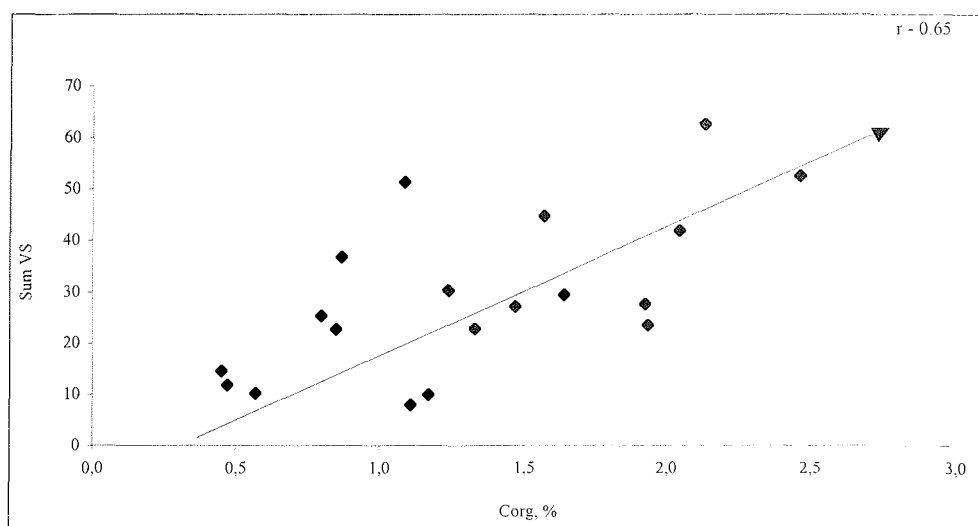


Fig.7.5. Correlation between V+S lignin structures and  $\text{C}_{\text{org}}$ -concentrations in the sediments.

The sediments recovered at stations 66 and 68 provide an example for the above mentioned influence of the Yenisei discharge and the resulting  $\delta^{13}\text{C}_{\text{org}}$  shift: The stations are situated northwards of the estuaries in an area of extremely low sedimentation rate (Fig.7.3). Organic carbon isotope compositions for both stations (-24,7 and -25,3‰) correspond to the  $^{13}\text{C}$  enriched part of the  $\delta^{13}\text{C}_{\text{org}}$  range defined for terrigenous OM (group II, Table 7.4), while the n-alkane distribution is typical of plankton-derived material. The presence of specific plankton biomarkers in sedimentary OM in areas northwards of the estuaries was also noticed in a previous study (Belyaeva & Eglinton 1997). Our Rock-Eval pyrolysis data for these samples ( $\text{HI} > 300 \text{ mgHC/gTOC}$ ) further support the planktonic nature of the  $^{12}\text{C}$  depleted sedimentary OM. We consider that the dissolved inorganic carbon of river water ( $\delta^{13}\text{C}_{\text{DIC}} = -6 \text{ ‰}$ ), assimilated in photosynthesis of phytoplankton microalgae may lead to similar isotope ratios of the planktonic and terrestrial organic matter.

Nitrobenzene oxidation of OM in the Kara Sea sediments was used to characterize the major lignin-derived phenolic compounds. According to their chemical structure, the oxidation products were summarized in the following groups:

$\Sigma\text{V}$ : Vanillyl-type compounds (vanillin, vanillic acid, acetovanillone)

$\Sigma\text{S}$ : Syringyl-type compounds (syringaldehyde, syringyl acid, acetosyringone)

$\Sigma\text{C}$ : Coumaric and ferulic acids (cinnamyl phenols)

$\Sigma\text{P}$ : p-Hydroxy-phenols

Figure 7.4 shows the concentration and distribution of lignin-derived phenols for the investigated samples. The sum of vanillyl-type compounds ( $\Sigma\text{V}$ , Fig. 7.4) is a distinguishing characteristic of lignin derivatives in the Kara Sea. Sediments of the

group II, directly influenced by the river discharge, in total display higher v-type phenol concentrations (max. 53,37  $\mu\text{g/g}$ ,  $\bar{O}$  28  $\mu\text{g/g}$ ) than sediments of group I (max. 37,48  $\mu\text{g/g}$ ,  $\bar{O}$  17,7  $\mu\text{g/g}$ , Tab. 7.4, Fig. 7.4). This agrees well with the abundance of coniferous forests (taiga) in the catchment areas of Ob and Yenisei rivers.

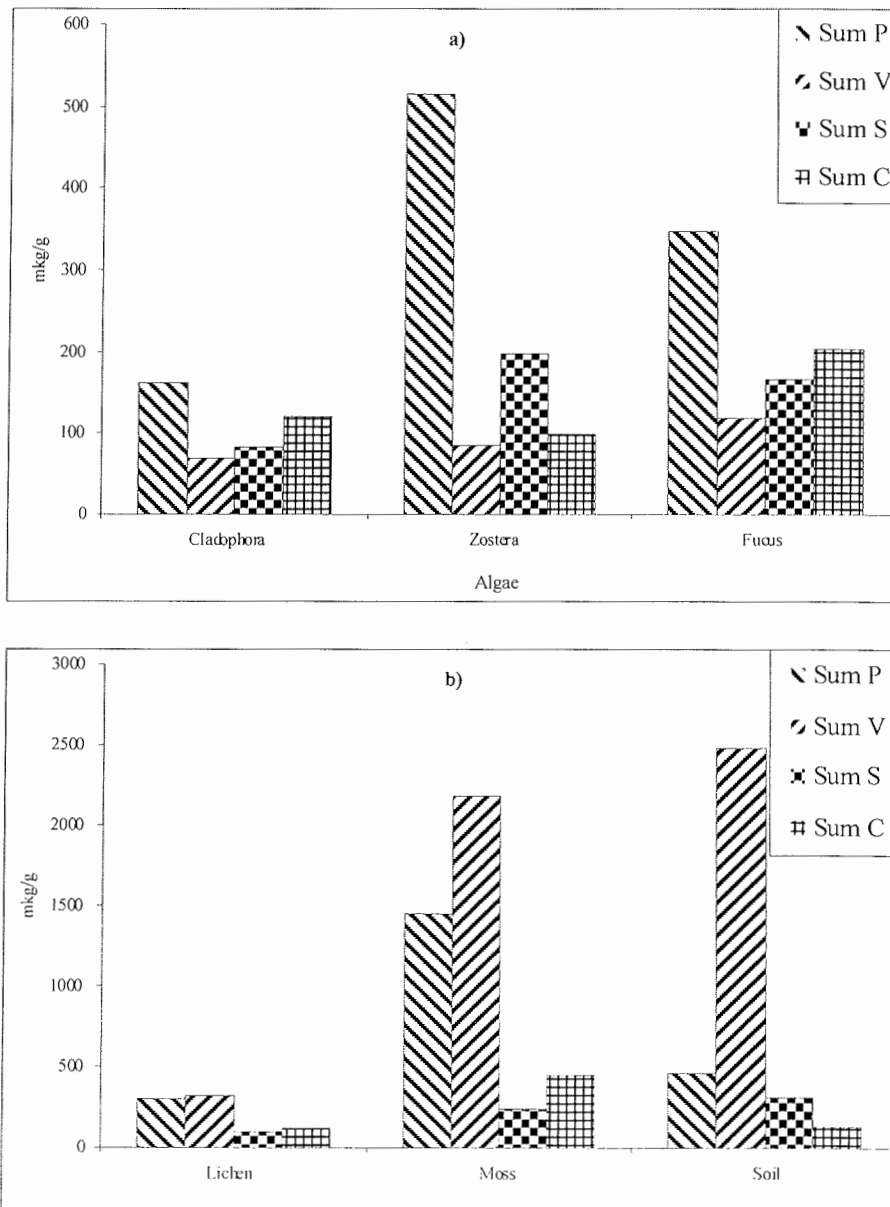


Fig.7.6. A. Lignin phenols of littoral algae (*Cladophora*, *Fucus*) and aquatic plant (*Zostera*), the White Sea; B. Lignin phenols of littoral non-vascular plants and soil, the White Sea.

Syringyl-type compounds belong to the minor compounds in the Kara Sea sediments. They are indicative for the presence of minor inputs of dicotyledon, land grasses and pollen derived lignin to the sediments.

Vanillyl-type phenols and, even though in minor quantities, syringyl-type phenolics were detected in sediments within the whole investigation area contributing to the sedimentary organic matter. This is also seen in the correlation of the sum of V- and S-type phenols and the sedimentary organic carbon content ( $\Sigma V+S$  vs.  $C_{org}$ ,  $r=0,65$ , Fig. 7.5) and thus once again reflects the impact of river discharge and sea-ice transportation of terrestrial derived OM to the sediments of the Kara Sea.

Another special feature of the distribution of phenolic compounds is the prevalence of p-Hydroxy phenols, as indicated in Table 7.4 by the ratio of  $\Sigma P/\Sigma V$  for almost all investigated samples, but especially in sediments of group I ( $\Sigma P/\Sigma V = 0,67-7,4$ ;  $\bar{\sigma} = 2,7$ ). In aquatic environment, additional, non-lignin sources of p-Hydroxy phenols have been identified. They might therefore derive from the oxidation of polymeric substances common in blue-green algae, brown algae or fungi (Hedges et al. 1988). Therefore, high p-phenol yields in aquatic environments can not be unequivocally attributed to plant lignins.

The composition of aromatic phenols – products of nitrobenzene oxidation of some algae and aquatic higher plant (*Zostera*), tundra moss, lichen and soil are given in Figure 7.6. Primitive non-vascular plants, including mosses (*Sphagnum*, *Marchantia*, *Polytrichum*), lichens, higher algae (*Fucus*, *Laminaria*) contain lignin-like compounds with p-coumaric structures being prevalent (Manskaya & Kodina 1975). Lignin is progressively degraded in soils, to produce smaller more oxidized products, which are washed out of soil and transported to marine basins.

Spores and pollen of land vegetation might be an additional source of the P- and C-, S-, V-compounds, which were detected in sediments of the south Kara Sea area (Matthiessen and Boucsein 1999). The presence of lignin in spore and pollen grain walls was established (Manskaya & Kodina 1975). The uniform distribution pattern of the minor compounds (S,C) over the entire Kara Sea area might be considered as an evidence of spore and pollen eolian transport from the land. Non-woody plant tissues (leaves, needles, grasses) can be distinguished by their lower yields of V- and S-compounds and by production of minor C-phenols (Sarkanen & Ludwig 1971; Hedges & Mann 1979).

### Acknowledgments

The work was supported by the Russian Foundation for Basic Research, grant 00-05-64575

Table 7.3. Carbon isotope composition and some geochemical parameters of organic matter from the Kara Sea surface sediments

Parameters	St.39, 62, 52, 98, 105, 30, 58, 57 (group I) Planktonogenous OM		St. 91, 88, 75, 79, 71, 72, 68, 66, 117, 111 (group II) Terrigenous OM	
	Average	Range	Average	Range
C <sub>org</sub> , %	0,80	0,45 to 2,47	1,40	0,40 to 2,14
$\delta^{13}\text{C}$ , ‰ vs. PDB	-23,1	-22,4 to -23,9	-26,0	-24,3 to -27,6
Vanillyl phenols ( $\Sigma\text{V}$ ), $\mu\text{g/g}$	17,7	4,48 to 37,48	28,0	9,24 to 53,37
$\Sigma\text{P}/\Sigma\text{V}$	2,7	0,67 to 7,4	1,2	0,40 to 3,7
$\Sigma\text{S}/\Sigma\text{V}$	0,25	0,09 to 0,77	0,15	0,05 to 0,27
n-Alkane concentration, $\mu\text{g/g}$	19,93	7,08 to 74,88	10,89	4,63 to 31,87
n-Alkane C max.	C <sub>17</sub> (St.105); C <sub>16</sub> (St.98); C <sub>15</sub> (St.52); C <sub>16</sub> , C <sub>31</sub> (St.62); C <sub>15</sub> , C <sub>25</sub> (St.30,); C <sub>17</sub> , C <sub>25</sub> (St.57); C <sub>17</sub> , C <sub>31</sub> (St.58)		C <sub>27</sub> (St.88,75); C <sub>25</sub> (St.111); C <sub>25</sub> , C <sub>17</sub> (St.117,72); C <sub>25</sub> , C <sub>27</sub> , C <sub>31</sub> (St.71,79); C <sub>17</sub> , C <sub>16</sub> (St.66,68)	
C <sub>10</sub> -C <sub>22</sub> /C <sub>23</sub> -C <sub>40</sub>	2,14	1,08 to 3,64	1,28	0,34 to 2,47
CPI	1,57	1,40 to 3,64	2,25	1,39 to 2,96

## 7.5 Carbon isotope composition of phytoplankton in the Yenisei river-estuary-open sea system and the application of isotopic approach for evaluation of phytoplankton contribution to the Yenisei POC load

L.A. Kodina

V.I. Vernasky Institute of Geochemistry and analytical Chemistry RAS, Moscow  
[kodina@gcokhi.ru](mailto:kodina@gcokhi.ru)

### Abstract

Measurement of the phytoplankton carbon isotope composition along the extended meridional section Yenisei-Kara Sea was carried out to identify the "marine" (plankton-derived) and terrestrial endmembers both types of organic matter contributions to the POC load in the framework of a two-compound mixing model. The phytoplankton samples were previously cleaned from detritus through a multiple decantation procedure. A high variability of the stable carbon isotope ratio caused by river run-off was revealed: plankton in the open sea differed from the freshwater plankton by about 12‰. A correlation was made between the plankton and particulate organic carbon isotope ratio distributions along the meridional section and the salinity. Both isotopic curves run in parallel each other, but in the frontal zone they intersect. The intersection point of the curves corresponds to the averaged  $\delta^{13}\text{C}$ -value of  $-27.5\text{‰}$ . This value is common to the plankton carbon, POC and hence to the second POC compound, namely to the terrigenous organic carbon. The value was used as the terrigenous endmember for calculation the both OM type contribution by the isotope-mass balance equation. The second endmember was represented by the  $\delta^{13}\text{C}$ -value of the clean phytoplankton sample for each station of the section. In the fresh water part, the contribution of plankton-derived carbon is 36-40%, in the open sea from 60 to 71%, with a very low particulate organic carbon concentration.

### Introduction

Stable carbon isotope analysis is commonly used for tracing sources of sedimentary organic matter (OM) in marine systems. The present work aims to continue our study of phytoplankton isotope composition of the both great Siberian rivers and adjacent Kara Sea area to get further proofs for the influence of the river run-off on the biogeochemical carbon cycle in the Kara Sea (Kodina 2001). Up to now, only few data on the carbon isotopic composition of Arctic phytoplankton exist. More typically, particulate organic carbon (POC) collected on a filter is measured. POC is representative of phytoplankton carbon in that it is largely derived from phytoplankton. However, two additional circumstances should be taken into account when studying the Arctic shelf seas. The first is that the POC load of the great Siberian rivers involves a substantial proportion of terrestrial material. Second, the dissolved inorganic carbon available for growth of phytoplankton algae might be depleted in the  $^{13}\text{C}$ -isotope due to input of dissolved inorganic carbon transported with river water from the land (Erlenkeuser et al. 1999; Kodina 2001).

The objective of the present work involved preparation of clean algae samples and to identify the “marine”(plankton-derived) and terrigenous endmembers for assessment of the both typeorganic matter contribution to POC load of the Yenisei.

### **Material and methods**

The work was carried out in the 35 cruise of R/V“Akademik Boris Petrov” (2000) along the meridional section river Yenisei-estuary-open sea, between 70 and 77°N, in the period of 7-19 September 2000. 14 phytoplankton sampling stations covered three basic part of the transect (Fig.7.7). Stations 17 and 19 were situated in the river part (fresh water from surface to bottom); estuary (surface water salinity is of 2,3-6,7 psu) included st. 16, 15 and 22; stations 23, 24, 8, 9, 28, 30, 35, 36 were taken in the open Kara Sea area. Most stations of the open sea situated close to drifting ice fields and were influenced by the ice thawing. The temperature of the thin uppermost water layer sank below 0°C, and the salinity sharply decreased. The stations 13-19 were taken 9-12 September, during the direct vessel trip southwards, stations 22-36 - on the vessel return trip in the period of 13-19 September. It is reasonable to consider separately the two parts of the cumulative section (direct and return vessel trips). Figure 7.8 shows the stations on the direct trip (upper part) and on the return trip (lower part of the Fig 7.8).

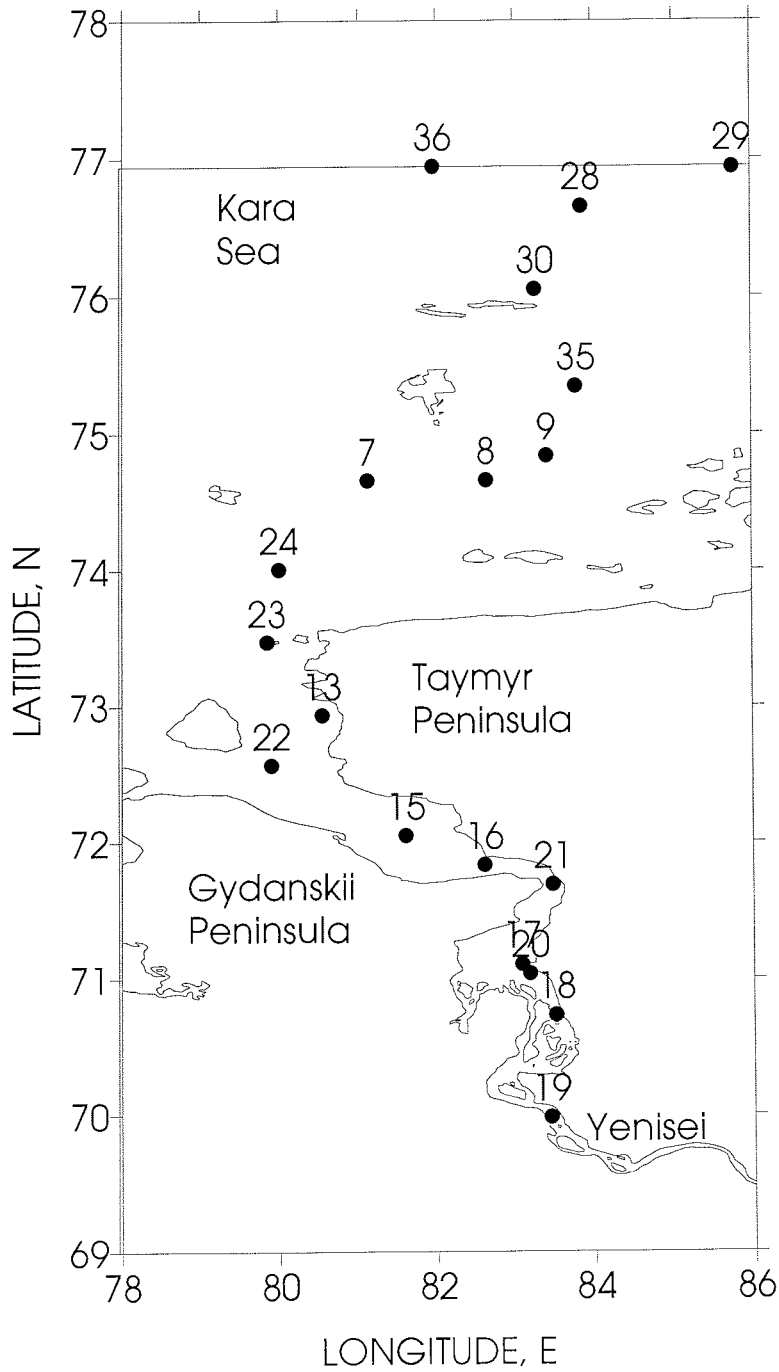


Figure 7.7. Map of phytoplankton sampling stations. 35 Cruise of R/V "Akademik Boris Petrov", September 2000.

## Results and discussion

### Plankton sample preparation

The starting material was sampled from subsurface water by traditional net technique. A hand net with pore size of 90  $\mu\text{m}$  was used. Sometimes, a ship pump and a bucket were used for water sampling. The raw samples were poisoned with saturated  $\text{HgCl}_2$  solution and left in a cold room until all particles settle down. The bulk of transparent water was removed, and the concentrated suspension was further separated into phytoplankton and detritus by a repeated careful decantation. The decantation procedure was repeated with the detritus samples as well to remove as much algae cells as possible. The cleaning of the algae samples was assessed by use of light microscopy. Within the species present in the raw material (natural population), usually only a few make up the bulk of biomass. Phytoplankton samples cleaned by this way, contained less than 5% detritus in most cases. The initial ratio of the dominating algae in the natural population was preserved with the following exception:

The samples from St. 15 and 16 (and to some extent St. 22) comprise mixture of separate freshwater algae cells and the bulk of brown colloidal aggregates and unidentified particles.

### Phytoplankton isotope composition

Data on the organic carbon isotope composition of the clean phytoplankton samples together with a short description of the dominating species (Dr. V. Larionov, Tab. 7.5). At St. 19-22, the algae population was represented almost exclusively by freshwater species. The main contribution to the total biomass was due to diatoms *Melosira granulata*, *Asterionella formosa*, *Fragillaria crotonensis*. At St. 17, 19 green algae (*Rhizolclonium*) and blue-green *Aphanizomenon flos-aquae* accounted for a great percentage of the total biomass. A typical marine population is present at St. 23, with rare freshwater algae cells being observed. St. 24 shows an exclusively marine species assemblage. Diatoms of *Chaetoceros* species and some *Dinophyceae* were predominant (Larionov & Makarevich 2001).

One can see a wide range of  $\delta^{13}\text{C}$  variations along the coupled Yenisei-Kara Sea transect : from - 36,2‰ and -35,6‰ in the Yenisey fresh water to -24,4‰ in the open sea, northwards of the estuary (Tab. 7.5). POC isotope composition along the transect ranged from -30,4 ‰ to -25,2 ‰ (Bogacheva et al. 2001). POC isotope composition in the Yenisei estuary has been found to fit well with the dissolved inorganic carbon isotope composition and water salinity (Kodina et al. 1999). The same regularity was valid as a whole for the Ob phytoplankton (Kodina 2001), as well as for the phytoplankton in this study. Curve 2 (Fig. 7.8) demonstrates the distribution of the phytoplankton isotope composition along the section, as compared with the POC isotope data (curve 1) and water salinity (curve 3). However, in the northerneastern part of the section the presence of the thawing ice and the stormy weather disturbed the regularity to some extent (e. g. St. 30 and 36 show anomalous depleted  $\delta^{13}\text{C}$ - values (-27,9‰ and -28,1‰).

Detritus and plankton differ in the carbon isotope composition (Tab. 7.5). The freshwater algae were noticeably depleted relative to reciprocal detritus. Conversely, in the marine part of the section (St. 23, 24, 28) the detritus is more depleted than the plankton.



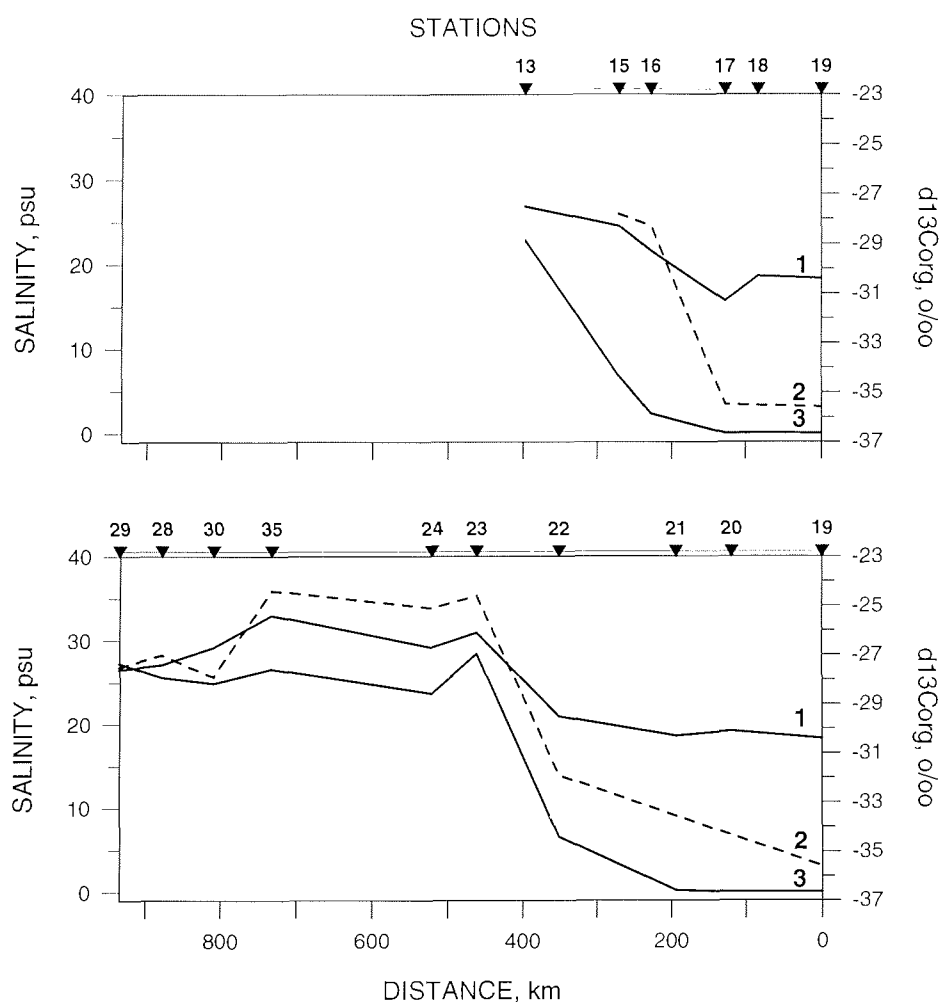


Figure 7.8. Distributions of  $\delta^{13}\text{C}$ - values (‰ PDB) for particulate organic carbon (curve 1), phytoplankton (curve 2) and subsurface water salinity (psu) along section Yenisey-Kara Sea in the periods of 9-12 September (upper part) and 12-19 September (lower part). Locations of the stations are shown in Figure 7.7.

#### Phytoplankton as a marker of the frontal zone.

Distribution pattern of the plankton carbon isotope composition along the section together with isotopic data for POC samples are given in Figure 7.8. One can see that a rather good agreement exists between the curves of water salinity,  $\delta^{13}\text{C}_{\text{plankton}}$  and  $\delta^{13}\text{C}_{\text{POM}}$ . It is particularly remarkable that the phytoplankton  $\delta^{13}\text{C}$  and salinity curves run almost parallel.

A sharp change of the phytoplankton isotopic signals in both parts of the cumulative transect are seen in Figure 7.8 (curve 2). The first is of 7,9‰ in magnitude and located between st. 17-16. The second - of 7,3‰ coincides with the frontal zone pronounced through salinity – temperature gradients between st. 22-23 (Stephantsev & Shmel'kov

2001). We suppose, that during the st. 13 and 14 (9 September, direct ship trip) due to the stormy weather, the hydrological front had been driven with a strong north-eastern wind at the distance of 224 km upstream. The frontal zone has been detected between the st. 16-17 through the sharp isotopic signal of the phytoplankton (Fig.7.8, upper part, curve 2). In the lower part of the Figure 7.8 we could observe that 53 hours later (return ship trip) the hydrological front came back to its initial position. Almost the same change of the phytoplankton isotopic signal of 7,3‰ was identified between st. 22 (salinity 6,6 psu) and st. 23 (salinity 28,4 psu).

The run of the POC curve is much more gentle than that of the plankton, in the frontal zone: 3,2‰ for POC against 7,3‰ for the clean plankton samples.

In the frontal zone POM sedimentation was shown to occur. The bulk of the river run-off POC was precipitated when water salinity changes from 6,6 psu to 28,4 psu (Bogacheva et al. 2001). The narrow interval (about 100 km) between st.22 and 23 corresponds to a depocenter of the marginal filter. It is known that about 90% of the sedimentary material carried with river water from the land, including freshwater plankton is precipitated in the marginal filter area (Lisitzin 1994).The freshwater plankton sedimentation is represented by the steep change of the carbon isotope composition from -31,9‰ (st. 22) to -24,6‰ (st. 23). An equal steep change of the species composition of algae population was observed in the marginal filter depocenter (Tab. 7.5).

It is significant that the  $\delta^{13}\text{C}_{\text{plankton}}$  and  $\delta^{13}\text{C}_{\text{POM}}$  curves cross at the point corresponding to the frontal zone. The intersection point corresponds to a  $\delta^{13}\text{C}$  value of -27,5‰. At this point, the phytoplankton, POC and hence the second averaged POC compound are of similar carbon isotopic composition.

#### Endmembers for the two-compound mixing model

The model of simple mixing of two endmembers – terrigenous and marine algae-derived organic material is widely accepted to explain variations of  $\delta^{13}\text{C}$  –values of marine particulate material and to determine the ratio between autochthonous material and terrigenous supply in organic carbon pools of sediment and water masses (Tan et al. 1991; Rachold & Hubberten 1999).

The central problem for a reliable application of the model consists in the selection of the both endmembers. A problem consists in, that for the system river-estuary-open sea it is not enough to get only the average value for primary bioproduction. The present paper demonstrates the wide variability of phytoplankton isotope composition (about 12‰) caused by the inorganic carbon variability and organic load transformation in the shallow shelf sea influenced by the great river run-off.

The study of isotope composition of phytoplankton in parallel with water particulates enables us to determine the representative  $\delta^{13}\text{C}$  –values for both endmembers.

We assume that the experimental  $\delta^{13}\text{C}$ - value for the bulk organic material precipitated in the depocenter of the marginal filter is representative of the average organic terrigenous load of the river water. We found it is equal to -27,5‰. The value seems to be rather reliable and fits well literature data on the tundra and taiga vegetation, soil and peat organic matter (Schell & Ziemann 1989; Balesdent et al.1993; Fogel & Cifuentes

1993; Huang et al. 1999), as well as an average of Kara Sea samples terrigenous UDOM  $\delta^{13}\text{C}$ - value of  $-27,3\text{‰}$  (Opsahl et al. 1999).

Many factors, involving temperature, DIC isotope composition, nutrient supply,  $\text{CO}_2$  availability, growth rate, as well as variations in both carbon source and carbon metabolism have been proposed to influence  $\delta^{13}\text{C}$  composition of marine phytoplankton. Species composition may be an additional controlling factor, as specific groups of marine phytoplankton may show significant difference in their carbon isotope ratio. Consequently, the calculation of the isotope ratios based on some of the available parameters seems to be problematic at the present time (Thompson & Calvert 1994; Fogel & Cifuentes 1993; Lajtha & Michener 1994).

We intend to get reliable data on the phytoplankton precisely and to use them as "marine" endmembers for three different parts of the extended meridional section "river-sea". The experimental data displayed in Table 7.5 were used as "marine" endmembers, different for each station to calculate the contribution of allochthonous supply and aquatic bioproductivity along the cumulative transect, except when a hydrological situation was unstable (exemplified by mixing zone or ice field vicinity). The standard equation of the isotope- mass balance for the two-member mixing model was applied. The experimentally determined average value of  $-27,5\text{‰}$  was used in each case as the terrigenous endmember.

In the freshwater part of the transect, the contribution of plankton-derived carbon in the POC pool is 36 - 40%; in the Yenisei Estuary, it is 45 - 50%. Selective sedimentation of the bulk freshwater plankton and flocculated terrestrial OM resulted in a drastic decline of the total POC concentration in the marine part of the transect, with the autochthonous bioproduction dominating (60-71%) in the open sea.

### Acknowledgement

I am grateful to Dr. S. Meschanov for his help in preparation of the hydrological material for this paper and discussion. The paper was prepared under support of the Russian Foundation of Basic Research, Grant N 00-05-64575

Table 7.5: Organic carbon isotope composition and description of the subsurface phytoplankton samples collected along the meridional transect Yenisei-Kara Sea (70-77° N)

Station number	Water salinity, psu	Detritus content, % $\delta^{13}\text{C}$ , ‰	Phytoplankton sample description (By Larionov V.V.) (Predominant species, rel.%)	$\delta^{13}\text{C}$ , ‰ PDB
19	0,0	< 5% -30,6	<i>Melosira granulata</i> (73), <i>Asterionella formosa</i> (13), <i>Chlorophyceae</i> (12), <i>Cyanophyceae</i> (2)	-35,6
17	0,0	<5%	<i>Asterionella formosa</i> (50), <i>Melosira sp.</i> (30), <i>Chlorophyceae</i> (20)	-36,2
16	2,3	<50% -28,3	<i>M. granulata</i> (70), <i>A. formosa</i> (10), <i>Synedra sp.</i> (5) <i>Chlorophyceae</i> (15)	-28,3
15	6,7	~50%	<i>M. granulata</i> (50), <i>Pennatophyceae</i> (23), <i>A. formosa</i> (10), <i>Synedra</i> (10), <i>Cyanophyceae</i> (5), <i>Chlorophyceae</i>	-27,8
22	6,6	<50%	<i>Melosira sp.</i> (80), <i>Thalassiosira nordenskiöldii</i> (5), <i>Nitzschia grunowii</i> , <i>Synedra</i> , <i>A.formosa</i> , <i>Chlorophyceae</i>	-31,9
23	28,5	<5% -25,4	<i>Chaetoceros socialis</i> (55), <i>Nitzschia grunowii</i> (20), <i>Thalassiosira sp.</i> (15), <i>Melosira sp.</i> (5) <i>Dinophyceae</i>	-24,6
24	23,7	5% -26,3	<i>Ch. socialis</i> (50), <i>Ch.sp.</i> (25), <i>Th.nordenskiöldii.</i> (15), <i>Dinophyceae</i> (5), <i>Nitzschia grunowii</i> <i>A.formosa</i>	-25,1
8	21,1	10%	<i>Nitzschia grunowii</i> (60), <i>Th.nordenskiöldii.</i> (30), <i>Ch.sp.</i> (10),	-25,9
9	23,8	10%	<i>Nitzschia grunowii</i> (75), <i>Th.nordenskiöldii</i> (15), <i>Chaetoceros sp.</i> ( 5), <i>Dinophyceae</i>	-25,9
26	19,2	<5%	<i>Ch. decipiens</i> (35), <i>Ch.sp.</i> (50), <i>Th.nordenskiöldii.</i> (15), <i>Ceratium arcticum</i>	-27,5
28	25,6	~10% -27,1	<i>Ch. sp.</i> (95), <i>Th.nordenskiöldii</i> , <i>Nitzschia grunowii</i> , <i>Ceratium arcticum</i>	-27,0
30	24,9	<5% -27,6	<i>Ch.sp</i> (85), <i>Dinophyceae</i> (10), <i>Nitzschia grunowii</i>	-27,9
35	26,6	<5%	<i>Ch. socialis</i> (90,) <i>Th.nordenskiöldii</i> (5); <i>Nitzschia grunowii</i> , <i>Dinophyceae</i> , <i>Anabaena</i>	-24,4
36	27,2	<5%	<i>Ch. decipiens</i> (>90), <i>Thalassionema sp.</i> , <i>Ceratium arcticum</i>	-28,1

## 7.6 POC isotope composition in the Ob estuary as compared with the Yenisei system

L.A. Kodina, M.P. Bogacheva

V.I. Vernadsky Institute of Geochemistry and Analytical Chemistry, RAS  
kodina@geokhi.ru

Our research in the Kara Sea are aimed to understand the pathway of organic carbon from biological sources to bottom sediments by the use of stable carbon isotope ratios in the different components of the carbon cycle with emphasis on organic matter in sea water, sediments, and sea-ice, as an integral part of the Arctic sedimentation. Data on organic carbon isotope composition of surface (0-2 cm) sediments in the Ob and Yenisei estuaries and adjacent sea area for samples of the expeditions BP-95 and BP-97 are shown in Figure 7.9 (Kodina 2000). As expected, all studied samples are isotopically depleted relative to the typical "marine"  $\delta^{13}\text{C}$  values of about 21-22‰ found somewhere in the west part of the Kara Sea area, being influenced by the Barents Sea water (Kodina et al. 2000; Kodina & Peresypkin, this volume). The gradual enrichment of the total organic carbon in the  $^{13}\text{C}$ -isotope towards the open sea is clearly manifested in both estuaries. It is particularly remarkable that there exists a well-pronounced difference between the two estuaries. Sediments of the Ob Bay are isotopically depleted (around -1,3‰) compared to the Yenisei estuary. The lowest  $\delta^{13}\text{C}$  value of -28,7‰ is situated in the center of the Ob Bay, whereas the highest  $\delta^{13}\text{C}$  value of -24,5‰ was found in the sea area under Yenisei influence.

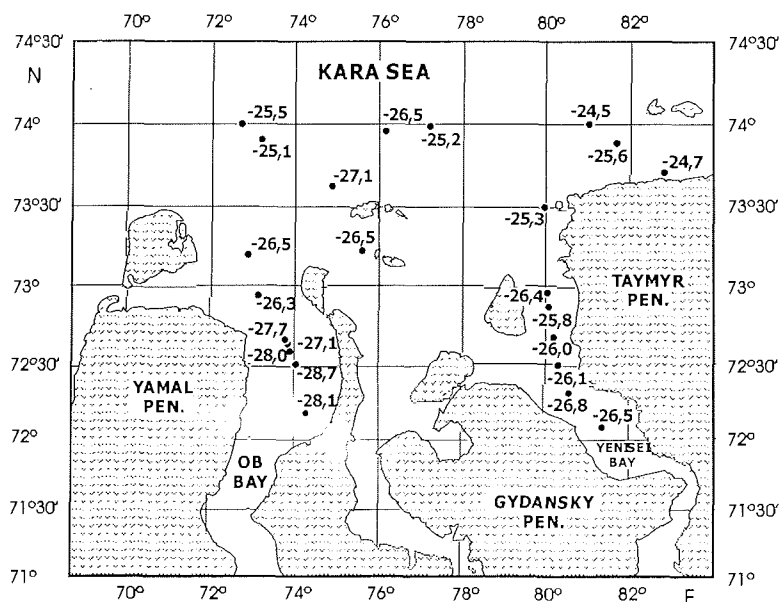


Fig 7.9. Organic carbon isotope composition of the top sediments (0-1cm) in the Ob and Yenisei estuaries and adjacent Kara Sea area (BP-95 and BP-97).

*Yenisei system*

The pattern of the stable carbon isotope ratio distribution in sediments of the Yenisei Bay was shown to correspond well with the correlation of the particulate organic carbon distribution and the salinity gradient in the Yenisei Estuary and adjacent Kara Sea area (Kodina et al. 1999). The  $\delta^{13}\text{C}$ -values in the area range from -28,8 to -24,5‰. The distribution of the POC isotope values against water salinity shows that there exists a rather good correlation between the two parameters ( $R=0,8$ ). It's notably, that the regularities occur both vertically through the water column and spatially throughout the study area.

In this way, in the study area the variations of the POC isotope composition are directly related to the variations of water salinity, with the isotopically lightest organic carbon (-28,8 ‰) being characteristic of the fresh water ( $S=1,2\text{‰}$ ), whereas the maximum  $\delta^{13}\text{C}$ -enrichment (-25,4‰) of the POC is observed in the marine surface water of highest salinity ( $S=14,9\text{‰}$ ).

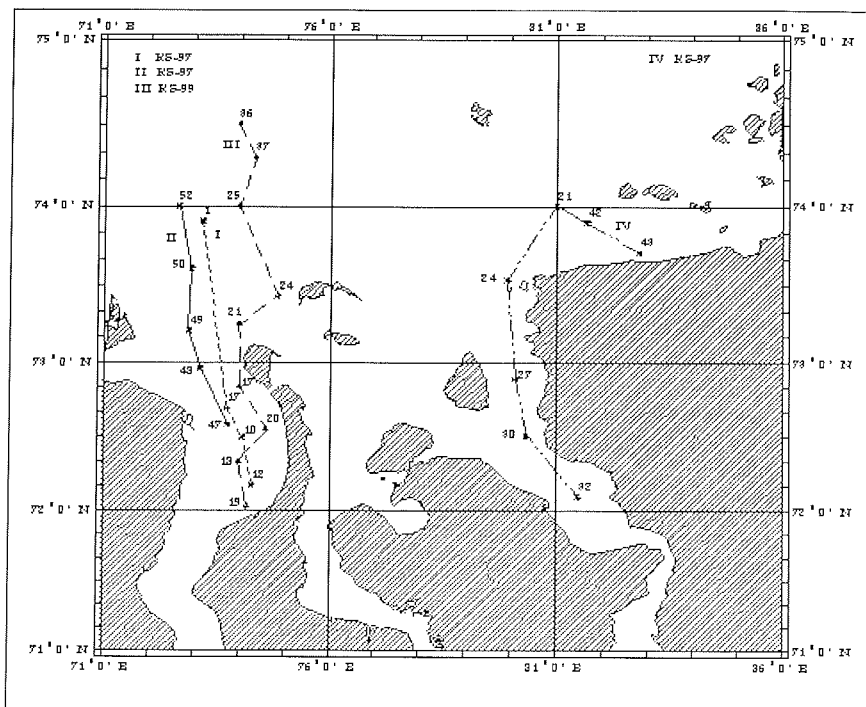


Fig. 7.10. POC sampling stations in BP-97 and BP-99 expeditions. I, II- meridional Ob sections , BP-97; III- meridional Ob sections , BP-99; IV- meridional Yenisei section, BP-97.

The regularity discussed above manifests itself spatially as well. The  $\delta^{13}\text{C}$ -values generally paralleled water salinity:  $\delta^{13}\text{C}$ -values were lower in the south river part of the section and increased gradually from -28,2 to -25,4‰ to the northern estuary and open sea.

This regularity is also true for the much more extended section “Yenisei-river-estuary-open sea”, BP-2000. The POC isotope data for this whole section are given in the Table 7.6. The presence of a hydrological front is a special feature of the section. Some peculiarities of the POC behavior in the frontal zone were presented earlier (Bogacheva et al. 2001). The sharp decrease of the POC concentration and the co-occurring enrichment of the POC in  $^{13}\text{C}$  by a value of 3,4‰ to the precipitation of the bulk terrestrial load.

#### Ob section

The Ob hydrology and hydrochemistry are characterized by some peculiarities, which appear noteworthy with respect to the POC isotope geochemistry.

The absence of a clearly defined local hydrological front resulted in a diffuse boundary between marine and riverine waters in the Ob Estuary. Limited penetration of marine water into the Ob Bay and a more pronounced influence of the Ob fresh water to the open sea area were suggested to be the most outstanding distinctions from the Yenisei section (Burenkov & Vasilkov 1994; Köhler & Simstich 2001). The overall phytoplankton biomass in Yenisei was more than one order of magnitude lower than in the Ob Bay and adjacent coastal areas of the Kara Sea (Larionov & Makarevich 2001).

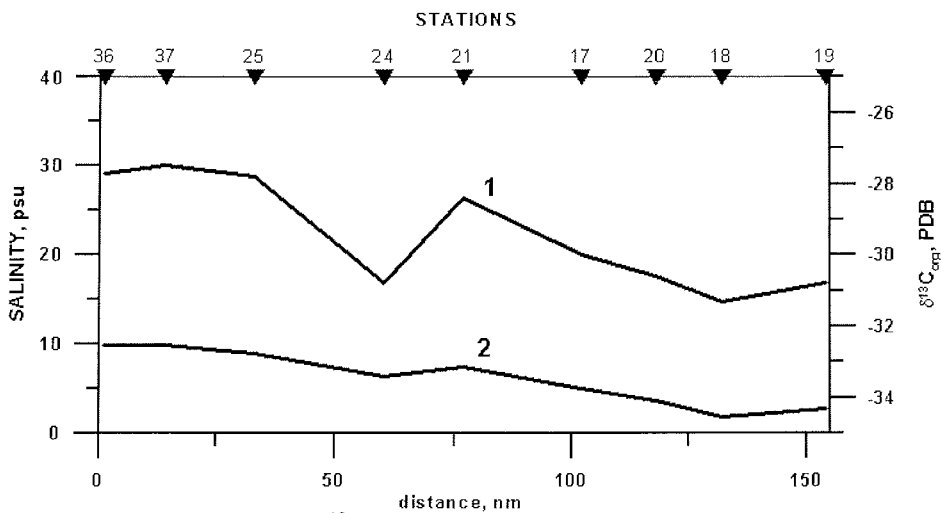


Fig. 7.11. Distribution of the  $\delta^{13}\text{C}_{\text{POC}}$  values (curve 1) against the surface water salinity (curve 2) along the Ob section III (BP-99).

Ob water contains a higher  $\text{HCO}_3^-$  concentration (76,3 mg/l) than Yenisei (55,2 mg/l) (Gaillardet et al. 1999; Gordeev 2000). In the Ob River, water  $\text{pCO}_2$  is much higher than in Yenisei because Ob watershed include mainly a marshland area with a swampy acidic soil. Oxidation of soil OM in the river water is responsible for  $\text{pCO}_2$  rise in Ob water (Makkaveev 1994). The degradation of organic material produces isotopically light  $\text{CO}_2$  that impacts the carbon balance and its isotopic composition in the Kara Sea (Erlenkeuser et al. 1999).

Samples for investigations were obtained during the two Joint Russian-German expeditions BP-97 and BP-99. Sea water area between the latitudes of 72° and 74° N was studied in 1997 and between 72° and 74°30'N in 1999. Water sampling for POC filtration was carried out in BP-97 along two short sections: in the R/V direct southward trip 13-15 September (section I, Fig. 7.10) and during the return R/V trip 22-23 September (section II, Fig. 7.10), with a time span of one week in between.

There is a principal difference in the hydrological situation between these both sections. The first section was carried out with a fresh water plume of a maximum salinity of 12,7 psu in the marine part. During work on the section II an increase in surface water salinity up to 13,8-20,8 psu occurred due to the strengthening of the Yamal current (Churun & Ivanov 1998).

$\delta^{13}\text{C}$ -values vary from -30,7 to -26,9‰ within section I (Tab. 7.7), when salinity rose from 2-3 psu in the southern estuary up to 12,7 psu in marine water. This reflects the normal correlation of the POC isotopic composition and salinity gradient and is similar to the observation for the Yenisei estuarine sections.

The change in the hydrological situation resulted in the occurrence of surface water with an irregular salinity trend within the section II (Fig. 7.10), and correspondingly in the absence of a correlation of salinity and the POC isotope distribution. The  $\delta^{13}\text{C}$ -values varied from -29,6 to -26,6 ‰ without any relation to the water salinity (Table 7.7).

Water sampling in BP-99 was performed from 30 August up to 7 September along the meridional section III, and consisted of 9 stations in estuary and adjacent sea area (Fig. 7.10). The influence of the river water to the north is seen throughout the section in the low surface water salinity ranged from 1,8 psu in southern estuary up to 9,9 psu in the open sea area. POC isotope composition ranged in surface water from -31,3 to -27,5‰, with the known correlation of  $\delta^{13}\text{C}$  values and salinity being preserved (Table 7.8, Fig. 7.11).

In summary, one can say, that in spite of a pronounced variability of the hydrological situation in the Ob Estuary and adjacent sea, variations of the POC isotope values between two years (sections I and III) are very close to each other: for minimal salinity (the average value is of 2,1 psu) the difference is 0,6‰, and the same magnitude is observed for the maximal salinity. For the Ob Estuary, the most  $^{13}\text{C}$ -depleted average POC isotope composition is -31‰, the most enriched is of -27,2‰. The corresponding values for Yenisei estuary (the average values for 1997 and 2000 years) are -29,0‰ and -25,8‰. This means, the difference in sedimentary organic carbon isotope composition between the Ob and Yenisei estuaries is inherited from the carbon isotopic signature of the water particulate material.

*The work was supported by the Russian Foundation for Basic Research, Grant 00-05-64575.*



Table 7.6: Particulate organic carbon isotope composition along the "Yenisei -Sea" section , 2000

Station N	Depth, m	S, psu	$\delta^{13}C_{POC}, \text{‰ PDB}$
19	0-1	0.00	- 30.4
	21.7	0.07	- 30.4
18	0-1	0.06	- 30.3
	15.0	0.00	- 30.9
20	0-1	0.00	- 30.1
	17.0	5.70	- 30.3
17	0-1	0.00	- 29.3
	17.0	0.40	- 30.9
21	0-1	0.20	- 30.3
	12.0	5.60	- 29.4
	24.5	22.90	- 27.6
	wood	-	- 26.2
16	0-1	2.30	- 29.3
	15.5	13.30	- 28.4
	23	20.1	-28.4
15	0-1	6.70	- 28.4
	6.5	7.30	- 27.9
22	0-1	6.60	- 29.7
	3.7	11.60	- 28.6
	10.0	29.90	- 27.3
13	0-1	22.80	- 27.6
	3,5-3,7	25,50	- 27.0
	10,5	29,6	-27.4
23	0-1	28.40	- 26.1
	11,5	30,70	- 26.6
	31,0	33,00	- 26.4
24	0-1	23,7	- 26.7
	11,5	26,00	- 26.6
	32,0	32,30	- 26.1
7	0-1	16,50	- 27.5
	11,0	25,30	- 25.9
	35,0	32,80	- 26.9
8	0-1	21,00	- 27.0
	9,5	26,40	- 26.4
	37,0	33,30	- 25.8
9	0-1	23,80	- 26.4
	14,0	27,90	- 25.2
	44,0	33,50	- 24.4
35	0-1	26,60	- 25.5
	14,5	30,40	- 25.2
	46,0	33,50	- 26.1
28	0-1	25,60	- 27.3
	16,0	29,20	- 26.6
	47,0	34,10	- 25.3
29	0-1	27,30	- 26.1
36	0-1	27,20	- 26.4
	17,0	31,20	-
	64.0	33,90	- 26.1

Table 7.7: Particulate organic carbon isotope composition along the "Ob - Sea" sections (1,2),1997.

Station N	Depth, m	S, psu	$\delta^{13}\text{C}_{\text{POC}}$ , ‰ PDB
<b>Section 1 (13 - 15.09).</b>			
12	0	3,1	-28,8
	8	3,8	-29,0
	12	20,1	- 29,7
10	0	2,4	- 30,7
	10	3,3	- 29,4
	11,5	25,1	- 29,8
	13	25,0	- 28,9
17	0	7,0	- 28,4
	5	14,0	- 27,8
	9	29,3	- 28,7
	16	29,8	-28,6
1	0,5	12,7	-26,9
	7,4	13,0	-27,0
	9,9	25,7	-27,4
<b>Section 2 (22 - 24.09)</b>			
47	0	18,9	-29,6
	10,1	29,4	- 28,9
	16	29,6	- 29,7
48	0	13,5	- 27,6
	7	16,5	- 27,5
	10,9	30,3	- 27,9
	23,9	31,4	- 27,3
49	0	16,4	- 28,6
	11,1	22,6	- 27,2
	15,9	30,5	- 25,8
	27,0	31,6	- 25,6
50	0	20,8	- 26,6
	9,4	20,8	- 26,7
	14,2	31,5	- 26,3
	26,0	31,8	- 26,6
52	0	18,2	- 28,2
	7	22,1	- 27,1
	10	31,0	- 27,0
	27	31,8	- 26,4

Table 7.8: Particulate organic carbon isotope composition along the "Ob - Sea" section, 1999.

Station N	Depth, m	S, psu	$\delta^{13}\text{C}_{\text{POC}}$ , ‰ PDB
19	3,0	2,7	- 30,8
	10,0	20,6	- 30,2
	11,6	21,5	- 30,9
18	2,0	1,8	- 31,3
	8,7	25,2	- 29,5
	11,7	26,1	- 30,1
20	3,2	3,7	- 30,6
	6,1	3,5	- 30,9
	11,0	10,8	- 29,6
	14,6	27,7	- 29,4
17	2,0	5,0	- 30,0
	7,0	22,6	- 30,3
	16,0	30,4	- 29,0
21	2,5	7,5	- 28,4
	9,0	21,6	- 28,0
	15,0	30,1	- 28,4
24	2,2	6,4	- 30,8
	12,0	27,3	- 27,6
	18,4	29,6	- 27,8
25	2,8	8,9	- 27,8
	8,4	21,7	- 26,2
	15,0	31,0	- 26,0
	22,7	32,0	- 26,9
37	3,0	9,8	- 27,5
	8,6	24,2	- 26,8
	28,2	32,2	- 26,7
36	3,2	9,9	- 27,7
	8,5	25,6	- 28,2
	28,7	32,0	- 27,6

## 7.7 Geochemistry of hydrocarbon gases in Kara Sea sediments

G.S. Korobeinik, V.G. Tokarev, T.I. Waisman

Vernadsky Institute of Geochemistry and Analytical Chemistry RAS, Moscow, Russia

Detailed gasometrical investigations in the Kara Sea were continued during the expedition of R/V "Academic Boris Petrov" (August - September, 2001). In this short paper we present preliminary results of a detailed study on the concentrations and distribution of hydrocarbon gases in the Kara Sea deposits. Sediments from four cores sampled at the stations BP01-26, BP01-55, BP01-47, BP01-34 were analyzed.

### Methods

The analytical procedures used for this work have been described previously (Korobeinik et al. 2001).

### Results and Discussion

The concentrations of the individual hydrocarbon gases ( $C_1$ - $C_5$ ) and the ratios of  $(C_{2=}-C_{4=})/(C_2-C_4)$  and  $\sum(C_4-C_5)/\sum(C_2-C_3)$  are shown in Table 7.9. Geochemical indices and methane distribution within the cores and along the Yenisei-Kara Sea profile are presented in Figures 7.12-7.15.

$C_1$  concentration in the sediments of the cores BP01-26, BP01-55 varies within a wide range from  $56 \times 10^{-4}$  ml/l in the subsurface layer to 10 ml/l at the core bottoms.  $C_1$  distribution within the sediments of the core BP01-26 is shown in Figure 7.12. Deposits are characterized by a down core increase of methane content and in the low parts of the cores a high concentration gradient is observed. Sediments taken at the stations BP01-26 and BP01-55 contain less  $C_{2=}$ ,  $C_{3=}$ ,  $C_{4=}$  hydrocarbons than  $C_2, C_3, i-C_4, n-C_4$  ( $(C_{2=}-C_{4=})/(C_2-C_4) < 1$ ). However, in the uppermost layer an oxidized layer as indicated by  $(C_{2=}-C_{4=})/(C_2-C_4)$  ratio of 4.99 can be distinguished (Fig. 7.13, curve A). In the upper layers (75 – 146 cm), higher homologues of hydrocarbon gases ( $i-C_4, n-C_4, i-C_5, n-C_5$ ) were observed in higher concentrations than  $C_2+C_3$  homologues, resulting in a  $\sum(C_4-C_5)/\sum(C_2-C_3)$  ratio of 7.02-7.20 (Fig. 7.13, curve B).

Hydrocarbon gases concentration and the distribution of the higher homologues within the sediments of cores BP01-26 and BP01-55 indicate active processes of gas generation and consumption in the deposits. The authigenic mineral ikaite as well as carbonate concretions were also described in these sediments (Kodina et al. 2001). The same regularities were revealed earlier in the sediments of the core BP00-37 (Korobeinik et al. 2001).

Sediments of the cores BP01-34 and BP01-37 show low methane concentrations and vary from  $300 \times 10^{-4}$  to  $660 \times 10^{-4}$  ml/l in the core BP01-47 (Fig. 7.14) and from  $150 \times 10^{-4}$  to  $974 \times 10^{-4}$  ml/l in the core BP01-34. Geochemical indices show  $(C_{2=}-C_{4=})/(C_2-C_4) > 1$  in the oxidized layer and  $\sum(C_4-C_5)/\sum(C_2-C_3) > 1$ . Hydrocarbon content and distribution pattern of these cores in the northern part of the Kara Sea (78°N) indicate that

Table 7.9: Methane and Other Hydrocarbon Gases in Sediment Cores of Kara Sea.

Station	Horizon cm	Concentration, ml/*10 <sup>-4</sup>										Gasgeochemical indices	
		C1	C2	C2=	C3	C3=	iC4	nC4	C4=	iC5	nC5	((C2=)-(C4=)) (C2-C4)	Σ(C4-C5) Σ(C2-C3)
26	5-7	56	6	44,8	3	10,76	1	3	5,3	3	3	4,99	1,22
	26-50	1 451	17	5,2	12	0,15	6	10	0,0	22	8	0,18	1,85
	75-95	277	9	0,6	7	0,16	4	77	0,0	14	16	0,04	7,02
	126-146	424	8	1,0	10	0,4	5	10	0,2	23	81	0,05	7,20
	175-195	511	27	1,8	34	0,48	15	29	0,3	34	30	0,02	1,78
	200-220	1 996	6	0,9	11	0,38	5	8	0,8	14	4	0,07	1,88
	226-246	1 939	3	0,4	4	0,03	2	4	0,0	7	4	0,06	2,19
	305-325	42 949	5	0,4	7	0,24	3	6	0,0	12	3	0,05	2,04
	350-370	105 993	16	2,2	12	0,15	5	9	0,0	18	7	0,08	1,37
	400-420	67 734	18	1,5	5	0,4	2	3	0,0	6	7	0,08	0,80
495-515	79 994	31	2,1	4	0,58	2	4	0,0	5	4	0,07	0,42	
55	16-36	1 074	30	0,4	28	0,25	13	23	0,0	30	9	0,01	0,73
	36-60	2 171	21	2,2	28	0,08	16	23	0,0	70	42	0,01	3,20
	105-125	3 153	42	1,6	25	0,2	12	21	0,7	45	20	0,02	1,47
	135-165	43 325	87	1,4	26	0,41	13	22	1,8	40	16	0,02	0,80
	190-217	112 715	227	17,2	17	0,41	11	17	3,0	24	11	0,08	0,26
	270-285	108 400	52	4,1	48	1,56	12	23	0,0	46	22	0,06	1,03
47	0-3	328	24	2	31	1,0	17	31	1,3	86	39	0,04	3,10
	6-10	298	25	2	29	0,5	17	28	0,0	64	59	0,05	3,10
	20-24	94	18	1	21	0,1	14	20	0,0	53	23	0,03	2,79
	34-38	310	7	0,2	18	0,04	9	15	0,0	43	14	0,01	3,64
	97-127	260	23	2	27	0,4	15	24	0,3	65	28	0,03	2,69
	170-192	531	20	1	25	0,6	11	22	0,3	68	26	0,03	2,84
	202-225	659	26	1	31	0,3	18	30	0,4	83	25	0,02	2,74
	230-259											0,03	2,97
34	24-29	4	0,5	0,04	1	0	0,2	0,4	0,0	4	0	0,08	4,20
	55-87	244	30	2	37	1,0	23	47	0,0	49	17	0,04	2,02
	150-180	150	24	1	24	0,02	15	22	0,0	43	15	0,02	2,00
	250-280	284	40	25	50	0,4	29	54	0,0	144	58	0,03	3,18
	280-380	974	28	2	21	0,2	8	12	0,0	42	37	0,04	2,02
	450-480	218	25	2	31	0,4	20	29	0,0	77	133	0,04	4,6

sedimentation and the diagenetic transformation of organic matter in sediments of this area differs from those located southernmost.

Fig. 7.12 Methane in bottom sediment.  
(Kara Sea, BP01-26)

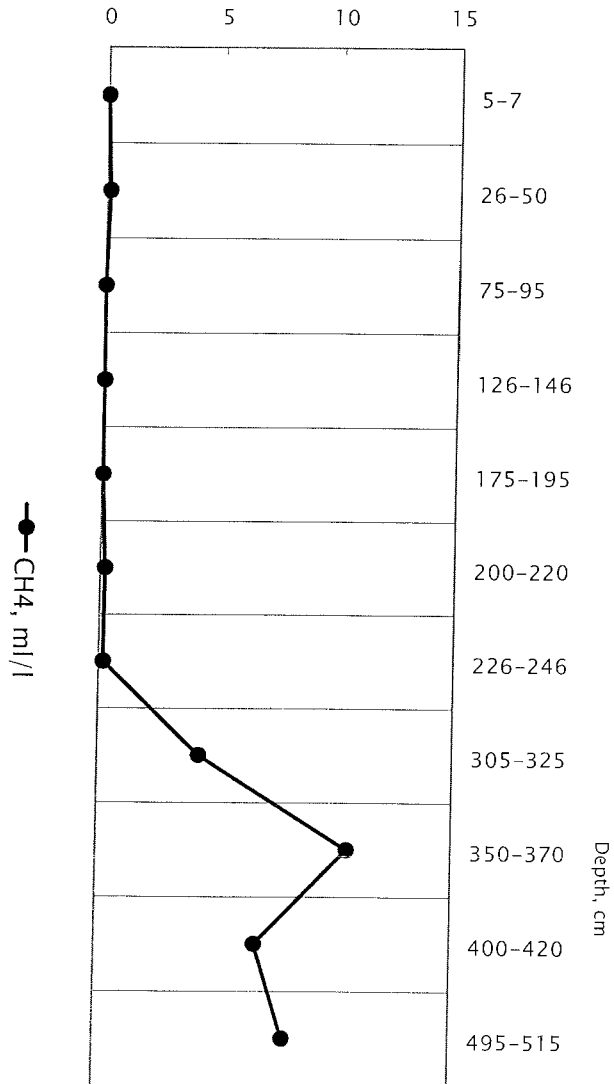


Fig. 7.13 Geochemical indices in bottom sediment, (Kara Sea, BP01-26)

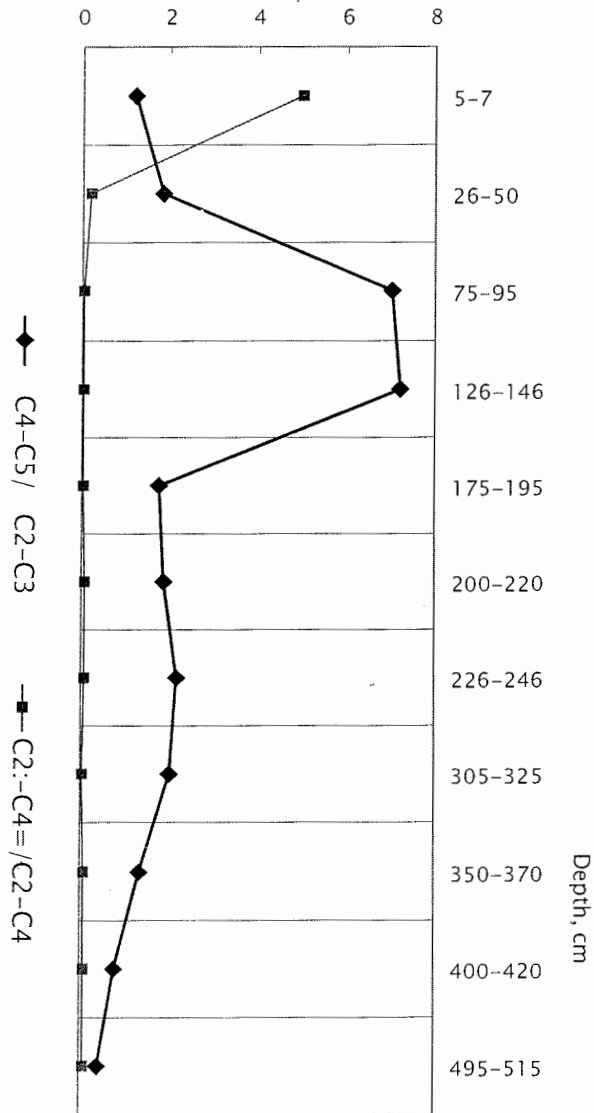


Fig. 7.14 Methane in bottom sediment.  
(Kara Sea, BP01-47) .

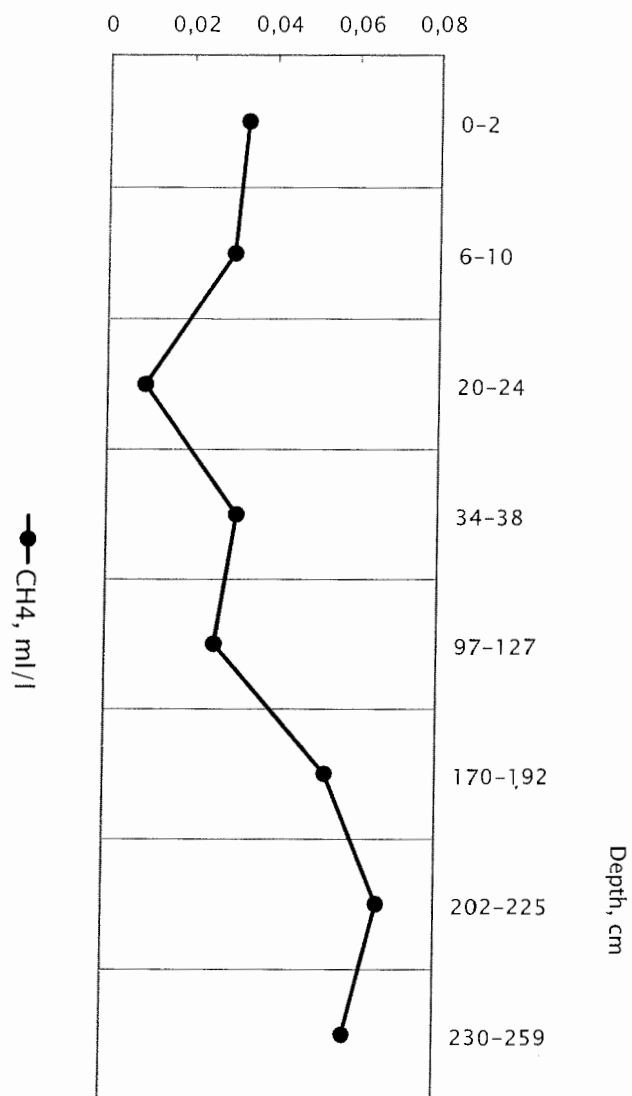
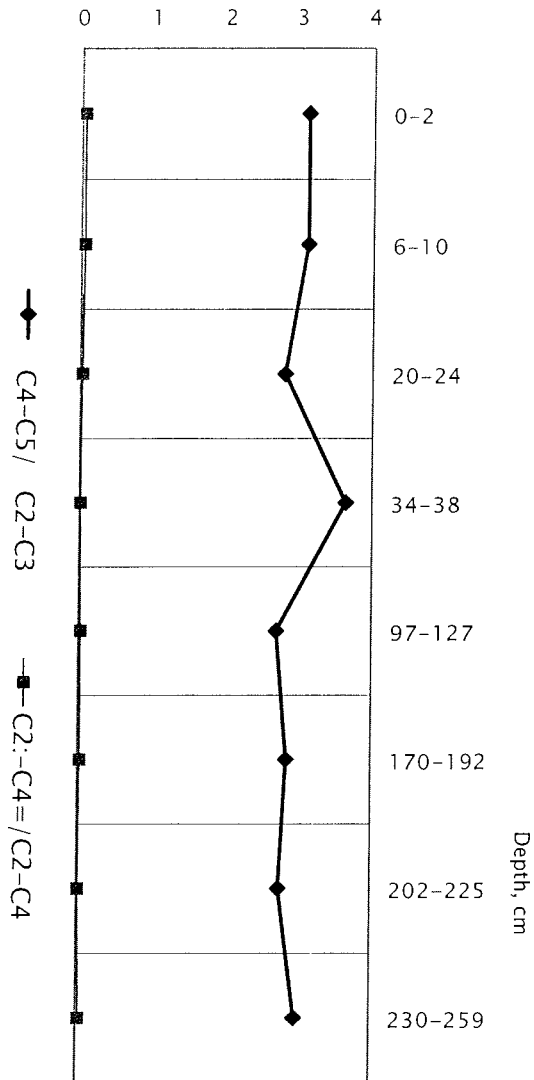




Fig.7.15 Geochemical indices in bottom sediment,  
(Kara Sea, BP01-47)



## 7.8 New findings of ikaite in the Kara Sea during R/V "Akademik Boris Petrov" Cruise 36, September 2001

L.A. Kodina, V.G. Tokarev, L.N. Vlasova, A.M. Bychkov, I.Yu. Mardanjan

V.I. Vernasky Institute of Geochemistry and analytical Chemistry RAS, Moscow

### Introduction

Only few findings of ikaite are known in the Arctic shelf seas up to the present (Schubert et al. 1997). Numerous findings of calcite pseudomorphs were described in Jurassic and L.Cretaceous sedimentary deposits in the large area (0,7 million km<sup>2</sup>) between river Pjasina and Vilyui, Lena basin and in the Laptev Sea shoreline area from Taymyr to the Lena delta (Kaplan 1978). Well-shaped crystals of different sizes, single or clustered were shown to be widespread in marine clayey or silty and sandy deposits (ball-shaped conglomerates of 0,5-8 cm in diameter, single crystals 1-8 cm in length). On the author's opinion, ikaite was the parent mineral of the carbonate pseudomorphs. This speculation fits well the geological situation and pseudomorph composition and was supported later (Suess et al. 1982).

In the joint German-Russian expeditions carried out onboard R/V "Akademik Boris Petrov" during the period of 1997-2001 ikaite and related authigenic carbonate inclusions in sediments have been repeatedly found in sediments (Kodina et al. 1998 2001; Geological core description, 2001). Most of them were observed along the Yenisei main channel, which is characterized by a high sedimentation rate (Stein 2001). Depositional environments, where ikaite occurs, are generally within silty clay or sandy silty clay, and often organic rich. Crystals occurred in the sediments at subbottom depths from 5-20 cm to 260 cm. During the last expedition (BP 2001) ikaite crystals were found at St. 26 and 55 and a carbonate crust ( $\delta^{13}\text{C} = -14,4\text{‰}$ ) was detected on the sediment surface at St. 45 and raised onboard (Fig 7.16.)

### Results and discussion

#### Core description.

The lithology of the ikaite bearing cores is presented in Figure 7.17. The detailed visual core description was made on board. The preliminary lithological description was supplemented by our onboard analytical data on the water content and the specific density of the raw sediments and comments of Drs R. Stein and M. Levitan. Geologists have made good use of the physical properties to study lithology and stratigraphy of sedimentary sections (Dunaev et al. 1995; Dittmers 2001). Both core sections exhibit a rather variable lithology. Within the sedimentary section St. 26, three lithological units could be distinguished. The upper part (0-195cm) of the core consisted of clayey sediments with a wet specific density (WSD) from 1,36 to 1,58 cm<sup>3</sup>. A sharp lithology and density boundary at 195-200cm marks the top of the second unit (195-385cm) comprising alternating sequences of very dense fine-grained silt, silty clay and more coarse-grained clayey silty sand and thin sandy (WSD=1,52-1,86 cm<sup>3</sup>) sediment intervals of variable thickness. The bottom part of the core (385-506 cm) was represented by dense silt and silty clay with diatoms (WSD= 1,56-1,64 cm<sup>3</sup>). Shell debris and intact bivalve

shells were abundant in the first unit and at the top interval of the second units (0-50 cm, 190-210 cm). The sediment was moderately reduced as observed by its grey, dark-grey, black color and slight H<sub>2</sub>S smell in the interval from 200-270 cm. At a depth of 226-230 cm, a weakly radiated spherical cluster (diameter of about 5 cm), of tightly connected, small (0,7-1 cm in length) yellowish to light-brown ikaite crystals was found.

The sedimentary sequence at St. 55 consisted mainly of sandy clay (WSD up to 1,80 cm<sup>3</sup>) in the uppermost part (0-70 cm) and partially of silty clay (WSD = 1,53- 1,72 cm<sup>3</sup>). The interval from 70 to 230 cm was represented by soft silty clay (WSD=1,48-1,58 cm<sup>3</sup>), with sand grains (sandy silty clay) below 170cm (WSD = 1,58- 1,62 cm<sup>3</sup>) being abundant. The bottom part of the section (230-310 cm<sup>3</sup>) consisted of highly reduced black sandy sediment (silty sand of WSD= 1,78-1.90 cm<sup>3</sup>). Intact bivalves (*Saxicava arctica*) and shell debris were present in the intervals from 10-20cm, 35-40cm, 120-130 cm. The sediments of the whole section were highly reduced, and strong H<sub>2</sub>S smell was present throughout the complete core.

Two ikaite crystal accumulations occurred close to each other in the silty clay core sections at depths from 135 - 145cm and 159 and 165 cm, respectively. The first one consisted of about 30 individual or doubled well-developed crystals of different sizes from less than 1 cm to 6,5 cm in length (Fig. 7.17). The weight of the crystal accumulation was about 300g. Within the second accumulation three small crystals and one giant, massive (169g), euhedral, magnificent crystal with a perfectly shaped front pyramidal termination (11,5 cm in length and 4,5 cm in diameter) occurred. To our knowledge, this is the largest known ikaite crystal up to now. All crystal specimens were translucent, dark amber in color. Few white points, consisting of calcite inclusions within the ikaite crystal are already visible by bare eye.

For the preservation of the ikaite crystals they were kept onboard in a freezer and could successfully be transported to the home laboratory.

#### X-Ray study of the crystals

X-ray study of the crystals was carried out on diffractometer DRON-3,0 using CoK $\alpha$  radiation. The study included phase identification and specification of the elementary cell parameters based on the random powder X-ray diffractometry data using silicon as an internal standard. Because of crystal metastability at room temperature, a rather high scanning rate of 1cm/min was used.

The following crystal specimens were investigated: small (0,8 – 1 cm in length) crystals of the crystal cluster from St. 26, a single crystal of about 5 cm in length and fragments from different parts of the giant crystal (St. 55). No compositional difference between the specimens has been detected; they all showed the typical reflections of stable ikaite and were accordingly identified as the natural, monoclinic mineral ikaite with a very low degree of replacement by calcite.

The transformation from ikaite to calcite at room temperature over a period of 12 to 24 hours was well documented by XRD on the ikaite sample from station BP00-37 (Kodina et al. 2001). However, some fragments of the crystals were found to be rather stable. After staying at room temperature for one day, some crystal fragments remained intact and X-ray diffractometry showed the typical ikaite structure.

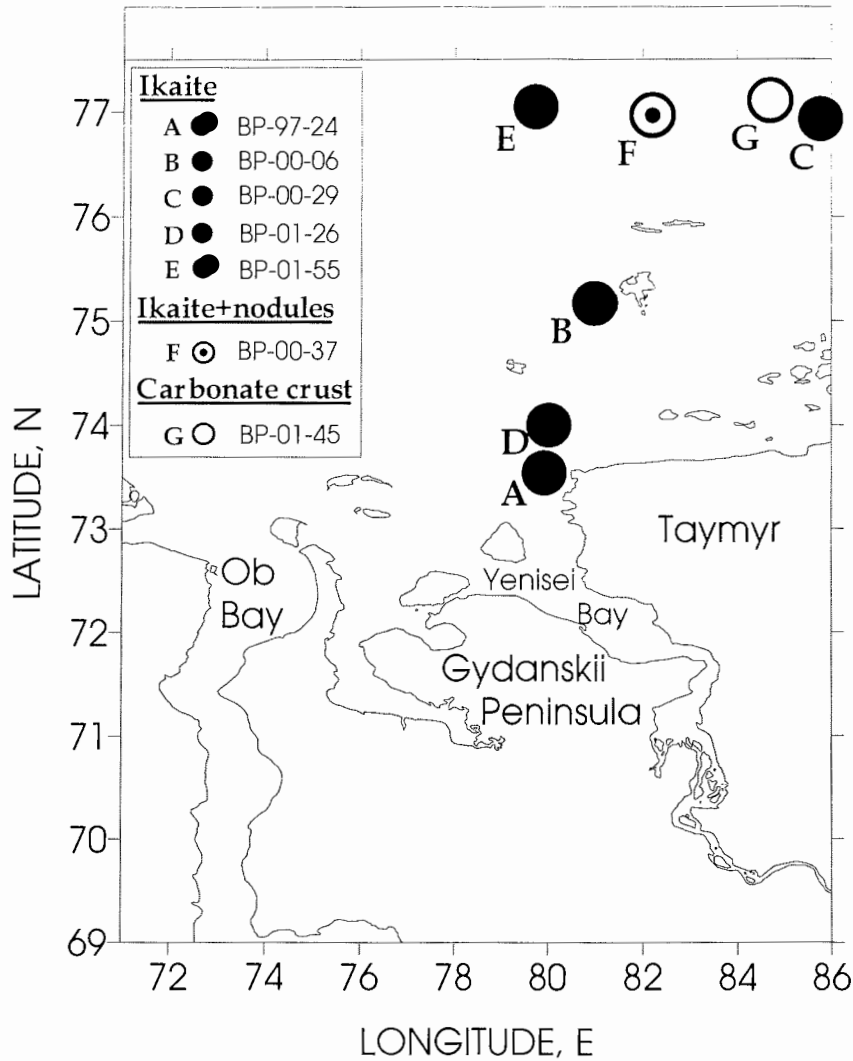


Fig. 7.16. Ikaite sampling stations in the Kara Sea German- Russian expeditions on board R/V "Akademik Boris Petrov", 1997-2001.

Determination of the elementary cell parameters was undertaken to get an additional efficient proof of the mineral nature. The data obtained were the following:  $a = 8,85$  (1);  $b = 8,25$  (1);  $c = 11,0(2)A$ ;  $\beta = 110,50(9)$ ;  $V = 7533(1,9)A^3$ . They are similar to the published data (Brown and Dickens 1970; Marland 1975; Schubert et al. 1997) for artificial and natural ikaite minerals.

#### Carbon isotope composition

Inorganic carbon isotope compositions of the ikaite samples from st. 55 and 26 are different (Table 7.10). This is evidence for different carbon sources, namely sedimentary organic carbon at St. 26 and a partial contribution of methane-derived  $CO_2$  at St. 55.

Table 7.10: Carbon isotope composition of the ikaite crystals

Station	Specimen	$\delta^{13}\text{C}_{\text{‰}}$	
BP01-26	Crystal № 1	-24.01	
	Crystal №2	-23.82	
	Crystal №3	-24.52	
	Crystal № 4	Random powder	-23.32
		Rest after sieving	-24.18
BP01-55	Giant crystal	Front pyramid termination	-41.64
		External part	-42.33
		Internal part	-42.26
	Crystal №1	-41.74	
	Crystal №2	-42.71	
	Crystal №3	-40.94	
	Crystal № 4	Random powder	-41.99
		Rest after sieving	-43.01

The stable carbon isotopic composition is variable between different crystals within one station as well as within different parts of the giant crystal. The magnitude of variations may be as large as 1,8‰ between different crystals and about 1‰ for different fragments inside single crystal. Isotopic variations are indicative of a complexity of isotope effects during formation of mineral phase and/or during the initial stage of the ikaite crystal pseudomorphism. Inclusion of organic or inorganic particles of the host sediment into the growing crystal can not be ruled out. Ikaite is generally believed to form near the sediment-water interface, and environmental conditions were favourable for this process (Larsen 1994).

#### Pore water hydrochemistry

The data on hydrochemistry of pore waters, pH, Eh of sediments and carbon isotope composition of dissolved inorganic carbon (DIC) throughout the sedimentary sequences at St. 55 and St. 26 are presented in Figures 7.18 A+B and 7.19). Both sedimentary sequences are characterized by a reducing regime. At St. 55 the most reduced interval occurs at a core depth of 135-165 cm as seen by the lowest Eh value of -320mV (Fig. 7.18A). St. 26 was found to be less reduced (Fig. 7.19). Development of anaerobic organic matter (OM) diagenesis in sediments with depth was noted by visual core description and a difference between the both cores was revealed.

Fig. 7.18A demonstrates a typical picture of anaerobic diagenetic OM decomposition in sediments, with increasing phosphate and silicate concentrations from the core top towards ~160 cm. Fig. 7.18B shows the distributions of the key parameters of organic matter diagenesis throughout the vertical section at St. 55. Common to earlier descriptions (Kodina et al. 2001), alkalinity increases as sulphate concentration decreases within the core section where ikaite precipitation occurs (135-165 cm). A change in the gradient of increasing alkalinity is notable. It corresponds to a synchronous drop of the  $\delta^{13}\text{C}_{\text{DIC}}$  due to the rapidly depleting DIC became constrained by the precipitation of isotopically depleted carbonate mineral ikaite ( $\delta^{13}\text{C}$  of about - 42‰). Methane is suggested as an additional

source of carbon dioxide depleted in the  $^{13}\text{C}$ -isotope. We have not yet all needed data, however the preliminary data evidence that methane concentrations as high as 11,2 ml/l were present in sediment interval of 200-226cm, sharply decreasing towards the overlying horizons. In other words, we suppose that St. 55 gives a typical example of ikaite precipitation resulting from methane cycle operation coupled with sulphate reduction in a highly reduced sediment (Kodina et al. 2001).

Isotope composition of the ikaite sample from St. 26 (about -24‰) suggests a different geochemical situation in the sediment, resulting from a different lithology and environment of sedimentation. This study is under progress. The vertical profiles for the geochemical parameters presented in Fig. 7.18 and 7.19 have much in common with the wet specific density curves for the corresponding sediment cores and might be an additional useful tool to determine environmental changes in the geological past, including the position of stratigraphic bounding in sedimentary sequences.

### **Acknowledgements**

The work was supported by Russian Foundation for Basic Research, Grant 00-05-64575.

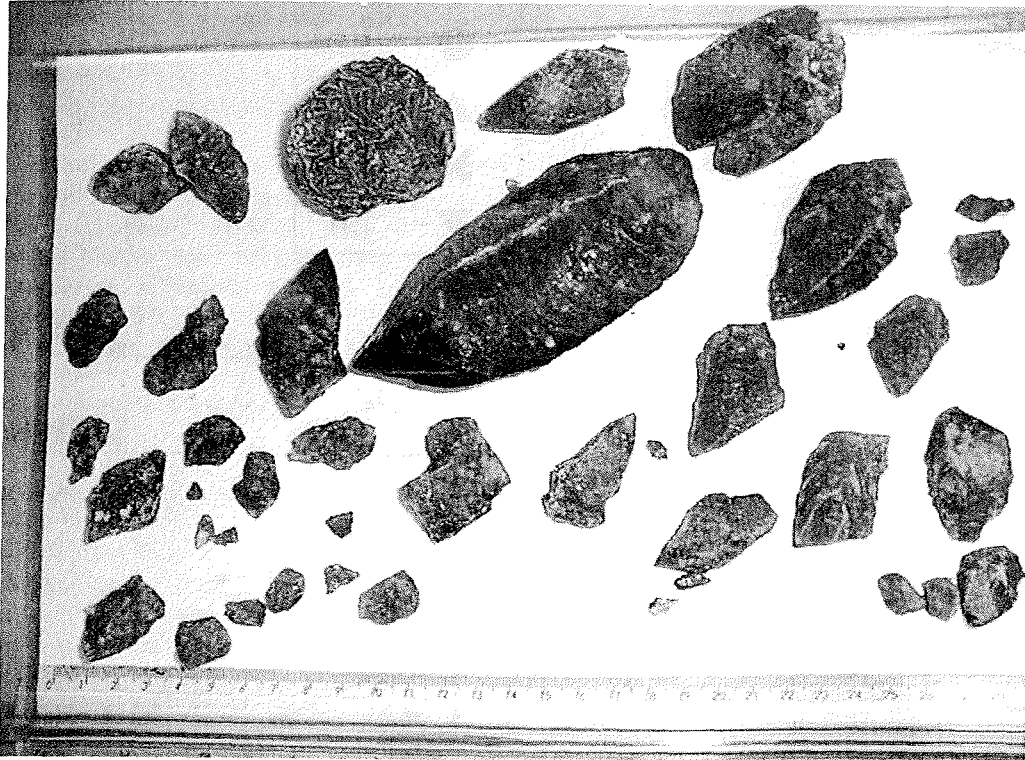


Fig. 7.17. Ikaite crystals from St. 26 (cluster spherical in shape , to the right of the giant crystal), from St. 55- giant crystal centrally positioned, single or doubled pyramidal and small bad-shaped crystals.

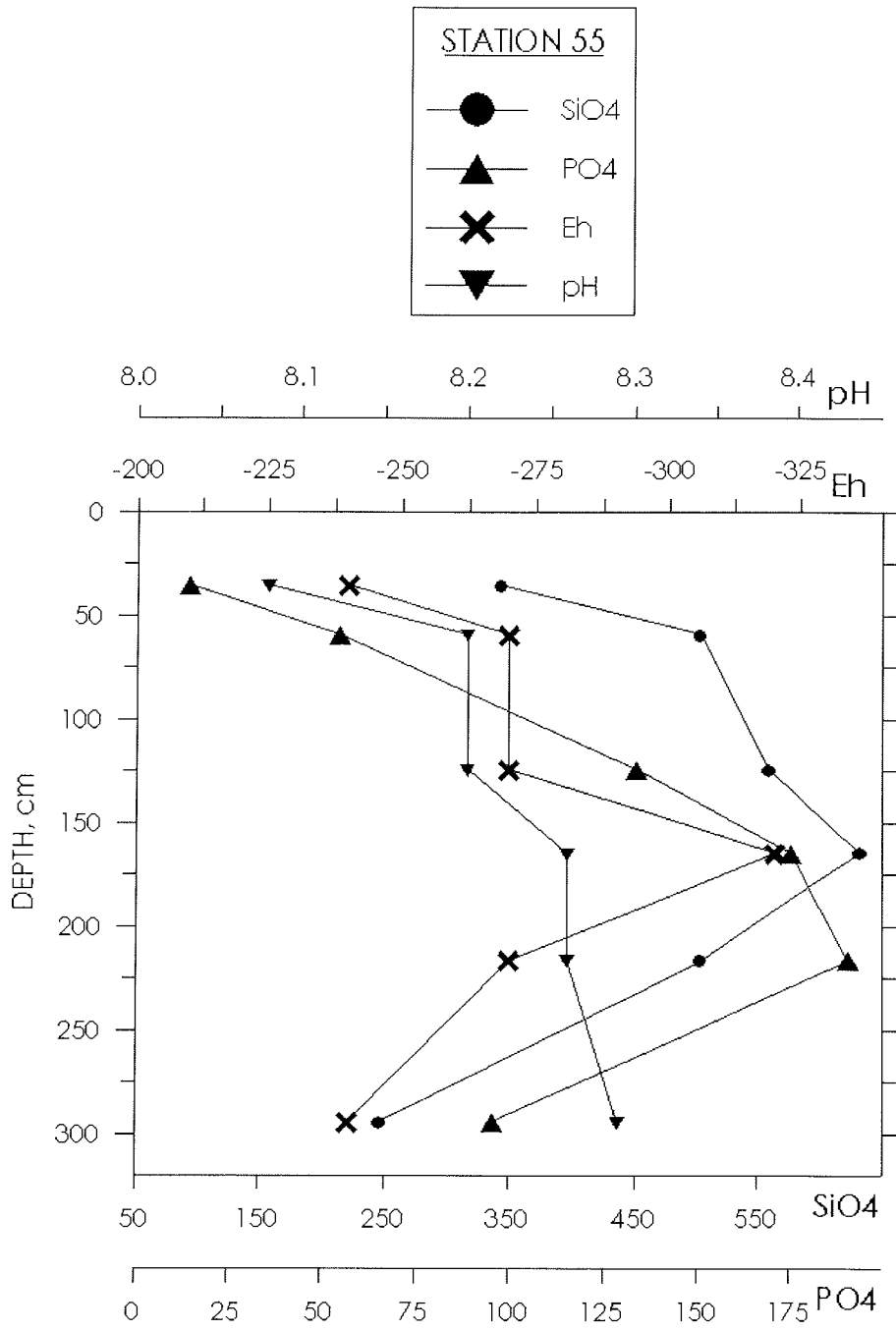


Fig. 7.18A.. Phosphate and silicate concentrations in pore water throughout the sedimentary sequence at St. 55.



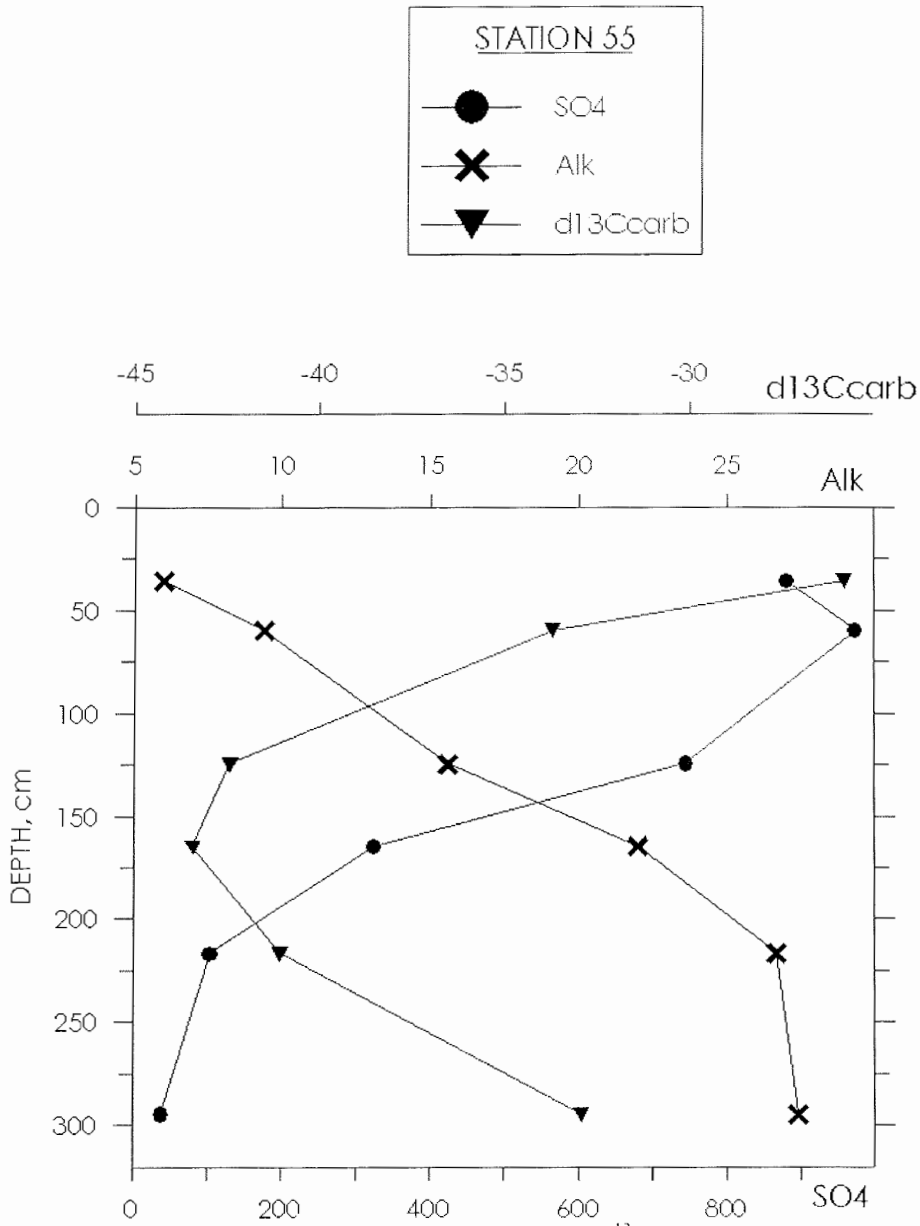


Fig. 7.18B. Alkalinity, sulphate concentration and  $\delta^{13}\text{C}_{\text{carb}}$  -values throughout the sedimentary sequence.

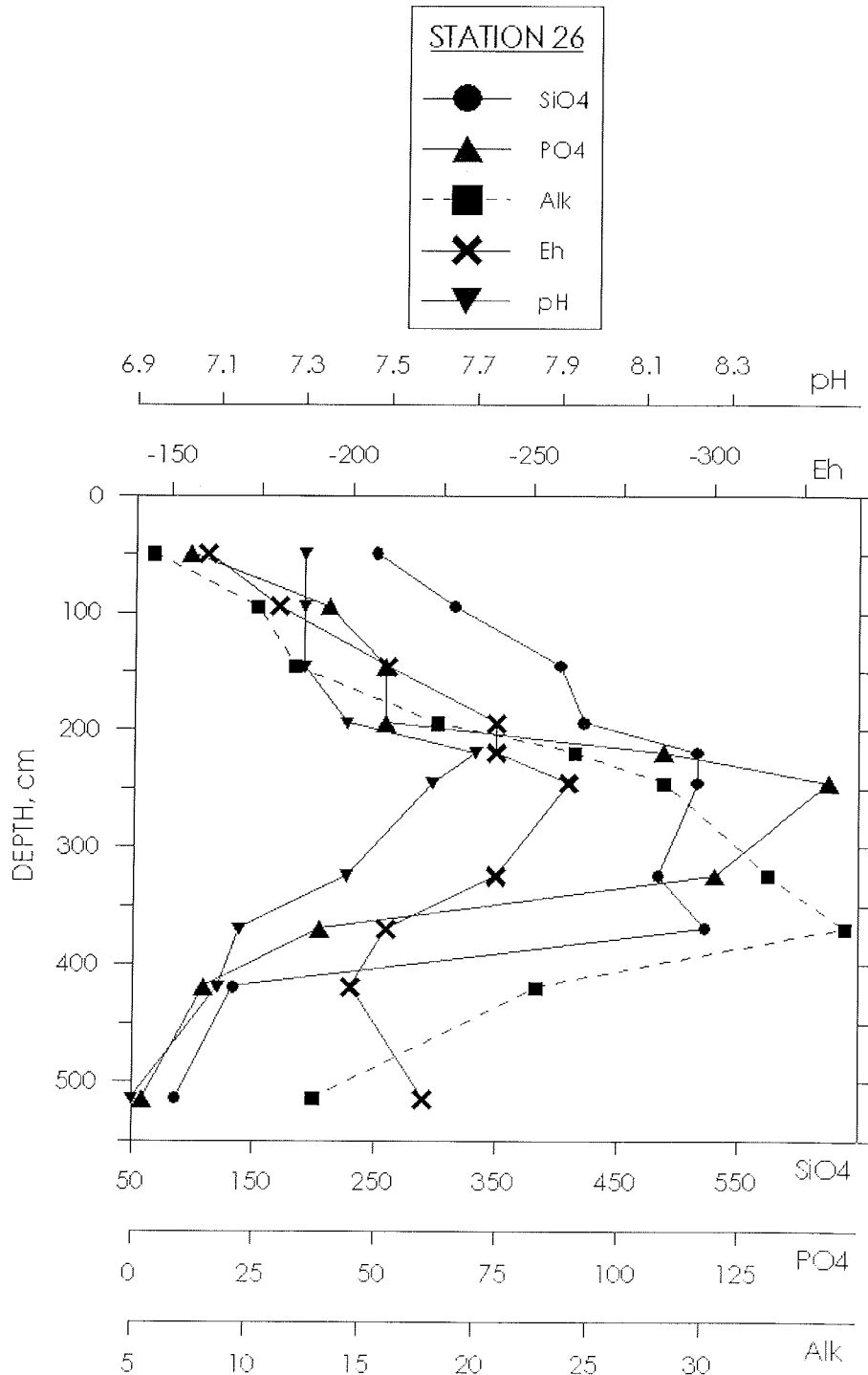


Fig. 7.19. Vertical profiles of Eh, pH and hydrochemical parameters of pore water throughout the sedimentary sequence at St. 26.

## 7.9 Variability of element concentrations in suspended matter and sediments of the Kara Sea and the Yenisei and Ob rivers

Schoster F.<sup>1</sup>, Eulenburg A.<sup>1</sup>, and Rachold V.<sup>1</sup>

<sup>1</sup>Alfred-Wegener-Institute for Polar- and Marine Research, Bremerhaven/Potsdam, Germany

### Introduction

The variability of element concentrations in suspended matter and sediments of the Kara Sea and the Yenisei and Ob rivers is quite high (Lukashin et al. 1999, Schoster et al. 2000). The Ob and Yenisei rivers transport huge amounts of terrigenous material from their sources to the estuaries and into the Kara Sea. Both rivers have large, but different catchment areas. The Ob River mainly drains the Siberian Lowland and the Altai Mountains far south, the Yenisei River mainly the Putoran Mountains with its Triassic Trapp Basalts, which show a significant chemical and mineralogical composition (Churkin et al. 1981, Lightfoot et al. 1990). Therefore, the surface sediments of the Kara Sea show high smectite content and enhanced Ti/Al-, Mg/Al-, Fe/Al-, Cr/Al-, and Ni/Al-ratios compared to the continental crust composition (Taylor and McLennan 1985, Schoster et al. 2000).

Changes in the salinity lead to rapid precipitation of particulate and dissolved material in the estuaries. In this "marginal filter" area mainly fine sediments, organic material and authigenic minerals like Fe- and Mn-oxides accumulate. So we have to distinguish between variability in sediment composition based on different source rocks and variability based on grain size fractionation and chemical processes.

The main objectives of our investigations: 1. Understanding of the distribution of the elements due to exchange reactions between water, suspended matter (SPM), and surface sediments, 2. Determining of the variations of elemental concentrations in sediments of the southern Kara Sea during the time from the last Termination until present time.

### 1. Major and minor elements in water, suspended matter and surface sediments

In order to understand the distribution of the elements due to exchange reactions between water, suspended matter (SPM) and surface sediments in the Ob and Yenisei rivers and the southern Kara Sea, the distribution of major and minor elements in the different components, water, SPM, and surface sediments will be investigated. In the Kara-Sea Expedition 2000, samples were mainly taken in the Yenisei River and in the adjacent southern Kara Sea (Schoster and Beeskow 2001, Beeskow and Rachold *subm.*). In the Kara-Sea Expedition 2001, mainly the Ob River and the adjacent southern Kara Sea were sampled. The focus of the examination is to understand the chemical processes in the estuarine environment of the Ob River and to compare it with the processes in the Yenisei Estuary. Variations in element ratios, which are caused by the exchange between dissolved and particulate phases in the transition zone between fresh water and seawater will be studied and interpreted. These data will provide

characteristic signatures for the estuarine mixing zone, which will serve as a basis for paleoenvironmental reconstructions.

### **Sampling program**

Water samples were taken on all stations in three depths:

- surface water: with bucket or a teflon water sampler;
- water of the pycnocline layer: with 24-bottles Niskin rosette sampler;
- bottom water: with 24-bottles Niskin rosette sampler and additional Multicorer-water.

All samples were immediately analyzed for conductivity, salinity, pH-value at 20°C, and alkalinity (Tab. 7.11, Fig. 7.20).

To obtain the river-transported SPM, surface water of every station was filtrated under slight vacuum through preweighted nucleopore filters with a pore size of 0.4 µm. The filters were dried at 40°C for two days. Depending on the sediment load, the volume of filtered water varied from 5 to 40 l. For river water SPM of three depths was separated. Surface sediments were sampled mainly by Multicorer (MUC), otherwise by Okeangrab or Large Box Corer. The samples are stored at 4°C.

### **Shipboard results**

The values of conductivity and salinity increase towards the north, the alkalinity is lower in the river area than in the Kara Sea regions. Measured pH-values show no significant variance. In all regions depth profiles of the water column are mainly characterized by an increase in salinity, conductivity, and alkalinity (Fig. 7.20. Tab. 7.11).

### **Analytical program**

In the laboratory detailed geochemical analyses will be performed. The concentrations of major and minor elements in all components (water, SPM and surface sediments) will be analyzed by Inductive-coupled plasma atom emission spectrometer (ICP-AES), Inductive-coupled plasma mass spectrometer (ICP-MS), Ionic chromatograph (IC), and additionally for sediments by X-ray fluorescence spectrometer (XRF).

## **2. Major and minor elements in sediments of the southern Kara Sea from the last Termination until present**

In order to get information about the quality and amounts of input of material into the Kara Sea from the last Termination until the present time, sediment cores from the shelf area will be studied. Major and minor element concentrations and mineralogy are used to characterize the sediments. The surface sediments of the Kara Sea show high contents of smectite and enhanced Ni/Al-, Ti/Al-, Fe/Al-, and Cr/Al-ratios compared to the continental crust composition (Taylor and McLennan 1985). The K/Al- and Rb/Al-ratios are rather low in the Yenisei Estuary. In comparison with the sediment compositions of the Yenisei Estuary K/Al- and Rb/Al-ratios are increased in the Ob Estuary, the other mentioned element/Al-ratios are reduced (Schoster et al. 2000). Therefore, it should be possible to distinguish between major input from one river or

from the other in order to reconstruct the paleoenvironment in the Kara Sea region for the last 12 ka.

### Sampling program

The sediment cores were taken with a 3 to 8 m long gravity corer and divided in one meter long sections. They were stored on board at ca. 5°C. At the Alfred-Wegener-Institute the cores will be measured for the magnetic susceptibility. According to this data samples for the determination of major and minor elements and the mineralogy will be taken.

### Analytical Program

After drying and grinding the samples will be analysed by XRF to get the major and minor element concentrations. To analyse for clay minerals the samples will be divided into sand, silt and clay fractions by sieving and grain-size fractionating after Atterberg (1912). In the clay fraction the contents of clay minerals will be determined.

Table 7.11: Hydrochemical data (A: surface water. B: pycnocline water. C: bottom near water. D: Bottom-near water. MUC, Teflon-WS: Teflon-water-sampler)

Stationno.	Sampling-device	Depth in m	Salinity	Temperature /Sampling (°C)	Conductivity (mS/cm) T <sub>Ref.</sub> 20°C	pH at ca. 20 °C	HCO <sub>3</sub> <sup>-</sup> (mg/l)
BP 01-01A	Teflon-WS	0.0	26.7	6.3	37.9	7.89	122.38
BP 01-01B	CTD	18.0	29.4	1.3	41.4	7.83	134.96
BP 01-01C	CTD	38.0	33.4	-1.42	46.2	7.58	141.06
BP 01-01D	MUC	38.0	29.4	/	41.7	7.76	132.68
BP 01-03A	Teflon-WS	0.0	4.0	10.7	6.57	7.69	49.94
BP 01-04A	Teflon-WS	0.0	0.0	15.3	0.130	7.86	64.43
BP 01-04C	CTD	18.0	0.0		0.160	7.59	62.14
BP 01-05A	Teflon-WS	0.0	0.0	14.5	0.127	7.89	62.91
BP 01-05C	CTD	11.0	0.0		0.127	7.45	62.91
BP 01-06A	Teflon-WS	0.0	0.0	14.7	0.126	7.60	63.67
BP 01-06C	CTD	14.0	0.0		0.153	7.69	62.91
BP 01-08A	Teflon-WS	0.0	0.0	14.5	0.130	7.86	62.53
BP 01-08C	CTD	27.0	0.0	14.3	0.139	7.64	63.29
BP 01-09A	Bucket	0.0	0.0	13.0	0.169	7.77	51.85
BP 01-09C	CTD	7.0	0.0		0.155	7.80	52.23
BP 01-09C	Teflon-WS	8.0	0.0	12.9	0.171	7.76	51.47
BP 01-11A	Teflon-WS	0.0	0.0	12.8	0.153	7.87	51.85
BP 01-11B	CTD	7.0	0.6		1.335	7.68	-
BP 01-11C	CTD	8.3	0.2		0.782	7.71	-

Stationno.	Sampling-device	Depth in m	Salinity	Temperature /Sampling (°C)	Conductivity (mS/cm) T <sub>Ref.</sub> 20°C	pH at ca. 20 °C	HCO <sub>3</sub> <sup>-</sup> (mg/l)
BP 01-11D	MUC	12.0	21.8		31.5	7.16	110.94
BP 01-16A	Bucket	0.0	0.0	12.8	0.129	7.81	62.14
BP 01-16B	CTD	13.0	0.0		0.121	7.85	59.48
BP 01-16C	CTD	27.0	0.0		0.120	7.84	61.00
BP 01-16D	MUC	28.0	0.0		0.123	7.91	61.76
BP 01-19A	Teflon-WS	0.0	6.0	9.8	9.63	7.70	56.04
BP 01-19B	CTD	5.0	27.6		39.6	7.66	127.72
BP 01-19C	CTD	23.0	32.0		44.9	7.54	139.16
BP 01-23A	Teflon-WS	0.0	4.7	9.8	7.67	7.79	56.81
BP 01-23B	CTD	7.0	17.7		26.1	7.74	91.50
BP 01-23C	CTD	18.0	33.3		46.1	7.64	142.21
BP 01-26A	Teflon-WS	0.0	12.3	8.0	18.57	7.78	77.78
BP 01-26B	CTD	5.5	17.8		26.3	7.73	94.17
BP 01-26C	CTD	30.0	33.1		46.3	7.69	141.83
BP 01-26D	MUC	33.0	25.3 ?		36.3	7.76	117.04
BP 01-28A	Bucket	0.0	23.0	3.6	33.1	7.87	109.42
BP 01-28B	CTD	17.0	29.4		41.4	7.81	133.82
BP 01-28C	CTD	50.0	33.7		46.7	7.82	141.83
BP 01-28D	MUC	51.0	33.7		46.6	7.83	141.44
BP 01-31A	Eimer	0.0	29.4	2.6	41.6	7.8	128.86
BP 01-31B	CTD	15.0	30.4		43.0	7.73	136.49
BP 01-31C	CTD	89.0	34.0		47.2	7.73	141.83
BP 01-31D	MUC	88.0	34.1		47.3	7.82	142.21
BP 01-35A	Bucket	0.0	28.8	3.2	40.2	7.82	128.10
BP 01-35B	CTD	17.0	32.4		44.8	7.85	135.34
BP 01-35C	CTD	150.0	34.7		47.4	7.67	142.21
BP 01-35D	MUC	160.0	34.7		47.4	7.76	143.35
BP 01-38A	Bucket	0.0	29.2	2.9	40.7	7.82	130.77
BP 01-38B	CTD	14.0	32.4		44.6	7.83	139.16
BP 01-38C	CTD	100.0	34.2		46.9	7.72	143.73
BP 01-38D	MUC	110.0	34.0		46.7	7.74	143.73
BP 01-43A	Bucket	0.0	20.6	5.5	30.4	7.83	103.32
BP 01-43B	CTD	10.0	23.9		35.1	7.81	115.90
BP 01-43C	CTD	40.0	33.4		47.5	7.75	142.97
BP 01-43D	MUC	48.0	33.7		46.9	7.78	145.26
BP 01-46A	Bucket	0.0	25.0	4.2	35.6	7.9	118.57
BP 01-46B	CTD	20.0	34.4		47.3	7.96	139.16
BP 01-46C	CTD	300.0	34.9		48.0	7.75	146.02
BP 01-46D	MUC	323.0	34.9		48.0	7.71	144.88

Stationno.	Sampling-device	Depth in m	Salinity	Temperature /Sampling (°C)	Conductivity (mS/cm) T <sub>Ref.</sub> 20°C	pH at ca. 20 °C	HCO <sub>3</sub> <sup>-</sup> (mg/l)
BP 01-46F	CTD	50.0	34.6		47.5	7.8	133.44
BP 01-51A	Bucket	0.0	23.8	4.4	34.9	7.87	117.81
BP 01-51B	CTD	10.0	29.6		42.5	7.95	133.06
BP 01-51C	CTD	140.0	33.8		48.0	7.75	142.21
BP 01-51D	MUC	158.0	33.5		47.6	7.84	142.97
BP 01-52A	Bucket	0.0	25.0	4.3	36.1	7.83	120.48
BP 01-52B	CTD	12.0	29.4		42.5	7.84	133.44
BP 01-52C	CTD	65.0	33.2		47.1	7.74	139.54
BP 01-52D	MUC	75.0	34.1		46.8	7.74	140.30
BP 01-56A	Bucket	0.0	21.7	5.5	31.2	7.86	109.80
BP 01-56B	CTD	16.0	31.9		44.4	7.94	138.78
BP 01-56C	CTD	170.0	34.7		47.7	7.85	141.06
BP 01-56D	MUC	176.0	34.5		48.5	7.86	142.59
BP 01-59A	Bucket	0.0	22.0	5.3	31.4	7.84	114.38
BP 01-59B	CTD	16.0	29.9		41.4	7.83	135.73
BP 01-59C	CTD	165.0	34.5		47.1	7.75	141.06
BP 01-59D	MUC	176.0	34.4		47.0	7.71	143.35
BP 01-62A	Bucket	0.0	23.1	4.8	33.4	7.91	113.61
BP 01-62B	CTD	12.0	29.4		41.0	7.87	128.10
BP 01-62C	CTD	120.0	34.2		47.1	7.79	134.20
BP 01-62D	MUC	135.0	33.9		47.4	7.78	143.35
BP 01-65A	Bucket	0.0	18.9	6.5	27.5	7.88	105.23
BP 01-65B	CTD	8.0	26.9		37.9	7.87	125.05
BP 01-65C	CTD	50.0	33.6		46.3	7.69	141.06
BP 01-65D	MUC	63.0	33.3		46.2	7.66	143.35
BP 01-66A	Bucket	0.0	13.2	7.1	19.77	7.61	86.16
BP 01-66B	CTD	10.0	26.6		37.4	7.83	124.29
BP 01-66C	CTD	45.0	33.4		45.9	7.64	139.54
BP 01-66D	MUC	55.0	33.5		46.2	7.63	141.83
BP 01-67A	Bucket	0.0	11.2	7.5	16.69	7.92	86.93
BP 01-67B	CTD	6.0	23.8		34.1	7.88	117.43
BP 01-67C	CTD	40.0	32.8		45.6	7.65	140.30
BP 01-67D	MUC	49.0	33.3		46.0	7.66	138.01
BP 01-68A	Bucket	0.0	9.8	7.9	15.11	7.66	84.64
BP 01-68B	CTD	6.0	21.4		31.1	7.64	110.56
BP 01-68C	CTD	20.0	32.1		45.2	7.48	138.78
BP 01-68D	MUC	31.0	32.7		44.8	7.62	140.30
BP 01-70A	Teflon-WS	0.0	0.7	9.4	1.533	7.46	42.32
BP 01-70B	CTD	7.0	29.9		40.7	7.41	130.01

Stationno.	Sampling-device	Depth in m	Salinity	Temperature /Sampling (°C)	Conductivity (mS/cm) T <sub>Ref.</sub> 20°C	pH at ca. 20 °C	HCO <sub>3</sub> <sup>-</sup> (mg/l)
BP 01-70C	CTD	15.0	31.0		42.8	7.46	135.73
BP 01-70D	MUC	22.0	29.8		42.3	7.5	146.40
BP 01-72A	Teflon-WS	0.0	0.0	11.4	0.09	7.42	39.27
BP 01-72A	Bucket	0.0	0.0		0.10	7.61	38.89
BP 01-72C	CTD	20.0	0.0		0.116	7.53	39.65
BP 01-73A	Teflon-WS	0.0	0.0	12.4	0.099	7.51	54.14
BP 01-73C	CTD	9.0	0.0		0.101	7.64	53.76
BP 01-73D	MUC	15.0	0.0		0.119	7.42	67.86
BP 01-74A	Bucket	0.0	0.0	?	0.03	7.06	19.83
BP 01-75A	Bucket	0.0	0.0	10.4	0.04	7.37	22.11
BP 01-77A	Bucket	0.0	0.0	11.4	0.029	7.19	22.88
BP 01-78A	Bucket	0.0	0.0	12.4	0.116	7.55	73.58
BP 01-79A	Bucket	0.0	0.0	12.1	0.104	7.62	56.43
BP 01-80A	Teflon-WS	0.0	0.7	8.7	1.522	7.73	44.23
BP 01-80B	CTD	7.0	11.1		16.95	7.29	83.11
BP 01-80C	CTD	10.0	22.1		31.7	7.36	115.14
BP 01-80D	MUC	16.0	24.0		34.3	7.38	121.24
BP 01-82A	Teflon-WS	0.0	10.0	6.7	15.8	7.70	77.39
BP 01-82B	CTD	7.0	23.6		33.5	7.55	117.81
BP 01-82C	CTD	20.0	33.1		45.1	7.49	139.54
BP 01-82D	MUC	29.0	32.8		45.0	7.44	140.30



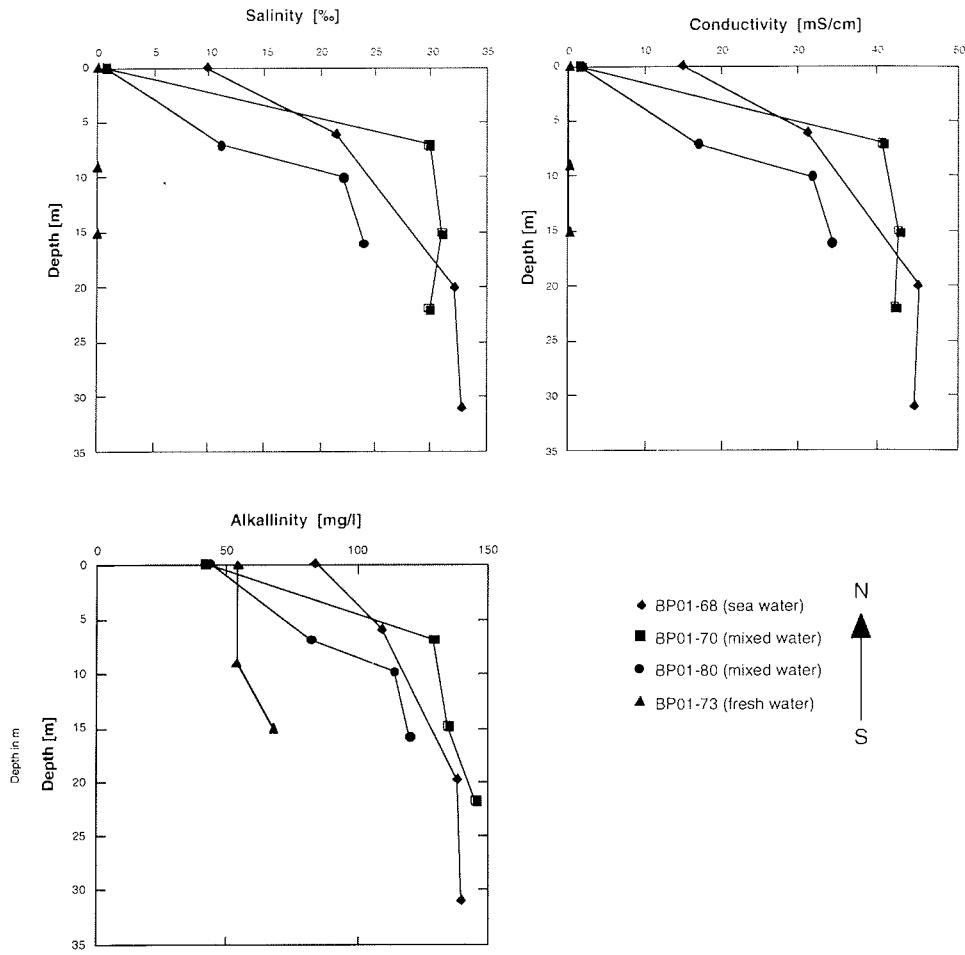


Figure 7.20: Hydrochemical parameter of the Ob Estuary.

## 7.10 Anthropogenic pollution of Kara Sea and estuaries of the Yenisei and Ob rivers based on data of the 2001 and 2000 cruises

O.V. Stepanets, A.P. Borisov, A.N. Ligaev, G.Yu. Solovjeva, E. M. Sisov,  
V.M. Komarevsky

Vernadsky Institute of Geochemistry and Analytical Chemistry, RAS, Moscow, Russia.

The great Siberian rivers jointly with the northern seas compose a part of the global hydrosphere within which the processes of continental erosion, transport and accumulation of sediments take place, i.e., the processes of geochemical interaction between the continent and ocean. The scale and nature of these processes in the territories of northern Russia and the Arctic seas remain rather uninvestigated.

From an ecological point of view the large Siberian rivers are potential sources of anthropogenic pollution of the Kara Sea and further of the Arctic basin. Therefore, the investigations connected with an assessment of levels of contents of radioactive and chemical admixing in surface sediments and in sediment cores obtained from fluvial medium, mixing zone and open part of the sea, help to estimate the modern ecological state of the local region and to reveal time intervals of massive fluvial input from radiochemical plants of Ural and Siberia into the marine area.

### Working Program

The main tasks of our radiogeochemical research of the cruise 2001 were to study the horizontal and vertical distribution of the Cs, Sr and Pu isotopes in water and sediments, and to estimate the influence of natural environmental parameters on laws governing the distribution and migration of radionuclides in the investigation area.

Other tasks are:

- the study of granulometric structure of upper layer sediments and level of radioactivity  $^{137}\text{Cs}$ ;
- the study of role of suspended matter on the behavior and migration of some radionuclides;
- the estimate of the Yenisei river role as source of anthropogenic pollution of the Kara Sea water;
- the evaluation of spreading of heavy metals with riverine suspension into the Kara Sea and the determination of anthropogenic elements in the Kara Sea, as consequence of the Norilsk plants production.

### Sampling and Analytical Methods.

Sediments were sampled with a box corer (50x50x60 cm), with subsequent subsampling with a plastic tube having an inner diameter of 10 cm. The cores were cut in 1-2 cm slices, and samples were dried at a temperature of 60 - 80<sup>o</sup> C. Water was sampled with a large volume sampler (200 l Batomat) or taken by a pump through a plastic pipe

system, and filled in storage tanks. Before analysis some samples were filtered through a cartridge filter to remove suspended matter  $>0.45\mu\text{m}$ .

The greatest amount of data was obtained for  $^{137}\text{Cs}$  contents, and to a smaller extent for  $^{90}\text{Sr}$  and  $^{239,240}\text{Pu}$ .  $^{137}\text{Cs}$ ,  $^{90}\text{Sr}$  and  $^{239,240}\text{Pu}$  in water samples, and  $^{90}\text{Sr}$  and  $^{239,240}\text{Pu}$  in sediment samples were determined with a radiochemical method. For the analysis of  $^{137}\text{Cs}$  in sediments we used direct  $\gamma$ -measurements without decomposition of the sample.

Measurement of the radioactivity of  $^{137}\text{Cs}$  in sediment samples was carried out in a low-background installation with semiconductor Ge detector.  $^{137}\text{Cs}$  was determined in water samples of 200 l volume using the sorption method under dynamic conditions with subsequent  $\gamma$ -spectrometer measurements on concentrates. Co-ferrocyanid, fixed on an organic matrix, was used as quality sorbent for concentrating Cs.

The determination of  $^{90}\text{Sr}$  in the water samples included precipitation of strontium carbonate. Then we use extraction chromatographic procedure with crown-ether dicyclohexano-18-crown-6 permitting to separate  $^{90}\text{Sr}$  from other radionuclides. At passage  $2\mu$  of solution on hydrogen nitrate keeping radionuclides through column on a column remain strontium and lead. After unabsorption of strontium from the column by hot water, we carried out a final precipitation of  $^{90}\text{Sr}$  as strontium oxalatum.

The analysis of Pu in water samples consisted of precipitation of Pu with iron hydroxide (from a volume of 150 l), subsequent radiochemical cleaning and adsorption of Pu on  $\text{LaF}_3$ . Precipitates were separated on a membrane filter and activity measured on  $\alpha$ -spectrometer. For extraction of Pu from sediments samples were boiled in 7M  $\text{HNO}_3$  with  $\text{KBrO}_3$ , and then were further processed as water samples Pu analysis.

## Results and Discussion

The data on  $^{137}\text{Cs}$  distribution in the top layer (0-2cm) of the bottom sediments from all stations are presented in Table 7.12. The data demonstrate that the distribution of  $^{137}\text{Cs}$  in the upper (0-2 cm) layer is irregular. In the Yenisei Bay high concentrations of this radionuclide are observed. The lowest values of  $^{137}\text{Cs}$  cluster are in the central part of our working area, and at some localities of the Ob Bay.

If we consider the data on  $^{137}\text{Cs}$  radioactivity, which we obtained during this expedition, in combination with the lithology and geochemical activity of 1995-cruise data (Tab. 7.13), we can estimate the peculiarities in the distribution of this radionuclide in the estuaries of rivers Ob and Yenisei. Thus, in the studied part of the Ob Bay, the reduced sediments are represented by sandy mud that does not absorb Cs, consequently, the  $^{137}\text{Cs}$  concentration is very low. On the contrary, in the Yenisei Bay, the bottom sediments are characterized by a high fraction of partially oxidized clays, with high capabilities of absorbing  $^{137}\text{Cs}$ , which resulted in the higher specific activity of  $^{137}\text{Cs}$  in the bottom sediments.

In the upper sedimentary layer the Pu-radionuclides activity distribution is recorded, although we have for this radionuclide less number of analysed samples (Table 7.14).

The investigation of the distribution of Cs and Sr radionuclides in water samples showed, that the concentration of these two radionuclides are low in filtrated samples of water. The concentrations of water-soluble Cs-species increase with increasing salinity (Fig. 7.21), where as the concentrations of Sr decrease with increasing salinity (Fig. 7.22).

The results of the Cs and Sr radionuclides distribution of solution and suspended matter showed, that for the sea water the suspended matter may absorb up to 1-10%  $^{137}\text{Cs}$  and  $^{90}\text{Sr}$ , for the water samples of rivers these value can be reach 15-30% (Tab. 7.15-7.16). This means, that the coefficient of  $^{137}\text{Cs}$  concentration (the first time) by suspended matter may be as high as  $10^3$ - $10^4$ . Therefore, suspended matter, together with mobile clay phase of the bottom sediments upper layer, may transfer considerable amounts of  $^{137}\text{Cs}$  (and other isotopes).

For  $^{90}\text{Sr}$ -radionuclide we confirm our previous data that  $^{90}\text{Sr}$  is able to form complex with dissolved organic matter (Tab. 7.16), especially in solutions with low salinity. These investigations are important for understanding of the behavior and transfer of radioactive elements – as marker of processes in the river-estuaries-sea geochemical system.

The second part of our investigations were to obtain additional analytical information about contents and distribution of heavy elements, including the presence of the anthropogeneous heavy metals in sea water which enters the Kara Sea as consequence of works of the mining plants. In this cruise, we have performed the determination of heavy metals in bottom sediments by X-Ray fluorescence method using X-Ray spectrometer SPARK-1.

The data of the Fe content in river and sea water show, that heavy metals together with the upper layer of bottom sediments spread far to north of the Sea (Fig. 7.23). The lateral distribution of the anthropogenic metals Pb and Cu and other elements are different (Fig. 7.24). We believe that the irregular distribution of Pb and Cu in the Kara Sea (Fig. 7.25) may be related to the influence of source-works mining plant in the town of Norilsk.

Thus, our studies yielded rather objective characteristics of the anthropogenic situation in the estuaries of the Yenisei and Ob rivers and adjacent part of the Kara Sea in 2001.

Table 7.12: The data on  $^{137}\text{Cs}$  distribution in the top layer of the bottom sediments.

	Number of station	Concentration of $^{137}\text{Cs}$ Bq/kg (P=0.95)
1	01-01	$8.0 \pm 1.0$
2	01-03	$33.7 \pm 3.0$
3	01-04	$8.6 \pm 1.8$
4	01-05	$2.8 \pm 0.6$
5	01-05	$4.4 \pm 0.6$
6	01-06	$16.0 \pm 1.5$
7	BP01-07	$15.9 \pm 2.2$
8	BP01-08	$7.6 \pm 1.1$
9	BP01-09	$24.0 \pm 2.0$
10	BP01-10	$27.4 \pm 2.2$
11	BP01-12	$46.2 \pm 3.7$
12	BP01-13	$24.0 \pm 2.2$
13	BP01-15	$21.0 \pm 3.0$
14	BP01-16	$3.0 \pm 1.0$
15	BP01-17	$21.7 \pm 3.0$
16	BP01-18	$39.3 \pm 4.5$
17	BP01-19	$47.0 \pm 5.0$
18	BP01-20	$363 \pm 4.0$
19	BP01-21	$28.0 \pm 4.0$
20	BP01-22	$6.2 \pm 1.5$
21	BP01-23	$6.8 \pm 1.4$
22	BP01-25	$19.0 \pm 2.0$
23	BP01-28	$7.0 \pm 1.2$
24	BP01-29	$7.1 \pm 2.3$
25	BP01-30	$5.6 \pm 0.9$
26	BP01-31	$7.0 \pm 1.4$
27	BP01-32	$4.9 \pm 1.0$
28	BP01-33	$3.8 \pm 0.5$
29	BP01-34	$2.0 \pm 0.4$
30	BP01-35	$6.4 \pm 1.0$
31	BP01-36	$2.2 \pm 0.6$
32	BP01-37	$5.0 \pm 1.1$
33	BP01-38	$6.1 \pm 0.9$
34	BP01-39	$5.8 \pm 0.9$
35	BP01-40	$5.7 \pm 0.8$
36	BP01-41	$6.0 \pm 0.8$
37	BP01-42	$16.7 \pm 2.0$
38	BP01-43	$14.4 \pm 2.0$
39	BP01-44	$1.4 \pm 0.5$
40	BP01-45	$10.2 \pm 1.4$
41	BP01-46	$2.1 \pm 0.6$
42	BP01-47	$9.2 \pm 0.9$
43	01-48	$6.0 \pm 1.5$
44	01-49	$5.0 \pm 0.8$
45	01-50	$3.8 \pm 0.6$
46	01-51	$6.8 \pm 1.6$
47	01-52	$7.1 \pm 1.3$

---

48	01-55	$5.6 \pm 0.8$
49	01-56	$5.0 \pm 0.8$
50	01-57	$5.2 \pm 0.8$
51	01-58	$7.0 \pm 2.0$
52	01-59	$7.6 \pm 2.0$
53	01-60	$3.8 \pm 0.7$
54	01-61	$11.9 \pm 1.7$
55	01-62	$12.7 \pm 1.6$
56	01-63	$5.2 \pm 0.9$
57	01-64	$10.9 \pm 1.3$
58	01-65	$4.2 \pm 1.2$
59	01-66	$9.6 \pm 1.2$
60	01-67	$11.7 \pm 1.5$
61	01-68	$4.5 \pm 0.8$
62	01-69	$13.5 \pm 2.0$
63	01-70	$7.2 \pm 0.8$
64	01-71	$1.9 \pm 0.5$
65	01-72	$2.1 \pm 0.5$
66	01-72	$9.2 \pm 1.2$
67	01-73	$10.1 \pm 1.4$
68	01-73-1	$11.1 \pm 1.3$
69	01-73-2	$9.5 \pm 1.2$
70	01-73-3	$14.9 \pm 1.7$
71	01-73-4	$9.8 \pm 1.0$
72	01-73-5	$7.1 \pm 1.0$
73	01-74	$10.8 \pm 1.4$
74	01-75	$15.9 \pm 2.0$
75	01-76	$14.4 \pm 2.4$
76	01-77	$12.8 \pm 2.1$
77	01-78	$11.8 \pm 1.5$
78	01-79	$6.8 \pm 0.9$
79	01-80	$2.4 \pm 0.4$
80	01-81	$17.4 \pm 2.6$
81	01-82	$14.4 \pm 2.6$
82	01-83	$10.0 \pm 0.9$

Table 7.13: Equilibrium partition coefficient ( $K_d$ ) of  $^{137}\text{Cs}$  for various types of bottom sediments (treatment of the cruise-1995 data).

Group no.	Type of bottom sediments	$K_d$	Sorption effect
1	Coarse-grained sediments with a low fraction of pelitic particles of organic-mineral composition of shallow bottom areas with intense exchange at media interface	10-20	Weak
2	Pelitic sediments of organic-mineral composition with high content of sand-silt fraction of shallow and moderately deep floor regions with an intense exchange of disperse phases at media interface	40-70	Medium
3	Pelitic sediments consisting mainly of organic-mineral colloids with intense exchange of disperse phases at media interface	>100	Strong

Table 7.14: Results of determination activity  $_{u-239,240}$  in upper layer of bottom sediments.

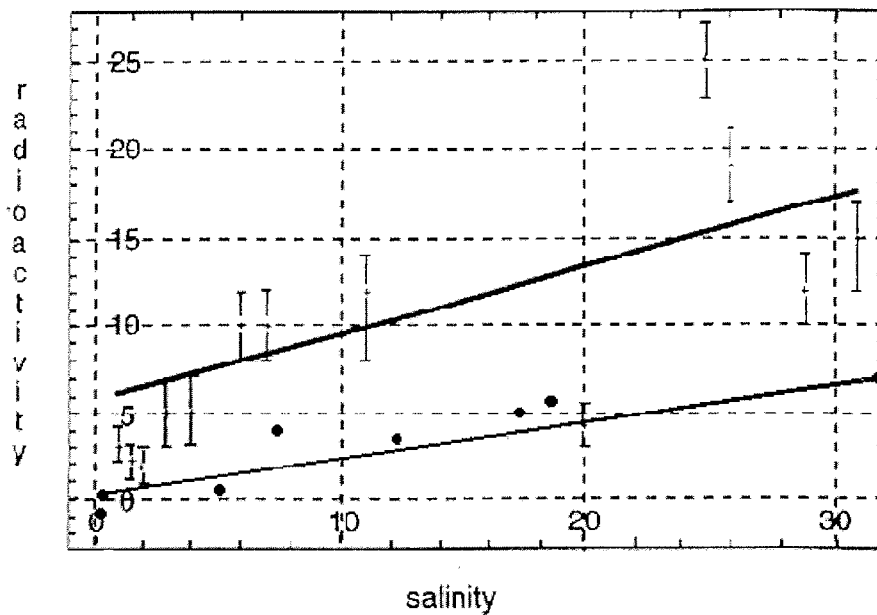
Station	Activity $_{u-239,240}$ , Bq/kg
BP2000-07	1.96
BP2000-14	0.595
BP2000-15	0.065
BP2000-16	0.19
BP2000-21	0.595
BP2000-22	0.595
BP2000-23	0.355

Table 7.15: Distribution of  $^{137}\text{Cs}$  between water and suspended matter fractions.

Number of station	Level of activity, Bq/sample.	
	Suspended matter	Water
BP95-36 (Kara Sea)	0.2	33
BP95-06 (Kara Sea)	0.3	46
BP01-70 (Ob bay)	0.4	2.2
BP01-25 (Yenisei bay)	0.7	4.8

Table 7.16: Results of measurement of Sr-90 in water, filtered water (0,2 µm) and ultrafiltered water(2000 Da)

Station	Depth, m	Salinity, ‰	Activity Sr-90, Bq/m <sup>3</sup>				
			Not filtered water	Filtered water, (0,2 µm)	Ultrafiltered water		
					2000 Da	800 Da	150 Da
BP01-08	3	0,1	3,9±1,1	3,1±0,6	-	-	-
	28	0,1	-	-	4,5±0,9	-	2,7±0,5
BP01-72	3	0,1	9,7±1,9	8,0±1,6	6,4±1,3	5,9	3,7±0,7
BP01-30	3	34,1	1,9±0,4	1,6±0,3	-	1,1±0,2	-
BP01-70	3	1,5	7,0±1,4	5,8±1,2	-	-	-



Cs-137 concentration (dissolved) in samples as function of salinity.

Figure 7.21: <sup>137</sup>Cs concentrations vs. salinity. × - data 1995, 1997; \_ - data 2001.



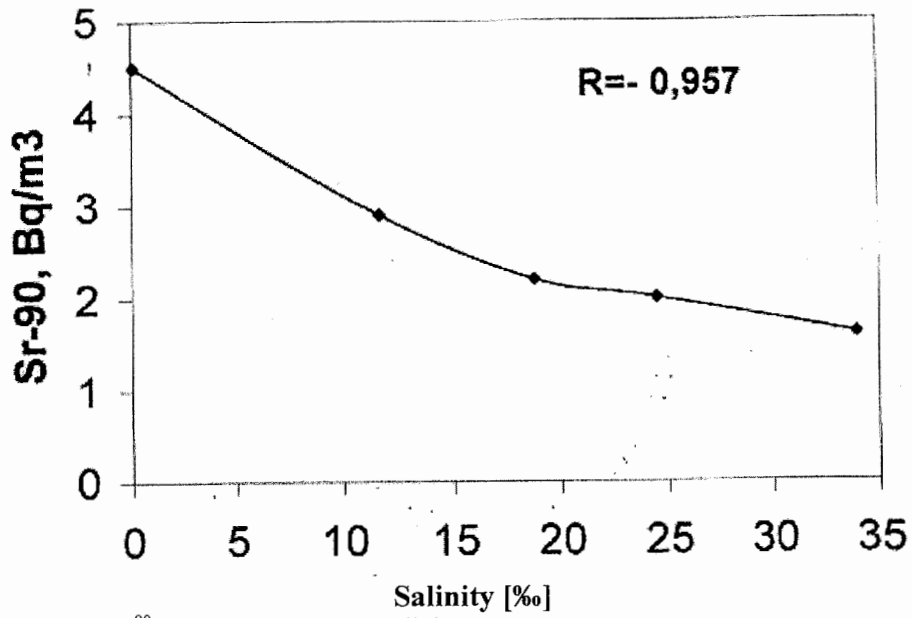


Figure 7.22: <sup>90</sup>Sr concentrations vs. Salinity

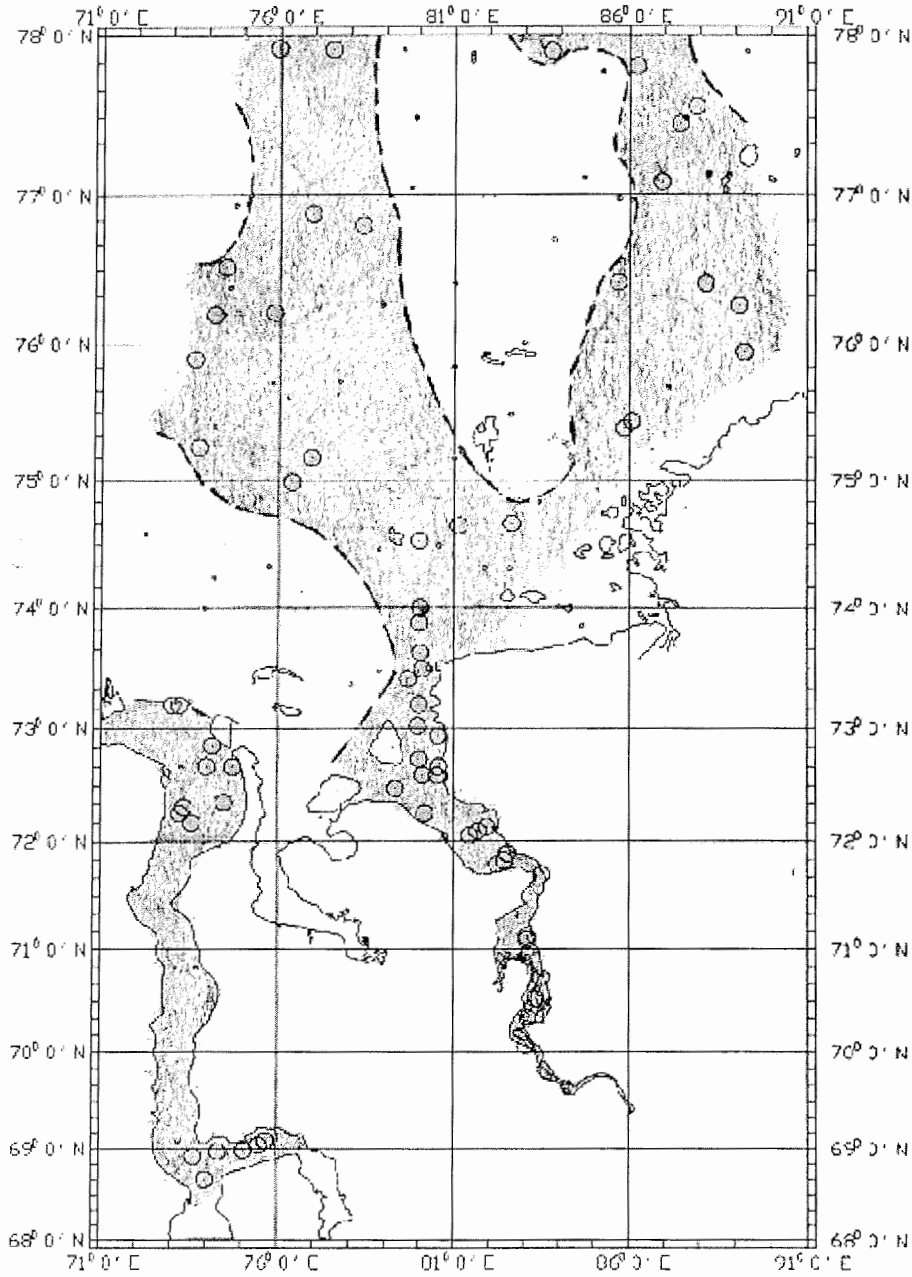


Figure 7.23: Spreading of the Yenisei river material to the Kara Sea on the Fe content in top layer of the bottom sediments.

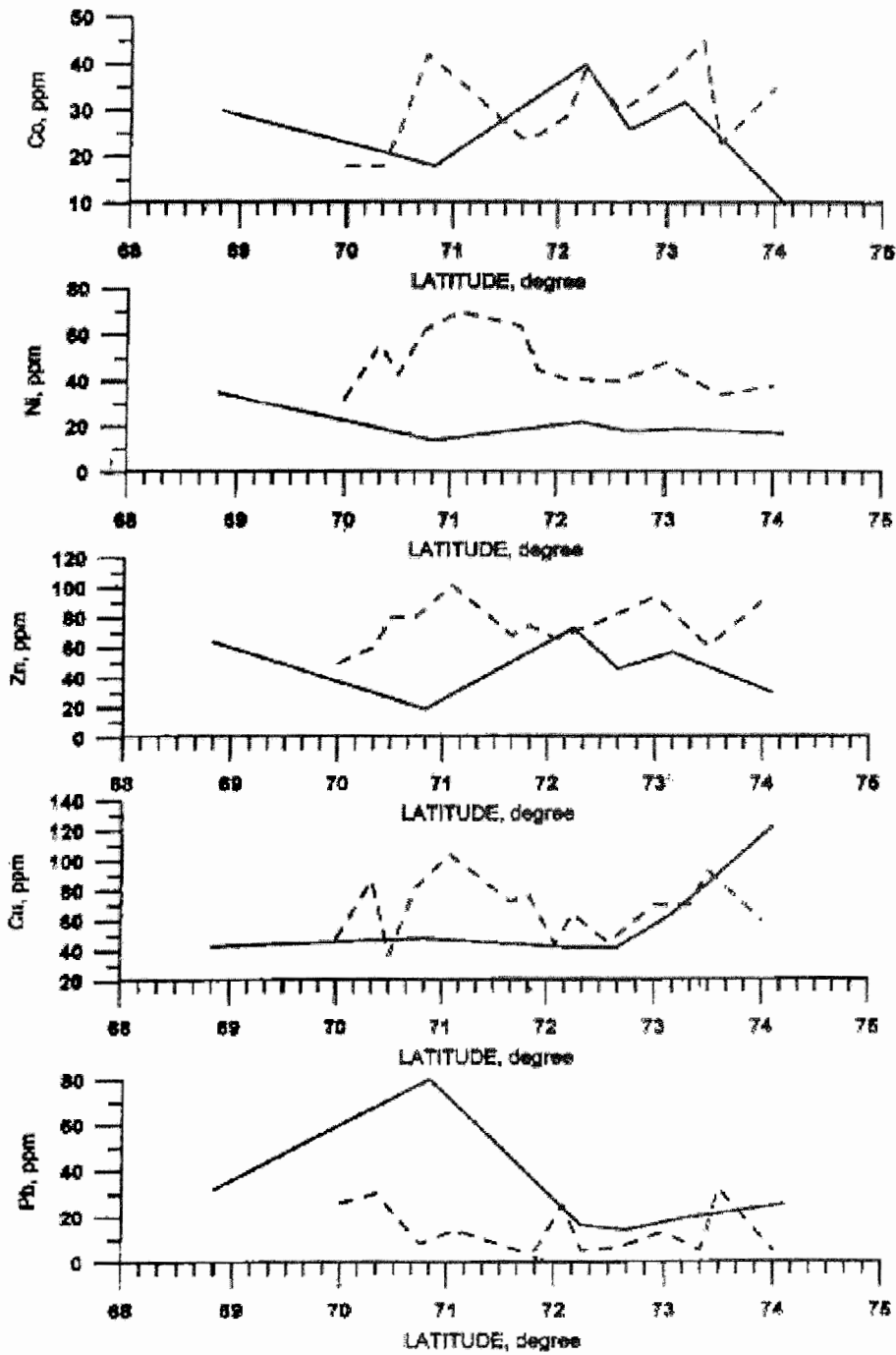


Figure 7.24: Lateral distribution of heavy metals in upper layer of bottom sediments. line: in Ob River; dotted line: in Yenisei River.

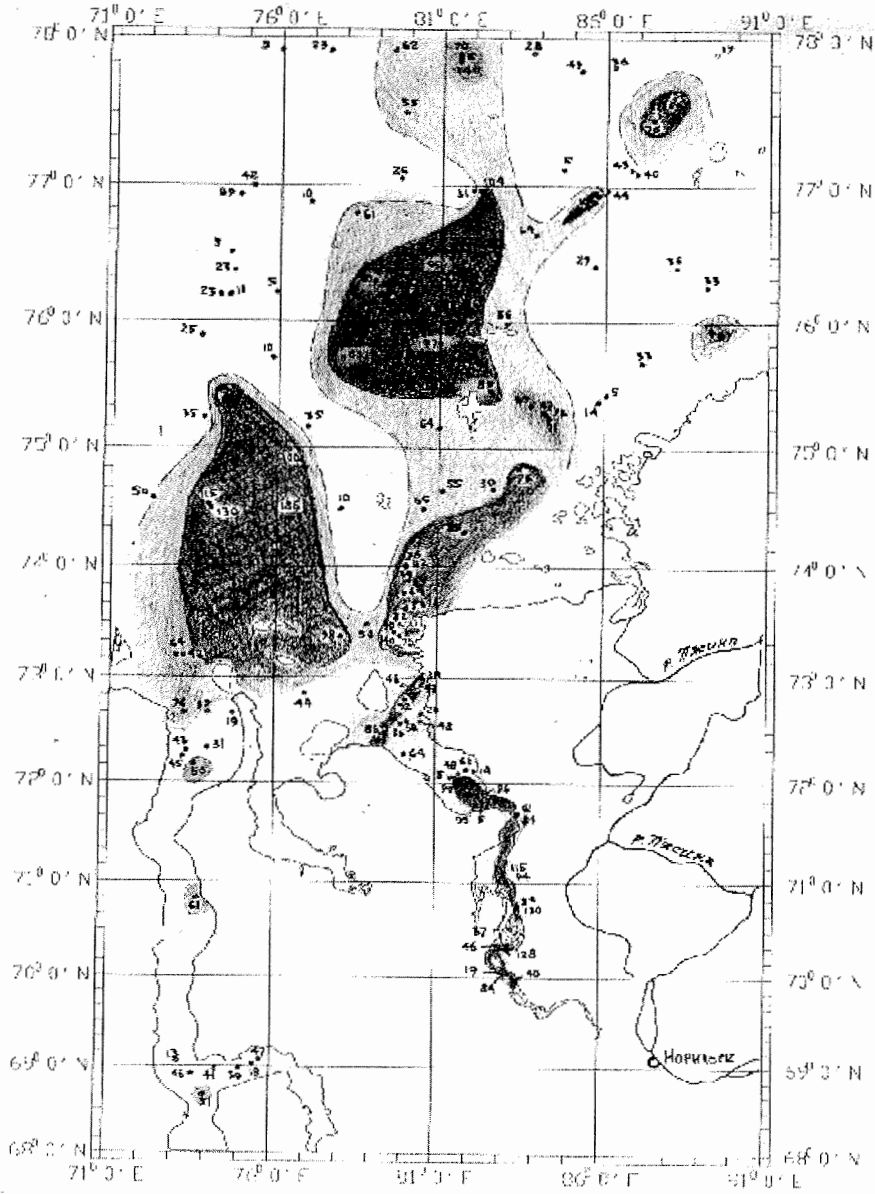
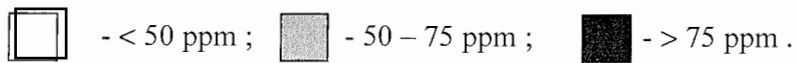


Figure 7.25: Distribution of the Cu in estuaries of the Yenisei and Ob rivers and adjacent area of the Kara Sea.



## 8.1 Studies on plutonium speciation and radionuclide concentrations in the Ob and Yenisey estuaries and the Kara Sea under the EU project ESTABLISH

M. Sickel<sup>1)</sup>, O. Chr. Lind<sup>2)</sup>, S. Gerland<sup>3)</sup>

<sup>1)</sup> Norwegian Radiation Protection Authority (NRPA), Grini Næringspark 13, 1361 Østerås, Norway

<sup>2)</sup> Institute for Soil and Water Sciences, Agricultural University Norway (AUN), Ås, Norway

<sup>3)</sup> Norwegian Radiation Protection Authority, Environmental Protection Unit, Polar Environmental Centre, 9296 Tromsø, Norway

### Background and Aims

The EU Copernicus project ESTABLISH (Estuarine Specific Transport and Biogeochemically Linked Interactions for Selected Heavy metals and radionuclides) focuses on the marine-freshwater interface in the Yenisey Estuary in connection with modelling of the transport of contaminants (heavy metals and radionuclides) from inland to the open sea. This important link received little attention within related studies in the past. However, in order to understand the biogeochemical behaviour and fate of contaminants in Siberian estuarine environments, it is crucial to take this link into account. The three main issues ESTABLISH is dealing with include: (i) Short-term transport processes, conservative and sediment-bound contaminant transport, (ii) Long-term fate of contaminants in sediment deposits, and (iii) Ocean-land interaction and estuarine living resources. ESTABLISH started officially on 1 October 2000, it will last three years. The participating institutions are: The Norwegian Radiation Protection Authority (NRPA, Norway), SPA Typhoon (Russia), the Vernadsky Institute of Geochemistry and Analytical Chemistry (GEOKHI, Russia), the Institute of Oceanography at the University Hamburg (IOH, Germany), the Arctic and Antarctic Research Institute (AARI, Russia) and the Agricultural University of Norway (AUN, Norway).

The main goals in connection with the “Akademik Boris Petrov” cruise in 2001 were collection of samples:

- In the Yenisey to perform process and speciation studies regarding the behaviour of plutonium in the mixing zone
- In the open Kara Sea to have a reference outside the mixing zones
- In the Ob bay to compare the mixing zone processes in the two large Arctic estuaries
- To increase our overall knowledge of levels of radioactive contamination in the Arctic areas

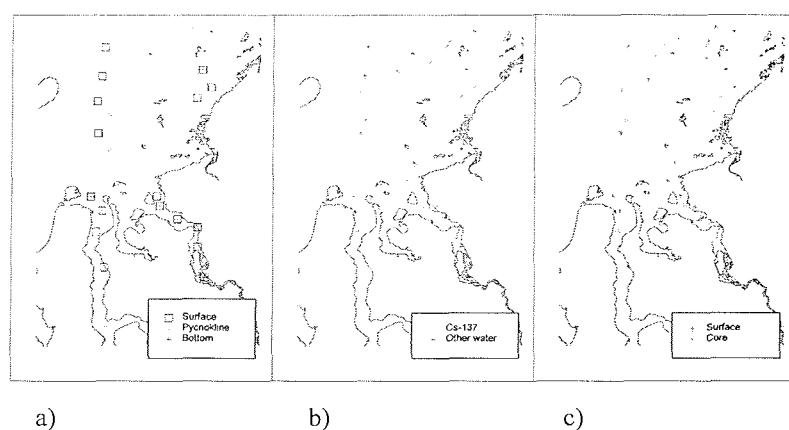
Studies in connection with samples from the “Akademik Boris Petrov” Cruise in 2000 by GEOKHI (Stepanets *et al.* 2001) and others, including the NRPA, were used as background information for the planning of the radioecological work during the cruise in 2001.

### Sampling and treatment of samples

An overview on the amount and locations where water and sediment samples were obtained is given in Fig. 8.1(a-c) and Table 8.1.

Station number	Area	<sup>238, 239+240</sup> Pu	<sup>137</sup> Cs	<sup>90</sup> Sr	<sup>129</sup> I	<sup>99</sup> Tc	Sediment cores	Surface sediments
2 – 21	Yenisey	13	9	4	13	4	7	13
1 and 22 – 64	Kara Sea	15	15	5	15	8	10	14
65 – 83	Ob	15	4	3	7	4	5	3

**Table 8.1:** Samples listed for regions and radionuclides.



**Figure 8.1 (a-c):** Sampling localities for radionuclide measurements a) Plutonium, b) <sup>137</sup>Cs and other water samples, c) Sediment samples.

### Plutonium

Being the main focus of the expedition, a major effort was undertaken to collect plutonium (<sup>238, 239+240</sup>Pu) samples through out the mixing zones in the Yenisey estuary. To get an as complete picture as possible, water samples (200 l each) were collected from the surface, bottom and pycnocline using pumps to collect the surface water and a large-volume water sampler (batomat) for the deeper water. (Tabs. 8.1 & 8.2). Due to the geographically shorter salinity gradient, the high particle load and less time available in the Ob estuary, it was not possible to get a complete supplement in Ob to the samples collected in the Yenisey. In the open Kara Sea, the sampling density was much lower than in the rivers. However, some samples could be collected from the different water bodies in the Kara Sea. To be able to distinguish between the particulate, colloidal and dissolved plutonium (Salbu 2000), the water samples (200 l) were filtrated using a 0.45µm filter and selected samples were ultra filtrated using a 10 kDa tangential flow cassette system (Salbu & Oughton 1994; Mitchell *et al.* 1995). Then, before the alpha counting process, the water samples were reduced in volume by a chemical precipitation procedure and further processing for α-spectrometry (Chen *et*

al. 1991). Following modern radiochemical separation and purification, plutonium and americium activities and isotope ratios will be also determined by means of Inductively Coupled Plasma Mass Spectrometry (ICP-MS), Accelerator Mass Spectrometry (AMS, see e.g. Oughton *et al.* 2000) for certain samples.

#### ***Caesium, technetium and strontium***

As for plutonium measurements, water samples for measurements of  $^{137}\text{Cs}$  (200 – 1000 l),  $^{90}\text{Sr}$  (50 l) and  $^{99}\text{Tc}$  (100 l) were collected using pumps for surface samples and the batomat for the deep-water samples. (Tab. 8.1). Due to time constraints, most of these samples were from surface water (Tab. 8.2). However, we anticipated achieving the largest possible geographical spread of the sampling. Samples collected for analyses of the conservative behaving radionuclide  $^{99}\text{Tc}$  for use in long-range transport studies were not treated. For the measurements of  $^{90}\text{Sr}$  water samples were acidified and a stable strontium carrier solution was added. Samples for  $^{137}\text{Cs}$  (200 l) were collected by pumping water through a particle filter and an adjacent adsorbent system. The sorbents will be ashed and measured using high-purity germanium (HPGe) gamma detectors.

#### ***Sediment samples***

Sediment samples were collected as sub-cores from the large box corer (GKG) for studies of vertical distribution of radionuclides (in total 22 cores), or as surface samples from the grab corer (22 samples) to be used for process studies in the laboratory (Tab. 8.1). Some sediment samples were collected to calculate *in situ*  $K_d$  values. In addition to those, samples were collected for use in process studies and for general monitoring and mapping of levels of radioactive contamination.

#### **Analytical work**

The analytical work is presently in the start-up phase. No samples are analysed yet. Measurements will be undertaken at the laboratories in Norway in Østerås and Tromsø (NRPA), in Ås (AUN), in Canberra (Australia, Australian National University) and at other foreign laboratories. Some first results are planned to be reported during the conference on Arctic and Antarctic Radioecology in St. Petersburg, Russia, in June 2002.

Station	Samples			Surface		Pyknokline depth	Bottom		
	Su	P	B	T	S		T	S	Depth
Yenisey	3	F		4.5	10.2	5	-0.9	32.2	14.5
	4	uf		13.7	0		12.7	0	19
	8	F	uf	14.4	0		14.3	0	27.4
	11	F	uf	13	0	7.4	5.5	22.4	8.4
	16	F		13	0		13	0	27.3
	19	F	uf	9.6	6.1	3.5	-1.1	32.5	24.1
Kara Sea	28	F		1.5	24.5	18.5	-1.1	33.8	50.6
	30	F	F	2.4	27.5	8	-1.4	34.1	46.1
	34		F	1.4	29.2	19.1	-1.4	34.3	90.7
	41	uf		3.4	23.8	10	-1.1	33.9	35
	46	F		4.2	26.4	18	-0.7	34.9	300
	56	F		5.5	22	12	-0.8	34.5	170
	59		F	5.2	21.9	9.5	-1.4	34.5	170
	62	F		4.8	23.3	7	-1.3	34.3	120
Ob	65		uf	5.9	19	15	-1.4	33.7	52
	67	F		7.4	11.2	5.5	-1.4	33.3	41
	68		uf	7.8	9.9	7	-1.2	32.6	21
	70	F	uf	9.2	0.9	7	-0.5	31.1	16
	72	uf		11.4	0		11.5	0	21
	73		uf	12.5	0		12.5	0	10
	80	F		8.6	0.9	8.7	2.9	22.7	11
82	uf	uf	6.7	9.9	6.7	-1.3	32.9	22	

**Table 8.2:** Overview of water samples prepared for plutonium measurements (Su: Surface, P: Pyknokline, B: Bottom, F: Filtered (0.45\_μm), uf: Ultra filtered (10kDa), T: Temperature °C, S: Salinity. Depths in meters).



## 8.2 Biological studies within the "ESTABLISH" project.

T.V. Panteleimonov, V.B. Pogrebov

SSC RF Arctic and Antarctic Research Institute (AARI), St.Petersburg, Russia

### Introduction

One of the main objectives within ESTABLISH project is to examine the uptake of contaminants (mainly of selected metals and radionuclides) to biota in order to assess, at a basic level, the impact of contamination levels on the environmental and man. As reliable indices of environmental impacts of human activities for marine and estuarine ecosystems, changes of benthic community composition, abundance and structure might be taken. The first priority given to bottom dwellers results from the fact that unlike plankton, fishes, sea birds and mammals, the benthos:

- \* is the most stable in time
- \* characterises the local situation in space, and
- \* can represent retrospective changes in the ecosystem (Pogrebov, 1994)

The aim of the studies in the year 2001 was to characterise the structure, species composition, abundance and biomass of benthic fauna within the Yenisei and Ob estuaries and the adjacent areas of the Kara Sea. An additional aim was species sampling (basically bottom fauna and fish) for subsequent analysis for heavy metals and radionuclides in the onshore laboratory.

### Methods and Materials

Macrofauna sampling was conducted by an ocean-grab with a sampling area of 0.25 m<sup>2</sup>. At each station 1-3 replicates were taken. The samples then washed over a sieve with a mesh size of 1 mm. The samples were fixed in 4 % borax buffered formalin. Meiofauna were taken from the grab or the box corer of the upper 4 cm layer of sediments by a tube sampler (20 cm<sup>2</sup> in area). Only one replicate was taken at each station. Each sample were labelled and fixed separately by a 40% neutralised formaline (up to 3-4% concentration of formalin in water). For the analysis of heavy metals and radionuclides in animals' tissues the bottom dwellers were collected from dredge samples and fish were bought in local settlements. All materials for the contaminant analysis were frozen and stored in a refrigerator until further investigations.

### Collected materials

During the cruise the bottom fauna of 34 stations was investigated. 13 stations were located in the Yenisei estuary, 16 stations in the Kara Sea and 5 stations in the Ob estuary. A total of 70 quantitative macrobenthos samples and 17 meiobenthos samples were collected (Tab. 5.5). For the contaminants analysis following species of animals were chosen: the fish *Coregonus muksun*, the isopoda *Saduria entomon* and *Saduria sabini*, the bivalves' *Tridonta borealis* and *Portlandia arctica*.

### Preliminary results

The macrobenthos samples were presorted aboard. The following groups of organisms dominate in the macrobenthos communities of the study area: polychaetes, crustaceans, bivalves, echinoderms and sipunculids.

In the Ob and Yenisei estuaries compositions of the bottom fauna were similar. Euryhaline forms as *Saduria entomon*, *Pontoporeia affinis* and *Portlandia aestuariorum* were most abundant in the estuarine zones of both rivers. At the southern station of the Yenisei (BP01-08) macrobenthos was absent in our samples. At the stations BP01-04-06, BP01-17 (Yenisei) the various species of chironomides, typical for fresh water, were observed. At the fresh water stations in the Ob (BP01-73, BP01-77) chironomides and fresh water bivalves compose the benthic community. Seaward, with increasing salinity of the bottom water amount of polychaetes increase and species *Saduria entomon* was exchanged by *Saduria sibirica* and *Saduria sabini*. In the estuarine areas species diversity, abundance and biomass increase with increasing of salinity of the bottom water.

At the majority of stations located in the open Kara Sea with a salinity of 33-34 the bivalves' *Tridonta borealis*, *Macoma calcarea* and *Portlandia arctica*, the polychaetes *Pectinaria hyperborea* and *Spiochaetopterus typicus* and the sipunculid *Phascolion strombi* were most abundant. The amount of brittle stars and holoturians increase with increasing depth of the stations.

The macrobenthos communities of the study area can be divided into three groups: (1) communities with dominating of the freshwater species, (2) communities of estuaries with dominating of the euryhaline organisms and (3) communities with marine fauna. Salinity of bottom waters governs the distribution of the benthos communities within the study area. The lowest biodiversity and abundance values are characteristic for the oligohaline parts of estuaries, whereas the highest ones for full-salinity marine biotopes. For understanding the influence on benthos of other environmental factors further investigations is needed.

### 8.3 Terrestrial investigations in the Lower Yenisei during the 36 voyage of the RV «Akademik Boris Petrov». Preliminary results.

E.M. Korobova<sup>1</sup>, N.G. Ukraintseva<sup>2</sup>, V.V. Surkov<sup>2</sup>, V.G. Linnik<sup>1</sup>

<sup>1</sup>Vernadsky Institute of Geochemistry and Analytical Chemistry, Russian Academy of Sciences

<sup>2</sup>Moscow State University;

#### Introduction

The main objective of the terrestrial study was to investigate distribution and migration of the ecologically significant elements in geochemically related landscapes of the Lower Yenisei. Landscape studies have been the first performed in the area simultaneously with the detailed Yenisei river and Kara Sea investigations carried out by the Vernadsky Institute since 1995. The work was an integral part of complex studies within the INCO project ESTABLISH “Estuarine Specific Transport And Biogeochemically Linked Interactions for Selected Heavy metals and radionuclides”. The aquatic part of the project was carried out on board by other scientists from the Vernadsky Institute, the Norwegian Radiation Protection Agency, Agricultural University of Norway, and SPA TYPHOON.

Unlike Yamal Peninsula the Yenisei estuary remains outside the impact zone the aerial masses moving from the European industrial areas. (Shaw, 1988). However there are regional sources of the Yenisei basin contamination including chemical, mining, oil-chemical, pharmaceutical, metallurgical, pulp and paper industries (GOSKOMEKOLOGIA, Annual State Report, 1997). The Krasnoyarsk Mining and Chemical Combine (KMCC), concern “Noril’sky Nickel”, the town of Tura noted for the gas-reprocessing industry are most significant for the Lower Yenisei area. Several investigations revealed considerable local contamination of the Yenisei flood plain soils and sediments by artificial radionuclides downstream KMCC as far as 2000 km (Kusnetsov et al. 2000, Kvasnikova et al. 2000).

Noril’sk industry releases annually 35,4 t of dust containing copper, nickel, sulfates, cobalt, lead, vanadium, nitrogen oxides, arsenic, antimony, phenols that are concentrating in the top layers of the peat soils on biogeochemical and sorption barriers. The established radius of the Noril’sk Combine impact zone extends up to 100 km km (Ford et al. 2000). According to wind rose the impact of the Noril’sk industry should be more significant for the estuary in winter period. The concentration of lead, copper and zinc in snow cover is 3-5 times higher in the lower reaches of the Yenisei river compared to the Yamal Peninsula and 10-15 times greater than that in Canadian Arctic (Solomatin et al. 1989).

Accounting of high interest to global ecology dynamics and vulnerable areas of the Arctic basin in particular the a study of trace element and radionuclide distribution in the regions difficult to access and subjected to global and possibly regional contamination seems to be an interesting and reasonable idea.

## Methods

Pre-selection of the study sites has been carried out on the basis of the landscape and soil maps (Soil Map of the USSR, 1988, Scale 1:2500 000; Landscape map, 1988, Scale 1:4000000) and space images helpfully provided by NUPI. Field selection of the plots was limited to the general executive plan of water and sediment sampling in the Yenisei estuary and the current weather conditions providing safe landing of the terrestrial group.

To characterize the contrasting conditions of trace element migration and deposition within the area the elaborated study sites were located in the main sections of the Yenisei estuary (the delta zone, the Yenisei Inlet and the Yenisei Bay). Every site was characterized by a landscape cross-section of the flood plain and the adjacent watershed area. On-site field work included leveling, a detailed description of geomorphological features, the soil and vegetation cover along the cross-section to evaluate the landscape structure and the flooding scenarios; determination of the permafrost table depth significant for water migration in the tundra landscapes. Altitude of the leveling points was referred to the current Yenisei water level that was 120-145 cm above the "zero" level of hydrological gauge station in set. Karaul and the standard sea level (Baltic system).

Soil depth profiles structure and texture were described in detail and sampled at elaborated plots with different conditions of the river deposition and atmospheric pollution. Flood plain profiles were sampled continuously with sampling increment ranging 2 to 10 cm to the depth of ground water or permafrost table or to 50-70 cm in case of their absence. Watershed profiles were sampled with due regard to the genetic soil horizons. Vegetation was characterized by description of the species composition and abundance and accompanied by herbarium collection. Sampling of the 1-3 m<sup>2</sup> plots located over the soil profiles was performed to calculate phytomass, to analyse dominating species for chemical elements. Every bulk vegetation sample has been separated into main agrobiological groups and species and weighted air dried to determine the phytomass structure. Soil samples were air dried and dried at 105 °C.

Surface and ground water samples were taken at selected points of the cross-section to characterize water migration parameters. Standard water parameters have been measured on-board. The radiation background has been determined along cross-sections with the help of a field scintillation detector. Several samples of fish, bird, berries and mushrooms were collected to determine chemical elements in local diet.

## First results

The studied landscape cross-sections characterize the Yenisei flood plain and the adjacent watershed area typical for the southern and typical tundra of the Taimyr Peninsula. The length of cross-sections varied from 500 to 880 m, relative altitude of watershed plots over the Yenisei low stage ranged from 26,8 m at the northern cross-section (Cape Shaitansky) to 60 m at the southern profile (set. Karaul) (Fig.8.2).



Table 8.3. Location of the landscape cross-sections

Landscape cross-sections	Sampling plots indices	Geographical coordinates	
		Latitude, N	Longitude, E
Yenisei Bay Cape Shaitansky  Typical tundra subzone	SK 1_0	72°04' 547	82°21' 408
	SK 1_6	72°04' 559	82°21' 444
	SK 1_10	72°04' 573	82°21' 490
	SK 1_15	72°04' 608	82°21' 595
	SK 1_25	72°04' 824	82°21' 650
	SAR 1	72°03' 408	82°25' 962
Yenisei Inlet Set. Vorontsovo	VR 1_16	71°43' 076	83°31' 301
	VR 1_14	71°43' 031	83°31' 039
	VR 1_8	71°42' 981	83°30' 504
	VR 1_6*	71°42' 889	83°30' 470
	VR 1_11a*	71°43' 016	83°30' 768
Yenisei delta zone Island Koroviy (Tysyara) Southern tundra subzone	TS 1_1a	70°32' 359	83°23' 336
	TS 1_4	nd*	nd
	TS 1_8	nd	nd
	TS 1_10	nd	nd
	TS 1_11	nd	nd
	TS 1_12*	nd	nd
	TS 1_12a*	nd	nd
	TS 2_7	nd	nd
Yenisei delta zone Right-coast flood plain Set. Karaul	KR 1_12	70°04' 394	83°10' 025
	KR 1_15	70°04' 408	83°10' 105
	KR 1_15a	70°04' 409	83°10' 116
	KR 1_25	70°04' 465	83°10' 432
	KR 2_0a	70°04' 551	83°10' 855
	KR 2_0	70°04' 551	83°10' 855
	KR 2_3	70°04' 546	83°10' 742
	KR 2_5	70°04' 521	83°10' 615

\*not determined

### Weather conditions and permafrost level

Fortunately, the weather conditions on the sampling dates were unusually favorable as registered on board the RV "Academic Boris Petrov" (Tab. 8.4). Air pressure was almost stable, air temperature varied from +5 to +19°C, wind velocity did not exceed 8-9 m/s during daylight hours. Wind direction changed from NE to SE not typical for the season and helped to study the right side of the river most suitable for landing.

Table 8.4: Weather conditions during sampling activity.

Date, m/d/y	Time, h/min	Cloudiness	Wind direction, compass degrees	Wind velocity m/s	Air pressure, mm of mercury	Air temperature, °C
08.17.01	04.00	clear		<3	761	10
08.17.01	08.00	clear		<3	761	13
08.17.01	12.00	clear		<3	762	16
08.17.01	16.00	clear		<3	763	15
08.17.01	20.00	clear		<3	763	11
08.17.01	24.00	clear	100	3	763	11
08.18.01	04.00	clear	25	10	764	8
08.18.01	08.00	clear	160	8	764	8
08.18.01	12.00	clear	90	9	764	8
08.18.01	16.00	overcast	50	8	764	11
08.18.01	20.00	overcast	20	9	764	10
08.18.01	24.00	clear	60	9	764	10
08.19.01	04.00	clear	55	6	765	4
08.19.01	08.00	clear	100	5	766	9
08.19.01	12.00	clear	90	5	767	9
08.19.01	16.00	clear	90	9	767	10
08.19.01	20.00	clear	90	8	767	5
08.19.01	24.00	clear	70	8	767	6
08.20.01	04.00	overcast	80	12	764	6
08.20.01	08.00	clear		<3	764	14
08.20.01	12.00	clear	80	10	764	19
08.20.01	16.00	overcast	60	6	763	16
08.20.01	20.00	clear	60	6	763	12
08.20.01	24.00	clear	90	18	762	12

The depth of permafrost in elaborated points is shown in Table 8.5. At some locations the ground thawed through to river bed alluvium while on watersheds the active layer thickness at some points did not exceed 40 cm despite a rather warm weather conditions.

Table 8.5: Depth of the permafrost table on the date of sampling at selected points of the landscape cross-section

Nature zone	Site Index	Landscape	Number of measurements	Thickness of active layer, cm
Southern tundra	KR	Hill tops and slopes, moss tundra	5	51,6±9,18
Southern tundra	KR	Hill tops and slopes, lichen and grasses communities	5	77±13,51
Southern tundra	TS	Flood plain, moss communities	5	62,6±11,45
Southern tundra	TS	Flood plain, grasses communities	8	No permafrost down to 180-200 cm, rarely 140 cm
Typical tundra	SK	Hill tops and slopes, moss tundra	11	43±12,2
Typical tundra	SK	Hill tops and slopes, lichen and grasses communities	12	86±18,2
Typical tundra	VR	Flood plain, moss communities	5	49,2±11,45
Typical tundra	VR	Flood plain, grasses communities	5	107 ±24,25 (5), or no permafrost down to 180-200 cm

As can be seen from the direct measurements at some plots the air temperature on top of the moss layer is 2-5 degrees higher than that at its bottom (Tab. 8.6). This supports the idea that moss layer plays a considerable buffering role in tundra landscapes isolating soil from heating in summer. Therefore on thick mossy areas seasonal thawing is shallower compared to thin ones or those without moss cover. This can be followed in both watershed and flood plain conditions. There is a clear tendency in decrease of the active layer from the southern tundra to the typical one.

Table 8.6: Air temperature above and below the moss layer

Index	Date	Time	Air, °C	Landscape	°C, moss top	°C, moss bottom	Moss height, cm	Moss species
KR_2_5	17.08.01	9-00	14	Hill top, herb-undershrub-lichen-moss tundra	15,2	11,3	4	Dicranum elongatum
KR_2_3	17.08.01	12-00	16	Eastern slope, grass-undershrub-moss tundra with shrubs	22,6	18,8	2,5	Dicranum elongatum
KR_2_0	17.08.01	15-00	15	Eastern slope, lake shore, high shrub(willow) tundra	15,4	13	4	Hylocomium splendens
SK_1_13	18.08.01	18-00	10	Western slope, grass-undershrub-moss tundra with shrubs	10,8	7	3,5	Hylocomium splendens
VR_1_8	19.08.01	16-45	10	Flood plain, ridge top, shrub(willow)-moss communities	12,5	7,8	5,5	Hylocomium splendens
VR_1_8	19.08.01	17-25	8	Flood plain, ridge top, shrub(willow)-moss communities	10,8	5,8	5,5	Hylocomium splendens



### A brief landscape description of the main geomorphological elevation levels

Reconnaissance of the areas in the landscape cross-section vicinity allowed find out characteristic landscape features of different geomorphological elements in the Yenisei flood plain.

The basement of the flood plain within the study area is formed of the channel alluvium facies presented by coarse and medium-grain gray and yellowish-brown sands outcropping on wide beaches with flat or slightly rolling relief typical for the coastal zones and island periphery. The thickness of the loamy and peat deposits covering alluvial sands at the back of the flood plain varies from 20 to 80 cm. At the northern cross-section (Cape Shaitansky) the coastal beach consisted of boulder-gravel -shingle sediments filled with coarse sand.

The lowest level flood plain studied on the islands and the Yenisei coast is up to 500-600 m wide; its elevation above the low water level varies from 0 to 0.5-1.5 m. Low flood plain often consists of the former sandy islands now attached to the coast, it has flat relief and is almost bare, especially along the shoreline where sandy beach surface acquire peculiar rolling wavy-striped microrelief. River sediments are sandy to the depth of available boring (down to 2 m). Pioneer vegetation presented by thin *Arctophylla* meadows and sparse specimens of horsetail and grasses rise up to 1.3-1.5 m above the mean river water level in the river delta and to 1.8-2.m in the estuary. No permafrost has been observed there.

The coastal part of the flood plain is usually the highest (up to 6 m on the studied plots) and vary in width from 30-50 m to 1500 m on big islands. It is well drained that is typical for accumulative type of the rivers. The area has rolling relief with pronounced ridges and is formed of medium-grain and fine sand with weakly developed primitive and laminated soils where gley conditions are found only in the bottom horizons. Vegetation consists of mainly shrubbery (willow and alder stands) and of relatively "dry" meadows with predominance of grasses and herbs. Permafrost lies here at the depth of 80-150 cm.

Back sides of the coastal flood plain and the central parts of the islands present medium-level Yenisei flood plain that is flat and 0.5-1.5 m lower compared to the coastal part. The elevation marks range from 3,5 to 4-4.5 m above the low water level. Sandy deposits are overlain by silt and loamy cover 20-40 cm to 1-1,5 m thick. Peat interbeds in peat-gley loamy soils locally reach 0.5 m. Permafrost 40-60 cm deep promotes swamping processes. At the lowest back side usually abundant in hollows and depressions with elevation marks equal to 2.5 - 3.0 m above the low water level wet meadows are replaced by marshes and marshy shrubbery. The main area exhibit different landscape features in the southern and typical tundra subzones. In southern tundra medium level surfaces are covered by willow and alder shrub thickets 2-2.5 m high with herbaceous-leguminous-grassy and grass meadows (e.g. set. Karaul). Fig. 8.3 shows a flood plain part of the landscape cross-section investigated in the Yenisei delta zone close to settlement Karaul. Due to considerable range in altitude of the flood plain and watershed parts it was not possible to show in details the whole cross-section. Complex landscape description of the sampling points within this cross-section is given in Table 8.7.

Table 8.7: Field description of the sampling points along the Karaul landscape cross-section

KR 1_12	Flood plain, flat ridge herb-tussock meadow (VCP+70-80%) with willow shrubs (H=30 cm, VCP=5-10%) with spots of bare silt deposits m in diameter occupying 10% of the area. Alluvial soddy laminated (interbedding of sandy and loamy layers).
KR 1_15	Flood plain, flat inter-ridge depression, moist cotton-grass-sedges meadow (H=40 cm, VCP=80-90%) with willow undergrowth (H=50 cm, VCP=10-20%). Alluvial peat-gley silty loam soil.
KR 1_15a	Flood plain, a round lake with marshy coast. Lake silt.
KR 1_26	Flood plain, grass-horsetail high-shrub (willow) communities (H= m, VCP=80%) on the edge of the high-level flood plain. Soddy-gley loamy soil with buried humus horizon.
KR 2_0a	Watershed area. Gravel-shingle beach of the lake.
KR 2_0	Watershed area. Coastal part of the lake at the foot of eastern slope (5-8 grad) 5 m from the the water level, mounded surface, alder(20%)-willow(80%) thicket , high-shrub(willow) tundra m high, VCP=80-90%), grass-horsetail and green moss-horsetail-grass cover. Humus-peat soil on sandy and loamy eluvium.
KR 2_3	Watershed area. Gently convex slope (3-5 grad), hillock-mounding micro-relief on 50% of the area, elevation variation - 10 cm, grass-undershrub-dwarf birch lichen-moss tundra (H=5-10%, VCP=70%) with solitary willow bushes (,7-1,3 m). Peat-gley loamy soil.
KR 2_5	Watershed area. Flat area on the convex hill top, micro-polygonal (1x1.5 m) herb-undershrub-lichen-moss (H=15-40 cm, VCP=70%) tundra with solitary spots 0.5 m in diameter and thick dwarf birch in fissures. Peaty illuvial-humus loamy soil.

In typical tundra the same level is marshy and covered by wet meadows, moss-sedge swamps and grassy or grass-moss willow shrubs not higher than 0.6-1.0 m. Leguminous species are almost absent. Succulent species may reflect the influence of marine environment releasing salts and bringing them to land with air.

Adjacent watershed areas rise 20 to 70 m above the Yenisei flood plain. They are abundant in lake depressions and crossed by medium-wide (1-1.5 km) trough-like valleys of the Yenisei tributaries (rivers Gal'chikha, Yakovleva, etc.). Elevation amplitude (between the ridge tops and local lake and river bottoms) reaches 20-40 m. Watershed landscapes near set. Vorontsovo and Karaul are formed on clay and detritus eluvium of the terrestrial bed rocks while near Cape Shaitansky the studied site is located in the zone of marine loamy deposits.

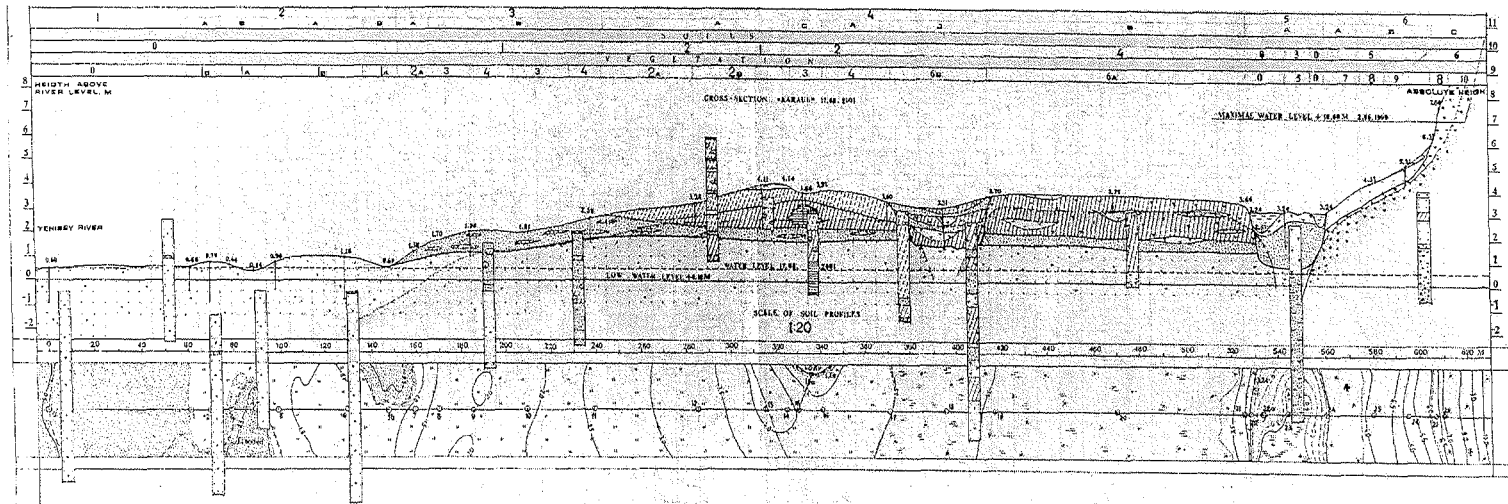


Fig.8.3: Vertical scheme and topographic plan of the landscape cross-section near set. Karaul (flood plain part). Made by V. V. Surkov.

**Landscapes:** 1 - Spits, middle-channel islands, coast-attached islands formed of medium- and small-sized sands locally covered by thin warp, rolling and flat barren soils; 2 - Low shoreline and island flood plain: A -ridges and elevations , primitive and laminated gley sandy soils overgrown by thin *Arctophylla* meadows; B - inter-ridge depressions overgrown by *Arctophylla* meadows; 3 - Middle and high-level shoreline and island flood plain composed of sands; A - ridges and levees with primitive soils covered by pioneer herbs; B - flat surfaces under horsetail-herbaceous-grassy and wet sedge-horsetail-grassy (cotton-grass-sedge-grassy) meadows with solitary willow shoots; 4 - Middle and high-level shoreline and island flood plain composed of loamy and peat deposits: A - ridges and elevations with primitive soils covered by pioneer grasses, horsetail and willow species; B - flat surfaces with bogged moss-cotton-grass-sedge willow shrubs; C - depressions and weakly pronounced inter-ridge depressions with meadow gley soils under wet sedge-cotton-grass-horsetail-grassy meadows; D - depressions under wet and marshy grass-horsetail-mossy willow scrubs; 5 - Ox-bow depressions and former river channels composed of sands; 6 - Deluvial slopes at the back of the flood plain: A - covered by tall shrubs of alder and willow with moss-herbaceous-sedge meadows on gley soils; B - with herbaceous-grassy meadows and shrubs on gley sandy soils; C- steep and gentle slopes, bumpy covered by alder thickets with willow and dwarf birch.

**Lithology:** litter peat fine sand small-grain sand medium-grain sand loamy sand sandy loam loam clay  
 detritus of parent rock shingle permafrost table  
 isohypse

### Soil moisture

Due to low rate of organic decomposition the tundra soils are enriched in plant debris noted for high water-holding capacity. Therefore variation in moisture capacity of soil horizons should be carefully accounted of in water migration and volumetric calculations of chemical element inventories.

Table 8.8 shows the results of moisture determination in soil samples of the Karaul cross-section that distinctly confirms higher humidity of the organic-bearing layers. Different temperature of drying and uneven distribution of organic debris in soil samples can lead in some samples to considerable discrepancy in moisture determination by means of standard soil beaks at 105°C and in air-dried larger samples 0.5-1.5 kg by weight (Tab. 8.8). This proves the necessity to take more replicates while measuring this parameter.

Table 8.8: Moisture in soil samples of the Karaul cross-section.

Sampling plot	Soil horizon symbol texture	Depth interval cm	Water content, % (sample volume - 90 cm <sup>3</sup> ), dried at 105°C	Water content, % (sample volume 400-900 cm <sup>3</sup> ), air dried
KR 2-5	A <sub>0</sub> Moss	0 2	-	106,6
	A <sub>t</sub> Peat	2 6	149,1	177,5
	A1Bg Peat-loam	6 18	27,7	48,7
	Big loam	20 30	28,9	46,9
	Big loam	30 40	26,3	41,5
	G (Bg)loam	50 55	54,2	73,9
KR 2-0	At Peat, sand	0 6	16,3	147,0
	G (Bg) Peat, sand	6 10	71,0	101,7
	BCg loamy sand	10 27	18,6	46,2
	Dg Loam	27 37	21,4	18,6
	Dg Loam	37 47	23,1	-
KR 2-3	A <sub>0</sub> Moss	0 6	60,6	191,1
	A <sub>t</sub> Peat	6 14	149,0	153,1
	A1Bg Peat-loam	14 24	128,9	128,9
	BCg loam	24 34	27,3	64,1
	BCg loam	34 42	27,2	-
KR 1-12	Sandy loam	3 10	25,0	-
	Silty sand	16 21	10,2	-
	Sandy loam	24 29	29,6	-
KR 1-15a	Silt	0 5	81,2	-
KR 1-15	Peaty loam	1 5	48,0	43,4
	Sandy clay	25 30	27,0	27,9
	Sandy clay	47 53	32,4	29,3

Moisture loss in 100 peat and soil samples dried at 105°C ranged from 5 to 280% with median value equal to 32,8%. Humidity of peat layers varied from 74 to 280%, the sandy ones – from 5 to 26%, silty and clay horizons produced intermediate values.

Field determination of pH and red-ox parameters of the surface and ground waters sampled along cross-section are presented in Table 8.9. Water samples have been stored

in flasks at the temperature of sampling. pH has been first roughly estimated by handheld pH-meter in situ. Other parameters were obtained next day of sampling in the on-board laboratory.

Table 8.9:

Study site	Plot	Sample	pH	Eh, mV	Alkalinity, meq l
Cape Shaitansky	SK1-7	Lake on landslide	9.00	+455	nd
	SK1-6	Lake on landslide	9.12	+410	12.0
	SK1-25	Ground water	7.60	+480	0.6
Set. Vorontsovo	VR-0	Yenisei	8.12	+370	1.2
	VR1-6	Ground water	6.40	+320	1.7
	VR1-11	Ox-bow lake	6.07	+420	0.7
	VR1-14	Ground water	6.75	+470	1.0
Tsyara Island	VR1-16	Ground water	7.20	+435	2.8
	TS1-8	Ground water	7.08	+450	5.8
	TS1-11	Stagnant water	7.10	+435	-
Set. Karaul	TS1-12	Ox-bow lake	8.12	+440	4.8
	KR1-15	Ox-bow lake	7.75	+470	1.5
	KR2-5	Ground water	-	-	1.1
	KR2-3	Ground water	6.20	+440	3.1
	KR2-3	Thawed water (permafrost)	8.20	+440	1.8

pH values measured in water in situ were approximately 0.5 units higher as compared to the laboratory data despite the undertaken sample preservation measures. Compared to other water samples a small lake formed on the land slip had considerably higher pH value and detectable salinity (1.3 promille) due to outcropping marine sediments.

Phytomass of the studied watershed plots is composed mainly of lichens and mosses varied from 500 to 750 g/m<sup>2</sup> irrespective of subzone. Lichens, mosses and their debris make up approximately 55-60% of the growing stock (Fig. 8.4.). In slope landscapes having similar structure phytomass increases to 900g/m<sup>2</sup>.

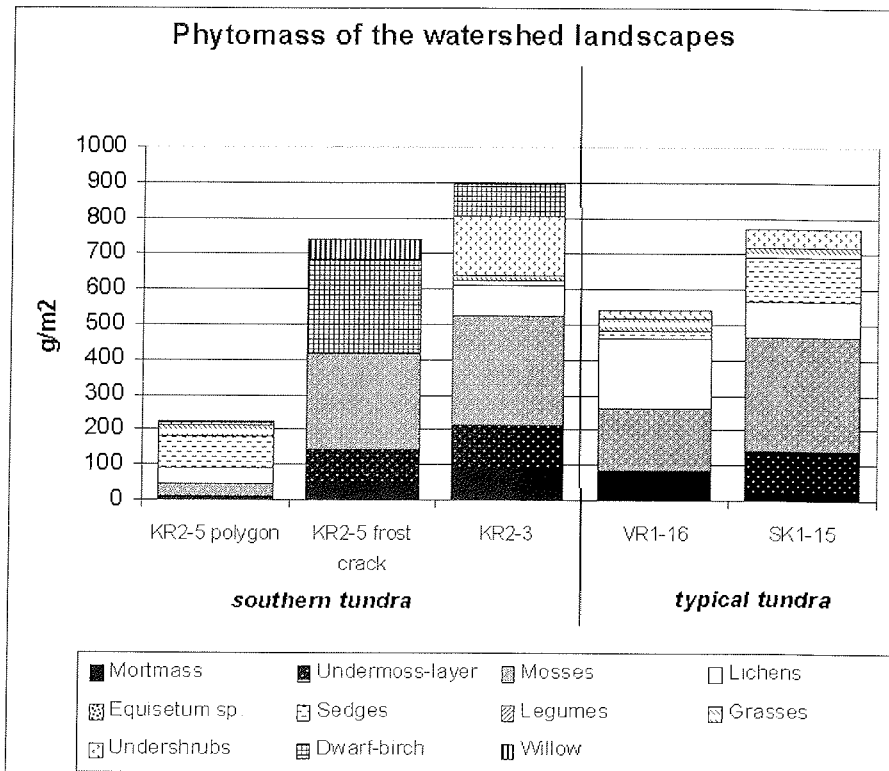


Fig. 8.4: Estimation of the overground phytomass parameters on the studied plots of watershed landscapes (DW)

Flood plain landscapes are characterized by predominance of herbaceous plants such as sedges, grasses and horsetails, locally legumes (Fig. 8.5). According to our earlier investigations on the Yamal Peninsular (1997-2000) in tall shrub thickets typical for swampy depressions the share of willow and alder in total phytomass can reach 70-80% (Ukrainseva et al., 2000).

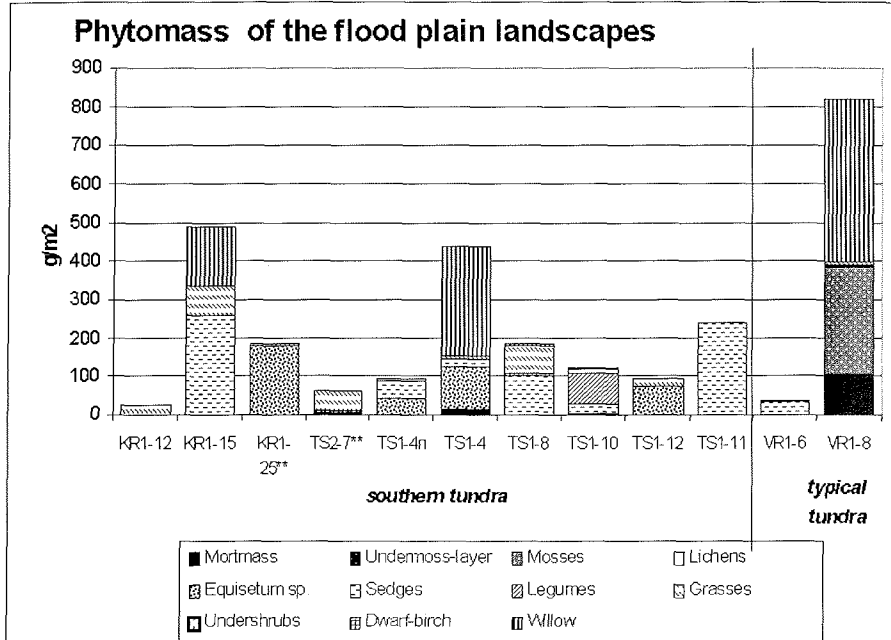


Fig. 8.5: Estimation of the overground phytomass parameters on the studied plots of flood plain landscapes (DW)

Density of the growing stock of the plots studied in the southern tundra subzone of the Yenisei delta ranged from 20 to 190 g/m<sup>2</sup> (100 on the average) for the grassy communities; approximated 400-500 g/m<sup>2</sup> in short willow thickets, and reached maximum values in tall scrub thickets that considerably exceeded phytomass of the watershed areas. In typical tundra subzone investigated in the Yenisy estuary the overground phytomass ranged from 36 to 820 g/m<sup>2</sup>. Maximum values correspond to the areas overgrown by shrubs presented mainly by willow surviving in both tundra subzones.

Concentration of trace elements in selected soil samples is presented in Table 8.10. A brief overview gives evidence of slightly enhanced content of Cu and Pb in the watershed soils compared to those on the flood plain part presumably due to the industry activity since the studied slope is windward facing Noril'sk.

Table 8.10. Concentration of chemical elements in soil samples (XRF determination performed by E.M. Sizov)

Number	Soil profile	Depth, cm	Sample type	Mn	Cu	Zn	Pb	Cr	Ni	Co	V	Ba
1.	KR 1 15	1 5	Peaty loam	0,13	0,0044	0,0041	<0,0010	0,0109	0,0028	0,0019	0,0125	0,064
2.		25_30	Peaty sandy loam	0,09	0,0109	0,0066	<0,0010	0,0087	0,0032	0,0016	0,0116	0,080
3.		47_53	Loam	0,10	0,0090	0,0059	<0,0010	0,0091	0,0039	0,0021	0,0127	0,089
4.	KR 1 15a	0 5	Silt	0,05	0,0050	0,0055	<0,0010	0,0088	0,0022	0,0015	0,0112	0,102
5.	KR 2 5	2 6	Peat	0,08	0,0100	0,0101	0,0075	0,0131	0,0034	0,0017	0,0131	0,091
6.		6 18	Loam	0,08	0,0048	0,0042	<0,0010	0,0120	0,0031	0,0021	0,0133	0,103
7.		30 40	Loam	0,11	0,0042	0,0029	0,0013	0,0092	0,0028	0,0028	0,0128	0,126
8.		50_56	Loam	0,10	0,0031	0,0042	<0,0010	0,0117	0,0028	0,0025	0,0144	0,125
9.	KR 2 0	0 6	Sandy peat	0,03	0,0090	0,0033	0,0070	0,0060	0,0023	0,0013	0,0108	0,081
10.		10 25	Loam	0,08	0,0023	0,0031		0,0099	0,0021	0,0025	0,0127	0,084
11.	KR 2 0a	0 5	Silt	0,06	0,0069	0,0045	<0,0010	0,0146	0,0043	0,0018	0,0127	0,074



## Conclusion

During the 36<sup>th</sup> voyage of the RV "Akademik Boris Petrov" within the INCO project ESTABLISH the first terrestrial studies have been performed in the three main sections of the Lower Yenisei. Landscape cross-sections established at four sites located in the Yenisei delta, estuary and its inlet characterize geomorphology, soil and vegetation cover of the flood plain and the adjacent watershed areas. Every cross-section included leveling, soil boring to determine the depth of permafrost table, a detailed description of soil and vegetation cover, as well as water, soil and plant sampling at the selected plots.

Subzonal differentiation has been revealed in landscape structure of the studied flood plain plots. Southern tundra is characterized by a predominance of tall shrub thickets and herbaceous-leguminous-graminea meadows on soddy sandy and loamy and humic-gley soils. In typical tundra the middle level flood plain is more waterlogged, the Yenisei middle flood plain is covered by wet meadows on humic-peat and peat soils and abundant in moss-sedge swamps and short (up to 1 m) grassy willow scrubs devoid of alder admixture. No structural difference has been found in watershed plots with tundra gley soils.

Overground phytomass of the watershed plots ranged on the average from 500 to 750 g/m<sup>2</sup> DM irrespective to the tundra subzone, with 55-60% share of mosses and lichens. On the slopes the total mass of the growing stock increased to 900 g/m<sup>2</sup> without significant changes in its structure.

Due to low temperature the tundra soils have peculiar water migration pattern depending upon dynamic active layer. Slow plant debris decomposition leads to interbedding of mineral and organic layers. Measurements of soil moisture confirmed considerable input of peat-bearing layers in soil water-holding capacity (up to 280%). Another peculiar feature confirmed during field studies is considerable alkalinity and mineralization of landslide soils due to outcrop of the frozen parent marine sediments. Moss layer play a buffering role in tundra landscape preventing soil from heating in summer both on watershed and flood plain areas. Thickness of active layer drops northward from southern to typical tundra.

Preliminary analysis of the heavy metal measurement in selected soil samples has not revealed ecologically significant contamination. Future chemical analysis of the whole set of samples for trace elements and radionuclides, soil properties is believed to allow to obtain patterns of distribution and migration of the ecologically significant elements in geochemically related landscapes of the Lower Yenisei.

## Acknowledgements

Authors express their deep gratitude to Dr. Stepanets, the head of the expedition, the Captain and the crew of RV "Academic Boris Petrov" for assistance in organizing the terrestrial work. We are indebted to Dr. V. Barchukov and navigator A. Moiseev for their help in the field work and sampling, to E. Sizov for XRF analysis and A. Borisov for gamma-spectrometry of the selected soil samples on board. We appreciate valuable advice and aid granted by Dr. L.Kodina, L.Vlasova, V. Tokarev, and G. Soloviova in the on-board sample processing

## 9. References

- Aargard, K., 1994. Contamination of the Arctic. Ocean Processes. Arctic Research of the U.S., 8: 21-33.
- AMAP Assessment Report: Arctic Pollution Issues. Radioactivity. By: Per Dtrand, Michel Balonov, Asker Aarkrog et al, Oslo, 1998.
- Amon, R. M. W. and Benner, R., 1996. Photochemical and microbial consumption of dissolved organic carbon and dissolved oxygen in the Amazon River system. *Geochimica et Cosmochimica Acta* 60: 1783-1792.
- Atterberg, A., 1912. Die mechanische Bodenanalyse und die Klassifikation der Böden Mittelschwedens. *Int. Mitt. f. Bodenkunde*. pp. 314.
- Azam, F., Fenchel, T., Field, J. G., Gray, J. S., Meyer-Reil, L. A., and Thingstad, F., 1983. The ecological role of water-column microbes in the sea. *Marine Ecology Progress Series* 10: 257-263.
- Balashov, Yu.A., 1976. Geochemistry of rare-earth elements. M.: Nauka, 266 p. (in Russian)
- Balesdent J.C., Girardin C., and Mariotti A., 1993. Site-related  $\delta^{13}\text{C}$  of tree leaves and soil
- Beeskov, B. and Rachold, V., submitted. Geochemical processes in the Yenisei River/Estuary system. In: Stein R. Fahl K. Fütterer. DK. Galimov EM (eds): Sierian River Run-Off in the Kara Sea: Characterisation. Quantification. Variability. and Environmental Significance. Proceedings in marine systems.
- Belyaeva A.N. and Eglinton G., 1997. Lipid biomarkers accumulation in the Kara Sea sediments. *Okeanologiya*, 37, 5, pp.705-714.
- Best, I.A. and Gunn, D.E., 1999. Calibration of marine sediment core loggers for quantitative acoustic impedance studies. *Marine Geology*, 160, 137-146.
- Bogacheva M.P., Kodina L.A., and Ljutsarev S.V., 2001. Particulate organic carbon in river and sea waters: Concentration and stable isotope ratio. *Ber. Polarforsch.*, B.393, S.161-164.
- Breitzke, M., 2000. Acoustic and elastic characterization of marine sediments by analysis, modeling, and inversion of ultrasonic P wave transmission seismograms. Union. Washington, DC, United States. 1996. *Journal of Geophysical Research, B, Solid Earth and Planets*. 105; 9, Pages 21, 411-21, 430. 2000. American Geophysical Union. Washington, DC, United States. 2000.
- Breitzke, M. Grobe, H. Kuhn, G., and Mueller, P., 1996. Full waveform ultrasonic transmission seismograms; a fast new method for the determination of physical and sedimentological parameters of marine sediment cores. *Journal of Geophysical Research, B, Solid Earth and Planets*. 101; 10, Pages 22,123-22,141. 1996. American Geophysical Union. Washington, DC, United States, 1996.
- Burenkov, V.I. and Vasilkov, A.P., 1994. Influence of River Discharge on Spatial Distribution of Hydrological Characteristics in the Kara Sea. *Okeanologiya*, 34, 5, pp.652-661.
- Burkovsky, IV, Udalov, AA, and Stoljarov, AP, 1997 The importance of juveniles structuring a littoral macrobenthic community. *Hydrobiologia* 355:1-9.
- Butman, CA, 1987 Larval settlement of soft - sediment invertebrates: the spatial scales of pattern explained by active habitat selection and emerging role of hydrodynamical processes. *Oceanogr Mar Biol A Rev* 25:113-165.
- Chen, Q.J., Aarkrog, A., Nielsen, S.P., Dahlgaard, H., Nies, H., Yu Yixuan and Mandrup, K., 1991: Determination of plutonium in environmental samples by controlled valence in anion exchange. Denmark, Risø National Laboratory RISØ-M-2856, 17 pages.
- Churkin, M., Soleimani, G., Carter, C., and Robinson, R., 1981. Geology of the Soviet Arctic: Kola Peninsula to Lena River. In: Nairn, A.E.M., Churkin, M., and Stehli, F.G. (eds.): *The Arctic Ocean*. New York (Plenum Press), 5, 331-375.
- Churun, V., and Ivanov, B., 1998. Investigations of the hydrophysical structure in the mixing zone between fresh and saline waters in the Ob and Yenisei estuaries. *Ber. Polarforsch.*, B.266, S.11-18.
- Dickens, B., and Brown, W.E., 1970. The crystal structure of calcium carbonate hexahydrate at  $-120^{\circ}\text{C}$ . *Inorganic Chemistry*. v.9. pp.480-486.

- Dittmers, K., Stein, R., and Steinke, T., 2001. Core logging: Magnetic susceptibility. *Ber.Polarforsch.*, B. 393, pp. 89-91.
- Dubinina, A.V., and Rozanov, A.G., 2001. Geochemistry of rare-earth elements and thorium in the Atlantic Ocean sediments and manganese nodules. *Lithology and mineral resources*, N 3: 311-323 (in Russian).
- Dunaev, N.N., Levitan, M.A., and Kutsov, V.M., 1995. Physical properties of the Late Quaternary sediments of the Kara Sea shelf area with relation to environmental conditions of sedimentation. *Okeanologiya*, 35, 6, pp. 916-923.
- Emiliani, C., 1955. Pleistocene temperatures. *Journal of Geology* 63, 538-578.
- Erlenkeuser, H., Spielhagen, R.F., and Taldenkova, E., 1999. Stable isotopes in modern water and bivalve samples from the southern Kara Sea. The Kara Sea Expedition of RV "Akademik Boris Petrov" 1997: First results of a joint Russian-German pilot study. *Berichte zur Polarforschung* 300: 80-90.
- Evans, C.A., O'Reilly, J.E., 1987. A handbook for the measurement of chlorophylla in netplankton and nanoplankton. *BIOMASS Handbook* 9, 1-14
- Fahl, K., and Stein, R., 1999. Biomarkers as organic- carbon- source and environmental indicators in the Late Quaternary Arctic Ocean: problems and perspectives. *Mar. Chem.*, 63, pp. 393-309.
- Fernandes, M.B., Sicre, M.-A., 2000. The importance of terrestrial organic carbon inputs on Kara Sea shelves as revealed by n-alkanes, OC and  $\delta^{13}\text{C}$  values. *Org. Geochem.*, 31, pp. 363-374.
- Fetzer, I., 2001. Distribution of meroplankton and juveniles along a transect in the eastern Kara Sea in: Stein R, Stephanets O (eds) The German-Russian project on Siberian river run-off (SIRRO): Scientific cruise report of the Kara Sea expedition 'SIRRO 2000' of RV 'Akademik Boris Petrov' and first results. *Ber Polarforsch.* 393, 68-71
- Fetzer, I., and Arndt, C., 1999. The distribution of zooplankton in the Kara Sea. In Stein, R. and Stepanets, O.V. (eds.), Scientific cruise report of the joint Russian-German Kara Sea expedition of RV "Akademik Boris Petrov" in 1999. *Ber. Polarforsch.*, 360: 37-45.
- Fetzer, I. and Hirche, H.-J., (in press). The influence of freshwater discharge on the distribution of zooplankton in the southern Kara Sea. *Polar Biology*.
- Fogel, M.L., Cifuentes, L.A., 1993. Isotope Fractionation during Primary Production In: *Organic Geochemistry. Principles and Applications*. M.H. Engel, Macko S.A. (Eds). Plenum Press, N.-Y., pp.73-98.
- Fomin, O.K., 1989. Some characteristic structures of the zooplankton ('Nekatorije strukturnije kharakteristiki zooplanktona') in: Matishov GG (ed) The ecology and bioresources of the Kara Sea ('Ekologiya i Bioresurci Karskovo Moria'). Murmansk Marine Biological Institute, Akademia Nauk SSSR, Apatiti, Russia, pp 65-85.
- Ford, J., Lacorsa, B.K., Monettift, and M., Vlasova, T., 2000. Contaminant landscapes of Arctic Alaska and Siberia. «Arctic Workshop 2000», INSTAAR, Boulder, CO USA, p.71.
- Gaillardet, J., Dupre, B., Louvat, P., and Allegre, C.J., 1999. Global silicate weathering and CO<sub>2</sub> consumption rates deduced from the chemistry of large rivers. *Chemical Geology*, v. 159, pp.3-30.
- Galimov, E.M., Laverov, N.P., Stepanets, O.V., and Kodina L.A., 1996. Preliminary results of ecological and geochemical investigations of the Russian Arctic Seas (Data obtained from Cruise 22 of R/V "Akademik Boris Petrov"). *Geokhimiya*, 7, pp. 579-597.
- Geodekyan, A.A., Levitan, M.A., and Shelekhova, E.S., 1997. Sorption potential of the Barents and Kara Seas sediments. *Repts. Russian Acad. Sci.*, 355(3): 361-364 (in Russian).
- Gloersen, P., Campbell, W.J.; and Cavalleri, D.J., 1992. Arctic and Antarctic sea ice, 1978 - 1987: satellite passive-microwave observations and analysis. Washington, D.C. NASA.
- Gordeev, V.V., 2000. River input of water, sediment, and major ions, nutrients and trace metals from Russian territory to the Arctic Ocean. In: Lewis E.L. et al.(eds). *The Freshwater Budget of the Arctic Ocean*. Kluwer Academic Publishers. Dordrecht.Boston.London. P. 297-321.

- Gribanov, V.A., Ivanov, B.V., Stanovoy, V.V., and Churun, V.N., 1999. Micro- and mesoscale oscillations of the thermohaline characteristics on the coastal zone in the vicinity of the Yenisey Gulf). *Berichte zur Polarforschung*, vol.300, p.27-34.
- Gribanov, V.A., Dmitrenko, I.A., and Stanovoy, V.V., 1997. Hydrophysical processes governing mesoscale variability of oceanographic characteristics in the coastal zone of the Kara and Laptev Seas. The Proc. of the Russian-Norwegian Workshop-95 "Nature conditions of the Kara and Barents Seas" (eds. V.Volkov et al.) Rapportserie No 97, Norsk Polarinstitut, Oslo, p. 118-120.
- Grossman, E.L. and Ku, T.-L., 1986. Oxygen and carbon isotope fractionation in biogenic aragonite: Temperature effects. *Chemical Geology (Isotope Geoscience Section)* 59: 59-74.
- Gurevich, V.I., 1995. Recent sedimentogenesis and environment on the Arctic shelf of Western Eurasia. *Norsk Polarinst. Medd.*, 131: 92 pp.
- Gurvich, E.G., Isaeva, A.B., Demina, L.V., Levitan, M.A., and Muraviov, K.G., 1994. Chemical composition of bottom sediments from the Kara Sea and estuaries of Ob and Yenisei rivers. *Oceanology*, N 5: 766-775 (in Russian).
- Gurvich, E.G., Lukashin, V.N., Lisitzin, A.P., and Kurinov, A.D., 1980. Rare-earth elements and itrium. In: Ronov, A.B. (Ed.). *Geochemistry of elements-hydrolisates*. M.: Nauka, p. 71-116 (in Russian).
- Halsband, C., and Hirche, H.-J., 1999. The role of Mesozooplankton for the transformation of organic matter in: Matthiessen J, Stephanets OV, Stein R, Fütterer DK, Galimov EM (eds) *The Kara Sea Expedition of RV 'Akademik Boris Petrov' 1997: First Results of a joint Russian-German Pilot Study*. *Ber Polarforschung* 300:45-50.
- Hargrave, B.T., von Bodungen, B., Stoffyn-Egli, P., and Mudie, P.J., 1993. Seasonal variability in particle sedimentation under permanent ice cover in the Arctic Ocean. *Ocean. Cont. Shelf Res.*, 14: 279-293.
- Hebbeln, D. and Wefer, G., 1991. Effects of ice coverage and ice-rafted material on sedimentation in the Fram Strait. *Nature*, 350: 409-411.
- Hedges J.I., Clark W.A., and Cowie G.L. 1988. Organic matter sources to the water column and surficial sediments of a marine bay. *Limnol. Oceanogr.* 33, 5, pp. 1116-1136.
- Hedges, J.I., and Mann, D.C., 1979. The characterization of plant tissues by their lignin oxidation products. *Geochim. Cosmochim. Acta*, 43, pp. 1803-1807.
- Hedges, J.I. and Oades, J.M., 1997. Comparative organic geochemistries of soils and marine sediments. *Organic Geochem.*, v.27, N7/8, pp. 319-361.
- Hedges, J., Keil, R., and Benner, R., 1997. What happens to terrestrial organic matter in the ocean? *Org. Geochem.* 27, 195-212.
- Hofmann, A., 1999. Kurzfristige Klimaschwankungen im Scotiameer und Ergebnisse zur Kalbungsgeschichte der Antarktis während der letzten 200 000 Jahre, *Ber. Polarforschg.*, 345, pp. 162 .
- Honjo, S., 1996. Fluxes of particles to the interior of the open oceans. In: V. Ittekkot, P. Schäfer, S. Honjo and P.J. Depetris (Editors), *Particle Flux in the Ocean*. SCOPE, Wiley and Sons, Chichester, pp. 91-154.
- Huang, Y., Freeman, K.H., Eglinton, T.I., and Street-Perrott, F.A., 1999.  $\delta^{13}\text{C}$  analysis of individual lignin phenols in Quaternary lake sediments: A novel proxy for deciphering past terrestrial vegetation changes. *Geology*, May 1999, v.27, N 5, pp.471-474.
- Hubberten, H.-W., Grobe, H., Jokat, W., Melles, M., Niessen, F., and Stein, R., 1995: *Glacial History of East Greenland Explored*.- EOS, Transactions, American Geophysical Union, 76 (36): 353-356
- Isachenko, A.G., Editor-in-chief. *Landscape map of the USSR*. Scale 1:4000000. 1988.
- Ittekkot, V., 1996. Particle flux in the ocean: Introduction. In: V. Ittekkot, P. Schäfer, S. Honjo and P.J. Depetris (Editors), *Particle Flux in the Ocean*. SCOPE, Wiley and Sons, Chichester, pp. 1-6.
- Kaplan, M.E., 1978. Calcite pseudomorphs from the Jurassic and Lower Cretaceous deposits of Northern East Siberia. *Geologiya and Greofyzyka*, 12, pp. 62-70 (in Russian).

- Kirchman, D.L., 1993. Leucine incorporation as a measure of biomass production by heterotrophic bacteria. In P. F. Kemp, B. Sherr, E. Sherr and J. J. Cole (eds.), *Handbook of Methods in Aquatic Microbial Ecology*. Lewis Publishers, Boca Raton, FL, pp. 509-513
- Kirchman, D.L., and Ducklow, H.W., 1993. Estimating conversion factors for the thymidine and Leucine methods for Measuring Bacterial Production. In P. F. Kemp, B. Sherr, E. Sherr and J. J. Cole [eds.], *Handbook of Methods in Aquatic Microbial Ecology*. Lewis Publishers, Boca Raton, FL, pp. 513-517.
- Kodina, L.A., 2001. The carbon isotope composition of phytoplankton along the Ob-Kara Sea transect in August-September 1999. *Ber.Polarforsch.*, 393, pp. 157-160.
- Kodina, L.A., Bogacheva, M.P., Vlasova, L.N., Meschanov, S.L., and Ljutsarev, S.V., 1999. Isotope geochemistry of particulate organic carbon in the Yenisei estuary: sources and regularities of distribution. *Ber. Polarforsch.*, 300, pp. 91-101.
- Kodina, L.A., Ljutsarev, S.V., and Bogacheva, M.P., 2000. Sources of sedimentary material of drifting ice in the Arctic Basin on evidence from the organic carbon isotope composition of the ice particulate material. *Doklady Rossiyskoy Akademii Nauk*, 371, 4, pp. 511-515.
- Kodina, L.A., Tokarev, V.G., Vlasova, L.N., and Pribylova, T.N., 2001. Karbonate minerals ikaite and glendonite and carbonate nodules in Holocene Kara Sea sediments. *Berichte zur Polarforsch.*, 393; pp. 189-196.
- Kodina, L.A., Tokarev, V.G., Vlasova, L.N., Pribylova, T.N., 2001. Carbonate minerals and clayey-carbonate nodules in the Holocene Kara Sea sediments: Geochemical and isotopic evidences. *Ber.Polarforsch.*, 393, pp. 189-197.
- Kodina, L.A., Tokarev, V.G., Vlasova, L.N., Pribylova, T.N., and Shpigun, L.K., 1998. Geochemistry of organic matter and other elements of the carbon cycle in the southern Kara Sea and estuarine zone (Ob, Yenisey). *Ber. Polarforsch.*, 266, pp. 54-62.
- Köhler, H., and Simstich, J., 2001. Distribution of surface-water salinity. *Ber.Polarforsch.*, 393, pp. 15 -17.
- Kolesov, G.M., 1994. Determination of minor elements: neutron-activation analysis in geochemistry and cosmochemistry. *J.of Analyt. Chem.*, 49(1): 56-66 (in Russian).
- Korobeinik, G.S., Tokarev, V.G., and Vaisman, T.I., 2001. Methane and other hydrocarbons in sediment cores along the Yenisei - Kara Sea Profile. *Ber. Polarforsch.*, 393; pp. 185-188.
- Krasnyuk, A.D., and Vanshtein, B.G., 1999. Heavy metals in bottom sediments from the estuaries of the rivers Ob and Yenisei. *Ber. Polarforsch.*, 300, pp. 188-195.
- Kuhn, G., 1995. Sedimentphysikalische Untersuchungen. In: R. Gersonde (ed.): *Die Expedition ANTARKTIS-XI/2 mit FS "Polarstern" 1993/1994*, *Ber. Polarforsch.*, 163, 66-74.
- Kulikov, N.N., 1961. Sedimentation in the Kara Sea. In: *Modern sediments of the seas and oceans*. M.: Nauka, p. 437-447 (in Russian).
- Kuznetsov, Yu., V., Legin, V.K., and Strukov V.N., 2000. Transuranic elements in the Yenisei river flood plain deposits. *Radiokhimiya*, 42, 5, pp. 470-477.
- Lajtha, K. and Michener, R.H., 1994. *Stable isotopes in ecology and environmental science*. Blackwell Scientific Publications.
- Larionov, V.V., Makarevich, P.R., 2001. The taxonomic and ecological description of the phytoplankton assemblages from the Yenisei Bay and adjacent waters of the Kara Sea in September 2000. *Ber. Polarforsch.*, 393, pp.48-62.
- Larsen, D., 1994. Origin and paleoenvironmental significance of calcite pseudomorphs after ikaite in the Oligocene Creede Formation, Colorado. *J. Sedimentary Research, Section A*, v.64, N 3, pp.593-603.
- Levitan, M.A., 2001. Facies variability of surface sediments along the Yenisey transect based on grain-size composition, heavy and light mineral data. *Ber. Polarforsch.*, 2001, 393: pp. 92-106.
- Levitan, M.A., Bourtman, M.V., Gorbunova, Z.N., and Gurvich, E.G., 1998. Quartz and feldspars in the surface layer of the Kara Sea bottom sediments. *Lithology and mineral resources*, 2, pp. 115-125 (in Russian).

- Levitan, M.A., Dekov, V.M., Gorbunova, Z.N., Gurvich, E.G., Muyakshin, S.I., Nürnberg, D., Pavlidis, M.A., Ruskova, N.P., Shelekhova, E.S., Vasilkov, A.P., and Wahsner, M., 1996. The Kara Sea: A reflection of modern environment in grain size, mineralogy and chemical composition of the surface layer of bottom sediments. *Ber. Polarforsch.*, 212: 58-81.
- Lightfoot, P.C., Naldrett, A.J., Gorbachev, N.S., Doherty, W., and Fedorenko, V.A., 1990. Geochemistry of the Siberian Trap of the Noril'sk area. USSR. with implications for the relative contributions of crust and mantle to flood basalt magmatism. *Contrib to Mineral Petrol* 104. 631-644.
- Lisitsyn, A.P., 1995. The marginal filter of the ocean. *Oceanology (engl. transl.)*, 34(5): 671-682.
- Lukashin, V.N., Ljutsarev, S.V., Krasnyuk, A.D., Shevchenko, V.P., and Rusakov, V.Yu., 1999. Suspended particulate material in the Ob and Yenisei estuaries. In: Matthiessen J. Stepanets O. Stein R. Fütterer DK. Galimov E (eds): *The Kara Sea Expedition of RV "Akademik Boris Petrov" 1997: First results of a Joint Russian-German Pilot Study*. *Ber Polarforsch* 300. 155-178.
- Makkaveev, P.N., 1994. Dissolved inorganic carbon in waters of the Kara Sea, Ob and Yenisey estuaries. *Okeanologiya*, 34, 5, pp. 668-672.
- Manskaya, S.M. and Kodina, L.A., 1975. Geochemistry of lignin. *Nauka, M.*, pp. 228 (in Russian).
- Marcus, N. H., 1996. Ecological and evolutionary significance of resting eggs in marine copepods: Past, present, and future studies. *DIAPAUSE IN THE CRUSTACEA*, *Hydrobiologia* 320 (1-3): 141-152.
- Marland, G., 1975. The stability of CaCO<sub>3</sub> 6H<sub>2</sub>O (ikaite). *Geochim.Cosmochim. Acta*, v.39, pp. 83-91.
- Matthiessen, J. and Boucsein, B., 1999. Palynomorphs in surface water of the Ob and Yenisei estuaries: Organic-walled tracers for riverine water. *Ber. Polarforsch.*, 300, pp. 71-78.
- Milliman, J.D., Fitznar, H.P., and Kattner, G., 2000. Biogeochemical characteristics of dissolved and particulate organic matter in Russian rivers entering the Arctic Ocean. *Geochimica et Cosmochimica Acta*, 64: 2973-2983.
- Mitchell, P.I., Batlle, J.V.I., Downes, A.B., Condren, O.M., Vintro, L.L. and Sanches-Cabeza J.A., 1995. Recent observation on the physico-chemical speciation of plutonium in the Irish Sea and the western Mediterranean. *Appl. Rad. Isot.*, 46, 1175-1190.
- Mopper, K. and D.J., Kieber, 2000. Marine photochemistry and its impact on carbon cycling. In S. De Mora, S. Demers and M. Vernet (eds.): *The effects of UV radiation in the marine environment*. Cambridge University Press, pp. 101-129.
- Niessen, F., Ebel, T., Kopsch, C., and Fedorov, G.B., 1999. High-resolution seismic stratigraphy of lake sediments on the Taymyr Peninsula, Central Siberia. In: Kassens, H., H.A. Bauch, I. Dmitrenko, H. Eicken, H.-W. Hubberten, M. Melles, J. Thiede and L. Timokhov (eds.), *Land-Ocean Systems in the Siberian Arctic: Dynamics and History*. Springer-Verlag, Berlin, pp. 437-456.
- Nowaczyk, N., 1991. Hochauflösende Magnetostratigraphie spätquartärer Sedimente arktischer Meeresgebiete. *Ber. Polarforsch.*, 78, pp. 187
- Obernosterer, I., Reitner, B., and Herndl, G.J., 1999. Contrasting effects of solar radiation on dissolved organic matter and its bioavailability to marine bacterioplankton. *Limnology and Oceanography* 44, 1645-1654.
- On the state of environment in the Russian Federation in 1997. The State Report of GOSKOMEKOLOGIA in 1997. Section 2. Surface and underground waters. Sea waters. (Internet version).
- O'Neil, J.R., Clayton, R.N., and Mayeda, T.K., 1969. Oxygen isotope fractionation in divalent metal carbonates. *The Journal of Chemical Physics* 51(12), 5547-5558.
- Opsahl, K., Benner, R., and Amon G.R., 1999. Major flux of terrigenous dissolved organic matter through the Arctic Ocean. *Limnol. Oceanogr.*, 44, pp. 2017-2023.

- Oughton, D.H., Fifield, K.L., Day, J.P., Cresswell, R.C., Skipperud, L., Di Tada, M., Salbu, B., Strand, P., Drozcho, E. and Mokrov, Yu., 2000. Plutonium from Mayak: Measurement of Isotope ratios and activities using Accelerator Mass Spectrometry Environ. Sci. Technol., 34, 1938-1945.
- Pavlov, V. K. and Pfirman, S. L., 1995. Hydrographic structure and variability of the Kara Sea: Implications for pollutant distribution. Deep-Sea Res. II, 42(6): 1369-1390.
- Pavlov, V.K., L.A. Timokhov, G.A. Baskakov, M.Yu. Kulakov, V.K. Kurazhov, P.V. Pavlov, S.V. Pivovarov and V.V. Stanovoy, 1996. Hydrometeorological regime of the Kara, Laptev and East-Siberian Seas. Technical Memorandum APL-UW TM 1-96: 179.
- Peresyupkin, V.I., 1990. Method of lignin determination in sediments. Okeanologiya, v.3, N 4, pp.678-681 (in Russian).
- Piepenburg D, and von Juterzenka, K., 1994. Abundance, biomass and spatial distribution pattern of brittle stars (Echinodermata: Ophiuroidea) on the Kobeinsey Ridge north of Iceland. Polar Biol 14:185-194.
- Pirrung, M., 2000. Physical properties of the sediments. - In: W. Jokat (ed.), The expedition ARKTIS-XV/2 of RV "Polarstern" 1999, Ber. Polarforsch. (einger.).
- Pogrebov, V.B., 1994. Biological evaluation of the environment quality in the course of Arctic offshore development. Development of Russian Arctic Offshore. Helsinki: JUSTNV-PAINO OY AJACTOS AB. P. 328-331.
- Rachold, V., and Hubberten, H.-W., 1999. Carbon isotope composition of particulate organic material in East Siberian Rivers. In Land-Ocean Systems in the Siberian Arctic. Dynamics and History. Kassens H., Bauch H.A., Dmitrenko I.A., Eicken H., Hubberten H.-W., Melles M., Thiede J., Timokhov L.A.(Eds). Springer, B.-Heidelberg, p.223-238.
- Romankevich, E.A., and Vetrov, A.A., 2001. Carbon cycle in the Russian Arctic Seas. M.: Nauka, 302 p. (in Russian).
- Salbu, B. and Oughton, D.H., 1994. Analytical strategies for the determination of physico-chemical forms of trace elements in natural waters. Trace Elements in Natural Waters (ed. B.Salbu & E. Steinnes), CRC Press, 41-69.
- Salbu, B., 2000. Speciation of Radionuclides in the Environment, R.A. Meyers Ed., Encycl. Anal. Chem. John Wiley & Sons Ltd, Chichester, 12993-13016.
- Sarkanen, K.V., Ludwig, C.H., 1971. Lignins: Occurrence, formation, structure and reactions. Wiley-Interscience, N.-Y.-L.-Sydney-Toronto, 915 p.
- Schell, D.M., and Ziemann, P.J., 1989. Natural carbon isotope tracers in Arctic aquatic food webs. In: Rundel P.W., Ehleringer J.R., Nagy K.A. (Eds). Stable isotopes in ecological research. SpringerVerlag, N.-Y., pp.231-250.
- Scheltema, R.S., 1986. On dispersal of planktonic larvae of benthic invertebrates: an eclectic overview and summary of problems. Bull Mar Sci 39:290-322.
- Schooster, F., and Stein, R., 1999. Major and minor elements in surface sediments of Ob and Yenisei estuaries and the adjacent Kara Sea. Ber. Polarforsch., 300: 196-207.
- Schooster, F and Beeskov B., 2001. Major and minor elements in suspended matter and sediments from the Yenisei River and the southern Kara Sea. In: Stein R. and Stepanets OV (eds): The German-Russian Project on Siberian River Run-Off (SIRRO): Scientific Cruise Report of the Kara-Sea Expedition "SIRRO 2000" of RV "Akademik Boris Petrov" and first results. Ber Polarforsch 393. 220-226.
- Schooster, F., Behrends, M., Müller, C., Stein, R., and Wahsner, M., 2000. Modern river discharge and pathways of supplied material in the Eurasian Arctic Ocean: Evidence from mineral assemblages and major and minor element distribution. In: Stein R (ed): Circum Arctic river discharge and its geological record. Int J Earth Sciences, 89, 486-495.
- Schubert C.J., Nürnberg, D., Scheele, N., Pauer, F., and Kriewis M., 1997.  $^{13}\text{C}$  isotope depletion in ikaite crystals: evidence for methane release from the Siberian shelves? Geo-Marine Letters, 17, pp. 169-174.
- Schubert, C.J., and Stein, R., 1997. Lipid distribution in surface sediments from the eastern central Arctic Ocean. Mar.Geol., 138, pp. 11-25.

- Shackleton, N.J., 1974. Attainment of isotopic equilibrium between ocean water and the benthonic foraminifera genus *Uvigerina*: Isotopic changes in the ocean during the last glacial. *Colloques Internationaux du C.N.R.S.* 219: 203-209.
- Shaw, G.E., 1988. Chemical air mass systems in Alaska. *Atmospheric Environment*, 22, 10, pp. 2239-2248.
- Simstich, J., 2001. Is water from the rosette sampler a suitable proxy for bottom water? - Comparison of salinity in rosette and multicorer. *Berichte zur Polarforschung - Reports on Polar Research. The German-Russian project on Siberian River Run-off (SIRRO): Scientific Cruise Report of the Kara Sea Expedition "SIRRO 2000" of RV "Akademik Boris Petrov" and first results* 393: 18-20.
- Sizov, E., Stepanets, O., Komarevsky, and V., Roschina, I., 2001. The identification of chemical elements in bottom sediments using X-ray fluorescence analysis. *Ber. Polarforsch.*, 393, 213-216
- Soil map of the USSR. Institute for Soil Science. 1988. Scale 1:2500000.
- Solomatina, V.I., Evseev, A.V., Korzun, A.V., and Kuznetsova, A.V., 1989. Geochemistry of the atmospheric precipitation, the surface waters and underground ice in Arctic landscapes. Moscow, VINITI, 590.
- Stein, R., 2001. Lithostratigraphy of gravity cores and correlation with sediment echograph profiles ("Akademik Boris Petrov" Kara Sea expeditions 1999 and 2000). *Ber. Polarforsch.*, 393, pp. 120-140.
- Stein, R., Niessen, F., Stepanets, O.V. and the SIRRO Scientific Party (submitted Polar Research): Siberian River Run-Off and Late Quaternary Glaciation in the Southern Kara Sea: First implications from the "Boris Petrov" Expedition 2001.
- Stein, R., and Stepanets, O., 2001. The German-Russian Project on Siberian River Run-off (SIRRO). Scientific Cruise Report of the Kara-Sea Expedition "SIRRO 2000" of RV "Akademik Boris Petrov" and first results. *Ber. Polarforsch.*, 393, pp. 287.
- Stepanets, O., Borisov, A., Komarevsky, V., Ligaev, A., Sisov, E., and Solovjeva, G., 2001. Radioecological research in the Yenisei and Ob rivers and adjacent Kara Sea shelf. in: *Reports on Polar and Marine Research 393* (edited by R. Stein & O. Stepanets: The German-Russian Project on Siberian River Run-Off (SIRRO): Scientific Cruise Report of the Kara Sea Expedition "SIRRO 2000" of RV "Akademik Boris Petrov" and First Results), 197-204.
- Stephantsev, L.A. and Shmelkov, B.S., 2001. Some peculiarities of the hydrological structure on a meridional section Kara Sea-Yenisei Estuary-Yenisei River. *Ber. Polarforsch.*, 393, pp. 6-14.
- Suck, I., 2001. The role of zooplankton for the turn-over of organic matter in the Kara Sea-First results and basic facts. In Stein, R. and Stepanets, O.V. (eds.), *The German-Russian project on Siberian river run-off (SIRRO): Scientific cruise report of the Kara Sea expedition "SIRRO 2000" of RV "Akademik Boris Petrov" and first results*. *Ber. Polarforsch.*, 393: 63-67.
- Suess E., Balzer W., Hesse, K.-F., Müller, P.J., Unger, C.A., Wefer, G., 1982. Calcium carbonate hexahydrate from organic-rich sediments of the Antarctic shelf: precursors of glendonites. *Sci.*, 216, 4550, pp. 1128-1130.
- Sukhoruk, V.I. and Tokarev, V.G., 2000. Sea water hydrochemistry and nutrients.// *Reports on Polar Res.*, 2000, 360, pp. 22-27.
- Tan, F.C., Cai, D.L., Edmond, J.M., 1991. Carbon isotope geochemistry of the Changjiang Estuary. *Estuar.Coast. Shelf Sci.*, 32, pp 395-403.
- Taylor, S.R. and McLennan, S.M., 1985. *The continental crust: its composition and evolution*. Blackwell. Oxford. pp 312.
- Telang, S.A., 1991. Carbon and mineral transport in major North American, Russian Arctic, and Siberian rivers: the St. Lawrence, the Mackenzie, the Yukon, the Arctic Alaskan, and the Arctic Basin rivers in the Soviet Union and the Yenisei. In: E.T. Degens, S. Kempe and J. Rickey (eds.), *Biogeochemistry of Major World Rivers*. SCOPE, pp. 75-104.



- Thompson, P.A., and Calvert, S.E., 1994. Carbon isotope fractionation by a marine diatom: The influence of irradiance, day length, pH, and nitrogen source. *Limnol. Oceanogr.* 39, 8. pp. 1835-1844.
- Thomson, R., and Oldfield, F., 1986. Environmental magnetism. Allen & Unwin, London pp. 227.
- Thorson, G. 1936. The larval development, growth and metabolism of Arctic marine bottom invertebrates compared with those of other seas. *Medd Gronl.* 100. pp. 1-155.
- Thorson, G., 1950. Reproductive and larval ecology of marine bottom invertebrates *Biol Rev* 25:1-45.
- Thurman, E. M. and Malcolm, R.L., 1981. Preparative isolation of aquatic humic substances. *Environ. Sci. Technol.*, 15, pp. 463-466.
- Ukrainitseva, N.G., 1997. Willow tundra of the Yamal as indicator of salinity of the surface sediments. Results of the fundamental study of the Earth's cryosphere in the Arctic and Sub-Arctic. Novosibirsk, Nauka. pp. 182-187.
- Ukrainitseva, N.G., Leibman, M.O., and Streletskaya, I.D., 2000. Peculiarities of Landslide process in saline frozen Deposits of Central Yamal, Russia. Proceedings of 8th International Symposium on Landslides, Cardiff, UK. Landslides. Telford Publishers, London, 1495-1500.
- Unger, D., Schayen, S., and Gaye, B., 2001. Sediment trap investigations in the Kara Sea. In: R. Stein and O. Stepanets (eds.), *Ber. Polarforsch.*, pp. 29-33.
- Urey, H.C., Lowenstam, H.A., Epstein, S., and McKinney, C.R., 1951. Measurements of paleotemperatures and temperatures of the Upper Cretaceous of England, Denmark and the southeastern United States. *Bulletin of the Geological Society of America.* 62, 399-416.
- Vil'chek, G.E., 1984. About productivity of the tundra phytocenoses neighboring Kharasavei Cape//*Nauchnye Doklady Vyssei Shkoly. Biologicheskie nauki.* 7, p. 67-71.
- Villinger, H., Spieß, V., and Pototzki, F., 1990. Sedimentphysikalische Untersuchungen. In: R. Gersonde & G. Hempel (eds.): *Die Expedition ANTARTIS-VIII/3 und VIII/4 mit FS "Polarstern" 1989*, 76-89.
- Vinogradov, M.E., Nikolaeva, G.G., Khoroshilov, V.S. and Vinogradov, G.M., 1995. The mesozooplankton of the West Kara Sea and the Baidara Bay. *Oceanology*, 34(5): 646-652 (English Translation).
- Weber, M.E., Niessen, F., Kuhn, G., and Wiedicke, M., 1997. Calibration and application of marine sedimentary physical properties using a multi-sensor core logger. *Marine Geology*, 136, 151-172.
- Williams, P.J., le, B., 2000. Heterotrophic bacteria and the dynamics of dissolved organic material. In D.L. Kirchman (eds.): *Microbial ecology of the oceans.* Wiley & Sons, pp. 153-200.
- Zakharchuk, Ye.A. and G.E. Presnyakova, 1997. High-frequency internal waves in the Kara Sea. The Proc. of the Russian-Norwegian Workshop-95 "Nature conditions of the Kara and Barents Seas" (eds. V.Volkov et al.) Rapportserie No 97, Norsk Polarinstittut, Oslo, p. 179- 181.

## 10.1 Station list

### Abbreviations of activities:

EBS-Epibenthos Sledge  
BD - Benthos Dredge  
CTD - Conductivity-Temperature-Depth probe for oceanography  
GC 500 - Gravity Corer with 500 cm core barrel  
GC 800 - Gravity Corer with 800 cm core barrel  
LBC - Large Box Corer (GKG)  
LVS - Large Volume Sampler (Batomat 200l)  
MUC - Multiple Corer  
PHN - Plankton Hand Net (10 $\mu$ m) (AWI, Geo)  
PN - Plankton Net (150 $\mu$ m) (AWI, Bio)  
Bucket - for surface water samples  
ST - Sediment Trap

Station	Date	Time (GMT)	Latitude ° N	Longitude ° E	Depth (uncor.) [m]	Depth (m)	Gear No.	Activity	Recovery (cm)
BP01-01	14.08.2001	12:00	74°59.12	76°23.41	33	38		CTD/RS/BAT/BUC PN	
							/01	LBC	35,5
							/02	OG	
							/03	OG	
							/04	LBC	
							/05	OG	
							/06	LBC	
							/07	MUC	
							/08	MUC	
							/09	GC 500	24
								EBS	
BP01-02	15.08.2001	4:12	74°00.1	80°01.3	28	33		ST-Recovery	
BP01-03	15.08.2001	16:45	72°56.0	80°31.8	12	17	/01	LBC	53
							/02	OG	
							/03	GC 800	689
							/04	GC 800	647
BP01-04	16.08.2001	8:54	71°05.5	83°06.2	17	22		CTD/RS/BAT/BUC PN	
BP01-05	16.08.2001	14:00	70°45.5	83°33.1	8	13		CTD/RS/BAT/BUC PN	
							/01	OG	
BP01-05a	16.08.2001		70°45.106	83°34.975				Katamaran	surface sample
BP01-06	17.08.2001	4:30	70°20.2	83°8.2	12	17		CTD/RS/BAT/BUC PN	
							/01	OG	
BP01-07	17.08.2001	8:44	70°21.08	82°59.14	10	15	/01	OG	
BP01-08	17.08.2001	11:00	70°04.1	83°3.9	23	28		CTD/RS/BAT/BUC PN	
							/01	OG	
BP01-08a	17.08.2001		70°02.4	83°05.96				Katamaran	170
BP01-09	18.08.2001	6:00	72°06.9	82°10.7	6	11		CTD/RS/BAT/BUC PN	
							/01	OG	
BP01-10	18.08.2001	10:00	72°05.5	81°56.9	9	13	/01	OG	

Station	Date	Time (GMT)	Latitude ° N	Longitude ° E	Depth (uncor.) [m]	Depth (m)	Gear No.	Activity	Recovery (cm)
BP01-11	18.08.2001	12:00	72°05.6	81°41.8	7	12		CTD/RS/BAT/BUC	
							/01	PN	
							/02	OG	
							/03	LBC	
BP01-12	18.08.2001	16:00	72°03.5	81°27.9				MUC	
BP01-13	19.08.2001	6:00	71°53.0	82°33	6	11		LBC	
BP01-14	19.08.2001	7:20	71°49.3	82°27.2	16	21		LBC	
								CTD/RS/BAT/BUC	
							/01	PN	
							/02	OG	
							/03	LBC	30
								LBC	
BP01-15	19.08.2001		71°50.0	82°04.8	7	12		BD	
BP01-16	19.08.2001	14:30	71°41.7	83°31.2	23	28		OG	
							/01	OG	
							/02	LBC	
BP01-17	20.08.2001	6:00	70°31.7	83°20.9	12	17		LBC	
								CTD/RS/BAT/BUC	
							/01	PN	
							/02	OG	
								LBC	
BP01-18	21.08.2001	8:30	72°28.3	79°20.4	8	13		LBC	
							/01	CTD	
							/02	OG	
BP01-19	21.08.2001	11:00	72°35.7	80°06.4	23	28		LBC	
								CTD/RS/BAT/BUC	
							/01	PN	
							/02	OG	
								LBC	
BP01-20	21.08.2001	15:00	72°35.4	80°37.2	11	16		CTD	34
							/01	OG	
							/02	LBC	
BP01-21	21.08.2001	17:00	72°40.5	80°32.7	11	16		CTD	
							/01	OG	
							/02	LBC	
BP01-22	22.08.2001	4:30	73°22.5	78°01.8	10	15		CTD	
							/01	OG	
							/02	LBC	

Station	Date	Time (GMT)	Latitude ° N	Longitude ° E	Depth (uncor.) [m]	Depth (m)	Gear No.	Activity	Recovery (cm)
BP01-23	22.08.2001	7:00	73°29.0	78°50.9	17	22		CTD	
							/01	PN	
							/02	OG	
BP01-24	22.08.2001	13:00	73°38.2	80°00.4	32	37		LBC	
								CTD	
BP01-25	22.08.2001	15:20	73°24.9	79°40.5	23	28		OG	
								CTD	
							/01	OG	
							/02	GC800	705
								CTD/RS/BAT/BUCC	
								PN	
							/01	LBC	
							/02	MUC	
							/03	GC800	526
								EBS	
								ST Deployment	
BP01-27	23.08.2001	10:06	74°00.07	80°19.87	31	36		CTD/RS/BAT/BUCC	
BP01-28	24.08.2001	4:15	75°56.34	89°15.9	46	51		CTD/RS/BAT/BUCC	
								PN	
							/01	OG	
							/02	LBC	
							/03	LBC	
							/04	LBC	47
							/05	MUC	
							/06	MUC	
							/07	GC 800	488
								BD	
								CTD	
BP01-29	24.08.2001	11:10	76°16.03	89°07.69	48	53		OG	
							/01	OG	
							/02	GC 500	174
								CTD/RS/BAT/BUCC	
								PN	
							/01	OG	
							/02	LBC	
							/03	LBC	
							/04	LBC	
							/05	MUC	30

Station	Date	Time (GMT)	Latitude °N	Longitude °E	Depth (uncor.)		Depth (m)	Gear No.	Activity	Recovery (cm)
					[m]					
BP01-31	25.08.2001	4:30	77°34.2	87°54.5	83	88	/06	GC 800	0	
								CTD/RS/BAT/BU		
								PN		
								OG		
								LBC	33	
								LBC		
								LBC		
								MUC		
BP01-32	25.08.2001	6:24	77°34.12	87°54.56	87	82	/01	GC 800	657	
								CTD/RS/BAT/BU		
								PN		
								OG		
								LBC	638	
								LBC	627	
								LBC		
								MUC		
BP01-33	25.08.2001	9:58	77°27.71	87°25.98	78	83	/01	GC 800	743	
								CTD/RS/BAT/BU		
								PN		
								OG		
								LBC		
								LBC		
								LBC		
								MUC		
BP01-34	25.08.2001	11:10	77°29.83	87°53.32	86	91	/02	GC 800		
								CTD/RS/BAT/BU		
								PN		
								OG		
								LBC	29	
								LBC		
								LBC		
								MUC		
BP01-35	26.08.2001	18:18	77°54.21	89°19.88	155	160	/01	GC 500	488	
								CTD/RS/BAT/BU		
								PN		
								OG		
								LBC	433	
								LBC		
								LBC		
								MUC		
BP01-36	26.08.2001	19:07	77°54.21	89°19.86	137	156	/01	GC 800	536	
								CTD/RS/BAT/BU		
								PN		
								OG		
								LBC	616	
								LBC		
								LBC		
								MUC		
BP01-36	26.08.2001	19:37	77°54.23	89°19.88	137	156	/02	GC 800	616	
								CTD/RS/BAT/BU		
								PN		
								OG		
								LBC	29	
								LBC		
								LBC		
								MUC		
BP01-36	26.08.2001	4:30	77°54.31	83°45.94	137	156	/01	GC 800	616	
								CTD/RS/BAT/BU		
								PN		
								OG		
								LBC	29	
								LBC		
								LBC		
								MUC		
BP01-36	26.08.2001	7:19	77°54.25	83°46.03	137	156	/02	GC 800	616	
								CTD/RS/BAT/BU		
								PN		
								OG		
								LBC	29	
								LBC		
								LBC		
								MUC		
BP01-36	26.08.2001	7:29	77°54.23	83°45.99	137	156	/03	GC 800	616	
								CTD/RS/BAT/BU		
								PN		
								OG		
								LBC	29	
								LBC		
								LBC		
								MUC		
BP01-36	26.08.2001	8:36	77°54.24	83°45.72	137	156	/04	GC 800	616	
								CTD/RS/BAT/BU		
								PN		
								OG		
								LBC	29	
								LBC		
								LBC		
								MUC		
BP01-36	26.08.2001	8:58	77°54.26	83°45.57	137	156	/05	GC 800	616	
								CTD/RS/BAT/BU		
								PN		
								OG		
								LBC	29	
								LBC		
								LBC		
								MUC		
BP01-36	26.08.2001	9:30	77°54.29	83°45.44	137	156	/06	GC 800	616	
								CTD/RS/BAT/BU		
								PN		
								OG		
								LBC	29	
								LBC		
								LBC		
								MUC		
BP01-36	26.08.2001	11:55	77°47.1	85°12.6	137	156	/01	GC 800	616	
								CTD/RS/BAT/BU		
								PN		
								OG		
								LBC	29	
								LBC		
								LBC		
								MUC		

Station	Date	Time (GMT)	Latitude ° N	Longitude ° E	Depth (uncor.) [m]	Depth (m)	Gear No.	Activity	Recovery (cm)
BP01-37	26.08.2001	13:52	77°48.9	86°11.9	139	144		CTD/RS/BAT/BUC	
							/01	PN	
							/02	OG	
							/03	LBC	37
							/04	LBC	
							/05	MUC	
		16:49	77°48.97	86°12.72			/06	MUC	
		17:06	77°48.97	86°12.71				GC 800	619
BP01-38	27.08.2001	4:30	77°5.29	86°55.48	105	110		CTD/RS/BAT/BUC	
								PN	
							/01	OG	
		7:41	77°5.07	86°54.97			/02	LBC	
							/03	LBC	38
							/04	LBC	
							/05	MUC	
		7:54	77°5.3	86°55.6			/06	MUC	
							/07	GC 800	624
							/08	GC 800	633
BP01-39	27.08.2001	11:45	77°06.7	86°44.9	101	106		CTD	
							/01	OG	
							/02	GC800	538
BP01-40	27.08.2001	16:30	76°25.2	85°39.9	47	52		CTD/RS/BAT/BUC	
								PN	
							/01	OG	
		17:39	76°25.22	85°39.98			/02	LBC	
							/03	LBC	30
							/04	LBC	
		18:27	76°25.16	85°40.0			/05	MUC	
		18:46	76°25.17	85°40.05			/06	GC 800	193

Station	Date	Time (GMT)	Latitude ° N	Longitude ° E	Depth (uncor.) [m]	Depth (m)	Gear No.	Activity	Recovery (cm)	
BP01-41	28.08.2001	4:00	75°41.4	87°07.8	37	42		CTD/RS/BAT/BUC		
								PN		
								/01	OG	
								/02	LBC	30
								/03	LBC	
								/04	LBC	
								/05	MUC	
BP01-42	28.08.2001	7:05	75°41.4	87°07.8				MUC		
		7:28	75°41.37	87°07.8				/06	MUC	
		10:28	75°26.2	86°03.73	40	49		/07	GC 800	457
BP01-43	28.08.2001	11:30	75°22.99	85°49.90	43	48		BD		
								CTD		
BP01-44	29.08.2001	5:09	76°58.4	86°02.75	72	84		OG		
								GC 800	572	
								CTD/RS/BAT/BUC		
								PN		
								/01	OG	
								/02	LBC	40
								/03	LBC	
								/04	LBC	
	/05	MUC								
BP01-45	29.08.2001	8:00	77°6.83	84°44.0	82	87		MUC		
								GC 500	344	
BP01-45	29.08.2001	10:28	77°6.83	84°42.54	82	87		GC 500	329	
								EBS		
BP01-45	29.08.2001	10:54	77°6.80	84°42.44	82	87		CTD		
								OG		
								/01	OG	
								/02	GC 800	309
								CTD/RS/BAT/BUC		
								PN		
BP01-45	29.08.2001	11:31	77°6.83	84°42.48	82	87		LBC		
								/01	OG	
								/02	LBC	45
								/03	LBC	
								/04	LBC	
								/05	MUC	
BP01-45	29.08.2001	11:31	77°6.83	84°42.48	82	87		GC 800	490	
								EBS		



Station	Date	Time (GMT)	Latitude ° N	Longitude ° E	Depth (uncor.) [m]	Depth (m)	Gear No.	Activity	Recovery (cm)
BP01-46	30.08.2001	4:53	77°55.43	75°57.35	290	323	/01	BD	234
								CTD/RS/BAT/BU	
								PN	
								OG	
								GC 500	
								MUC	
								MUC	
BP01-47	30.08.2001	14:48	77°54.55	77°22.49	154	174	/01	LBC	35
								LBC	
								LBC	
								LBC	
								LBC	
								LBC	
								LBC	
BP01-48	31.08.2001	4:30	77°53.49	81°29.94	197	202	/01	BD	53
								CTD	
								OG	
								LBC	
								LBC	
								LBC	
								LBC	
BP01-49	31.08.2001	8:52	77°53.45	81°30.54	175	198	/01	GC 500	469
								GC 500	
								GC 500	
								GC 500	
								GC 500	
								GC 500	
								GC 500	
BP01-50	31.08.2001	10:30	77°52.48	81°30.03	135	154	/01	CTD/RS/BAT/BU	384
								PN	
								OG	
								LBC	
								LBC	
								LBC	
								LBC	
BP01-50	31.08.2001	11:41	77°50.91	81°30.13	135	154	/01	GC 800	211
								GC 800	
								CTD	
								OG	
								GC 500	
								CTD	
								GC 500	

Station	Date	Time (GMT)	Latitude ° N	Longitude ° E	Depth (uncor.) [m]	Depth (m)	Gear No.	Activity	Recovery (cm)
BP01-51	31.08.2001	14:30	77°54.68	79°29.48	153	158		CTD/RS/BAT/BUC	
							/01	PN	
		16:28	77°54.3	79°30.17			/02	OG	
		17:09	77°54.03	79°28.96			/03	LBC	31
		17:56	77°55.02	79°30.0			/04	MUC	
BP01-52	01.09.2001	4:19	77°29.94	79°52.0	70	75	/05	GC 800	392
								CTD/RS/BAT/BUC	
							/01	PN	
							/02	OG	
							/03	LBC	30
BP01-53	01.09.2001	8:25	77°29.99	79°50.63	58	69	/04	MUC	369
							/05	GC 800	
								CTD	
							/01	OG	
							/02	GC 500	0
BP01-54	01.09.2001	8:56	77°30.1	79°49.5	60	71	/01	CTD	10
BP01-55	01.09.2001	11:48	77°2.97	79°43.99	71	83		GC 500	
								CTD/RS/BAT/BUC	
							/01	PN	
							/02	OG	
							/03	LBC	20
							/04	LBC	
BP01-56	02.09.2001						/05	MUC	317
							/06	GC 500	424
								EBS	
							/06	GC 500	
								CTD/RS/BAT/BUC	
							/01	PN	
							/02	OG	
					/03	LBC	31		
					/04	LBC			
					/05	MUC			
		7:20	76°59.0	75°20.27			/06	MUC	
							/06	GC 500	245

Station	Date	Time (GMT)	Latitude ° N	Longitude ° E	Depth (uncor.) [m]	Depth (m)	Gear No.	Activity	Recovery (cm)
BP01-57	02.09.2001		76°52.85	76°56.02	98	113		BD CTD	
BP01-58	02.09.2001	12:20	76°48.12	78°21.24	79	94	/01	GC 500	274
							/01	OG	38
							/02	LBC	
							/03	LBC	
		14:53	76°48.1	78°21.3			/04	MUC	
BP01-59	03.09.2001	4:30	76°31.16	74°30.95	155	176	/05	GC 800	589
								CTD/RS/BAT/BUC	
								PN	
							/01	OG	
							/02	LBC	
							/03	LBC	40
							/04	MUC	
BP01-60	03.09.2001	9:28	76°31.23	74°30.94	75	88	/05	GC 800	606
			76°23.02	74°37.19				CTD	
							/01	OG	
BP01-61a	03.09.2001	12:53	76°12.08	75°45.3	89	94	/02	GC 500	29
BP01-61b	03.09.2001	13:15	76°12.9	75°53.15	106	111		ST-Deployment	
								CTD/RS/BAT/BUC	
								PN	
							/01	OG	
							/02	LBC	
							/03	LBC	45
							/04	LBC	
							/05	MUC	
							/06	MUC	
			76°11.9	76°05			/07	GC 800	566
BP01-62	04.09.2001	4:30	76°12.05	74°12.15	130	135		EBS	
								CTD/RS/BAT/BUC	
								PN	
							/01	OG	
							/02	LBC	
							/03	LBC	46
							/04	MUC	
							/05	GC 800	580

Station	Date	Time (GMT)	Latitude ° N	Longitude ° E	Depth (uncor.) [m]	Depth (m)	Gear No.	Activity	Recovery (cm)
BP01-63	04.09.2001		76°12.02	74°29.33		80	/06	GC 800 CTD OG	582
BP01-64	04.09.2001		75°53.4	73°38.9	85	99	/01 /02	GC 300 CTD/RS/BAT/BU PN	14
							/01 /02 /03 /04 /05	LBC LBC LBC MUC	56
BP01-65	05.09.2001	4:18	75°42.98	75°50.79	58	63	/06 /07	MUC GC 500 GC 800 CTD/RS/BAT/BU	492 536
							/01 /02 /03 /04 /05 /06	PN OG LBC LBC MUC MUC GC 500	28
BP01-66	05.09.2001	11:28	75°10.04	76°55.13	50	55		GC 500 CTD/RS/BAT/BU	56
							/01 /02 /03 /04 /05	PN OG LBC LBC MUC MUC EBS BD	37
BP01-67	06.09.2001	4:30	75°14.65	73°45.78	44	49		CTD/RS/BAT/BU PN OG LBC LBC	47
							/01 /02 /03 /04	PN OG LBC LBC	

Station	Date	Time (GMT)	Latitude °N	Longitude °E	Depth (uncor.) [m]	Depth (m)	Gear No.	Activity	Recovery (cm)
BP01-68	06.09.2001	12:25	74°35.05	72°14.97	26	31	/05	MUC	71
							/06	MUC	
							/07	GC 500	
								BD	
								CTD/RS/BAT/BUCC	
								PN	
								OG	
BP01-69	07.09.2001	4:30	72°39.87	74°45.05	9	16	/01	LBC	68
							/02	LBC	
							/03	LBC	
							/04	MUC	
							/05	MUC	
							/06	GC 500	
								CTD	
BP01-70	07.09.2001	7:15	72°40.16	17	22	/01	OG	45	
						/02	LBC		
							CTD/RS/BAT/BUCC		
							PN		
						/01	OG		
						/02	LBC		
						/03	LBC		
BP01-71	07.09.2001	14:30	72°39.96	16	23	/01	OG	639	
						/02	LBC		
						/03	LBC		
						/04	LBC		
						/05	MUC		
						/06	MUC		
						/07	GC 500		
BP01-72	08.09.2001	4:20	70°49.88	73°44.34	19	26	BD	23	
							CTD		
							OG		
							LBC		
							GC 500		
							GC 500		
							CTD		
BP01-72a	08.09.2001	9:30	70°51.43 70°51.03 70°51.06	73°42.52 73°43.07 73°43.06	20	27	/01	OG	467
							/01	OG	
							/02	GC 500	
							/03	LBC	

Station	Date	Time (GMT)	Latitude ° N	Longitude ° E	Depth (uncor.) [m]	Depth (m)	Gear No.	Activity	Recovery (cm)
BP01-73	09.09.2001	4:24	68°54.89	73°39.99	9	15	/01 /02 /03 /04 /05	CTD/RS/BAT/BUC OG LBC LBC MUC GC 500	60 222
BP01-73a	09.09.2001	8:46	68°52.144	73°37.833	8	14	/01	OG	
BP01-73b	09.09.2001	9:23	68°52.063	73°48.899	7	13	/01	OG	
BP01-73c	09.09.2001	9:50	68°49.883	73°43.576	7	13	/01	OG	
BP01-73d	09.09.2001	10:20	68°48.205	73°38.118	7	13	/01	OG	
BP01-73e	09.09.2001		68°52.063	73°48.899	7	13	/01	OG	
BP01-74	09.09.2001	12:25	68°58.024	74°22.033	7	13		Bu OG	
BP01-75	09.09.2001	15:10	69°5.04	75°41.853	6	12	/01	Bu OG	
BP01-76	09.09.2001	15:54	69°1.954	75°29.857	7	13	/01	Bu OG	
BP01-77	09.09.2001	16:58	68°58.79	75°4.92	7	13	/01 /02	Bu OG LBC	
BP01-78	09.09.2001	19:43	68°40.074	73°59.74	7	13	/01	Bu OG	
BP01-79	09.09.2001	22:30	69°03.27	73°13.65	7	13	/01	Bu OG	
BP01-80	10.09.2001	14:30	72°14.99	73°15.18	10	16	/01 /02 /03 /04 /05 /06	OG OG LBC LBC LBC MUC GC 500	30 150
BP01-81	10.09	17:23	72°18.35	73°21.36	9	15	/01	OG	
BP01-82	11.09	4:17	73°11.83	73°01.65	22	29		CTD/RS/BAT/BUC PN	
							/01 /02 /03	OG LBC LBC	40

Station	Date	Time (GMT)	Latitude °N	Longitude °E	Depth (uncor.) [m]	Depth (m)	Gear No.	Activity	Recovery (cm)
BP01-83	11,09	9:30	73°11.8	73°14.4	17	24	/04	LBC	229 213
							/05	MUC	
							/06	MUC	
							/07	GC 500	
							/08	GC 500	
								EBS	
							/01	BD	
							/02	OG	
	GC800	730							

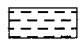
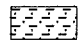

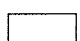
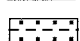
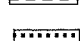
10.2

(Core description: R. Stein, AWI Bremerhaven  
Smear-slide data: M. Levitan, GEOKHI/IORAS Moscow)




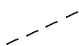
## Geological Core Descriptions

**Legend:**

**Lithology**

	clay
	silty clay
	sandy silty clay
	sand
	sandy clay
	clayey sand

**Structure**

	bioturbation
	sharp boundary
	gradational boundary
	transition zone



Core description

BP01-03/4 (SL-8)

Yenisei Estuary

Boris Petrov 2001

Recovery: 6.47 m

72° 56.04' N, 80° 31.80' E

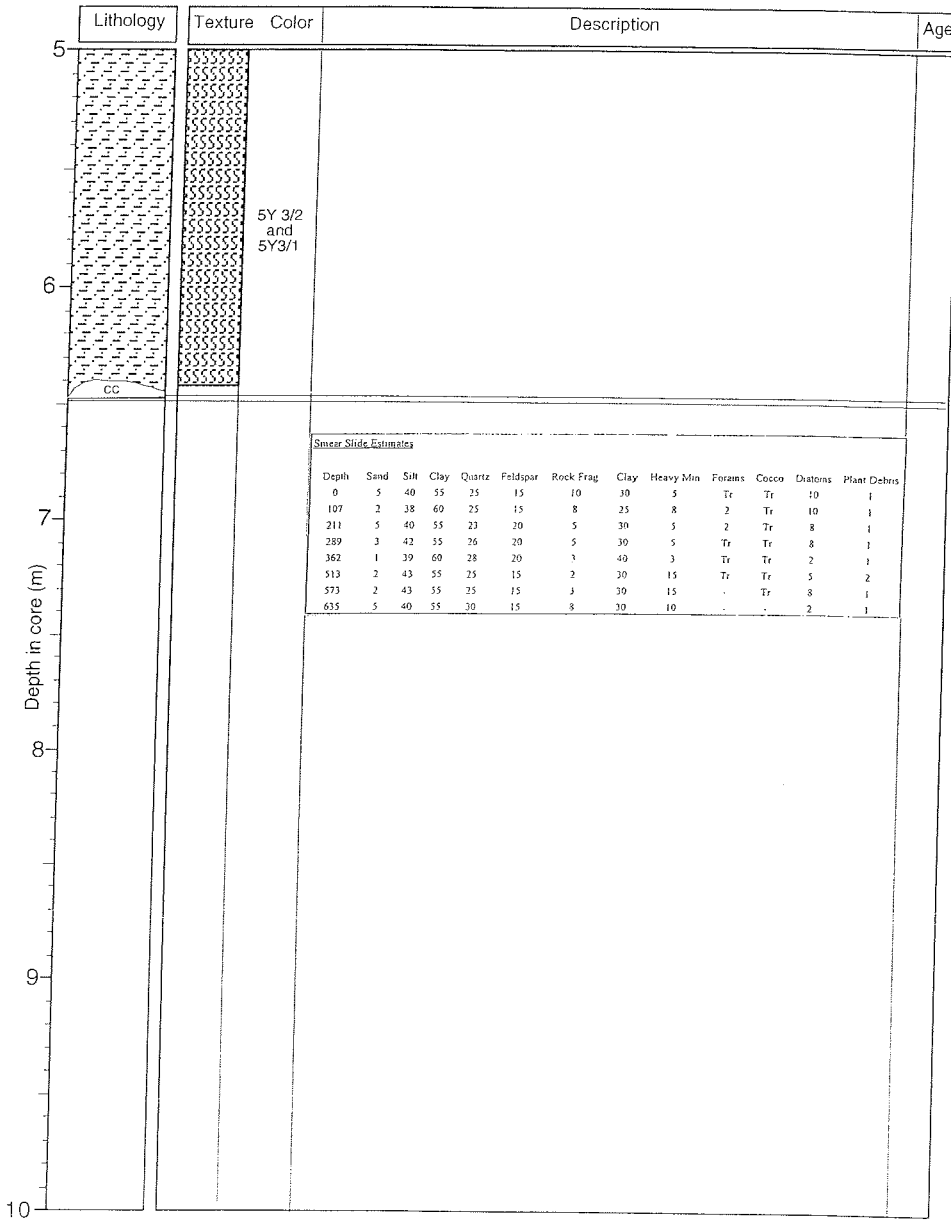
Water depth: 17 m

Lithology	Texture Color	Description	Age
	<p>10YR 4/3 5Y 4/2</p> <p>5Y 3/1 and 5Y 3/2</p>	<p>0-6 cm: dark brown (10YR 4/3) silty clay</p> <p>6-16 cm: olive gray (5Y 4/2) silty clay</p> <p>16-647 cm: very dark gray (5Y 3/1) and dark olive gray (5Y 3/2) silty clay, slightly to moderately to strongly bioturbated (bioturbation increasing downcore), abundant black spots throughout, sharp boundary at 74 cm</p> <p>bivalves at 154 and 291 cm; shell debris at 72, 179, 197, 260, and 346 cm</p>	

BP01-03/4 (SL-8)

cont.

Boris Petrov 2001



BP01-26/3 (SL-8)

Southern Kara Sea

Boris Petrov 2001

Recovery: 5.26 m

74° 0.0' N, 80° 01.4' E

Water depth: 33 m

	Lithology	Texture Color	Description	Age
0		5Y 4/2	0-73 cm: dark olive (5Y 4/2) to very dark olive (5Y 3/2) silty clay, soft, slightly to moderately bioturbated, black spots	
		5Y 3/2 and 5Y 4/2	73-126 cm: very dark gray (5Y 3/1) and black (5Y 2.5/1) silty clay, moderately bioturbated	
			126-145 cm: very dark gray (5Y 3/1) silty clay to clayey silt, slightly bioturbated	
			145-165 cm: dark gray (5Y 4/1) silty clay to clayey silt, moderately bioturbated (mottled)	
1		5Y 3/1 and 5Y 2.5/1	165 - 200 cm: black (5Y 2.5/1) silty clay to clayey silt, above 180 cm moderately bioturbated	
		5Y 3/1	200-230 cm: olive gray (5Y 4/2) silty clay to clayey silt, some amount of sand and more stiff than previous interval; large ikaite crystal (diameter of about 5 cm) at 225-230 cm	
		5Y 3/1	230-263 cm: olive gray silty clay to clayey silt with sandy layers (sandy silt)	
		5Y 4/1	263-526 cm: silty clay to clayey silt with minor amount of sand, stiff, distinct color variations (cycles) with sharp boundaries of olive gray (5Y 4/2), dark olive gray (5Y 3/2), dark gray (5Y 4/1), very dark gray (5Y 3/1) and black (5Y 2.5/1); sandy silt layers at 390 and 398-401 cm	
		5Y 2.5/1	bivalves at 4 cm (intact), 28, 37, 43, and 109 cm	
2		5Y 4/2		
		5Y 3/1		
		5Y 4/2		
		5Y 2.5/1		
		5Y 3/1		
3		5Y 2.5/1		
		5Y 3/1		
		5Y 3/2		
		5Y 3/1		
		5Y 2.5/2		
		5Y 4/2		
		5Y 3/2		
		5Y 3/2		
4		5Y 3/2		
		5Y 3/2		
		5Y 4/1		
		5Y 3/1		
		5Y 3/1		
5		5Y 3/2		

BP01-26/3 (SL-8)

cont.

Boris Petrov 2001

Lithology	Texture	Color	Description	Age								
5		5Y 2.5/2										
		5Y3/1										
Smear Slide Estimates												
Depth	Sand	Silt	Clay	Quartz	Feldspar	Rock Frag.	Clay	Heavy Min.	Forams	Cocco	Diatoms	Plant Debris
18	1	24	75	27	14	5	50	1	-	-	-	-
34	5	20	75	12	7	5	20	2	-	-	-	-
89	3	22	75	10	7	5	20	2	-	-	-	-
134	40	30	30	28	20	15	25	2	-	-	-	-
210	10	55	35	33	20	6	30	3	1	-	3	-
250	45	50	5	46	30	10	-	4	1	-	1	-
280	5	70	25	23	20	5	15	5	1	-	15	-
365	55	40	5	44	30	10	5	4	-	-	-	1
410	5	80	15	43	20	8	12	3	1	-	10	Tr
429	10	70	20	44	20	5	15	5	1	-	5	-
470	2	88	10	42	20	5	5	2	1	-	10	-
473	5	80	15	46	20	5	10	2	1	-	10	Tr
6												
7												
8												
9												
10												

BP01- 33/02 (SL-8)

Southern Kara Sea

Boris Petrov 2001

Recovery: 7.43 m

77° 29.83' N, 87° 35.32' E

Water depth: 83 m

Lithology	Texture Color	Description	Age
0	5Y 4/2 and 5Y3/1	0-1 cm: dark brown (10YR 4/3) silty clay 1-43 cm: olive gray (5Y 4/2) and very dark gray (5Y 3/1) silty clay, some amount of sand, bioturbated 43-240 cm: very dark gray (5Y 3/1) and dark olive gray (5Y 3/2) silty clay, black spots, bioturbated, some amount of sand; black horizons at 107-108, 119, 123, 125, 127, 129, 132, and 138 cm; dropstone (gneiss?) of 2 cm in diameter at 208-209 cm 240-251 cm: very dark gray (5X 3/1) clayey sandy silt to clayey silty sand (more sandy at base)	
	5Y 3/1 and 5Y 3/2	251-450 cm: very dark gray (5Y 3/1) and dark olive gray (5Y 3/2) silty clay, more firm/stiff than previous section; bioturbated, black spots 450-690 cm: (finely) laminated dark olive gray (5Y 3/2) and very dark gray (5Y 3/1) silty clay to clayey silt, stiff; two dark reddish brown (5YR 3/4) horizons (each 0.5cm thick) between 459-461 cm 690-714 cm: dark olive gray (5Y 3/2) and very dark gray (silty) clay 714-719 cm: dark olive gray (5Y 3/2) clayey silty sand 719-729 cm: dark olive brown (2.5Y 3/2) clayey silty sand 729-743 cm: black (5Y 2.5/1) clayey silty sand	
1		shell debris at 24 cm, bivalve at 144 cm	
2	5Y 3/1		
3			
4	5Y 3/1 and 5Y 3/2		
5			

BP01- 33/02 (SL-8)

cont.

Boris Petrov 2001

	Lithology	Texture Color	Description	Age
5				
6				
7			5Y 3/2 and 5Y3/1  2.5Y 3/2 5Y 2.5/1	
8				
9				
10				

Core description

BP01-34/7 (SL-5)

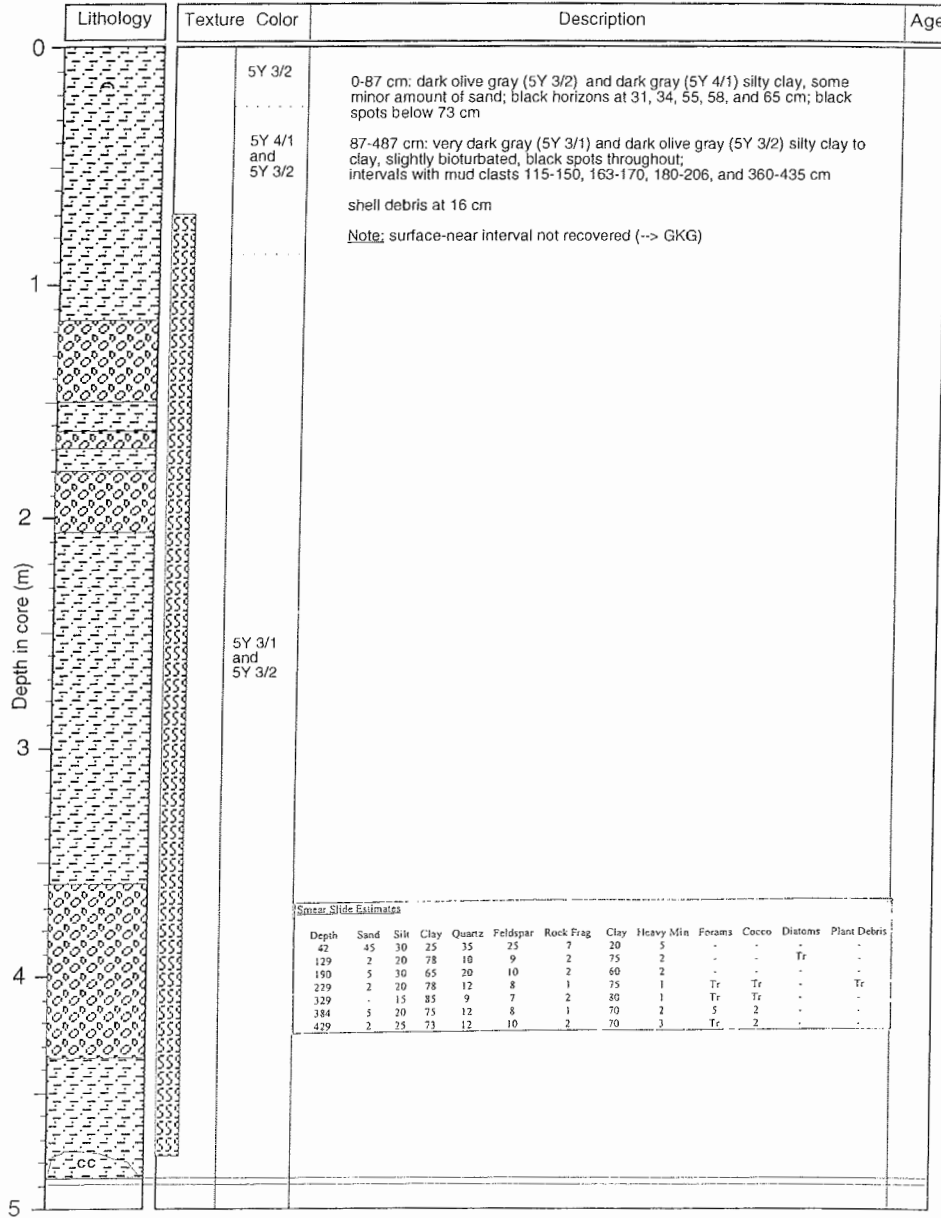
Southern Kara Sea

Boris Petrov 2001

Recovery: 4.87m

77° 54.21' N, 89° 19.88' E

Water depth: 91 m



Core description

BP01- 37/06 (SL-8)

Southern Kara Sea

Boris Petrov 2001

Recovery: 6.19 m

77° 48.9' N, 86° 11.9' E

Water depth: 144 m

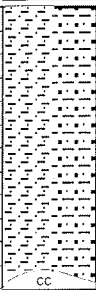
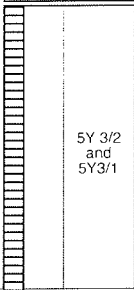
	Lithology	Texture Color	Description	Age
0			0-1 cm: dark brown (10YR 4/3) silty clay	
			1-119 cm: olive gray (5Y 4/2) and dark gray (5Y 4/1) silty clay, few black spots, bioturbated	
		5Y 4/2 and 5Y4/1	119-460 cm: very dark gray (5Y 3/1) and dark olive gray (5Y 3/2) silty clay, abundant black spots, bioturbated, below 440 cm some amount of sand	
			460- 619 cm. very dark gray (5Y 3/1) and dark olive gray (5Y 3/2) silty clay, thin more silty/sandy laminae throughout	
1			bivalves at 128, 160, 174, 195, 245, 260, 284, and 308 cm	
5		5Y 3/1 and 5Y 3/2		



BP01- 37/06 (SL-8)

cont.

Boris Petrov 2001

Lithology	Texture	Color	Description	Age
		<p>5Y 3/2 and 5Y3/1</p>		

5  
6  
7  
8  
9  
10

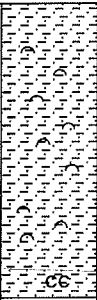

Depth in core (m)



BP01- 38/07 (SL-8)

cont.

Boris Petrov 2001

	Lithology	Texture	Color	Description	Age
5			5Y 3/1 and 5Y 3/2 and 5Y 2.5/1		
6					
7					
8					
9					
10					

BP01-38/8 (SL-8)

Southern Kara Sea

Boris Petrov 2001

Recovery: 6.33 m

77° 05.29' N, 86° 55.48' E

Water depth: 110 m

	Lithology	Texture Color	Description	Age
0				
		5Y 4/2 and 5Y 4/1	0-133 cm: olive gray (5Y 4/2) to dark gray (5Y4/1) silty clay, black spots, slightly to moderately bioturbated; dark brown color (7.5YR 3/4) at 8-12 cm	
		5Y 4/2 and 5Y 4/1	133- 633 cm: dark olive gray (5Y 3/2) and very dark gray (5Y 3/1) silty clay, abundant black spots throughout, slightly to moderately bioturbated; small nodule (lithified sediment? incrustated shell?)	
		5Y 4/2 and 5Y 4/1	bivalves at 442, 488, 545 (intact), and 554 cm, shell debris at 276 cm	
1				
5		5Y 3/1 and 5Y 3/2		

BP01-38/8 (SL-8)

cont.

Boris Petrov 2001

Lithology	Texture	Color	Description	Age
5				
6		5Y 3/2 and 5Y3/1		
7				
8				
9				
10				

Depth	Sand	Silt	Clay	Quartz	Feldspar	Rock Frag	Clay	Heavy Min	Forams	Cocco	Diatoms	Plant Debris
11	5	35	60	17	10	2	50	3	2	-	Tr	-
82	-	25	75	37	15	3	50	4	1	-	Tr	-
182	10	50	40	39	20	5	30	3	2	-	-	-
284	2	38	60	35	14	3	50	7	1	-	-	-
359	10	50	40	35	20	5	30	6	2	-	Tr	-
459	5	60	35	29	30	1	25	3	1	-	-	-
609	5	40	55	23	20	2	45	5	1	-	-	-

**BP01- 39/02 (SL-8)**

Southern Kara Sea

**Boris Petrov 2001**

Recovery: 5.38 m

77° 06.7' N, 86° 44.9' E

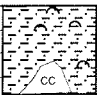

Water depth: 106 m

	Lithology	Texture Color	Description	Age
0 1 2 3 4 5 Depth in core (m)		5Y 3/1 and 5Y 3/2 and 5Y 2.5/1	<p>0-538 cm: very dark gray (5Y 3/1), black (5Y 2.5/1), and dark olive gray (5Y 3/2) silty clay, black spots, bioturbated</p> <p>Bivalves/shell debris at 51, 60, 76, 121, 127 (large gastropode, 3 cm), 128, 152, 169, 170, 172, 179, 187, 195, 200, 256, 262.5, 280, 287.5, 296, 349, 391, 460, 470, 480, 481, 500, 509, 511, and 525 cm</p>	

BP01- 39/02 (SL-8)

cont.

Boris Petrov 2001

Lithology	Texture	Color	Description	Age
		5Y 3/2 and 5Y3/1		

Depth in core (m)

5  
6  
7  
8  
9  
10

BP01- 42/02 (SL-8)

Southern Kara Sea

Boris Petrov 2001

Recovery: 5.72 m

75° 26.2' N, 86° 03.73' E

Water depth: 49 m

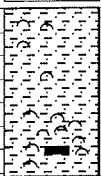

	Lithology	Texture Color	Description	Age
0		5Y 3/2 and 5Y 3/1 and 5Y 2.5/1	0-1 cm: dark brown (10YR 4/3) silty clay  1-572 cm: very dark gray (5Y 3/1), dark olive gray (5Y 3/2), and black (5Y 2.5/1) silty clay, abundant black spots, bioturbated; upper 72 cm very soft; below 520 cm some amount of sand; large drop stone (4cm x 1cm x 0.5cm; black siltstone?) at 562 cm	
1			Bivalves and/or shell debris at 120, 200, 214, 217.5, 232, 246.5, 275, 293.5, 330, 342, 427.5, 450, 468, 477, 487, 494, 504, 508, 516, 530, 545, 547.5, 550, 553, 554, 558, 560, 562, and 567 cm	
2				
3				
4				
5				



BP01- 42/02 (SL-8)

cont.

Boris Petrov 2001

Lithology	Texture	Color	Description	Age
		5Y 3/2 and 5Y3/1 and 5Y 2.5/1		

Depth in core (m)

5

6

7

8

9

10

BP01-43/8 (SL-5)

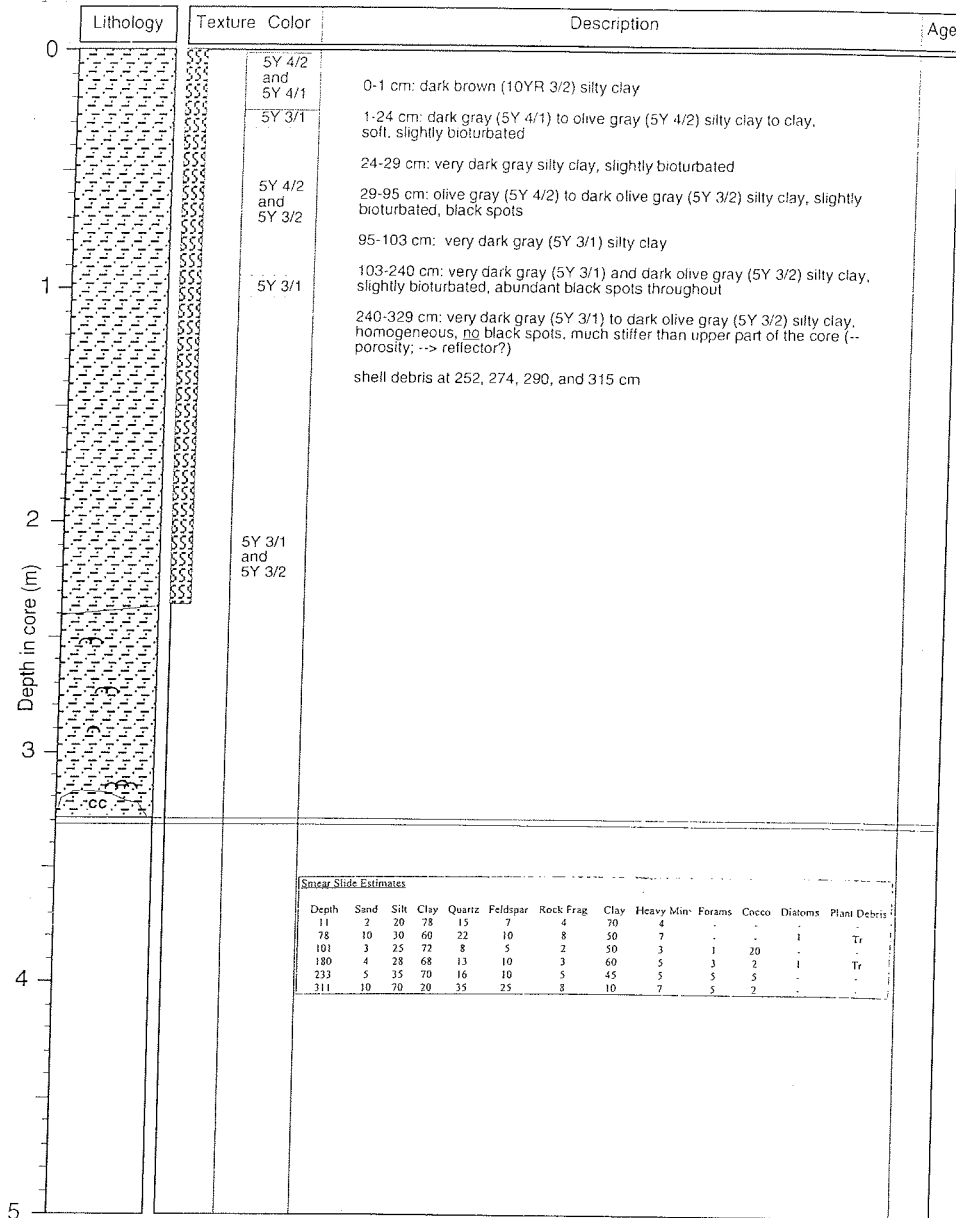
Southern Kara Sea

Boris Petrov 2001

Recovery: 3.29m

75° 22.99' N, 85° 49.9' E

Water depth: 48 m



BP01- 45/06 (SL-8)

Southern Kara Sea

Boris Petrov 2001

Recovery: 6.00 m

77° 06.83' N, 84° 42.48' E

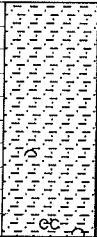

Water depth: 87 m

Lithology	Texture Color	Description	Age
	<p>5Y 3/1 and 5Y 3/2 and 5Y 2.5/1</p>	<p>0-1 cm: dark brown (10YR 4/3) silty clay</p> <p>1-600 cm: very dark gray (5Y 3/1), dark olive gray (5Y 3/2) and black (5Y 2.5/1) silty clay, black spots, bioturbated; ikaite/glendonite at 199-200 and 245-247 cm</p> <p><u>Note:</u> 580-600 cm coring disturbance</p> <p>Bivalves and/or shell debris at 13, 15, 27, 52, 63, 65, 70, 85, 169, 170-171 (4 cm in diameter), 210, 267, 277-278 (intact, 4 cm in diameter), 285, 302, 304, 308, 326, 350, 365, 375, 380, 460, 488, 491, 499, 567, and 599 (CC) cm</p>	

BP01- 45/06 (SL-8)

cont.

Boris Petrov 2001

	Lithology	Texture	Color	Description	Age
5			5Y 3/1 and 5Y 3/2 and 5Y 2.5/1		
6					
7					
8					
9					
10					

Core description

BP01- 46/07 (SL-5)

Southern Kara Sea

Boris Petrov 2001

Recovery: 2.34m

77° 55.5' N, 75° 59.2' E

Water depth: 323 m

Lithology	Texture	Color	Description	Age
0-1.75 m	[Pattern: vertical lines]	5Y 3/1 and 5Y 3/2	0-1cm: very dark brown (10YR 3/3) silty clay 1-34 cm: very dark gray (5Y 3/1) and dark olive gray (5Y 3/2) silty clay, black spots, some bioturbation; dark brown lenses at 5 and 17 cm	
		5Y 3/1 and 5Y 3/2 and 2.5YR 3/2	34-129 cm: very dark gray (5Y 3/1), dark olive gray (5Y 3/2), and very dark grayish brown (2.5YR 3/2) silty clay, abundant black spots (less below 128 cm), bioturbated 129-145 cm: dark olive gray (5Y 3/2) silty clay 145-149 cm: olive brown (2.5Y 4/3) silty clay 149-209 cm: dark olive gray (5Y 3/2) silty clay, very dark gray (5Y 3/1) to black (5Y 2.5/1) horizons below 160 cm 209-211 cm: very dark gray silty clay (laminated?)	
1.75-2.34 m	[Pattern: vertical lines]	5Y 3/2	211-234 cm: very dark gray (5Y 3/1) to black (5Y 2.5/1) clayey sandy silt, firm; conglomerates at 231-234 cm (diameter 3 cm), and 220 cm (diameter of 0.5 and 1 cm); two stones at 215 cm (1 cm in diameter)	
		5Y 3/1 and 5Y 3/2 and 5Y 2.5/1		
2.34-2.34 m	[Pattern: vertical lines]	5Y 3/1 and 5Y 2.5/1		
2.34-5.00 m	[Pattern: vertical lines]			

BP01-47/03 (SL-5)

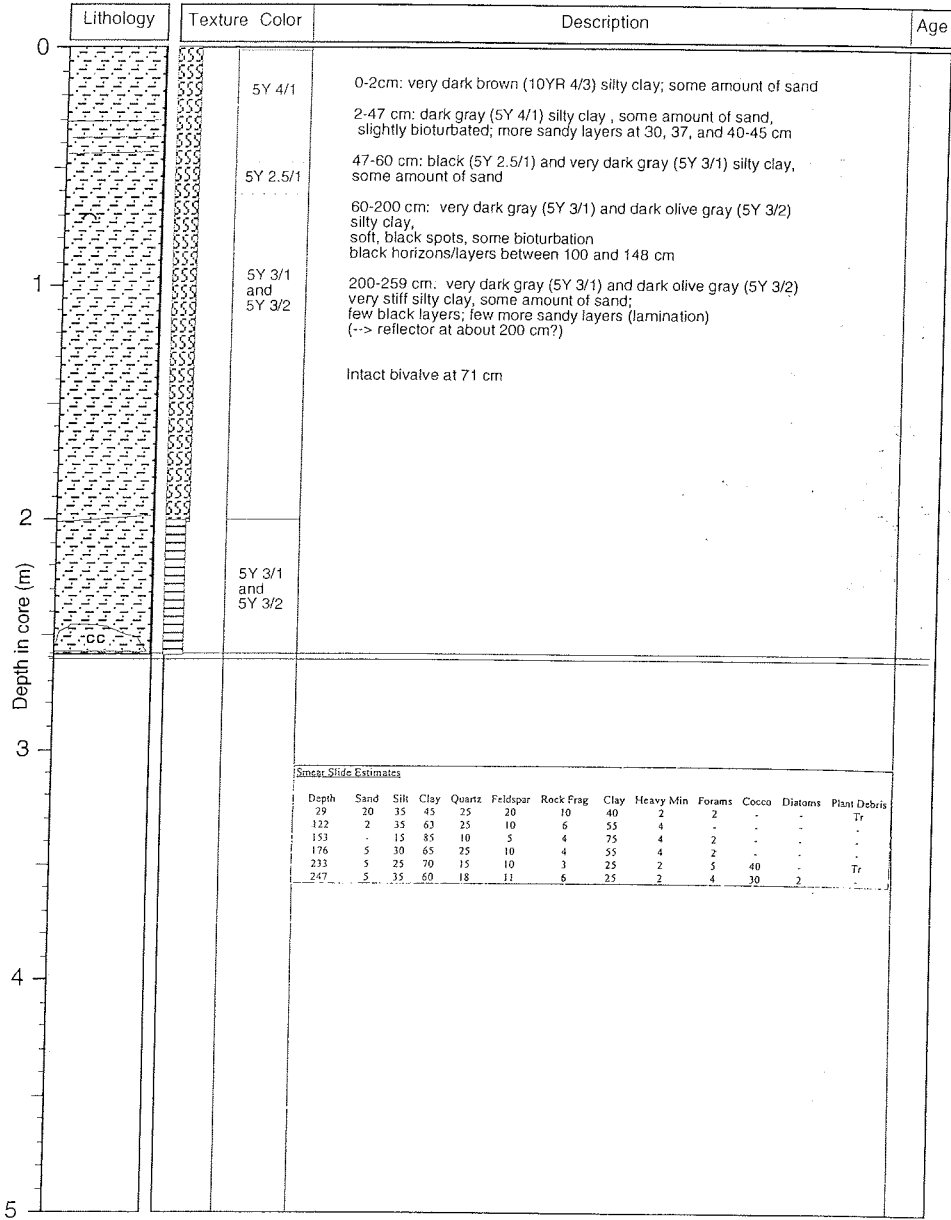
Southern Kara Sea

Boris Petrov 2001

Recovery: 2.59m

77° 54.93' N, 77° 26.64' E

Water depth: 174 m





BP01- 49/02(SL-5)

Southern Kara Sea

Boris Petrov 2001

Recovery: 3.84m

77° 52.48' N, 81° 30.03' E

Water depth: 198 m

Depth in core (m)	Lithology	Texture	Color	Description	Age
0				0-1cm: very dark brown (10YR 2/2) sandy silty clay	
			5Y 3/2	1-3 cm: dark grayish brown (10YR 4/2) silty clay with dark brown more sandy lenses/laminae	
				3-7 cm: olive brown (2.5 YR 4/3) sandy silty clay	
				7-13 cm: dark gray (5Y 4/1) silty sandy clay	
				13-20 cm: olive gray (5Y 4/2) silty sandy clay with thin sandy laminae	
				20-29 cm: dark olive gray (5Y 3/2) silty clay, few black spots, bioturbated	
1			5Y 3/1 and 5Y 3/2	29-32 cm: greenish gray (5GY 5/1) silty clay	
				32-37 cm: dark olive gray (5Y 3/2) silty clay	
				37-192 cm: very dark gray (5Y 3/1) and dark olive gray (5Y 3/2) silty clay, some amount of sand; abundant black spots, bioturbation;	
				192-284 cm: alternation of dark olive gray silty clay and clayey sandy silt (lamination)	
				284-384 cm: very dark grayish brown (2.5YR 3/2) sandy silty clay to silty sandy clay, very stiff (overconsolidated?); black stone (0.5 cm in diameter) at 329 cm	
2			5Y 3/2		
3			2.5YR 3/2		
4					
5					



BP01- 50/02(SL-5)

Southern Kara Sea

Boris Petrov 2001

Recovery: 2.11m

77° 50.91' N, 81° 30.13' E

Water depth: 154 m

Lithology	Texture	Color	Description	Age
	5Y 3/2		0-2cm: very dark brown (10YR 2/2) sandy silty clay	
	5Y 3/1 5Y 3/2		2-7 cm: dark grayish brown (10YR 4/2) silty clay with dark brown more sandy laminae	
			7-11 cm: dark gray (5Y 4/1) silty clay. some amount of sand	
	5Y 3/1 and 5Y 3/2		11-20 cm: dark olive gray (5Y 3/2) silty clay. very few black spots. bioturbated	
			20-42 cm: dark olive gray (5Y 3/2) and very dark gray (5Y 3/1) silty clay. abundant black spots	
			42-87 cm: dark olive gray (5Y 3/2) and very dark gray (5Y 3/1) silty clay with intercalated sandy laminae (increase in sand below 60 cm)	
			87-92 cm: (sandy) silty clay	
			92-99 cm: diamicton (abundant stones of 1-4 cm in diameter, sand, silt)	
	5Y 3/2		99-111 cm: dark olive gray (5Y 3/2) (sandy) silty clay	
			111-137 cm: dark olive gray (5Y 3/2) (sandy) silty clay. laminated. sandy laminae at 114, 115, 124, 127, 128, 132, and 137 cm	
		137-151 cm: dark olive gray (5Y 3/2) clayey silty sand		
		151-211 cm: alternation of dark olive gray silty clay and more sandy laminae		

BP01- 55/05 (SL-5)

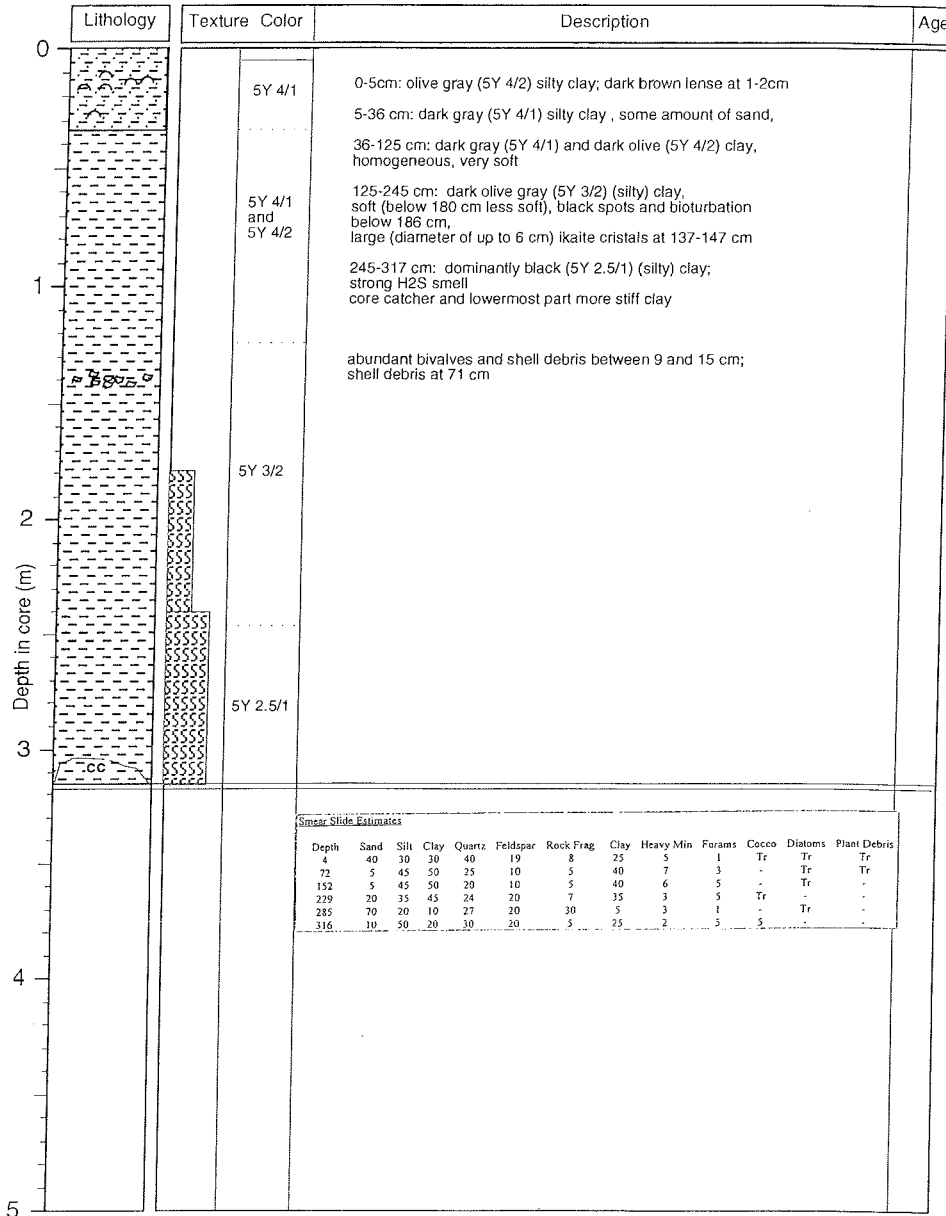
Southern Kara Sea

Boris Petrov 2001

Recovery: 3.17m

77° 02.97' N, 79° 43.99' E

Water depth: 83 m



Core description

BP01- 59/05 (SL-8)

Southern Kara Sea

Boris Petrov 2001

Recovery: 6.06 m

76° 31.23' N, 74° 30.94' E

Water depth: 176 m

Lithology	Texture Color	Description	Age
	<p>5Y 3/2</p>	<p>0-9 cm: very dark brown (10YR 3/2), dark brown (10YR 4/3), and dark grayish brown (sandy) silty clay, mottled/bioturbated</p> <p>9-18 cm: dark olive gray (5Y 3/2) soft (sandy) silty clay, sandy lenses; bioturbated</p> <p>18-606 cm: very dark gray (5Y 3/1) and dark olive gray (5Y 3/2) silty clay, black spots, bioturbated; minor amount of sand</p> <p>Bivalves at 386 and 502 cm</p>	
	<p>5Y 3/1 and 5Y 3/2</p>		

BP01- 59/05 (SL-8)

cont.

Boris Petrov 2001

	Lithology	Texture	Color	Description	Age
5			5Y 3/2 and 5Y3/1		
6					
7					
8					
9					
10					

Core description

BP01- 60/02 (SL-5)


Southern Kara Sea

Boris Petrov 2001

Recovery: 0.29m

76° 23.02' N, 74° 37.19' E

Water depth: 88 m

Lithology	Texture Color	Description	Age
	5Y 3/2 5Y 3/1	0-1cm: dark brown (10YR 4/3) silty clay: some sand 1-2 cm: olive brown silty clay: some sand 2-9 cm: olive gray (5Y 4/2) sandy silty clay 9-18 cm: dark olive gray (5Y 3/2) sandy silty clay and clayey silty sand (alternation) 18-29 cm: very dark gray (5Y 3/1) sandy silty clay, sand lenses	
0			
1			
2			
3			
4			
5			

BP01- 61/07 (SL-8)

Southern Kara Sea

Boris Petrov 2001

Recovery: 5.66 m

76° 12.9' N, 75° 53.15' E

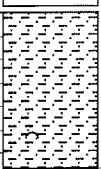
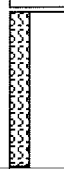
Water depth: 111 m

Depth in core (m)	Lithology	Texture Color	Description	Age
0		5Y 4/2 and 5Y 3/2 and 5Y 3/1	0-1 cm: dark brown (10YR 4/3) silty clay 1-66 cm: olive gray (5Y 4/2), dark olive gray (5Y 3/2), and very dark gray (5Y 3/1) silty clay; black spots, bioturbated 66-566 cm: very dark gray (5Y 3/1), black (5Y 2.5/1), and dark olive gray (5Y 3/2) silty clay, black spots (most abundant between 166 and 366 cm), bioturbated; ikatte/glendonite at 250-252 cm	
1		5Y 3/1 and 5Y 3/2 and 5Y 2.5/1	Bivalves/shell debris at 43 (gastropode), 60, 120, 127, 130 (intact), 157, 160, 183, 190, 194, 200, 203, 215, 218, 225, 239, 242, 265, 313, 407, 478, and 552 cm	
2				
3				
4				
5				

BP01- 61/07 (SL-8)

cont.

Boris Petrov 2001

	Lithology	Texture	Color	Description	Age
5			5Y 3/2 and 5Y3/1		
6					
7					
8					
9					
10					

BP01- 62/05 (SL-8)

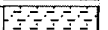
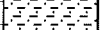
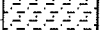
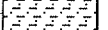
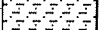
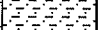
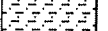
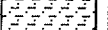
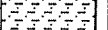
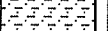
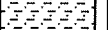
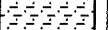
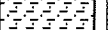
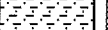
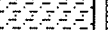
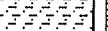
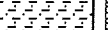
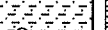

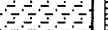
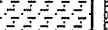
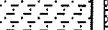
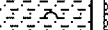
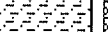
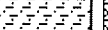
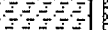
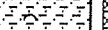
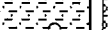
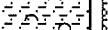
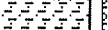
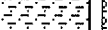
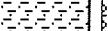
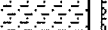
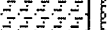
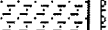

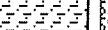
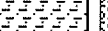
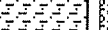
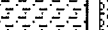
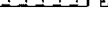


















Southern Kara Sea

Boris Petrov 2001

Recovery: 5.80 m

76° 12.05' N, 74° 12.15' E

Water depth: 135 m

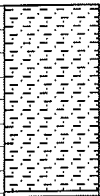

	Lithology	Texture Color	Description	Age
0			0-5 cm: dark brown (10YR 4/3) silty clay; sharp base	
			5-12 cm: dark olive gray (5Y 3/2) silty clay	
		5Y 3/2 and 5Y3/1	12-103 cm: very dark gray (5Y 3/1) and dark olive gray (5Y 3/2) silty clay, black spots, bioturbated, very soft	
			103-118 cm: very dark gray (5Y 3/1) to black (5Y 2.5/1) silty clay, bioturbated	
			118-178 cm: very dark gray (5Y 3/1) and dark olive gray (5Y 3/2) silty clay, black spots, bioturbated	
			178-580 cm: very dark gray (5Y 3/1), black (5Y 2.5/1), and dark olive gray (5Y 3/2) silty clay, black spots, bioturbated; lithified "worm tube" at 225-231 cm	
			Bivalves/shell debris at 222, 280, 330, 346, 355, 360, and 440 cm	
				
				
				
				
				
				
				
				
				
				
				
				
				
				
		5Y 3/1 and 5Y 3/2 and 5Y 2.5/1		
				
				
				
				
				
				
				
				
				
				
				
				
				
				
				
				
				
				
				
				
				
				
				
				
				
				
				
				
				
				
				
				
				
				
				
				
				



BP01- 62/05 (SL-8)

cont.

Boris Petrov 2001

Lithology	Texture	Color	Description	Age
		<p>5Y 3/2 and 5Y3/1 and 5Y 2.5/1</p>		

5  
6  
7  
8  
9  
10

Depth in core (m)

**BP01- 63/02 (SL-5)**

Southern Kara Sea

**Boris Petrov 2001**

Recovery: 0.14m

76° 12.02' N, 74°29.33' E

Water depth: xx m

Depth in core (m)	Lithology	Texture	Color	Description	Age
0			5Y 3/2	0-1 cm: dark brown (10YR 4/3) (sandy) silty clay 1-14 cm: dark olive gray (5Y 3/2) clayey sandy silt	
1					
2					
3					
4					
5					



Core description

BP01- 67/07 (SL-5)

Southern Kara Sea

Boris Petrov 2001

Recovery: 0.71m

75° 14.65' N, 73° 45.78' E

Water depth: 49 m

Litholog	Texture	Color	Description	Age																																																																																																																																			
0																																																																																																																																							
		5Y 3/1 and 5Y 3/2	0-71 cm: very dark gray (5Y 3/1) and dark olive gray (5Y 3/2) silty clay, black spots, bioturbated																																																																																																																																				
1																																																																																																																																							
	<table border="1"> <thead> <tr> <th colspan="13">Smear Slide Estimates</th> </tr> <tr> <th>Depth</th> <th>Sand</th> <th>Silt</th> <th>Clay</th> <th>Quartz</th> <th>Feldspar</th> <th>Rock Frag</th> <th>Clay</th> <th>Heavy Min</th> <th>Forams</th> <th>Cocco</th> <th>Diatoms</th> <th>Plant Debris</th> </tr> </thead> <tbody> <tr> <td>2</td> <td>5</td> <td>15</td> <td>80</td> <td>8</td> <td>4</td> <td>3</td> <td>75</td> <td>3</td> <td>2</td> <td>-</td> <td>2</td> <td>-</td> </tr> <tr> <td>10</td> <td>7</td> <td>20</td> <td>73</td> <td>15</td> <td>5</td> <td>3</td> <td>70</td> <td>3</td> <td>-</td> <td>-</td> <td>1</td> <td>-</td> </tr> <tr> <td>20</td> <td>15</td> <td>35</td> <td>50</td> <td>25</td> <td>15</td> <td>5</td> <td>40</td> <td>5</td> <td>-</td> <td>-</td> <td>2</td> <td>-</td> </tr> <tr> <td>30</td> <td>7</td> <td>15</td> <td>78</td> <td>10</td> <td>5</td> <td>3</td> <td>70</td> <td>3</td> <td>-</td> <td>-</td> <td>2</td> <td>-</td> </tr> <tr> <td>40</td> <td>5</td> <td>15</td> <td>80</td> <td>10</td> <td>5</td> <td>2</td> <td>75</td> <td>2</td> <td>-</td> <td>-</td> <td>-</td> <td>-</td> </tr> <tr> <td>50</td> <td>15</td> <td>35</td> <td>50</td> <td>25</td> <td>15</td> <td>6</td> <td>40</td> <td>5</td> <td>-</td> <td>-</td> <td>-</td> <td>-</td> </tr> <tr> <td>60</td> <td>7</td> <td>63</td> <td>30</td> <td>35</td> <td>22</td> <td>5</td> <td>25</td> <td>5</td> <td>-</td> <td>-</td> <td>Tr</td> <td>Tr</td> </tr> <tr> <td>71</td> <td>10</td> <td>35</td> <td>55</td> <td>20</td> <td>10</td> <td>6</td> <td>50</td> <td>5</td> <td>Tr</td> <td>-</td> <td>1</td> <td>Tr</td> </tr> </tbody> </table>				Smear Slide Estimates													Depth	Sand	Silt	Clay	Quartz	Feldspar	Rock Frag	Clay	Heavy Min	Forams	Cocco	Diatoms	Plant Debris	2	5	15	80	8	4	3	75	3	2	-	2	-	10	7	20	73	15	5	3	70	3	-	-	1	-	20	15	35	50	25	15	5	40	5	-	-	2	-	30	7	15	78	10	5	3	70	3	-	-	2	-	40	5	15	80	10	5	2	75	2	-	-	-	-	50	15	35	50	25	15	6	40	5	-	-	-	-	60	7	63	30	35	22	5	25	5	-	-	Tr	Tr	71	10	35	55	20	10	6	50	5	Tr	-	1	Tr	
Smear Slide Estimates																																																																																																																																							
Depth	Sand	Silt	Clay	Quartz	Feldspar	Rock Frag	Clay	Heavy Min	Forams	Cocco	Diatoms	Plant Debris																																																																																																																											
2	5	15	80	8	4	3	75	3	2	-	2	-																																																																																																																											
10	7	20	73	15	5	3	70	3	-	-	1	-																																																																																																																											
20	15	35	50	25	15	5	40	5	-	-	2	-																																																																																																																											
30	7	15	78	10	5	3	70	3	-	-	2	-																																																																																																																											
40	5	15	80	10	5	2	75	2	-	-	-	-																																																																																																																											
50	15	35	50	25	15	6	40	5	-	-	-	-																																																																																																																											
60	7	63	30	35	22	5	25	5	-	-	Tr	Tr																																																																																																																											
71	10	35	55	20	10	6	50	5	Tr	-	1	Tr																																																																																																																											
2																																																																																																																																							
3																																																																																																																																							
4																																																																																																																																							
5																																																																																																																																							

BP01- 71/04 (SL-5)

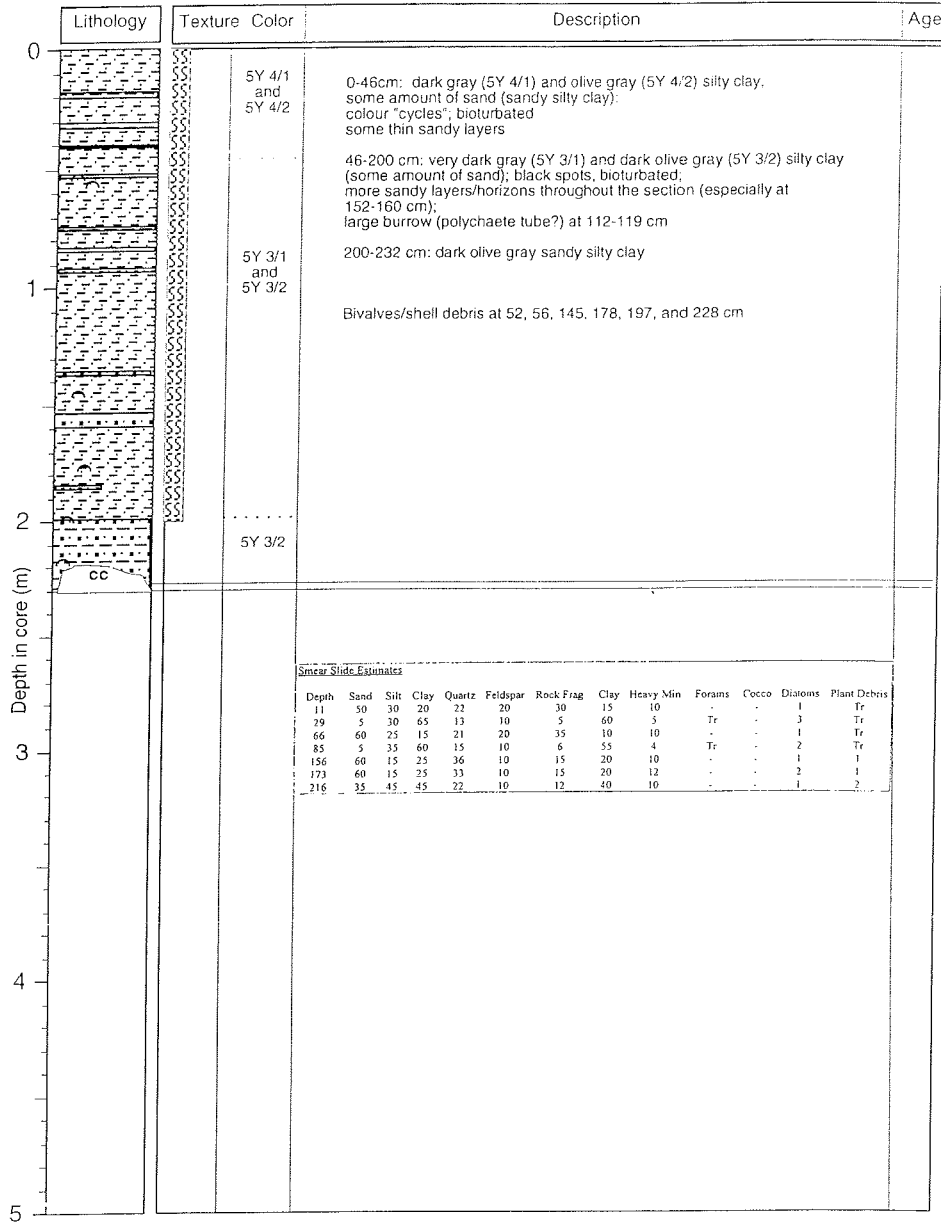
Ob Estuary

Boris Petrov 2001

Recovery: 2.32m

72° 39.96' N, 73° 17.94' E

Water depth: 23 m



BP01- 72a/02 (SL-5)

Southern Ob Estuary

Boris Petrov 2001

Recovery: 4.67m

70° 51.03' N, 73° 43.07' E

Water depth: 27 m

Lithology	Texture	Color	Description	Age
			0-4 cm: black (5Y 2.5/1) silty clay	
		5Y 3/1 and 5Y 3/2	4-10 cm: very dark gray (5Y 3/1) clayey sandy silt	
			10-45 cm: very dark gray (5Y 3/1) and dark olive gray (5Y 3/2) clayey silty sand, bioturbated	
			45-48 cm: black (5Y 2.5/1) silty clay	
		5Y 2.5/1	48-55 cm: very dark gray (5Y 3/1), black (5Y 2.5/1), and dark olive gray (5Y 3/2) clayey silty sand	
			55-68 cm: black (5Y 2.5/1) and dark olive gray (5Y 3/2) silty clay, bioturbation; more sandy interval at 63-64 cm	
		5Y 2.5/1	68-90 cm: dominantly black (5Y 2.5/1) silty clay; some dark olive gray mottling/bioturbation; ++ black at 84-90 cm	
			90-103 cm: black (5Y 2.5/1) and dark olive gray (5Y 3/2) silty clay, very minor amount of sand; mottled	
			103-125 cm: black (5Y 2.5/1) silty clay	
			125-467 cm: alternation of black (5Y 2.5/1) and dark olive gray (5Y 3/2) silty clay, partly slightly bioturbated; dominance of black	
		Bivalves 80, 95, 129, 304 (intact), 326, 364 (intact), 379 (intact), and 408 cm		
	5Y 2.5/1 and 5Y 3/2			
cc				

BP01- 73/05 (SL-5)

Southern Ob Estuary

Boris Petrov 2001

Recovery: 2.22m

68° 54.89' N, 73° 39.99' E

Water depth: 15 m

Lithology	Texture Color	Description	Age
		<p>0-222 cm: alternation of dark olive gray sandy clayey silt and clayey silty sand; thickness of more fine-grained layers 0.5 - 2 cm, of more coarse-grained layers 0.2-0.5 cm; "slump structures" between 55 and 74 cm and 85 and 100 cm</p>	

BP01- 82/08 (SL-5)

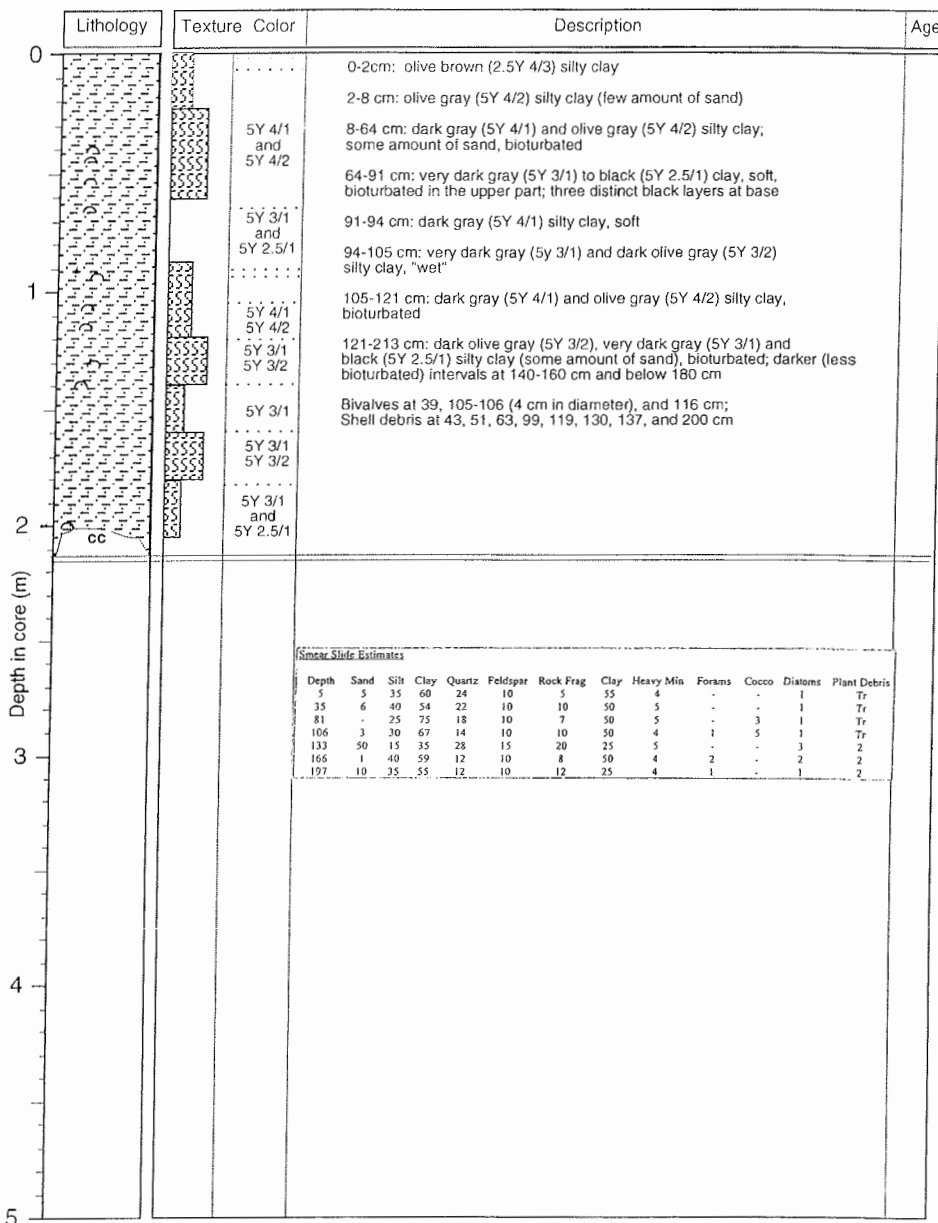
Ob Estuary

Boris Petrov 2001

Recovery: 2.13m

73° 11.83' N, 73° 01.65' E

Water depth: 29 m





10-3: Summary of biological, geochemical, and geological studies performed at Russian and German institutes on water and sediment samples obtained during the "Akademik Boris Petrov" Kara Sea Expedition 2001.

	Institute	Methods	Parameter
<b>1. Water samples</b>			
Sea (river) water	GEOKHI	Classical chemical analyses	Nutrients (PO <sub>4</sub> , NO <sub>3</sub> , NO <sub>2</sub> , SiO <sub>2</sub> ), alkalinity, pH, chlorinity
Sea water	GEOKHI	GC	Concentration and distribution of CH <sub>4</sub> and C <sub>2</sub> -C <sub>6</sub> homologues
Dissolved organic matter	IFBM-AWI	HTC, HPLC, GC/MS, IRMS, CHN, NMR	DOC, DON; C, N; Amino acids, lignin phenols; structure
Carbon and silica cycle	IFBM	CN, HPLC, MS, Photometry	POC, PON, CaCO <sub>3</sub> , Opal, aminoacids, carbohydrates; δ <sup>15</sup> N
Particulate organic matter	AWI	GC, GC/MS	Biomarkers (n-alkanes, fatty acids, sterols, hopanoids etc.)
Particulate organic matter	GEOKHI	CNS, MS	POC, PON; stable carbon and nitrogen isotopes
Particulate organic matter	GEOKHI	Radiochemistry	<sup>137</sup> Cs and other radionuclides
Geochemistry	GEOMAR	MS	Stable inorganic carbon and oxygen isotopes
Geochemistry	GEOKHI	MS	Stable inorganic carbon isotopes
Phytoplankton	GEOKHI	MS	Stable carbon and nitrogen isotopes
Phytoplankton	MMBI	Microscopy, statistical analysis	Abundances, species composition, community structure
Zooplankton	AWI	Microscopy, REM, statistical analysis	Abundances, biomass, species composition, community structure

Parameter	Methods	Institute
Benthos ecology	AWI Microscopy, statistical analysis	
Benthos	GEOKHI Gamma-spectrometry	
Sedimentology/Mineralogy	AWI XRD	
Sedimentology/Mineralogy	IORAS Microscopy	
Organic geochemistry	AWI CNS, Rock-Eval, GC, GC/MS; Microscopy	
Organic geochemistry	IFBM CN, HPLC, MS, Photometry	
Organic geochemistry	GEOKHI CNS, Rock-Eval, GC, GC/MS	
Organic geochemistry		C, N, S; pyrolysis parameter; lignin; stable carbon and nitrogen isotopes
Hydrocarbon gases	GEOKHI GC, GC/MS	Concentration and distribution of hydrocarbon gases; stable isotopes CH4
Pore-water chemistry	GEOKHI classical chemistry analyses	Nutrients (PO4, NO3, NO2, SiO2), alkalinity, pH, chlorinity
Radio-geochemistry	GEOKHI Radiochemistry, gamma-spectrometry	137-Cs, 90-Sr, 239-Pu, 240-Pu, 210-Pb
Radio-geochemistry	IGEM Radiochemistry, gamma-spectrometry	137-Cs, 90-Sr, 239-Pu, 240-Pu, 210-Pb
Micropalaeontology	AWI Microscopy	Palytomorphs, diatoms; pollen stratigraphy
Micropalaeontology	IORAS Microscopy	Benthic foraminifera
Geochemistry	GEOMAR MS	Stable inorganic carbon and oxygen isotopes
Inorganic geochemistry	AWI RFA	Major and minor elements
Inorganic geochemistry	GEOKHI XRS	Heavy elements
Core logging	AWI Multi-sensor core logging	Magnetic susceptibility, density, velocity
Dating of sediment cores	AWI AMS 14C	Chronology; flux rates
Sediment profiling	AWI	Sediment echograph, 3.5 khz profiling

**10.4: Research Participants**

<b>Name</b>	<b>Discipline</b>	<b>Institution</b>
Stepanets, Oleg	Chief of Expedition	GEOKHI
Stein, Ruediger	Co - chief Scientist	AWI
Borisov, Alexander	Radio- Geochemistry	GEOKHI
Barchukov, Valeriy	Biology	GEOKHI
Beude, Rafaela	Biology	AWI
Deubel, Hendrik	Biology	AWI
Dittmers, Klaus	Geophysics	AWI
Gebhardt, Andrea Catalina	Organic Geochemistry	IFBM
Eulenburg, Antje	Inorganic Geochemistry	AWI
Engel, Marcus	Biology	AWI
Fetzer, Ingo Marcus	Biology	AWI
Hollman, Beate	Organic Geochemistry	AWI
Kabanov, Alexander	Radionuclides	TAIPHUN
Kodina, Ludmilla	Organic Geochemistry	GEOKHI
Korobova, Elena	Radionuclides	GEOKHI
Köhler, Hayo	Organic Geochemistry	IFBM
Lahajnar, Niko	Organic Geochemistry	IFBM
Larionov, Viktor	Biology	MMBI
Levitan, Michael	Geology	GEOKHI
Ligaev, Alexander	Radio - Geochemistry	GEOKHI
Lind Ole - Christian	Radiochemistry	NLH
Niessen, Frank	Geophysics	AWI
Meon, Benedikt	Organic Geochemistry	AWI
Miroshnikov, Alexey	Radionuclides	IGEM
Osadchiy, Nikolay	Engineer	GEOKHI
Panteleymonov, Timophej	Biology	AARI
Pegoev, Nikolay	Radionuclides	TAIPHUN
Schoster, Frank	Inorganic Geochemistry	AWI
Schmelkov, Boris	Engineer	GEOKHI
Sickel, Morten	Radiochemistry	NRPA
Simstich, Johannes	Geology	GEOMAR
Sizov, Yevgeniy	Radio - Geochemistry	GEOKHI
Solovjeva, Galina	Radio - Geochemistry	GEOKHI
Stanovoy, Vladimir	Oceanography	AARI
Steinke, Tatjana	Geology	AWI
Suhoruk, Vladimir	Marine Chemistry	IORAS
Tokarev, Viktor	Organic Geochemistry	GEOKHI
Ukrainzeva, Nataliya	Radionuclides	MSU

Vlasova, Ludmilla                      Organic Geochemistry                      GEOKHI

### **Ships Crew**

Vtorov, Igor	Captain
Dmitrenko, Peter	Chief mate
Moiseev, Alexey	2nd Mate
Vaulin, Alexander	2nd Mate
Opekunov, Viner	3rd Mate
Krytin, Alexey	Chief Radio
Horshev, Viktor	Scientific - Engineer
Latko, Alexander	Scientific - Engineer
Reyzkiy, Anatoliy	Doctor
Yakybovskiy, Pavel	Hauptmechaniker
Kuryshv, Viktor	2nd Mechaniker
Zentner, Boris	3rd Mechaniker
Yazenko, Sergei	4nd Mechaniker
Ganoshenko, Anatoliy	Elektro - Engineer
Drosdov, Ruslan	2nd Elektro - Engineer
Golikov, Yuriy	Motorman
Markovskiy, Vladimir	Boatswain
Nesterchuk, Yuriy	Seaman
Domrachev, Alexey	Seaman
Levkin, Vladimir	Seaman
Vasilchenko, Alexander	Seaman
Moriz, Igor	Seaman
Vtorov, Andrey	Seaman
Smirnov, Vladimir	Seaman
Slepchenko, Vladimir	Motorman
Spakovskiy, Yuriy	Motorman
Phil, Vladimir	Motorman
Saizev, Anatoliy	Motorman
Pereversa, Alexander	Cook
Oblapinskiy, Alexander	Cook
Gavrilyuk, Irina	Stewardess
Dolmatova, Irina	Stewardess
Grizeshina, Irina	Stewardess
Demyanovich, Galina	Stewardess
Titova, Irina	Stewardess